Four dimensional hyperbolic link complements via Kirby calculus

Hemanth Saratchandran

Balliol College

University of Oxford

A thesis submitted for the degree of

Doctor of Philosophy

Hilary 2015

For Jaya, Chandran and Para

"Any man that can sing like that can't be all bad"

Lt. Columbo; Swan Song

Acknowledgements

First and foremost I must thank my supervisor Marc Lackenby for his continual support and encouragement during the writing of this thesis. I am indebted to him for the time and effort he has put in helping me through my graduate research here at Oxford. His deep insight and dedication in helping me understand various difficult concepts has proved invaluable in the writing of this thesis.

I must also thank Andras Juhasz and Panos Papazoglou for reading parts of an earlier draft of this thesis. Their comments on the mathematical contents and stylistic aspects proved very helpful. I would also like to thank Manuel Araújo and Mark Penney for their help with Mathematica, which proved vital for the many diagrams that are present in this thesis, and their friendship along with the great times we had in sharing an office together.

I wish to acknowledge the constant support and encouragement of Ben Andrews, Christopher Douglas, Frances Kirwan and Ulrike Tillmann. The advice they have given me throughout my degree has proved very useful, and I am extremely grateful for the many times they have helped me without any hesitation. I must also thank Douglas Dupree in making my time at Balliol College a very pleasant experience, and always offering a helping hand.

I thank my good friends Lashi Bandara, Alejandro Betancourt, Antonio De Capua and Alejandra Garrido for their constant encouragement, the many times they have come to my office to see how I am doing, and the countless amount of great moments we have had together. It is a truly magnificent feeling to know such good people. A special mention must be given to Salvador Izquierdo-Bueno Martín who has come to be a remarkable friend of mine. I am greatly indebted to him for his constant support and the countless amount of times he has looked out for my general well being. I am very lucky to have such a genuine person as a friend and housemate, and will treasure the great moments we have had together. I would also like to thank Carlos Javier Bernárdez García, Adrian King (the "boss") and Maca Roni for their friendship and constant encouragement during the writing of this thesis. It has been a real pleasure living with such good people, and I will always remember the great times we had together.

I must also thank Bruce Bartlett, Dario Beraldo, Alberto Cazzaniga, Emily Cliff, Simon Day, Chris Hopper, Robert Laugwitz, Brent Pym and Benjamin Volk for their friendship along with

the many great moments we have had at Oxford.

A thank you must be given to the wonderful administrative and care taking staff here at the Mathematical Institute part of whom are, Stu Burchell, Helen Cullen, Keith Gillow, Cathy Hunt, Naomi Kraker, Sally Mullins, Sandhya Patel and Timmy!

I owe a huge thank you to my wonderful brother Para for taking the time and effort to come and see me in Oxford on more than one occasion, and always taking a keen interest in what I am doing.

Finally, I would like to acknowledge the ongoing support of the two greatest people in my life, my parents. They have given me endless encouragement throughout my life, always showering me with constant love and affection, and during every minute of the day take the time to make sure that I am doing well.

Abstract

The primary aim of this thesis is to construct explicit examples of four dimensional hyperbolic link complements. Using the theory of Kirby diagrams and Kirby calculus we set up a general framework that one can use to attack such a problem. We use this framework to construct explicit examples in a smooth standard S^4 and a smooth standard $S^2 \times S^2$. We then characterise which homeomorphism types of smooth simply connected closed 4-manifolds can admit a hyperbolic link complement, along the way giving constructions of explicit examples.

Contents

Introduction

In the 1970's W. Thurston initiated a grand study of the topology of 3-manifolds motivated by the realisation that many 3-manifolds admitted homogeneous Riemannian metrics. Thurston's insight was that one could use this geometry to study the topology of a 3-manifold, the ultimate goal being a unification of the worlds of geometry and topology in dimension three. Two worlds thought to be completely distinct before Thurston's time. Part of Thurston's study involved a detailed understanding of how various link complements in 3-manifolds could admit homogeneous geometries. He was able to show that many link complements admitted a hyperbolic geometry thereby throwing the world of hyperbolic geometry to the forefront (see [20] chap.3, p.27 and [21] cor.2.5, p.360). This grand vision of Thurston came to be known as the "geometrisation conjecture" and was finally proved by G. Perelman in 2003. The geometrisation theorem together with the classification of surfaces leads to a complete understanding of the worlds of two and three dimensional manifolds.

The quest for a complete understanding of the world of 4-manifolds, analogous to the two and three dimensional cases, is a futile quest. The main reason being that, every finitely presented group can arise as the fundamental group of a compact 4-manifold. As there is no algorithm to tell whether two finitely presented groups are isomorphic, there is no algorithm to tell if two 4-manifolds have the same fundamental groups. Motivated by Thurston's work on which link complements, in dimension 3, admit hyperbolic geometries, we can restrict our attention to the class of hyperbolic 4-manifolds and try to understand which 4-manifolds have link complements that admit a hyperbolic geometry. The main problem here is that hyperbolic 4-manifolds are characteristically different from hyperbolic 3-manifolds, and the techniques used to show that a 3-manifold admits a link complement that is hyperbolic simply do not have four dimensional counter parts. Due to this, the quest to understand which 4-manifolds admit link complements that are hyperbolic takes on a very different feel right from the start.

In the last decade there have been quite a few constructions of hyperbolic 4-manifolds. One of the simplest constructions was given by J. Ratcliffe and S. Tschantz in their paper [17]. Each of the 4-manifolds they construct are non-compact and have ends of the form $E \times [0, \infty)$, with E a closed flat 3-manifold that is a circle bundle over a surface. We can take these ends, chop them

off at a certain point, and produce a compact 4-manifold M_0 with boundary a certain number of flat closed 3-manifolds E_i. The region near the boundary is a copy of $E_i \times [0, t]$, for some $t > 0$. These boundary 3-manifolds, being circle bundles, bound a 4-manifold F_i, the associated disk bundle. We can then glue the manifold F_i to M_0 by identifying the boundary components via the identity, we will call this a "filling" of M_0.

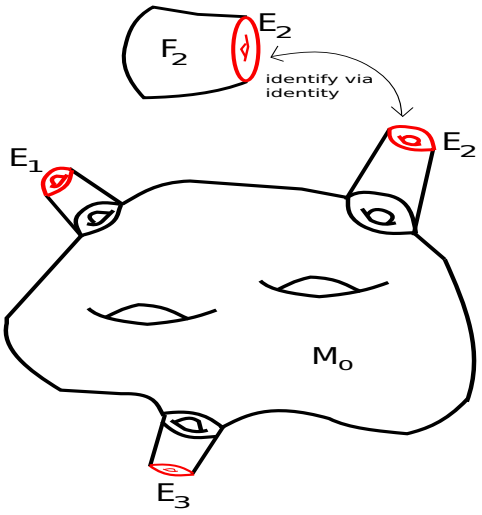

It could be the case that the 3-manifold E fibres over a surface in more than one way, hence the filling process will depend on the choice of S^1-fibre. Carrying out this gluing procedure for each boundary component of M_0 produces a closed 4-manifold $\widetilde{M}$. The original hyperbolic 4-manifold can then be seen to be a complement inside of the closed 4-manifold $\widetilde{M}$. At this point one of the most basic questions we can ask is, can we explicitly identify the manifold $\widetilde{M}$? This question is related to the above problem of finding 4-manifolds that have a hyperbolic link complement in that the ability to classify such an $\widetilde{M}$ would then result in an explicit example of a four dimensional hyperbolic link complement. However, one has to be very careful in using the word "classify". The main reason being that the world of 4-manifolds is a truly wild world, there are 4-manifolds out there that do not admit a single smooth structure, others out there that admit countably many smooth structures, and some even admitting uncountably many smooth structures! This exotic behaviour of 4-manifolds shows the mathematician that the problem of characterising a 4-manifold up to homeomorphism is a very different problem than to characterise it up to diffeomorphism, something one does not witness when restricting to manifolds of dimensions two and three.

In general the identification of the topological/smooth type of the manifold $\widetilde{M}$ can prove to be an impossible task. However, if for example the filled in manifolds one obtains are simply connected then there is certainly hope. A good way to try and smoothly identify a simply connected 4-manifold is to resort to a "calculus of links" developed by R. Kirby towards the

end of the 70's (see [14]). Kirby showed that given a handle decomposition of a closed 4-manifold, the one and two handles were really what one had to worry about in trying to understand the manifold. The one and two handle structure of such a manifold can be neatly encoded in a link diagram in S^3, which we can view as $\mathbb{R}^3 \cup \{\infty\}$. Therefore, the one and two-handle structure of such a manifold could be explicitly visualised by a link diagram in $\mathbb{R}^3$, which we now call a Kirby diagram. Kirby was able to prove that if one applied certain elementary moves to the link diagram, obtaining a new link diagram, the 4-manifold that corresponded to this new link diagram would be diffeomorphic to the original 4-manifold. In this way Kirby set up a "calculus" that one could appeal to in order to simplify their link diagram but without any compensation being paid on the diffeomorphism type of their closed 4-manifold.

Armed with the knowledge that the Kirby calculus provides a means for exposing the diffeomorphism type of a filling of a hyperbolic link complement, we set our sights on understanding how one can build a Kirby diagram for a non-compact finite volume hyperbolic 4-manifold. The thesis starts by showing how to produce a Kirby diagram for any one of the Ratcliffe-Tschantz manifolds and then shows how it changes when a filling procedure is carried out, in turn producing an explicit diagram for any such filling. We then take a particular example and appeal to Kirby's calculus of links, showing how to simplify the associated Kirby diagram all the way down to the Kirby diagram of a standard smooth S^4. This leads us to our first main theorem:

Theorem. *(theorem 2.3.1) There exists a collection L of five linked tori embedded in a standard smooth S^4 such that the complement $S^4 - L$ admits a finite volume hyperbolic geometry.*

We would like to mention that D. Ivanšić proves in his paper [10] (see thm.4.3, p.18) that there exists a system of five linked tori embedded in a smooth manifold X that is homeomorphic to S^4 such that $X - L$ admits a finite volume hyperbolic geometry. The manifold he uses to construct X is the same manifold we use to prove the above theorem. However, he does not prove that X is diffeomorphic to S^4 and in particular does not consider constructions to do with Kirby diagrams and the Kirby calculus. Furthermore, D. Ivanšić, J. Ratcliffe and S. Tschantz in their paper [11] construct several more examples of hyperbolic link complements in 4-manifolds that are homeomorphic to S^4, they do not prove that any of the fillings they construct are diffeomorphic to S^4, and they only consider fillings that can be homeomorphic to S^4. We were unaware of the existence of these two papers when we were constructing the proof of the above theorem, and during the writing of this whole thesis. In fact we were only made aware of these two papers very recently, we should also point out that the rest of our theorems have no counter parts in their paper, and the techniques we use to analyse the fillings we obtain are completely different from the techniques they employ.

The above theorem showing the existence of a hyperbolic link complement in a standard smooth S^4 raises the question of whether there exist other 4-manifolds with hyperbolic link complements, and if so can we identify their diffeomorphism type? The next main theorem we prove provides an answer to this question by constructing an explicit example in a standard smooth $(S^2 \times S^2)$.

Theorem. *(theorem 3.3.1) There exists a collection L of ten linked tori embedded in a standard smooth $(S^2 \times S^2)$ such that the complement $(S^2 \times S^2) - L$ admits a finite volume hyperbolic geometry.*

Following on from the work of R. Kirby it was soon realised that many topological structures, such as a spin structure, that a 4-manifold could posses could be investigated through the knowledge of a Kirby diagram. This led to the knowledge of a Kirby diagram being a useful tool to study the homeomorphism type of a 4-manifold. Chapters 4 and 5 are dedicated to understanding the topological type of various fillings associated to the Ratcliffe-Tschantz manifolds via knowledge of their Kirby diagram. The study is initiated with a discussion on how using a Kirby diagram one can understand whether the Ratcliffe-Tschantz manifolds and certain fillings associated to them posses a spin structure. Coupled with M. Freedman's and S. Donaldson's classification of the homeomorphism types of smooth simply connected closed 4-manifolds (see [6] and [5]) we are able to classify the homeomorphism type of various fillings. The main theorem we prove along these lines is the following.

Theorem. *(theorem 4.2.6) There exists a collection L of linked tori embedded in a closed 4-manifold X, such that X is homeomorphic to $\#_n(S^2 \times S^2)$ with $n \geq 2$ even, and $X - L$ admits a finite volume hyperbolic geometry.*

Using a classification theorem of A. Kawauchi on closed 4-manifolds with infinite cyclic fundamental group we are able to construct a hyperbolic complement in a non-simply connected 4-manifold and explicitly identify its topological type.

Theorem. *(theorem 4.3.2) There exists a collection L consisting of seven tori and one Klein bottle embedded in a closed 4-manifold X, such that X is homeomorphic to $(S^1 \times S^3)\#(S^2 \times S^2)$ and $X - L$ admits a finite volume hyperbolic geometry.*

The work of M. Freedman and S. Donaldson on smooth simply connected closed 4-manifolds gives a very nice list on the homeomorphism types a 4-manifold can be. Looking at such a list one could try and understand which of these types could posses a link complement that admits a finite volume hyperbolic geometry. The thesis ends by giving necessary conditions on the homeomorphism type of those simply connected closed 4-manifolds that have a link complement that admits a finite volume hyperbolic geometry.

Theorem. *(theorem 5.0.8) Let X be a smooth closed simply connected 4-manifold that has a link complement that admits a finite volume hyperbolic geometry. Then the homeomorphism type of X falls into one of the following three categories:*

- S^4
- $\#_k(S^2 \times S^2)$, $k > 0$.
- $\#_k\mathbb{CP}^2\#_k\overline{\mathbb{CP}^2}$, $k > 0$.

We now briefly outline the contents of each chapter.

In **Chapter** 1 we give details of the construction of the 24-cell, the fundamental domain for each of the hyperbolic 4-manifolds that Ratcliffe and Tschantz construct. We then give a brief survey of how Ratcliffe and Tschantz constructed their hyperbolic manifolds, giving explicit details on the side pairing transformations they use. We then show how all this information can be used to produce a Kirby diagram for any one of the 1179 manifolds they construct, giving explicit examples with several pictures along the way.

Chapter 2 initiates the study of the smooth topology of the boundary fillings of the Ratcliffe-Tschantz manifolds. In order to make sense of such a procedure, one needs a good understanding of the cusp structure of each of the Ratcliffe-Tschantz manifolds. We explain how to compute parabolic generators associated to the stabiliser subgroups of each cusp, and how to identify translations in these stabiliser subgroups. We then explain how these translations give us a way to produce a boundary filled manifold, and show how the boundary filling takes place on the level of the Kirby diagram. The next step is to try and reduce the Kirby diagram of such a boundary filled manifold, we explicitly explain what this entails and why it works in our examples, along the way giving several pictures of examples of reduction moves. Finally, we end with an explicit example of a boundary filled manifold that we reduced all the way down to a smooth copy of a standard smooth S^4 culminating in our theorem on the existence of a hyperbolic link complement in a standard smooth S^4. Another purpose of this example (done in great detail) is to show the reader how our general framework for producing a Kirby diagram can be constructively put to use for many particular examples, thereby making the techniques of practical value.

Chapter 3 continues the study initiated in chapter 2, we show how to construct a smooth hyperbolic link complement in a standard smooth $S^2 \times S^2$ using the methods from the previous two chapters.

Chapter 4 begins the study of trying to understand the homeomorphism type of a boundary filling. The starting point for this chapter is to show the reader how one can try and understand whether a Ratcliffe-Tschantz manifold is spin via its associated Kirby diagram. We give

explicit examples of such manifolds and use them to construct fillings that are homeomorphic to $\#_{2k}(S^2 \times S^2)$ for each $k > 0$. The chapter ends with an explicit construction of a non-simply connected filling with homeomorphism type $(S^1 \times S^3)\#(S^2 \times S^2)$.

Chapter 5 seeks to understand which smooth simply connected closed 4-manifolds can admit a link complement that is hyperbolic. We prove a characterisation theorem that rules out many possible 4-manifolds from admitting a complement with such a structure.

Chapter 1

A Handle Decomposition for the Ratcliffe-Tschantz Manifolds

This chapter begins with some basic properties of the 24-cell, a four dimensional polyhedron that is the fundamental domain of all the manifolds we will be concerned with. We then move on to explain how Ratcliffe and Tschantz constructed an assortment of non-compact hyperbolic 4-manifolds each having the 24-cell as their fundamental domain. Using Ratcliffe and Tschantz' construction and the geometry of the 24-cell, we show how one can obtain a handle decomposition for each of the hyperbolic 4-manifolds that Ratcliffe and Tschantz construct. The chapter ends by giving an explicit handle decomposition for two of the hyperbolic 4-manifolds.

1.1 Dualising the 24-cell

In this section we will explain to the reader how the 24-cell is constructed, and how we can visualise the boundary of the 24-cell in $\mathbb{R}^3$. In the sections to follow we will then show how this leads one to obtain a Kirby diagram for any of the manifolds constructed by Ratcliffe and Tschantz.

Let $S_{(*,*,*,*)}$ denote a sphere of radius 1 centred at a point in $\mathbb{R}^4$ whose coordinates have two ± 1's and whose other two coordinates are both zero. For example $S_{(+1,+1,0,0)}$ denotes the sphere of radius 1 centred at the point $(1,1,0,0)$ in $\mathbb{R}^4$. If we let $\mathbb{H}^4$ denote the ball model of hyperbolic 4-space, then we find that all the spheres $S_{(*,*,*,*)}$ intersect the sphere at infinity orthogonally. This implies that each such sphere determines a hyperplane in $\mathbb{H}^4$. If we let $Q_{(*,*,*,*)}$ denote the corresponding half-space that contains the origin, and then take the intersection of all such half-spaces, we find that we obtain a 24-sided polyhedron P in $\mathbb{H}^4$. This polyhedron is known as the hyperbolic 24-cell and we will denote it by P. It is a four dimensional self dual polyhedron. We will denote the side of P that lies on the sphere $S_{(*,*,*,*)}$ also by $S_{(*,*,*,*)}$. All the dihedral angles of P are $\pi/2$ and it has 24 vertices which are all ideal vertices. We can

explicitly describe each ideal vertex: We have 8 vertices of the form $v_{(\pm1,0,0,0)} = (\pm1, 0, 0, 0)$, $v_{(0,\pm1,0,0)} = (0, \pm1, 0, 0)$, $v_{(0,0,\pm1,0)} = (0, 0, \pm1, 0)$, $v_{(0,0,0,\pm)} = (0, 0, 0, \pm1)$ plus 16 vertices of the form $v_{(\pm1/2,\pm1/2,\pm1/2,\pm1/2)} = (\pm1/2, \pm1/2, \pm1/2, \pm1/2)$. Finally let us mention that it has twenty four codimension 1 sides, ninety six codimension 2 sides, and ninety six codimension 3 sides.

In our study of the 24-cell it will be very useful for us to know which sides intersect in codimension 2 faces and which vertices lie on a particular side. Two sides of P intersect in $\mathbb{H}^4$ if their identifying spheres have coordinates that have equal nonzero entries in one place and the remaining nonzero entries lie in different positions. For example the sides $S_{(+1,0,-1,0)}$ and $S_{(+1,+1,0,0)}$ intersect, however the sides $S_{(+1,+1,0,0)}$ and $S_{(0,0,-1,-1)}$ do not. In the case of vertices with one nonzero ±1 (those from the first 8 described above) we find that such a vertex lies on a side if the side has an equal nonzero entry in the same position as the vertex. For example the vertex $v_{(-1,0,0,0)}$ lies on the side $S_{(-1,0,0,+1)}$ but not on the side $S_{(0,+1,+1,0)}$. In the case of a vertex in the group $v_{(\pm1/2,\pm1/2,\pm1/2,\pm1/2)}$ we find that such a vertex lies on a side provided the sign of the nonzero entries of the side coincides with the sign of the entries of the vertex in the same position. For example the vertex $v_{(+1/2,+1/2,-1/2,+1/2)}$ lies on the side $S_{(+1,0,-1,0)}$ but does not lie on the side $S_{(-1,+1,0,0)}$. We also mention that when two sides of P intersect they do so at right angles.

The hyperbolic manifolds that we will be considering will be obtained by a side pairing identification of the 24-cell. In this regard it will be very helpful if we had some way to visualise the 24-cell. The 24-cell is a 4-dimensional polyhedron, hence its boundary is 3-dimensional. We will now outline a procedure that will allow us to visualise this boundary. This will prove useful when we start looking at a Kirby diagram of a particular manifold obtained from a side pairing transformation of the 24-cell.

Each side of the polyhedron P corresponds to a sphere of the form $S_{(*,*,*,*)}$, which itself is identified by the co-ordinate $(*, *, *, *)$. We can then radially project this point to the boundary $\partial B^4 = S^3$. For example, if we are focusing on the side corresponding to the sphere $S_{(+1,0,+1,0)}$, then the radial projection of the point $(1, 0, 1, 0)$ is $(1/\sqrt{2}, 0, 1/\sqrt{2}, 0)$. Thus each side in P uniquely corresponds to a point in S^3.

Using the Mobius transformation that transforms the ball B^4 onto the upper half-plane $\mathbb{R}^4_{x_4>0}$ we obtain a map from S^3 onto $\mathbb{R}^3 \cup \{\infty\}$. We will use this map to transfer information about the boundary of P into $\mathbb{R}^3 \cup \{\infty\}$.

We define the map:

$$\phi : S^3 \to \mathbb{R}^4 \cup \{\infty\}$$

by

$$\phi(x_1, x_2, x_3, x_4) = (0, 0, 0, 1) + \frac{2}{x_1^2 + x_2^2 + x_3^2 + (x_4 - 1)^2}(x_1, x_2, x_3, x_4 - 1).$$

This is just the usual Mobius transformation from $\overline{B^4}$ to $\mathbb{R}^4_{x_4 \geq 0} \cup \infty$ restricted to the boundary sphere S^3. Using the above map we can map each point in S^3 that corresponds to a sphere onto a point in $\mathbb{R}^3$. For example if we take the sphere $S_{(+1,0,+1,0)}$, then we know that the associated point on S^3 has coordinates $(1/\sqrt{2}, 0, 1/\sqrt{2}, 0)$. Applying ϕ to this point we get the point $(1/\sqrt{2}, 0, 1/\sqrt{2})$. Doing this for all the points corresponding to the sides of P we get a collection of points in $\mathbb{R}^3$.

Suppose we have two sides of the polyhedron P call them S_1 and S_2 that intersect along a codimension two face (a codimension two face is sometimes called a ridge). Associated to these sides we have points x_1 and x_2 respectively that reside on S^3. We can then choose a path in S^3 from x_1 to x_2 that when projected to P will intersect the codimension 2 side $S_1 \cap S_2$ transversely in one point. Let us note that there will be many paths we can choose between x_1 to x_2, but if we give S^3 the round metric induced from the standard Euclidean inner product on $\mathbb{R}^4$, then there will be a unique length minimising geodesic segment joining x_1 to x_2. It is this segment that we choose as our path, and from here on in when we spoke of such a path between two such points we keep it fixed that it is the geodesic segment we are taking as the path. We can think of this path in S^3 as representing the intersecting face $S_1 \cap S_2$. For example if we took the sides $S_{(+1,+1,0,0)}$ and $S_{(+1,0,+1,0)}$ then we know that the corresponding points in S^3 are given by the points $(1/\sqrt{2}, 1/\sqrt{2}, 0, 0)$ and $(1/\sqrt{2}, 0, 1/\sqrt{2}, 0)$. The corresponding path is taken to be the geodesic segment between these two points. If we then use our map ϕ these paths between such points will give us a path in $\mathbb{R}^3$ between the images of these points. In this way we view the image path in $\mathbb{R}^3$ as representing a codimension 2 face in the polyhedron P, its endpoints correspond to the sides in P that intersect to give this codimension 2 face. We mention that since the path we are taking in S^3 that corresponds to the intersection $S_1 \cap S_2$ is a geodesic segment (with respect to the round metric on S^3) the image will in general not be a straight line. However, the image path will be homotopic (fixing endpoints) to a straight line and when drawing pictures we will always take the image paths to be straight line segments.

Thus far we have explained how to visualise the faces and edges (codimension 2 faces) of the polyhedron P, before we draw these edges let us explain how we can also visualise the codimension 3 faces. Fix three sides S_1, S_2 and S_3, and suppose they all triply intersect in a codimension 3 face. Let x_1, x_2, x_3 denote the respective points in S^3. As we explained above each pair of intersections defines a geodesic segment in S^3 whose endpoints are precisely the points corresponding to the intersecting side. Thus associated to the triply intersecting sides S_1, S_2 and S_3 we have a geodesic triangle in S^3 whose vertices are x_1, x_2 and x_3, and whose sides correspond to the pair of intersections of S_1, S_2 and S_3. This geodesic triangle in S^3 will

get mapped to a triangle in $\mathbb{R}^3$ via ϕ. In general this triangle will not be made up of straight line segments, however when we draw such triangles we will always take straight line segments. This tells us that codimension 3 faces correspond to triangles made up of paths that correspond to codimension 2 faces.

Putting together the above information gives us a way to picture the boundary of P in $\mathbb{R}^3$. What we are really visualising is the dual polyhedron of ∂P, but since we will be interested in a handle decomposition this is very useful for our purposes.

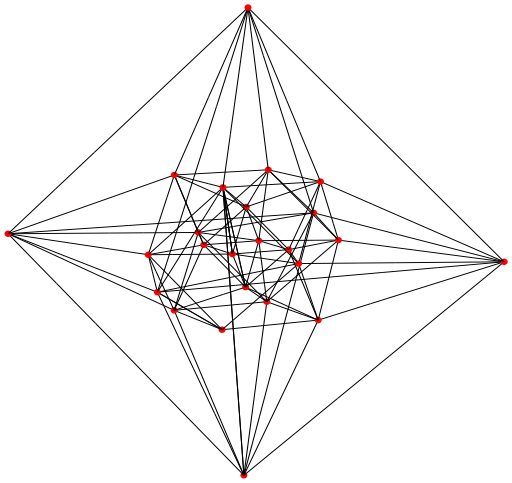

The red vertices in the above diagram correspond to the codimension 1 sides of P and recall that we obtained these by picking the centre point of each sphere, radially projecting it to S^3, then mapping it to $\mathbb{R}^3$ using the Mobius transformation ϕ. The following table shows the co-ordinates of each of the red vertices and their corresponding sphere.

$S_{(+1,+1,0,0)}$	$(\frac{1}{\sqrt{2}}, \frac{1}{\sqrt{2}}, 0)$	$S_{(-1,+1,0,0)}$	$(\frac{-1}{\sqrt{2}}, \frac{1}{\sqrt{2}}, 0)$
$S_{(+1,-1,0,0)}$	$(\frac{1}{\sqrt{2}}, \frac{-1}{\sqrt{2}}, 0)$	$S_{(-1,-1,0,0)}$	$(\frac{-1}{\sqrt{2}}, \frac{-1}{\sqrt{2}}, 0)$
$S_{(+1,0,+1,0)}$	$(\frac{1}{\sqrt{2}}, 0, \frac{1}{\sqrt{2}})$	$S_{(+1,0,-1,0)}$	$(\frac{1}{\sqrt{2}}, 0, \frac{-1}{\sqrt{2}})$
$S_{(-1,0,+1,0)}$	$(\frac{-1}{\sqrt{2}}, 0, \frac{1}{\sqrt{2}})$	$S_{(-1,0,-1,0)}$	$(\frac{-1}{\sqrt{2}}, 0, \frac{-1}{\sqrt{2}})$
$S_{(0,+1,+1,0)}$	$(0, \frac{1}{\sqrt{2}}, \frac{1}{\sqrt{2}})$	$S_{(0,-1,-1,0)}$	$(0, \frac{-1}{\sqrt{2}}, \frac{-1}{\sqrt{2}})$
$S_{(0,+1,-1,0)}$	$(0, \frac{1}{\sqrt{2}}, \frac{-1}{\sqrt{2}})$	$S_{(0,-1,+1,0)}$	$(0, \frac{-1}{\sqrt{2}}, \frac{1}{\sqrt{2}})$
$S_{(+1,0,0,+1)}$	$(1+\sqrt{2}, 0, 0)$	$S_{(-1,0,0,-1)}$	$(1-\sqrt{2}, 0, 0)$
$S_{(+1,0,0,-1)}$	$(-1+\sqrt{2}, 0, 0)$	$S_{(-1,0,0,+1)}$	$(-1-\sqrt{2}, 0, 0)$
$S_{(0,+1,0,+1)}$	$(0, 1+\sqrt{2}, 0)$	$S_{(0,-1,0,+1)}$	$(0, -1-\sqrt{2}, 0)$
$S_{(0,+1,0,-1)}$	$(0, -1+\sqrt{2}, 0)$	$S_{(0,-1,0,-1)}$	$(0, 1-\sqrt{2}, 0)$
$S_{(0,0,+1,+1)}$	$(0, 0, 1+\sqrt{2})$	$S_{(0,0,+1,-1)}$	$(0, 0, -1+\sqrt{2})$
$S_{(0,0,-1,+1)}$	$(0, 0, -1-\sqrt{2})$	$S_{(0,0,-1,-1)}$	$(0, 0, 1-\sqrt{2})$

1.2 Preliminaries on the Ratcliffe-Tschantz 4-manifolds

In their paper [17] Ratcliffe and Tschantz construct several examples of non-compact hyperbolic 4-manifolds of finite volume. We briefly describe how this construction process works. The interested reader is referred to page 109 of their paper [17] for more details.

Recall, a real $(n+1)\times(n+1)$ matrix A is said to be *Lorentzian* if A preserves the Lorentzian inner product:

$$x \cdot y := x_1y_1 + \ldots + x_ny_n - x_{n+1}y_{n+1}.$$

The hyperboloid model of hyperbolic n-space is the metric space

$$\mathbb{H}^n := \{x \in \mathbb{R}^{n+1} : x \cdot x = -1 \text{ and } x_{n+1} > 0\}$$

with the metric d defined by the equation:

$$cosh(d(x,y)) := -x \cdot y.$$

A Lorentzian $(n+1)\times(n+1)$ matrix A is said to be positive if A maps $\mathbb{H}^n$ to $\mathbb{H}^n$. The isometries of $\mathbb{H}^n$ are the positive Lorentzian matrices.
Let Γ^n be the group of $(n+1)\times(n+1)$ positive Lorentzian matrices with integer entries. The group Γ^n is an infinite discrete subgroup of the group $O(n,1)$ of Lorentzian $(n+1)\times(n+1)$ matrices. The principal congruence two subgroup of Γ^n is the group Γ^n_2 of all matrices in Γ^n that are congruent to the identity matrix modulo two.

In their paper [17] Ratcliffe and Tschantz classify all the hyperbolic space forms $\mathbb{H}^4/\Gamma$ where Γ is a torsion free subgroup of minimal index in the group Γ^4_2 (they actually do the case $n = 2, 3$ as well but as we are only interested in the $n = 4$ case we will not worry about these other two). The main theorem takes the form:

Theorem 1.2.1. *There are, up to isometry, exactly 1171 hyperbolic space-forms $\mathbb{H}^4/\Gamma$ where Γ is a torsion free subgroup of minimal index in the group Γ^4_2. Only 22 of these manifolds are orientable.*

The proof of this theorem which leads to the construction of the 1171 hyperbolic space-forms $\mathbb{H}^4/\Gamma$ involves finding suitable side pairings of the 24-cell that will give rise to hyperbolic 4-manifolds. The interested reader can consult p.111 of [17] for the details of the proof. The actual side-pairings they use will be important for our understanding of a Kirby diagram, so we go through in some detail exactly how they code their side pairings.

All their side pairings are of the form rk, where k is a diagonal matrix with diagonal entry taking the form $(\pm1, \pm1, \pm1, \pm1)$, which is to be interpreted as a composition of reflections in the coordinate planes $x_i = 0$ for $1 \leq i \leq 4$. In order to identify a particular element k it

suffices to simply give the diagonal $(\pm 1, \pm 1, \pm 1, \pm 1)$, where a -1 in some position tells us that we reflect in the coordinate corresponding to that position, and $+1$ tell us that we do nothing. For example $(-1, +1, -1, +1)$ is the composition of the reflection in the hyper-planes $x_1 = 0$ followed by reflection in $x_3 = 0$. When we want to speak of a particular side pairing rk and make reference to its k-part we will always write the k-part in the form $k_{(\pm 1, \pm 1, \pm 1, \pm 1)}$, the k is to remind us that we are only dealing with the k part of rk and the subscript $(\pm 1, \pm 1, \pm 1, \pm 1)$ tells us what the diagonal is. Ratcliffe and Tschantz develop a coding system for the k-part of each side pairing which we now describe.

The polyhedron P has 24 three dimensional sides, since a side pairing transformation must identify pairs of sides we need to give twelve transformations. We will denote these transformations by the letters $a, b, \ldots, k, l$. We then group the letters $a, b, \ldots, l$ and the sides of P into the following groups:

$$\{a, b, S_{(\pm 1, \pm 1, 0, 0)}\}, \{c, d, S_{(\pm 1, 0, \pm 1, 0)}\}, \{e, f, S_{(0, \pm 1, \pm 1, 0)}\},$$

$$\{g, h, S_{(\pm 1, 0, 0, \pm 1)}\}, \{i, j, S_{(0, \pm 1, 0, \pm 1)}\}, \{k, l, S_{(0, 0, \pm 1, \pm 1)}\}.$$

In each of the above sets the letters are pairings between the spheres in that set (remember the spheres represent the sides of the 24-cell P by the way we constructed it). We give the sides the ordering $(+1, +1) < (+1, -1) < (-1, +1) < (-1, -1)$. So for example taking the first group above our order tells us that

$$S_{(+1, +1, 0, 0)} < S_{(+1, -1, 0, 0)} < S_{(-1, +1, 0, 0)} < S_{(-1, -1, 0, 0)}$$

The first letter always pairs the side with $+1, +1$ to one of the other sides (we will show how to determine this side), and the second letter pairs the next unused side (with respect to the above ordering) with the last side. The actual side pairing transformations are encoded by a string of six characters from the set

$$\{1, 2, 3, 4, 5, 6, 7, 8, 9, A, B, C, D, E, F\}$$

one character for each of the above sets. Each character represents a particular k-part, and the following table shows the correspondence:

Character	**k-part**
1	$k_{(-1,+1,+1,+1)}$
2	$k_{(+1,-1,+1,+1)}$
3	$k_{(-1,-1,+1,+1)}$
4	$k_{(+1,+1,-1,+1)}$
5	$k_{(-1,+1,-1,+1)}$
6	$k_{(+1,-1,-1,+1)}$
7	$k_{(-1,-1,-1,+1)}$
8	$k_{(+1,+1,+1,-1)}$
9	$k_{(-1,+1,+1,-1)}$
A	$k_{(+1,-1,+1,-1)}$
B	$k_{(-1,-1,+1,-1)}$
C	$k_{(+1,+1,-1,-1)}$
D	$k_{(-1,+1,-1,-1)}$
E	$k_{(+1,-1,-1,-1)}$
F	$k_{(-1,-1,-1,-1)}$

The coding of a particular manifold will take the form of six characters from the above set of characters. For example, a code can look like

1428BD.

Each character in the above code tells us what the k-part of each pair of transformations in the group

$$\{(a,b),(c,d),(e,f),(g,h),(i,j),(k,l)\}$$

is. For example for the code **1428BD** the first character is **1**, this tells us that for the particular manifold corresponding to this code the side pairings a and b have k-parts given by $k_{(-1,+1,+1,+1)}$. The next character in the code is **4**, this tells us that the side pairings c and d have k-part $k_{(+1,+1,-1,+1)}$. Continuing in this way we can determine all the k-parts of each of the side pairings $a, b, c, d, \ldots, k, l$.

$$S_{(+1,+1,0,0)} \xrightarrow[k_{(-1,+1,+1,+1)}]{a} S_{(-1,+1,0,0)} \qquad S_{(+1,-1,0,0)} \xrightarrow[k_{(-1,+1,+1,+1)}]{b} S_{(-1,-1,0,0)}$$

$$S_{(+1,0,+1,0)} \xrightarrow[k_{(+1,+1,-1,+1)}]{c} S_{(+1,0,-1,0)} \qquad S_{(-1,0,+1,0)} \xrightarrow[k_{(+1,+1,-1,+1)}]{d} S_{(-1,0,-1,0)}$$

$$S_{(0,+1,+1,0)} \xrightarrow[k_{(+1,-1,+1,+1)}]{e} S_{(0,-1,+1,0)} \qquad S_{(0,+1,-1,0)} \xrightarrow[k_{(+1,-1,+1,+1)}]{f} S_{(0,-1,-1,0)}$$

$$S_{(+1,0,0,+1)} \xrightarrow[k_{(+1,+1,+1,-1)}]{g} S_{(+1,0,0,-1)} \qquad S_{(-1,0,0,+1)} \xrightarrow[k_{(+1,+1,+1,-1)}]{h} S_{(-1,0,0,-1)}$$

$$S_{(0,+1,0,+1)} \xrightarrow[k_{(-1,-1,+1,-1)}]{i} S_{(0,-1,0,-1)} \qquad S_{(0,+1,0,-1)} \xrightarrow[k_{(-1,-1,+1,-1)}]{j} S_{(0,-1,0,+1)}$$

$$S_{(0,0,+1,+1)} \xrightarrow[k_{(-1,+1,-1,-1)}]{k} S_{(0,0,-1,-1)} \qquad S_{(0,0,+1,-1)} \xrightarrow[k_{(-1,+1,-1,-1)}]{l} S_{(0,0,-1,+1)} \ .$$

The above is to be understood as the letter above the arrow tells you which side of the polyhedron P is being paired to another side, and the k-part of that transformation is on the bottom of the arrow.

We have still not explained what the r-part of the side pairing transformations are, they are just reflections in the image side, viewed as a hyperplane in $\mathbb{H}^4$. For example for the code **1428BD**, described above, we know that the side pairing transformation a pairs side $S_{(+1,+1,0,0)}$ to side $S_{(-1,+1,0,0)}$, and has k-part given by $k_{(-1,+1,+1,+1)}$. Using the fact that the r-part is just reflection in the image side we have that

$$a := rk_{(-1,+1,+1,+1)}$$

where r is reflection in the side $S_{(-1,+1,0,0)}$.

To summarise, Ratcliffe and Tschantz construct 1171 distinct non-compact finite volume hyperbolic 4-manifolds, 22 of which are orientable and all others non-orientable. Each such 4-manifold is obtained by giving side pairing transformations for the sides of the 24-cell P (described in the previous section). The side pairing transformations for any fixed such manifold are labelled by the letters $a, b, \ldots, k, l$, and each such transformation is given in the form rk, where r is always reflection in the image side. The k-part of each transformation is understood through a six character code, which can be decoded using the above table, showing what each characters k-part is.

We would like to point out that we have not said anything about the proof of why these side pairing transformations on the polyhedron P actually lead to hyperbolic 4-manifolds. This is all explained in their paper [17] from p.109-117, with details on the side-pairing coding from p.112-117. We are taking it for granted that such manifolds exist and are well defined via side pairing transformations as described above.

Towards the end of their paper (see p. 117-124 [17]) Ratcliffe and Tschantz have tables of the 1171 manifolds giving various information about these manifolds, in particular the tables tell what the side pairing code for each manifold is. As we will be interested in the side pairing codes of certain particular manifolds and some other information coming from these tables we reproduce these tables here for convenience of the reader.

N	SP	S	H_1	H_2	H_3	LT
1	1428BD	16	330	700	4	AAABF
2	14278D	16	240	600	4	AABBF
3	1477B8	16	240	600	4	AABBF
4	1477BE	16	240	600	4	AABBF
5	1478ED	16	240	600	4	AABBF
6	14278E	16	240	600	4	ABBBF
7	142DBE	48	150	500	4	ABBBF
8	1427BD	16	150	500	4	ABBBF
9	1477EB	16	150	500	4	ABBBF
10	1477ED	16	150	500	4	ABBBF
11	1478EB	16	150	500	4	ABBBF
12	147BDE	16	150	500	4	ABBBF
13	14B8ED	16	150	500	4	ABBBF
14	1427BE	16	150	500	4	BBBBF
15	1477DE	16	150	500	4	BBBBF
16	14B7E8	16	060	400	4	BBBBF
17	14B7ED	16	060	400	4	BBBBF
18	14BDE7	16	060	400	4	BBBBF
19	14B7DE	16	060	400	4	BBFFF
20	14B8E7	16	051	400	4	ABFFF
21	14BD7E	16	051	400	4	ABFFF
22	17BE8D	16	051	400	4	ABFFF

Table 1.1: Orientable Ratcliffe-Tschantz hyperbolic 4-manifolds

The above table gives the information corresponding to the 22 orientable hyperbolic 4-manifolds. Before we show tables of the non-orientable ones let us explain what some of the headers in the table mean. To start with the the header **N** is simply referring to the number of the manifold. As their are 1171 manifolds in total, each one is assigned a number, giving a convenient way to refer to it (one can just think of it as the row number of the table). The column headed by **SP** lists the side-pairing for the manifold in the coded form we explained previously. The column headed by **S** lists the number of symmetries of the manifolds, for our work we will not need to worry about this column. The columns headed by H_1, H_2, H_3, lists the first, second and third homology groups respectively. The three digit number abc represents $\mathbb{Z}^a \oplus \mathbb{Z}_2^b \oplus \mathbb{Z}_4^c$, and the single digit entry a in the column H_3 represents $\mathbb{Z}^a$.

The column headed by **LT** lists the link types of the cusps corresponding to the ends of the manifolds. The orientable manifolds are all five cusped manifolds, hence have five non-compact ends each diffeomorphic to $E \times \mathbb{R}$, where E is a closed Euclidean manifold. The link type tells us which Euclidean manifold E is, here $A, B, \ldots, J$ represent the ten closed Euclidean 3-manifolds in the order given by *Hantzsche* and *Wendt* in [9], these are also given in *Wolf's* text [22] p.122, where in his notation $\mathcal{G}_1$, $\ldots$, $\mathcal{G}_6$ correspond to $A, \ldots, F$ respectively, and $\mathcal{B}_1$, $\ldots$, $\mathcal{B}_4$ correspond to $G, \ldots, J$. The orientable ones are given by $A, \ldots, F$ and the non-orientable ones are $G, \ldots, J$. Only C, D, E do not occur as links of cusps of any of their manifolds.

We will end this section by giving tables of the non-orientable Ratcliffe-Tschantz manifolds. These manifolds are either five cusped or six cusped, the ones numbered 23-1090 are all five cusped, and the remaining ones are all six cusped.

N	SP	S	H_1	H_2	H_3	LT	N	SP	S	H_1	H_2	H_3	LT	N	SP	S	H_1	H_2	H_3	LT
23	1569A4	32	420	620	2	AAGGH	49	134A3F	16	330	520	2	AAHIJ	75	1358BD	16	330	430	1	AGGHI
24	134B2E	16	420	620	2	AAGHH	50	1369A4	16	330	520	2	AAIIJ	76	13C8B4	16	330	430	1	AGGHI
25	134B3E	16	420	620	2	AAGHH	51	156A9C	16	330	520	2	ABGGH	77	13CB36	16	330	430	1	AGGHI
26	13483D	16	420	620	2	AAGHJ	52	13D834	16	330	520	2	ABGGJ	78	13EFCA	16	330	430	1	AGGHI
27	1348BD	16	420	620	2	AAGHJ	53	136F8A	32	330	520	2	ABGHH	79	157B9D	16	330	430	1	AGGHI
28	13492C	16	420	620	2	AAHHI	54	134B6E	16	330	520	2	ABGHH	80	13483E	16	330	430	1	AGGHJ
29	1349AC	16	420	620	2	AAHHI	55	134B7E	16	330	520	2	ABGHH	81	1348FC	16	330	430	1	AGGHJ
30	1429AC	48	420	620	2	AFGGG	56	13D935	16	330	520	2	ABGHI	82	134B2C	16	330	430	1	AGGHJ
31	13C835	16	420	530	1	AGGGJ	57	13482E	16	330	520	2	ABGHJ	83	13583C	16	330	430	1	AGGHJ
32	13482C	16	420	530	1	AGGHH	58	13487D	16	330	520	2	ABGHJ	84	135B2E	16	330	430	1	AGGHJ
33	1348AC	16	420	530	1	AGGHJ	59	1348AD	16	330	520	2	ABGHJ	85	136B2E	16	330	430	1	AGGHJ
34	1348BC	16	420	530	1	AGHHI	60	134B3C	16	330	520	2	ABGHJ	86	136F2A	16	330	430	1	AGGHJ
35	146928	64	420	440	0	GGGGH	61	136DA8	16	330	520	2	ABGHJ	87	13EE64	16	330	430	1	AGGHJ
36	1468AF	32	330	610	3	AAAJJ	62	1439AC	16	330	520	2	ABGHJ	88	13C875	16	330	430	1	AGGIJ
37	156F8C	32	330	610	3	AABJJ	63	143B9C	16	330	520	2	ABGHJ	89	13EA35	16	330	430	1	AGGIJ
38	143BD8	16	330	610	3	ABFGH	64	13483F	16	330	520	2	ABGJJ	90	134B3D	16	330	430	1	AGGJJ
39	14378D	16	330	610	3	ABFHH	65	13496C	16	330	520	2	ABHHI	91	136D28	16	330	430	1	AGGJJ
40	143CF9	16	330	520	2	AAGGJ	66	1349BC	16	330	520	2	ABHHI	92	1348EC	16	330	430	1	AGHHI
41	13FF8A	32	330	520	2	AAGHH	67	134A2C	16	330	520	2	ABHIJ	93	13593D	16	330	430	1	AGHHI
42	13482D	16	330	520	2	AAGHJ	68	1368A4	16	330	520	2	AFGGI	94	135A2F	16	330	430	1	AGHHI
43	1348FD	16	330	520	2	AAGHJ	69	1347B8	16	330	520	2	AFGII	95	136CA8	16	330	430	1	AGHHI
44	136B84	16	330	520	2	AAGIJ	70	1437C9	16	330	520	2	BFGGH	96	13EFC4	16	330	430	1	AGHHI
45	13ED28	16	330	520	2	AAGIJ	71	13EB34	16	330	430	1	AGGGH	97	147B9C	16	330	430	1	AGHHJ
46	13493C	16	330	520	2	AAHHI	72	13EB64	16	330	430	1	AGGGH	98	1347A8	16	330	430	1	AGHIJ
47	1349EC	16	330	520	2	AAHHI	73	13582D	16	330	430	1	AGGHH	99	13486C	16	330	430	1	AGHIJ
48	134A2F	16	330	520	2	AAHIJ	74	135B3F	16	330	430	1	AGGHH	100	13487C	16	330	430	1	AGHIJ

Table 1.2: non-orientable, five cusped, Ratcliffe-Tschantz hyperbolic 4-manifolds

101	13492E	16	330	430	1	AGHIJ	156	1359AD	16	330	331	0	GHHHI	211	134A3D	16	240	420	2	ABIJJ
102	13592C	16	330	430	1	AGHIJ	157	3579BF	32	250	430	2	ABGII	212	136A3D	16	240	420	2	ABIJJ
103	135A3E	16	330	430	1	AGHIJ	158	1437F9	16	240	510	3	ABBGJ	213	136E39	16	240	420	2	ABIJJ
104	1367A8	16	330	430	1	AGHIJ	159	14378E	16	240	510	3	ABBJJ	214	136E84	16	240	420	2	ABIJJ
105	1368AE	16	330	430	1	AGHIJ	160	143DF8	16	240	510	3	ABFGH	215	13EE75	16	240	420	2	ABIJJ
106	13692C	16	330	430	1	AGHIJ	161	14779C	16	240	510	3	ABFGH	216	1429FA	16	240	420	2	AFGGG
107	1359AC	16	330	430	1	AGIIJ	162	14F7C9	16	240	510	3	ABFGJ	217	136F84	16	240	420	2	AFGHI
108	1349BD	16	330	430	1	AGIJJ	163	14386D	16	240	510	3	ABFHH	218	1439FA	16	240	420	2	AFGHI
109	1369AE	16	330	430	1	AHHHI	164	143E8D	16	240	510	3	ABFHH	219	13487E	16	240	420	2	AFGHJ
110	1347B9	16	330	430	1	AHIIJ	165	1437FA	16	240	510	3	ABFHI	220	134B6C	16	240	420	2	AFGHJ
111	1349AD	16	330	430	1	AHIIJ	166	14279C	16	240	510	3	BBFGG	221	143B9E	16	240	420	2	AFGHJ
112	13C874	16	330	430	1	BGGGH	167	1427AC	16	240	510	3	BBFGG	222	136DA4	16	240	420	2	AFGIJ
113	1358AC	16	330	430	1	BGGGJ	168	1437D8	16	240	510	3	BBFGH	223	156F9C	16	240	420	2	AFGIJ
114	13EECA	16	330	430	1	BGGGJ	169	143D68	16	240	510	3	BBFGH	224	134B7D	16	240	420	2	AFGJJ
115	13682E	16	330	430	1	BGGHH	170	1CFF38	32	240	420	2	AAGJJ	225	1347FC	16	240	420	2	AFHII
116	136C2A	16	330	430	1	BGGHH	171	153CF4	32	240	420	2	AAHII	226	1367A9	16	240	420	2	AFHII
117	1359BD	16	330	430	1	BGGHI	172	13D864	16	240	420	2	ABGGJ	227	157DB9	16	240	420	2	AFHII
118	136E28	16	330	430	1	BGGHJ	173	143DE8	16	240	420	2	ABGGJ	228	13496E	16	240	420	2	AFHIJ
119	13EEC4	16	330	430	1	BGGHJ	174	13DB37	16	240	420	2	ABGHI	229	156DA9	16	240	420	2	AFHIJ
120	13C837	16	330	430	1	BGGIJ	175	13486D	16	240	420	2	ABGHJ	230	1347A9	16	240	420	2	AFIII
121	157A9C	16	330	430	1	BGHHH	176	1348ED	16	240	420	2	ABGHJ	231	1569F4	32	240	420	2	BBGGH
122	136A2C	16	330	430	1	BGHHI	177	136B3C	16	240	420	2	ABGHJ	232	13D8A4	16	240	420	2	BBGGJ
123	153A9C	16	330	430	1	BGHHI	178	136F38	16	240	420	2	ABGHJ	233	143EC9	16	240	420	2	BBGGJ
124	1539AD	16	330	430	1	BGHHJ	179	13D8B4	16	240	420	2	ABGHJ	234	143FD8	16	240	420	2	BBGGJ
125	143AC9	16	330	430	1	FGGGH	180	13EE84	16	240	420	2	ABGHJ	235	5EFF7A	32	240	420	2	BBGHH
126	1539BD	16	330	430	1	FGGGH	181	13EED4	16	240	420	2	ABGHJ	236	136B3E	16	240	420	2	BBGHH
127	1439BC	16	330	430	1	FGGHH	182	1477B9	16	240	420	2	ABGHJ	237	136F3A	16	240	420	2	BBGHH
128	136B8C	16	330	421	1	AGHHH	183	1479BE	16	240	420	2	ABGHJ	238	13EB74	16	240	420	2	BBGHH
129	13678A	16	330	421	1	AGHIJ	184	1347E8	16	240	420	2	ABGIJ	239	13EA74	16	240	420	2	BBGHI
130	13CB35	16	330	340	0	GGGGJ	185	136B8D	16	240	420	2	ABGIJ	240	15FA9C	16	240	420	2	BBGHI
131	13583D	16	330	340	0	GGGHH	186	13EEDB	16	240	420	2	ABGIJ	241	13683D	16	240	420	2	BBGHJ
132	136F28	16	330	340	0	GGGHH	187	14BC79	16	240	420	2	ABGIJ	242	136D38	16	240	420	2	BBGHJ
133	13C836	16	330	340	0	GGGHI	188	134B2D	16	240	420	2	ABGJJ	243	13D874	16	240	420	2	BBGHJ
134	135B3E	16	330	340	0	GGGHJ	189	13683F	16	240	420	2	ABGJJ	244	13EE74	16	240	420	2	BBGHJ
135	136C28	16	330	340	0	GGGHJ	190	1368AF	16	240	420	2	ABGJJ	245	1437BD	16	240	420	2	BBGHJ
136	136D2A	16	330	340	0	GGGHJ	191	136D3A	16	240	420	2	ABGJJ	246	13D836	16	240	420	2	BBGIJ
137	13C935	16	330	340	0	GGGIJ	192	13DD64	16	240	420	2	ABGJJ	247	13D974	16	240	420	2	BBGIJ
138	136E2A	16	330	340	0	GGGJJ	193	143B68	16	240	420	2	ABGJJ	248	1437CA	16	240	420	2	BBGIJ
139	13EF64	16	330	340	0	GGHHH	194	13497C	16	240	420	2	ABHHI	249	1539AF	16	240	420	2	BBGIJ
140	135A3F	16	330	340	0	GGHHI	195	1349FC	16	240	420	2	ABHHI	250	13DD74	16	240	420	2	BBGJJ
141	13EA64	16	330	340	0	GGHHI	196	136CA9	16	240	420	2	ABHII	251	13EF74	16	240	420	2	BBHHH
142	1358AD	16	330	340	0	GGHHJ	197	13D975	16	240	420	2	ABHII	252	13693C	16	240	420	2	BBHHI
143	13593C	16	330	340	0	GGHIJ	198	13493E	16	240	420	2	ABHIJ	253	136C39	16	240	420	2	BBHHI
144	156B9D	16	330	340	0	GHHHI	199	134A7F	16	240	420	2	ABHIJ	254	13D9B5	16	240	420	2	BBHHI
145	1359BC	16	330	340	0	GHIJJ	200	13693E	16	240	420	2	ABHIJ	255	13DC74	16	240	420	2	BBHHJ
146	135B2F	16	330	331	0	GGGHH	201	136C3B	16	240	420	2	ABHIJ	256	156AD9	16	240	420	2	BBHHJ
147	136B2C	16	330	331	0	GGGHH	202	136CA4	16	240	420	2	ABHIJ	257	153CA4	32	240	420	2	BBHII
148	13582C	16	330	331	0	GGGHJ	203	13DCF4	16	240	420	2	ABHIJ	258	136A3F	16	240	420	2	BBHIJ
149	13682C	16	330	331	0	GGGHJ	204	156A3C	16	240	420	2	ABHIJ	259	136E3B	16	240	420	2	BBHIJ
150	13592D	16	330	331	0	GGHHI	205	156DAE	16	240	420	2	ABHIJ	260	143C69	16	240	420	2	BFGGH
151	13692E	16	330	331	0	GGHHI	206	1347F9	16	240	420	2	ABIIJ	261	147CA9	16	240	420	2	BFGGH
152	1358BC	16	330	331	0	GGHHJ	207	13D9A4	16	240	420	2	ABIIJ	262	14379C	16	240	420	2	BFGHH
153	13C8B5	16	330	331	0	GGHHJ	208	13DA36	16	240	420	2	ABIIJ	263	14396C	16	240	420	2	BFGHH
154	135A2E	16	330	331	0	GGHIJ	209	13EA75	16	240	420	2	ABIIJ	264	14B7C9	16	240	420	2	BFGHI
155	136A2E	16	330	331	0	GGHIJ	210	13492F	16	240	420	2	ABIJJ	265	1437BE	16	240	420	2	BFGHJ

266	1358EC	16	240	330	1	AGGIJ	321	156FC9	16	240	330	1	BGGHJ	376	13EEC5	16	240	330	1	BGHJJ
267	1368B4	16	240	330	1	AGGIJ	322	1357A8	16	240	330	1	BGGIJ	377	13EED5	16	240	330	1	BGHJJ
268	13E837	16	240	330	1	AGGIJ	323	1359FC	16	240	330	1	BGGIJ	378	156E9D	16	240	330	1	BGHJJ
269	143FCA	16	240	330	1	AGGIJ	324	1368E4	16	240	330	1	BGGIJ	379	1357B9	16	240	330	1	BGIIJ
270	13482F	16	240	330	1	AGGJJ	325	136DB8	16	240	330	1	BGGIJ	380	136AC4	16	240	330	1	BGIIJ
271	143A9F	16	240	330	1	AGGJJ	326	13C7A8	16	240	330	1	BGGIJ	381	13D936	16	240	330	1	BGIIJ
272	13EF84	16	240	330	1	AGHHJ	327	13CA35	16	240	330	1	BGGIJ	382	15396A	16	240	330	1	BGIIJ
273	1359FD	16	240	330	1	AGHII	328	1539BF	16	240	330	1	BGGIJ	383	13597C	16	240	330	1	BGIJJ
274	13E936	16	240	330	1	AGHII	329	13582E	16	240	330	1	BGGJJ	384	135A2C	16	240	330	1	BGIJJ
275	13EA94	16	240	330	1	AGHII	330	13583E	16	240	330	1	BGGJJ	385	135A3C	16	240	330	1	BGIJJ
276	134A3C	16	240	330	1	AGHIJ	331	13587C	16	240	330	1	BGGJJ	386	135A7E	16	240	330	1	BGIJJ
277	136C29	16	240	330	1	AGHIJ	332	135B7E	16	240	330	1	BGGJJ	387	13693F	16	240	330	1	BGIJJ
278	13EE9B	16	240	330	1	AGHIJ	333	136B3D	16	240	330	1	BGGJJ	388	136D3B	16	240	330	1	BGIJJ
279	14AB9C	16	240	330	1	AGHIJ	334	136E38	16	240	330	1	BGGJJ	389	13D9B4	16	240	330	1	BGIJJ
280	14FB9C	16	240	330	1	AGHJJ	335	1439BE	16	240	330	1	BGGJJ	390	14396A	16	240	330	1	BGIJJ
281	136A94	16	240	330	1	AGIIJ	336	143A69	16	240	330	1	BGGJJ	391	13D9A5	16	240	330	1	BHHHI
282	13CA37	16	240	330	1	AGIIJ	337	1579ED	16	240	330	1	BGGJJ	392	13DC65	16	240	330	1	BHHHI
283	13493F	16	240	330	1	AGIJJ	338	1369EC	16	240	330	1	BGHHI	393	13DC75	16	240	330	1	BHHHI
284	134A2D	16	240	330	1	AGIJJ	339	136A3E	16	240	330	1	BGHHI	394	156A3E	16	240	330	1	BHHHJ
285	136E2B	16	240	330	1	AGIJJ	340	136CB9	16	240	330	1	BGHHI	395	13D965	16	240	330	1	BHHII
286	1347EC	16	240	330	1	AHHIJ	341	136F29	16	240	330	1	BGHHI	396	13EF75	16	240	330	1	BHHIJ
287	1349FD	16	240	330	1	AHIIJ	342	136F3B	16	240	330	1	BGHHI	397	13EFD5	16	240	330	1	BHHIJ
288	1347FD	16	240	330	1	AHIJJ	343	13C974	16	240	330	1	BGHHI	398	156B3D	16	240	330	1	BHHIJ
289	13678C	16	240	330	1	AHIJJ	344	13CCE6	16	240	330	1	BGHHI	399	156D39	16	240	330	1	BHHIJ
290	13496D	16	240	330	1	AIIJJ	345	13EFD4	16	240	330	1	BGHHI	400	143CE9	16	240	330	1	FGGGH
291	136DA9	16	240	330	1	AIJJJ	346	357B9D	16	240	330	1	BGHHI	401	136B94	16	240	330	1	FGGGI
292	1358ED	16	240	330	1	BGGGH	347	13CCE5	16	240	330	1	BGHHJ	402	136BC4	16	240	330	1	FGGGI
293	13EB94	16	240	330	1	BGGGH	348	13DC64	16	240	330	1	BGHHJ	403	143F9C	16	240	330	1	FGGHH
294	13EBC4	16	240	330	1	BGGGH	349	1479EC	16	240	330	1	BGHHJ	404	13679A	16	240	330	1	FGGHI
295	13DB34	16	240	330	1	BGGGJ	350	157A3C	16	240	330	1	BGHHJ	405	1367B8	16	240	330	1	FGGHI
296	13683C	16	240	330	1	BGGHH	351	15EA9C	16	240	330	1	BGHHJ	406	14BAC9	16	240	330	1	FGGHI
297	136BCE	16	240	330	1	BGGHH	352	136A9C	16	240	330	1	BGHII	407	14B93C	16	240	330	1	FGGHJ
298	136C38	16	240	330	1	BGGHH	353	13C936	16	240	330	1	BGHII	408	15397D	16	240	330	1	FGGHJ
299	13EC64	16	240	330	1	BGGHH	354	15FB9D	16	240	330	1	BGHII	409	153B9F	16	240	330	1	FGGHJ
300	13EF9A	16	240	330	1	BGGHH	355	13592F	16	240	330	1	BGHIJ	410	1569ED	16	240	330	1	FGGHJ
301	1368BE	16	240	330	1	BGGHI	356	13593F	16	240	330	1	BGHIJ	411	1369B4	16	240	330	1	FGGII
302	136F9A	16	240	330	1	BGGHI	357	13597D	16	240	330	1	BGHIJ	412	1369E4	16	240	330	1	FGGII
303	13C9B4	16	240	330	1	BGGHI	358	135A7F	16	240	330	1	BGHIJ	413	13C7B8	16	240	330	1	FGGII
304	13CB74	16	240	330	1	BGGHI	359	13692F	16	240	330	1	BGHIJ	414	1357B8	16	240	330	1	FGGIJ
305	13D837	16	240	330	1	BGGHI	360	13693D	16	240	330	1	BGHIJ	415	156AC9	16	240	330	1	FGHHI
306	13DA35	16	240	330	1	BGGHI	361	1369BE	16	240	330	1	BGHIJ	416	157D39	16	240	330	1	FGHHI
307	13E964	16	240	330	1	BGGHI	362	136A3C	16	240	330	1	BGHIJ	417	157A3E	16	240	330	1	FGHHJ
308	1569BF	16	240	330	1	BGGHI	363	136D2B	16	240	330	1	BGHIJ	418	157F9C	16	240	330	1	FGHJJ
309	13587D	16	240	330	1	BGGHJ	364	136D39	16	240	330	1	BGHIJ	419	1357A9	16	240	330	1	FGIIJ
310	135B2D	16	240	330	1	BGGHJ	365	136E9B	16	240	330	1	BGHIJ	420	13EB85	16	240	321	1	AGHIJ
311	135B3D	16	240	330	1	BGGHJ	366	136F39	16	240	330	1	BGHIJ	421	153B8F	16	240	321	1	AHHJJ
312	135B7F	16	240	330	1	BGGHJ	367	13D964	16	240	330	1	BGHIJ	422	157F8C	16	240	321	1	AHHJJ
313	13683E	16	240	330	1	BGGHJ	368	13DCE4	16	240	330	1	BGHIJ	423	1367AE	16	240	321	1	AHIJJ
314	136B2D	16	240	330	1	BGGHJ	369	13EAC4	16	240	330	1	BGHIJ	424	13EFDA	16	240	321	1	BGHHI
315	136B3F	16	240	330	1	BGGHJ	370	13EB75	16	240	330	1	BGHIJ	425	13EFDB	16	240	321	1	BGHII
316	136B9C	16	240	330	1	BGGHJ	371	13EEC6	16	240	330	1	BGHIJ	426	146F28	32	240	240	0	GGGGH
317	136C3A	16	240	330	1	BGGHJ	372	13EECB	16	240	330	1	BGHIJ	427	13FFC8	32	240	240	0	GGGHH
318	136E3A	16	240	330	1	BGGHJ	373	14A93C	16	240	330	1	BGHIJ	428	13C8F4	16	240	240	0	GGGHI
319	13EEDA	16	240	330	1	BGGHJ	374	15396D	16	240	330	1	BGHIJ	429	13583F	16	240	240	0	GGGHJ
320	1569EA	16	240	330	1	BGGHJ	375	1569FD	16	240	330	1	BGHIJ	430	13E935	16	240	240	0	GGGIJ

```
431 13EE6A 16 240 240 0 GGGIJ
432 135B3C 16 240 240 0 GGGJJ
433 13EE9A 16 240 240 0 GGGJJ
434 136FC8 32 240 240 0 GGHHH
435 1358FD 16 240 240 0 GGHHH
436 13586D 16 240 240 0 GGHHI
437 1368EC 16 240 240 0 GGHHI
438 136C2B 16 240 240 0 GGHHI
439 136DEA 16 240 240 0 GGHHJ
440 13ED64 16 240 240 0 GGHHJ
441 157DA4 32 240 240 0 GGHII
442 157DF4 32 240 240 0 GGHII
443 135A3D 16 240 240 0 GGHIJ
444 135B6E 16 240 240 0 GGHIJ
445 136E29 16 240 240 0 GGHIJ
446 136F2B 16 240 240 0 GGHIJ
447 13CB75 16 240 240 0 GGHIJ
448 13CC65 16 240 240 0 GGHIJ
449 1539EA 16 240 240 0 GGHIJ
450 136CB8 16 240 240 0 GGHJJ
451 13EB95 16 240 240 0 GGHJJ
452 157E9D 16 240 240 0 GGHJJ
453 13C937 16 240 240 0 GGIIJ
454 13593E 16 240 240 0 GGIJJ
455 136B9D 16 240 240 0 GGIJJ
456 136D29 16 240 240 0 GGIJJ
457 13EE65 16 240 240 0 GGIJJ
458 136E9A 16 240 240 0 GGJJJ
459 13EFC6 16 240 240 0 GHHHI
460 5BFFDA 32 240 240 0 GHHII
461 135A6F 16 240 240 0 GHHII
462 136ACE 16 240 240 0 GHHII
463 13EFCB 16 240 240 0 GHHII
464 156CEA 16 240 240 0 GHHII
465 1359EC 16 240 240 0 GHHIJ
466 13CDE6 16 240 240 0 GHHIJ
467 13EF65 16 240 240 0 GHHIJ
468 13EFC5 16 240 240 0 GHHIJ
469 156ACE 16 240 240 0 GHHIJ
470 15EB9D 16 240 240 0 GHHIJ
471 357AB9 16 240 240 0 GHHIJ
472 153A9E 16 240 240 0 GHHJJ
473 13596C 16 240 240 0 GHIIJ
474 13C975 16 240 240 0 GHIIJ
475 156DB9 16 240 240 0 GHIIJ
476 13C9B5 16 240 240 0 GHIJJ
477 13CD65 16 240 240 0 GHIJJ
478 13CD75 16 240 240 0 GHIJJ
479 157DA9 16 240 240 0 GHIJJ
480 1369BF 16 240 240 0 GIIJJ
481 367B9C 32 240 240 0 HHHJJ
482 13582F 16 240 231 0 GGGHJ
483 13682F 16 240 231 0 GGGHJ
484 135B2C 16 240 231 0 GGGJJ
485 135B6F 16 240 231 0 GGHHI
486 1368BF 16 240 231 0 GGHHJ
487 13EDA8 16 240 231 0 GGHHJ
488 13EF6A 16 240 231 0 GGHHJ
489 367AB5 16 240 231 0 GGHII
490 13586C 16 240 231 0 GGHIJ
491 135A2D 16 240 231 0 GGHIJ
492 136A2D 16 240 231 0 GGHIJ
493 136CEA 16 240 231 0 GGHIJ
494 13C865 16 240 231 0 GGHIJ
495 1358FC 16 240 231 0 GGHJJ
496 13C8F5 16 240 231 0 GGHJJ
497 13592E 16 240 231 0 GGIJJ
498 1367C8 16 240 231 0 GGIJJ
499 1367EA 16 240 231 0 GGIJJ
500 13E9A6 16 240 231 0 GHHHI
501 13596D 16 240 231 0 GHHII
502 136F9B 16 240 231 0 GHHII
503 13EF9B 16 240 231 0 GHHII
504 1359ED 16 240 231 0 GHHIJ
505 136A9D 16 240 231 0 GHHIJ
506 13EA95 16 240 231 0 GHHIJ
507 135A6E 16 240 231 0 GHIIJ
508 13679B 16 240 231 0 GHIIJ
509 1367B9 16 240 231 0 GHIIJ
510 136DB9 16 240 231 0 GHIIJ
511 13C7B9 16 240 231 0 GHIIJ
512 13C9A5 16 240 231 0 GHIIJ
513 13EA65 16 240 231 0 GHIIJ
514 357BAF 32 240 231 0 HHHII
515 357B9A 16 240 231 0 HHHII
516 367B95 16 240 231 0 HHHIJ
517 1569AF 32 231 510 3 ABBGG
518 1579BF 32 231 420 2 AAGII
519 1347AC 16 231 420 2 ABHIJ
520 134A6F 16 231 420 2 ABHIJ
521 1369AF 16 231 420 2 ABIIJ
522 1347BD 16 231 420 2 ABIJJ
523 1539FA 16 231 420 2 AFGGI
524 1479FC 16 231 420 2 BFGGH
525 13E7A8 16 231 330 1 AGGIJ
526 13682D 16 231 330 1 AGGJJ
527 136FC4 16 231 330 1 AGHIJ
528 13E9AC 16 231 330 1 AGIIJ
529 1349ED 16 231 330 1 AGIJJ
530 136A2F 16 231 330 1 AGIJJ
531 136DE4 16 231 330 1 AGIJJ
532 13C8A5 16 231 330 1 BGGHJ
533 13E8AC 16 231 330 1 FGGGI
534 1579FD 16 231 330 1 FGGGI
535 136CE4 16 231 330 1 FGGHI
536 136EC4 16 231 330 1 FGGIJ
537 15397A 16 231 330 1 FGGIJ
538 13EB65 16 231 231 0 GGGIJ
539 136B2F 16 231 231 0 GGGJJ
540 13C965 16 231 231 0 GGIIJ
541 13692D 16 231 231 0 GGIJJ
542 1367CE 16 231 231 0 GHHIJ
543 1367EC 16 231 231 0 GHHIJ
544 357ABE 16 231 231 0 GHHIJ
545 367ABF 32 222 321 1 BGGGG
546 13E7AC 16 160 330 2 BBGII
547 143DFA 16 150 410 3 ABBIJ
548 143EDB 16 150 410 3 ABBIJ
549 1477AF 16 150 410 3 ABFGH
550 14A79C 16 150 410 3 ABFGI
551 14A78D 16 150 410 3 ABFHH
552 143B6E 16 150 410 3 ABFHJ
553 14386F 16 150 410 3 ABFJJ
554 14F7CA 16 150 410 3 BBBGJ
555 1437AC 16 150 410 3 BBBHJ
556 1437DB 16 150 410 3 BBBIJ
557 14279F 16 150 410 3 BBFGG
558 1427AF 16 150 410 3 BBFGG
559 14779A 16 150 410 3 BBFGH
560 1477A9 16 150 410 3 BBFGH
561 14A7C9 16 150 410 3 BBFGI
562 143E69 16 150 410 3 BBFGJ
563 14F79C 16 150 410 3 BBFGJ
564 143E6B 16 150 410 3 BBFHI
565 1437AF 16 150 410 3 BBFHJ
566 143D6A 16 150 410 3 BBFIJ
567 1477A8 16 150 320 2 ABGGJ
568 153CFA 16 150 320 2 ABIII
569 157CEA 16 150 320 2 ABIII
570 14AB3C 16 150 320 2 ABIJJ
571 13EE85 16 150 320 2 ABJJJ
572 14AB78 16 150 320 2 AFGGJ
573 134A7C 16 150 320 2 AFHIJ
574 15BA79 16 150 320 2 AFHIJ
575 15AD69 16 150 320 2 AFIII
576 3579CF 16 150 320 2 AFIII
577 1347ED 16 150 320 2 AFIIJ
578 13497F 16 150 320 2 AFIJJ
579 13678D 16 150 320 2 AFIJJ
580 1367AF 16 150 320 2 AFIJJ
581 15AD6E 16 150 320 2 AFIJJ
582 13D8F4 16 150 320 2 BBGGJ
583 13EED8 16 150 320 2 BBGGJ
584 1437E8 16 150 320 2 BBGGJ
585 14779B 16 150 320 2 BBGGJ
586 13EBD4 16 150 320 2 BBGHH
587 136BDE 16 150 320 2 BBGHI
588 136CFA 16 150 320 2 BBGHI
589 13DB75 16 150 320 2 BBGHI
590 156CFA 16 150 320 2 BBGHI
591 1368FD 16 150 320 2 BBGHJ
592 136FD8 16 150 320 2 BBGHJ
593 13D8E4 16 150 320 2 BBGHJ
594 13DDE7 16 150 320 2 BBGHJ
595 13E874 16 150 320 2 BBGHJ
```

596 13E8B7 16 150 320 2 BBGHJ
597 13EF7A 16 150 320 2 BBGHJ
598 1477DF 16 150 320 2 BBGHJ
599 1477EC 16 150 320 2 BBGHJ
600 147CEB 16 150 320 2 BBGHJ
601 136BD4 16 150 320 2 BBGIJ
602 136ED8 16 150 320 2 BBGIJ
603 13DA64 16 150 320 2 BBGIJ
604 13E875 16 150 320 2 BBGIJ
605 13EDB8 16 150 320 2 BBGIJ
606 13EE7B 16 150 320 2 BBGIJ
607 14BEC9 16 150 320 2 BBGIJ
608 156CBF 16 150 320 2 BBGIJ
609 136DFA 16 150 320 2 BBGJJ
610 13DB74 16 150 320 2 BBGJJ
611 13DDA4 16 150 320 2 BBGJJ
612 13EE7A 16 150 320 2 BBGJJ
613 13EED7 16 150 320 2 BBGJJ
614 14379F 16 150 320 2 BBGJJ
615 13DCF7 16 150 320 2 BBHHI
616 13ECB9 16 150 320 2 BBHHI
617 13EC74 16 150 320 2 BBHHJ
618 1369FC 16 150 320 2 BBHII
619 13E974 16 150 320 2 BBHII
620 13E9B6 16 150 320 2 BBHII
621 156DFB 16 150 320 2 BBHII
622 136ADF 16 150 320 2 BBHIJ
623 13D9F5 16 150 320 2 BBHIJ
624 13EC75 16 150 320 2 BBHIJ
625 13ED74 16 150 320 2 BBHIJ
626 156BDF 16 150 320 2 BBHIJ
627 157DEB 16 150 320 2 BBHIJ
628 357F9B 16 150 320 2 BBHIJ
629 13DCA4 16 150 320 2 BBHJJ
630 13DDF7 16 150 320 2 BBHJJ
631 143E6D 16 150 320 2 BBHJJ
632 156F3B 16 150 320 2 BBHJJ
633 1369F4 16 150 320 2 BBIIJ
634 13D7B9 16 150 320 2 BBIIJ
635 13DA74 16 150 320 2 BBIIJ
636 156D3B 16 150 320 2 BBIIJ
637 13D9F4 16 150 320 2 BBIJJ
638 13DDF6 16 150 320 2 BBIJJ
639 143D6E 16 150 320 2 BBJJJ
640 147CAF 16 150 320 2 BFGGH
641 1357E8 16 150 320 2 BFGGI
642 1368F4 16 150 320 2 BFGGI
643 14AC79 16 150 320 2 BFGGI
644 143F68 16 150 320 2 BFGGJ
645 14BA97 16 150 320 2 BFGGJ
646 1437EB 16 150 320 2 BFGHI
647 143ECB 16 150 320 2 BFGHI
648 143F6A 16 150 320 2 BFGHI
649 143FDA 16 150 320 2 BFGHI
650 14BCE9 16 150 320 2 BFGHI
651 1569FA 16 150 320 2 BFGHI
652 143A6F 16 150 320 2 BFGHJ
653 143CAF 16 150 320 2 BFGHJ
654 143DBE 16 150 320 2 BFGHJ
655 14B79C 16 150 320 2 BFGHJ
656 14B9EC 16 150 320 2 BFGHJ
657 1357F9 16 150 320 2 BFGII
658 136AD4 16 150 320 2 BFGII
659 1367D8 16 150 320 2 BFGIJ
660 1367FA 16 150 320 2 BFGIJ
661 13D7B8 16 150 320 2 BFGIJ
662 143C6B 16 150 320 2 BFGIJ
663 153CAF 16 150 320 2 BFGIJ
664 14396E 16 150 320 2 BFGJJ
665 14B7CE 16 150 320 2 BFGJJ
666 15BF9C 16 150 320 2 BFGJJ
667 156ADE 16 150 320 2 BFHHJ
668 157BDF 16 150 320 2 BFHII
669 13D7A9 16 150 320 2 BFIII
670 135B7D 16 150 320 2 FFGGH
671 13587E 16 150 320 2 FFGGJ
672 13597F 16 150 320 2 FFGHI
673 153C7A 16 150 320 2 FFGII
674 135A7C 16 150 320 2 FFGIJ
675 14AB97 16 150 230 1 AGJJJ
676 157CBF 16 150 230 1 AHIIJ
677 13EF85 16 150 230 1 AHJJJ
678 13DB64 16 150 230 1 BGGHJ
679 13EE94 16 150 230 1 BGGHJ
680 143CEB 16 150 230 1 BGGIJ
681 13C9F4 16 150 230 1 BGHHI
682 13EED6 16 150 230 1 BGHHJ
683 13EF94 16 150 230 1 BGHHJ
684 147ADF 16 150 230 1 BGHHJ
685 136FC9 16 150 230 1 BGHII
686 13DB65 16 150 230 1 BGHII
687 13EAD4 16 150 230 1 BGHII
688 13EFC9 16 150 230 1 BGHII
689 157CFA 16 150 230 1 BGHII
690 1357FD 16 150 230 1 BGHIJ
691 136BDF 16 150 230 1 BGHIJ
692 136CEB 16 150 230 1 BGHIJ
693 136F94 16 150 230 1 BGHIJ
694 13CA74 16 150 230 1 BGHIJ
695 13D7A8 16 150 230 1 BGHIJ
696 13ECA9 16 150 230 1 BGHIJ
697 13EE6B 16 150 230 1 BGHIJ
698 13EED9 16 150 230 1 BGHIJ
699 13EFC7 16 150 230 1 BGHIJ
700 1579EA 16 150 230 1 BGHIJ
701 15ADE6 16 150 230 1 BGHIJ
702 13CCA5 16 150 230 1 BGHJJ
703 13CCE7 16 150 230 1 BGHJJ
704 13DCB4 16 150 230 1 BGHJJ
705 13DDE6 16 150 230 1 BGHJJ
706 143F6C 16 150 230 1 BGHJJ
707 14F96C 16 150 230 1 BGHJJ
708 157F39 16 150 230 1 BGHJJ
709 35AFE6 16 150 230 1 BGHJJ
710 153CEA 16 150 230 1 BGIII
711 136DEB 16 150 230 1 BGIIJ
712 13CA75 16 150 230 1 BGIIJ
713 13D9E4 16 150 230 1 BGIIJ
714 13EA9C 16 150 230 1 BGIIJ
715 15A9FD 16 150 230 1 BGIIJ
716 15AC36 16 150 230 1 BGIIJ
717 1357EC 16 150 230 1 BGIJJ
718 136DB4 16 150 230 1 BGIJJ
719 136EC9 16 150 230 1 BGIJJ
720 13CDE7 16 150 230 1 BGIJJ
721 13EBD5 16 150 230 1 BGIJJ
722 13EEC9 16 150 230 1 BGIJJ
723 156F9B 16 150 230 1 BGIJJ
724 15AE9D 16 150 230 1 BGIJJ
725 13EEC7 16 150 230 1 BGJJJ
726 143C6F 16 150 230 1 BGJJJ
727 15B9ED 16 150 230 1 BGJJJ
728 136CFB 16 150 230 1 BHHHI
729 13DA75 16 150 230 1 BHHII
730 13EFD6 16 150 230 1 BHHII
731 136ED9 16 150 230 1 BHHIJ
732 13D9E5 16 150 230 1 BHHIJ
733 13DCE7 16 150 230 1 BHHIJ
734 13DCF6 16 150 230 1 BHHIJ
735 367F9A 16 150 230 1 BHHIJ
736 13DCA5 16 150 230 1 BHHJJ
737 156E3A 16 150 230 1 BHHJJ
738 357ECF 16 150 230 1 BHIII
739 35AD69 16 150 230 1 BHIII
740 1369FD 16 150 230 1 BHIIJ
741 13DA65 16 150 230 1 BHIIJ
742 13DCE6 16 150 230 1 BHIIJ
743 13E975 16 150 230 1 BHIIJ
744 13EDB9 16 150 230 1 BHIIJ
745 156C3A 16 150 230 1 BHIIJ
746 15AD36 16 150 230 1 BHIIJ
747 357ACE 16 150 230 1 BHIIJ
748 357BDF 16 150 230 1 BHIIJ
749 367BDE 16 150 230 1 BHIIJ
750 136ADE 16 150 230 1 BHIJJ
751 13EAD5 16 150 230 1 BHIJJ
752 13ED75 16 150 230 1 BHIJJ
753 13EF7B 16 150 230 1 BHIJJ
754 13EFD7 16 150 230 1 BHIJJ
755 153A6E 16 150 230 1 BHIJJ
756 153B6F 16 150 230 1 BHIJJ
757 153DAE 16 150 230 1 BHIJJ
758 156F39 16 150 230 1 BHIJJ
759 357FDE 16 150 230 1 BHIJJ
760 157ADE 16 150 230 1 BHJJJ

761 1367FB 16 150 230 1 BIIJJ
762 136DFB 16 150 230 1 BIIJJ
763 153C6F 16 150 230 1 BIIJJ
764 153D6E 16 150 230 1 BIIJJ
765 15AF36 16 150 230 1 BIIJJ
766 13E9B7 16 150 230 1 BIJJJ
767 15AE36 16 150 230 1 BIJJJ
768 136CB4 16 150 230 1 FGGHI
769 14BC69 16 150 230 1 FGGHI
770 14BF9C 16 150 230 1 FGGHJ
771 13E79A 16 150 230 1 FGGII
772 136E94 16 150 230 1 FGGIJ
773 13EB9C 16 150 230 1 FGGIJ
774 35FAB6 16 150 230 1 FGHHI
775 15BA96 16 150 230 1 FGHHJ
776 156DBE 16 150 230 1 FGHII
777 15ADE9 16 150 230 1 FGHII
778 1357ED 16 150 230 1 FGHIJ
779 13679C 16 150 230 1 FGHIJ
780 1367BE 16 150 230 1 FGHIJ
781 157ACE 16 150 230 1 FGHIJ
782 157E3A 16 150 230 1 FGHIJ
783 15AF9C 16 150 230 1 FGHIJ
784 153A7E 16 150 230 1 FGHJJ
785 153B7F 16 150 230 1 FGHJJ
786 156E9A 16 150 230 1 FGHJJ
787 1367C9 16 150 230 1 FGIIJ
788 1367EB 16 150 230 1 FGIIJ
789 13C7A9 16 150 230 1 FGIIJ
790 157CAF 16 150 230 1 FGIIJ
791 15BE36 16 150 230 1 FGIIJ
792 367AFB 16 150 230 1 FGIIJ
793 1357FC 16 150 230 1 FGIJJ
794 153C7F 16 150 230 1 FGIJJ
795 153D7E 16 150 230 1 FGIJJ
796 157F9B 16 150 230 1 FGIJJ
797 15EDA6 16 150 230 1 FGIJJ
798 367C9D 16 150 230 1 FHHII
799 367BEA 16 150 230 1 FHHIJ
800 157F8B 16 150 221 1 AJJJJ
801 13EFD8 16 150 221 1 BGHIJ
802 1368FC 16 150 221 1 BGHJJ
803 13EFD9 16 150 221 1 BHIII
804 136FD9 16 150 221 1 BHIIJ
805 35AFEC 16 150 221 1 BHIIJ
806 357FAE 16 150 221 1 BHIJJ
807 1367D9 16 150 221 1 BIIJJ
808 357AC9 16 150 221 1 FHHII
809 357AFC 16 150 221 1 FHHII
810 35FB9D 16 150 221 1 FHIIJ
811 14BA69 16 150 140 0 GGIJJ
812 13EE95 16 150 140 0 GGJJJ
813 13CDF6 16 150 140 0 GHIIJ
814 13EF6B 16 150 140 0 GHIIJ
815 13EC65 16 150 140 0 GHIJJ
816 157DAE 16 150 140 0 GHIJJ
817 15AB96 16 150 140 0 GHIJJ
818 15BA69 16 150 140 0 GHIJJ
819 13EF95 16 150 140 0 GHJJJ
820 15BE9D 16 150 140 0 GHJJJ
821 15BD69 16 150 140 0 GIIIJ
822 367AC5 16 150 140 0 GIIIJ
823 367ECF 16 150 140 0 GIIIJ
824 13C9F5 16 150 140 0 GIIJJ
825 13ED65 16 150 140 0 GIIJJ
826 13EDA9 16 150 140 0 GIIJJ
827 15ACE6 16 150 140 0 GIIJJ
828 15AD79 16 150 140 0 GIIJJ
829 367DB5 16 150 140 0 GIIJJ
830 367EB9 16 150 140 0 GIIJJ
831 13CDF7 16 150 140 0 GIJJJ
832 157E9A 16 150 140 0 GIJJJ
833 13CDA5 16 150 140 0 GJJJJ
834 367EFD 16 150 140 0 HHIII
835 367DFA 16 150 140 0 HHIJJ
836 367EF5 16 150 140 0 HIIII
837 367EC5 16 150 140 0 HIIIJ
838 357AFB 16 150 140 0 HIIJJ
839 357BEA 16 150 140 0 HIIJJ
840 35ACE6 16 150 140 0 HIIJJ
841 35ACED 16 150 140 0 HIIJJ
842 367F95 16 150 140 0 HIIJJ
843 35ADCE 16 150 140 0 HIJJJ
844 367C9B 16 150 140 0 HIJJJ
845 367FD5 16 150 140 0 HIJJJ
846 367BEC 16 150 140 0 HJJJJ
847 367DFC 16 150 140 0 IIJJJ
848 367FDE 16 150 140 0 IIJJJ
849 13586F 16 150 131 0 GGHJJ
850 135B6C 16 150 131 0 GGJJJ
851 13E79B 16 150 131 0 GHIIJ
852 135A6D 16 150 131 0 GHIJJ
853 157BCF 16 150 131 0 GHIJJ
854 15EF6C 16 150 131 0 GHJJJ
855 13596E 16 150 131 0 GIJJJ
856 13679D 16 150 131 0 GIJJJ
857 1367BF 16 150 131 0 GIJJJ
858 35ADC9 16 150 131 0 HIIIJ
859 35FAB9 16 150 131 0 HIIIJ
860 367DC5 16 150 131 0 HIIIJ
861 367DCE 16 150 131 0 HIIIJ
862 367EC9 16 150 131 0 HIIIJ
863 367BD5 16 150 131 0 HIIJJ
864 367DF5 16 150 131 0 HIIJJ
865 35ABE6 16 150 131 0 HIJJJ
866 14A86F 32 141 410 3 AABJJ
867 15BF8C 32 141 410 3 ABBJJ
868 143B6C 16 141 410 3 ABFHJ
869 156CAF 16 141 410 3 ABFII
870 156F8B 16 141 410 3 ABFJJ
871 136CF4 16 141 320 2 ABHIJ
872 136ED4 16 141 320 2 ABIJJ
873 14BA79 16 141 320 2 AFGIJ
874 13486F 16 141 320 2 AFGJJ
875 13E78C 16 141 320 2 AFIIJ
876 15BD79 16 141 320 2 AFIIJ
877 134A6D 16 141 320 2 AFIJJ
878 157DBE 16 141 320 2 AFIJJ
879 156DEB 16 141 320 2 BBGGI
880 1479FA 16 141 320 2 BFGGH
881 13C7E8 16 141 320 2 BFGGI
882 13E7CA 16 141 320 2 BFGGI
883 14F97C 16 141 320 2 BFGGJ
884 1357BD 16 141 320 2 BFGHI
885 136FD4 16 141 320 2 BFGHI
886 13E7B8 16 141 320 2 BFGHI
887 143A6D 16 141 320 2 BFGHJ
888 156BCF 16 141 320 2 BFGHJ
889 1357AC 16 141 320 2 BFGIJ
890 136DF4 16 141 320 2 BFGIJ
891 1367DE 16 141 320 2 BFHHI
892 1367FC 16 141 320 2 BFHHI
893 357F9C 16 141 320 2 BFHHI
894 13E9BC 16 141 320 2 BFHII
895 14B93E 16 141 320 2 FFGGJ
896 15397F 16 141 320 2 FFGGJ
897 153A7C 16 141 320 2 FFGHH
898 157DFB 16 141 230 1 AGIIJ
899 367ACF 16 141 230 1 BGGII
900 1368ED 16 141 230 1 BGGIJ
901 13C7EA 16 141 230 1 BGGIJ
902 13C8E5 16 141 230 1 BGGJJ
903 13E8A7 16 141 230 1 BGGJJ
904 14BA3D 16 141 230 1 BGGJJ
905 13E8BC 16 141 230 1 BGHIJ
906 136ACF 16 141 230 1 BGIIJ
907 13E9A7 16 141 230 1 BGIIJ
908 157C3A 16 141 230 1 BGIIJ
909 357EBF 16 141 230 1 BGIIJ
910 367CD9 16 141 230 1 BGIIJ
911 367EFB 16 141 230 1 BGIIJ
912 13EAC5 16 141 230 1 BGIJJ
913 157D3B 16 141 230 1 BGIJJ
914 13E7B9 16 141 230 1 BHIIJ
915 1367DF 16 141 230 1 BHIJJ
916 13C7FA 16 141 230 1 FGGHI
917 13E7A9 16 141 230 1 FGGII
918 15BD36 16 141 230 1 FGGII
919 367AC9 16 141 230 1 FGGII
920 367EBF 16 141 230 1 FGGII
921 153DBE 16 141 230 1 FGGIJ
922 1579FA 16 141 230 1 FGGIJ
923 15A9ED 16 141 230 1 FGGIJ
924 15B9FD 16 141 230 1 FGGIJ
925 367DBE 16 141 230 1 FGGIJ

```
926 15A9E6 16 141 230  1  FGGJJ    981 14BF97  16  060 220  2  FFGGJ   1036 13D7FA 16 051 220  2  BFGIJ
927 13E96C 16 141 230  1  FGHII    982 17AF9C  16  060 220  2  FFGHJ   1037 13E87C 16 051 220  2  BFGIJ
928 1367CF 16 141 230  1  FGHIJ    983 15BC6F  16  060 220  2  FFGIJ   1038 13D8F6 16 051 220  2  BFGJJ
929 1367ED 16 141 230  1  FGHIJ    984 16BF9C  16  060 220  2  FFGJJ   1039 13EBD7 16 051 220  2  BFGJJ
930 157F3B 16 141 230  1  FGHJJ    985 57EC6D  96  060 220  2  FFHHH   1040 15B9E6 16 051 220  2  BFGJJ
931 367F9C 16 141 230  1  FGHJJ    986 35FA6B  16  060 220  2  FFHHI   1041 1B57ED 16 051 220  2  BFGJJ
932 15BF36 16 141 230  1  FGIJJ    987 36ABE7  16  060 220  2  FFHHJ   1042 1B57FD 16 051 220  2  BFGJJ
933 13EB6C 16 141 221  1  BGGIJ    988 14BF68  16  060 130  1  BGGJJ   1043 13ECB6 16 051 220  2  BFHHJ
934 13C7F9 16 141 221  1  BGIIJ    989 15ACF6  16  060 130  1  BHIIJ   1044 13D7EB 16 051 220  2  BFHII
935 1367FD 16 141 221  1  BHIJJ    990 15ADF6  16  060 130  1  BHIIJ   1045 35AEF6 16 051 220  2  BFHIJ
936 35ADF9 16 141 221  1  FGGHI    991 36CEBF  16  060 130  1  BIIIJ   1046 35AFDE 16 051 220  2  BFHIJ
937 13EBC6 16 141 221  1  FGGHJ    992 36FEBD  16  060 130  1  BIIIJ   1047 15EAD6 16 051 220  2  BFHJJ
938 13C9E6 16 141 221  1  FGHIJ    993 15ECB6  16  060 130  1  BIJJJ   1048 15EB7D 16 051 220  2  BFHJJ
939 357BED 16 141 221  1  FGHIJ    994 15EFD6  16  060 130  1  BIJJJ   1049 15FAD6 16 051 220  2  BFHJJ
940 13C7AE 16 141 221  1  FGIIJ    995 15AD7E  16  060 130  1  FGIJJ   1050 35AFD9 16 051 220  2  BFIII
941 13C8F6 16 141 131  0  GGHJJ    996 15AF79  16  060 130  1  FGIJJ   1051 13D7AF 16 051 220  2  BFIIJ
942 13E865 16 141 131  0  GGIIJ    997 16AE9D  16  060 130  1  FGIJJ   1052 35FE6D 16 051 220  2  BFIIJ
943 13CB65 16 141 131  0  GGIJJ    998 15AE96  16  060 130  1  FGJJJ   1053 13ED7B 16 051 220  2  BFIJJ
944 136BCF 16 141 131  0  GGJJJ    999 15BE96  16  060 130  1  FGJJJ   1054 13EDB7 16 051 220  2  BFJJJ
945 13EBC5 16 141 131  0  GGJJJ   1000 36AEF9  16  060 130  1  FHIII   1055 15FB7D 16 051 220  2  FFGHI
946 13ED6A 16 141 131  0  GGJJJ   1001 35ABED  16  060 130  1  FHIIJ   1056 13ECA7 16 051 220  2  FFGHJ
947 367CDF 16 141 131  0  GHIIJ   1002 35ADF6  16  060 130  1  FHIIJ   1057 15FBC6 16 051 220  2  FFGHJ
948 153CBF 16 141 131  0  GHIJJ   1003 36ABD5  16  060 130  1  FHIJJ   1058 15FCB6 16 051 220  2  FFGIJ
949 367AFD 16 141 131  0  GHIJJ   1004 36AFD5  16  060 130  1  FHIJJ   1059 36FEB7 16 051 220  2  FFIII
950 13EDA6 16 141 131  0  GHJJJ   1005 37DE6F  16  060 130  1  FHIJJ   1060 13E7DB 16 051 211  2  BBIIJ
951 15EBC6 16 141 131  0  GHJJJ   1006 36ADF7  16  060 130  1  FHJJJ   1061 13D7EA 16 051 130  1  BGIIJ
952 13C7FB 16 141 131  0  GIIIJ   1007 36AFE7  16  060 130  1  FHJJJ   1062 14F96A 16 051 130  1  BGJJJ
953 13CA65 16 141 131  0  GIIIJ   1008 36CDB5  16  060 130  1  FIIJJ   1063 13EAD6 16 051 130  1  BHIJJ
954 13E965 16 141 131  0  GIIJJ   1009 36CEB9  16  060 130  1  FIIJJ   1064 13D9E6 16 051 130  1  BIJJJ
955 1369ED 16 141 131  0  GIJJJ   1010 36CF97  16  060 130  1  FIIJJ   1065 13EC6B 16 051 130  1  FGHIJ

956 13C9E5 16 141 131  0  GIJJJ   1011 14FF28 320 060 040  0  GGGGG   1066 36ACD9 16 051 130  1  FGIII
957 367CD5 16 141 131  0  HIIIJ   1012 DEFF7B  64  060 040  0  GJJJJ   1067 37AFD9 16 051 130  1  FGIII
958 367CE5 16 141 131  0  HIIJJ   1013 37DEBF  32  060 040  0  HIIJJ   1068 13C7EB 16 051 130  1  FGIIJ
959 367CED 16 141 122  0  HIIJJ   1014 36ADC5  16  060 040  0  IIJJJ   1069 13E7C9 16 051 130  1  FGIIJ
960 14A7F9 16 060 400  4  BBBFI   1015 14FBD7  16  051 310  3  ABFJJ   1070 15BDF6 16 051 130  1  FGIIJ
961 14F7A9 16 060 400  4  BBBFJ   1016 15BC7F  16  051 310  3  AFFIJ   1071 36CDBE 16 051 130  1  FGIIJ
962 14A79F 16 060 310  3  BBBGJ   1017 15BF79  16  051 310  3  AFFIJ   1072 13C9F7 16 051 130  1  FGIJJ
963 14FD6A 16 060 310  3  BBBJJ   1018 15BF86  16  051 310  3  AFFJJ   1073 15FE7D 16 051 130  1  FGIJJ
964 15EC7A 16 060 310  3  BBFIJ   1019 13D7F9  16  051 310  3  BBFII   1074 37ACDF 16 051 130  1  FHIII
965 14F79A 16 060 310  3  BFFGJ   1020 13EA7C  16  051 310  3  BBFII   1075 36AEFD 16 051 130  1  FIIJJ
966 1BFFD8 32 060 220  2  BBGJJ   1021 13EC7A  16  051 310  3  BFFGH   1076 13E7D9 16 051 121  1  BIIIJ
967 1B6FD8 32 060 220  2  BBHJJ   1022 15FD7B  16  051 310  3  BFFGI   1077 35AFE9 16 051 121  1  BIIJJ
968 1C6F38 32 060 220  2  BBHJJ   1023 14A7CF  16  051 310  3  BFFGJ   1078 13E79C 16 051 121  1  FGIIJ
969 14A7DF 16 060 220  2  BBJJJ   1024 15EA7C  16  051 310  3  BFFHH   1079 36ACDF 16 051 121  1  FHIII
970 14B7EC 16 060 220  2  BBJJJ   1025 13D9F7  16  051 310  3  BFFHI   1080 36CFE7 80 051 050  0  JJJJJ
971 14BE69 16 060 220  2  BFGIJ   1026 14FB6C  16  051 220  2  ABJJJ   1081 37EDBC 64 051 031  0  HJJJJ
972 14BCE7 16 060 220  2  BFGJJ   1027 13D7E8  16  051 220  2  BBGIJ   1082 36CF9E 16 051 031  0  IIIJJ
973 14BD6E 16 060 220  2  BFGJJ   1028 13D7FB  16  051 220  2  BBIIJ   1083 37ADC9 16 051 031  0  IIIJJ
974 17BE9D 16 060 220  2  BFGJJ   1029 13E97C  16  051 220  2  BBIIJ   1084 37AFE9 16 051 031  0  IIIJJ
975 15BCE6 16 060 220  2  BFHII   1030 14B96E  16  051 220  2  BFGGJ   1085 15B97F 32 042 400  4  ABFFG
976 15BDE6 16 060 220  2  BFHII   1031 13E7D8  16  051 220  2  BFGHI   1086 35FEBD 32 042 220  2  BBGII
977 35AEFD 16 060 220  2  BFHII   1032 15BCF6  16  051 220  2  BFGHI   1087 13C8E7 16 042 220  2  FFGGJ
978 15EF7C 16 060 220  2  BFHJJ   1033 13D8E7  16  051 220  2  BFGHJ   1088 14F97A 16 042 220  2  FFGGJ
979 15FDA6 16 060 220  2  BFIJJ   1034 14FA6D  16  051 220  2  BFGHJ   1089 13EAC7 16 042 220  2  FFGIJ
980 14AC7F 16 060 220  2  FFGGJ   1035 15FA7C  16  051 220  2  BFGHJ   1090 36ACD5 16 042 121  1  FGIIJ
```

N	SP	S	H_1	H_2	H_3	LT	N	SP	S	H_1	H_2	H_3	LT	N	SP	S	H_1	H_2	H_3	LT
1091	53FF35	32	510	820	3	AGHHAA	1118	56FF95	16	240	340	1	BHIJGG	1145	56CCF5	16	141	420	3	FHIIBB
1092	53FFCA	64	430	630	2	AAGGGG	1119	56FF9A	16	240	340	1	BHIJGG	1146	36AAF9	16	141	330	2	BFGIII
1093	53AA35	16	420	630	2	GHIJAA	1120	36AC65	16	240	340	1	BIIJGG	1147	35AAF9	16	141	330	2	BFHIGG
1094	53FF3A	16	420	540	1	AGHHGG	1121	36CC65	16	240	340	1	FIIJGG	1148	53AC35	16	141	330	2	GHIJBB
1095	5CFF3A	64	420	450	0	HHHHGG	1122	53FAC5	16	240	250	0	GHHJII	1149	53AF36	16	141	240	1	AIIJII
1096	56CC65	48	330	620	3	FIIIAA	1123	53AA6F	16	240	250	0	HHHIII	1150	56CA6F	16	141	240	1	BGHIII
1097	53AA9F	16	330	440	1	AHIIGG	1124	56FF3A	16	240	250	0	HHHJII	1151	36AACF	16	141	240	1	BGHJII
1098	53FF36	16	330	440	1	AHIJGG	1125	53AA36	16	240	250	0	HIIJGG	1152	36CC6F	16	141	240	1	BIJJGG
1099	56FF35	16	330	440	1	BGHHGG	1126	56AF95	16	240	250	0	HIJJII	1153	36AF65	16	141	240	1	BIJJII
1100	56FA65	16	330	440	1	BGIJGG	1127	56AA3F	16	240	241	0	GHHJII	1154	56CF35	16	141	240	1	FGHIII
1101	56AF35	16	330	350	0	GHJJGG	1128	53AFC5	16	231	340	1	AGHIII	1155	36CF65	16	141	240	1	FIJJII
1102	53AA65	16	330	350	0	HHIIGG	1129	53FF6A	16	231	340	1	AGHJII	1156	56AC35	16	141	150	0	GIJJII
1103	53AA3F	16	330	350	0	HHIJGG	1130	56FAC5	16	231	340	1	BGGJII	1157	36AAC5	16	141	150	0	GJJJII
1104	53FA65	16	330	350	0	HHIJGG	1131	36AA65	16	231	340	1	BGIJGG	1158	53AC36	16	141	150	0	HIIJII
1105	53FA35	16	330	341	0	GHHHGG	1132	56CA65	16	231	340	1	FGIIGG	1159	36FF65	16	132	330	2	BFIJGG
1106	56FF65	16	321	620	3	BHIJAA	1133	36AAC9	16	231	340	1	FGIJGG	1160	56AAC9	16	132	240	1	FGGIII
1107	53AF35	16	321	440	1	AGIJGG	1134	56FF6A	32	231	250	0	HHJJGG	1161	36CC9F	32	070	230	2	BBIIII
1108	56AACF	16	321	440	1	BGGHGG	1135	56CC6F	16	150	420	3	BIIJBB	1162	35FFAC	128	061	410	4	BBBBGG
1109	56AA35	16	321	350	0	GGJJGG	1136	36FC65	16	150	330	2	BFIIII	1163	35AAFC	32	051	230	2	FFHHII
1110	53FF9A	16	250	430	2	ABGIII	1137	36CC69	16	150	330	2	HIJJBB	1164	39FF65	16	051	230	2	FFHIII
1111	59FF9A	32	250	430	2	BBIIGG	1138	36AC69	16	150	240	1	BHIIII	1165	36FF95	16	051	140	1	BJJJII
1112	53FF39	16	240	520	3	AHIJBB	1139	35AA69	16	150	240	1	BHIJII	1166	35AAF6	16	051	140	1	FHJJII
1113	56FFC5	16	240	520	3	BGHHBB	1140	36AC6F	16	150	240	1	BHIJII	1167	39CC6F	32	051	050	0	JJJJII
1114	53AAC5	16	240	430	2	GHIJBB	1141	35AAC9	16	150	240	1	FHIJII	1168	35FF6C	16	042	320	3	BBFJII
1115	53AF95	16	240	340	1	AIIJII	1142	53AA96	16	150	150	0	HHIIII	1169	36FF6A	16	042	320	3	FHJJBB
1116	53AACF	16	240	340	1	BGHIII	1143	53FA36	16	150	150	0	HHIJII	1170	36FF6C	32	042	230	2	FFJJGG
1117	59FF3A	16	240	340	1	BHHIII	1144	36AA6F	32	141	420	3	BGHHBB	1171	36FF9C	32	042	230	2	FFJJGG

Table 1.3: non-orientable, six cusped, Ratcliffe-Tschantz hyperbolic 4-manifolds

1.3 Handle Decomposition of the Ratcliffe-Tschantz manifolds

In this section we want to explain how to obtain a handle decomposition of any of the Ratcliffe-Tschantz manifolds.

Recall from the previous section that each of the Ratcliffe-Tschantz manifolds is obtained via the 24-cell P in $\mathbb{H}^4$ by appropriate side pairing transformations. Therefore it should come as no surprise that the approach to finding such a handle decomposition starts by trying to decompose the polyhedron P into various pieces that glue up appropriately when we apply the side pairing transformations. One must keep in mind that the polyhedron P is not a manifold so we cannot really speak of a handle decomposition of it. The main idea is that the dual cell decomposition we gave previously will lead to a handle decomposition for any of the Ratcliffe-Tschantz manifolds.

In section 1.1 we constructed a diagram of the dual polyhedron of ∂P. The red dots in the diagram will constitute pieces of the 1-handles for the manifolds. The lines joining these red dots will be parts of the 2-handles, and the triangles formed by these lines will be parts of 3-handles. As for the 0-handle, just observe that the interior of P can be identified with the interior of a 4-ball and as any side pairing transformation is injective on the interior of P we find that we can think of the interior as the 0-handle of any of the Ratcliffe-Tschantz manifolds.

Let us explain in slightly more detail how exactly we get this handle decomposition from the dual cell diagram we drew.

Suppose we have obtained a manifold M from side pairing transformations of the polyhedron P. The side pairing transformations form a group, which we denote by G, we obtain M by taking the quotient of P by G. The polyhedron P has a natural stratification into codimension k sides. The codimension 0 side is just the interior of P, so the zeroth level of the stratification of P comprises of the interior of P. Codimension 1 sides of P comprise of the faces of P, and we know that there are 24 such faces, thus the first level of the stratification comprises of these 24 sides. There are 96 codimension 2 sides, hence the second level of the stratification comprises of these 96 codimension 2 sides. There are 96 codimension 3 sides, which tells us that the third level of the stratification consists of these 96 codimension 3 sides. The side pairing group G preserves this stratification, and the orbit of each codimension k side in the k^{th}-level forms a codimension k equivalence class. For example since G does not identify any points in the interior of P we have that the codimension 0 equivalence class simply consists of the interior of P. Each side pairing transformation takes a side of P and pairs it with another unique side of P, distinct from the original side. This implies that each codimension 1 equivalence class will consist of precisely two elements, a pair of codimension 1 sides that are paired together by some side pairing transformation. For the codimension 2 sides there are exactly four elements in each equivalence class (this is because the dihedral angles of a 24-cell are all $\pi/2$, hence four copies are needed around each codimension 2 side in order to give a total angle of 2π), since there are 96 codimension 2 sides it follows that there are a total of 24 codimension 2 equivalence classes. Finally, there are eight codimension 3 sides in each codimension 3 equivalence class, and since there are 96 codimension 3 sides there are a total of twelve codimension 3 equivalence classes. From here it is easy to obtain a handle decomposition of M, each equivalence class of codimension k sides corresponds to one k handle. As there is only one equivalence class for the codimension 0 side we have that M has exactly one 0-handle. As there are twelve equivalence classes of codimension 1 sides, it follows that M has twelve 1-handles. Similarly one can conclude that M has twenty four 2-handles and twelve 3-handles. Finally, there are no 4-handles as all the vertices of P are ideal. We can now see why the dual cell diagram we drew in section 1.1 gives us the handle structure information. The vertices in the diagram corresponded to codimension 1 sides in P, hence pairs of vertices will correspond to 1-handles for M. Lines joining vertices corresponded to codimension 2 sides, so collections of such lines (four to be exact) will form a 2-handle. Triangles filling in triples of lines that join vertices corresponded to codimension 3 sides, so collections of such triangles (8 to be exact) will constitute a 3-handle.

It is time to start giving some explicit examples, so let us start with manifold no. 3 in table 1.1. The code for this manifold is **1477B8**, decoding this we find that the side pairing transformations are given by:

$$S_{(+1,+1,0,0)} \xrightarrow[k_{(-1,+1,+1,+1)}]{a} S_{(-1,+1,0,0)} \qquad S_{(+1,-1,0,0)} \xrightarrow[k_{(-1,+1,+1,+1)}]{b} S_{(-1,-1,0,0)}$$

$$S_{(+1,0,+1,0)} \xrightarrow[k_{(+1,+1,-1,+1)}]{c} S_{(+1,0,-1,0)} \qquad S_{(-1,0,+1,0)} \xrightarrow[k_{(+1,+1,-1,+1)}]{d} S_{(-1,0,-1,0)}$$

$$S_{(0,+1,+1,0)} \xrightarrow[k_{(-1,-1,-1,+1)}]{e} S_{(0,-1,-1,0)} \qquad S_{(0,+1,-1,0)} \xrightarrow[k_{(-1,-1,-1,+1)}]{f} S_{(0,-1,+1,0)}$$

$$S_{(+1,0,0,+1)} \xrightarrow[k_{(-1,-1,-1,+1)}]{g} S_{(-1,0,0,+1)} \qquad S_{(+1,0,0,-1)} \xrightarrow[k_{(-1,-1,-1,+1)}]{h} S_{(-1,0,0,-1)}$$

$$S_{(0,+1,0,+1)} \xrightarrow[k_{(-1,-1,+1,-1)}]{i} S_{(0,-1,0,-1)} \qquad S_{(0,+1,0,-1)} \xrightarrow[k_{(-1,-1,+1,-1)}]{j} S_{(0,-1,0,+1)}$$

$$S_{(0,0,+1,+1)} \xrightarrow[k_{(+1,+1,+1,-1)}]{k} S_{(0,0,+1,-1)} \qquad S_{(0,0,-1,+1)} \xrightarrow[k_{(+1,+1,+1,-1)}]{l} S_{(0,0,-1,-1)} \ .$$

From our above discussion we know that the 1-handles of this manifold correspond to pairs of identified sides of P. We are going to label the 1-handles as follows, each side pairing transformation pairs a domain side to an image side. We label the domain side by a capital letter, the letter corresponding to the letter of the side pairing transformation. We label the image side by a primed capital letter, the letter being the same as what we used for the domain side. For example, from the above we see that the transformation a pairs $S_{(+1,+1,0,0)}$ to $S_{(-1,+1,0,0)}$, hence we label $S_{(+1,+1,0,0)}$ by A and $S_{(-1,+1,0,0)}$ by A'. The following table summarises this information for manifold no. 3.

A	$S_{(+1,+1,0,0)}$	$(\frac{1}{\sqrt{2}}, \frac{1}{\sqrt{2}}, 0)$	A'	$S_{(-1,+1,0,0)}$	$(\frac{-1}{\sqrt{2}}, \frac{1}{\sqrt{2}}, 0)$
B	$S_{(+1,-1,0,0)}$	$(\frac{1}{\sqrt{2}}, \frac{-1}{\sqrt{2}}, 0)$	B'	$S_{(-1,-1,0,0)}$	$(\frac{-1}{\sqrt{2}}, \frac{-1}{\sqrt{2}}, 0)$
C	$S_{(+1,0,+1,0)}$	$(\frac{1}{\sqrt{2}}, 0, \frac{1}{\sqrt{2}})$	C'	$S_{(+1,0,-1,0)}$	$(\frac{1}{\sqrt{2}}, 0, \frac{-1}{\sqrt{2}})$
D	$S_{(-1,0,+1,0)}$	$(\frac{-1}{\sqrt{2}}, 0, \frac{1}{\sqrt{2}})$	D'	$S_{(-1,0,-1,0)}$	$(\frac{-1}{\sqrt{2}}, 0, \frac{-1}{\sqrt{2}})$
E	$S_{(0,+1,+1,0)}$	$(0, \frac{1}{\sqrt{2}}, \frac{1}{\sqrt{2}})$	E'	$S_{(0,-1,-1,0)}$	$(0, \frac{-1}{\sqrt{2}}, \frac{-1}{\sqrt{2}})$
F	$S_{(0,+1,-1,0)}$	$(0, \frac{1}{\sqrt{2}}, \frac{-1}{\sqrt{2}})$	F'	$S_{(0,-1,+1,0)}$	$(0, \frac{-1}{\sqrt{2}}, \frac{1}{\sqrt{2}})$
G	$S_{(+1,0,0,+1)}$	$(1+\sqrt{2}, 0, 0)$	G'	$S_{(-1,0,0,-1)}$	$(1-\sqrt{2}, 0, 0)$
H	$S_{(+1,0,0,-1)}$	$(-1+\sqrt{2}, 0, 0)$	H'	$S_{(-1,0,0,+1)}$	$(-1-\sqrt{2}, 0, 0)$
I	$S_{(0,+1,0,+1)}$	$(0, 1+\sqrt{2}, 0)$	I'	$S_{(0,-1,0,+1)}$	$(0, -1-\sqrt{2}, 0)$
J	$S_{(0,+1,0,-1)}$	$(0, -1+\sqrt{2}, 0)$	J'	$S_{(0,-1,0,-1)}$	$(0, 1-\sqrt{2}, 0)$
K	$S_{(0,0,+1,+1)}$	$(0, 0, 1+\sqrt{2})$	K'	$S_{(0,0,+1,-1)}$	$(0, 0, -1+\sqrt{2})$
L	$S_{(0,0,-1,+1)}$	$(0, 0, -1-\sqrt{2})$	L'	$S_{(0,0,-1,-1)}$	$(0, 0, 1-\sqrt{2})$

The following diagram shows the 1-handles.

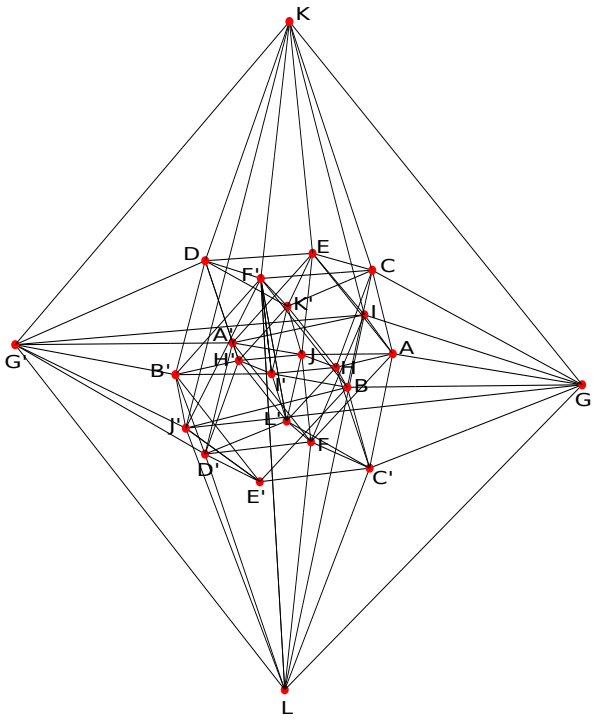

We should really think of the red vertices as very small 3-balls as a 1-handle is a copy of $D^1 \times D^3$, hence the attaching sphere is $S^0 \times D^3$, which is a pair of 3-balls. The standard convention, for orientable manifolds, of visualising a 1-handle is by drawing its attaching region, which is $S^0 \times D^3$, in $\mathbb{R}^3$ with the understanding that the boundaries of these two balls are identified via a reflection (an orientation reversing diffeomorphism). For the non-orientable case the convention is that attaching regions of 1-handles are attached by an orientation preserving diffeomorphism. In our situation the 1-handles are in correspondence with pairs of codimension one faces of P (the 24-cell), and each such pair is identified via a side-pairing transformation. Therefore for our case the attaching regions of 1-handles will be identified via their corresponding side-pairing transformation, these could be orientation reversing or preserving depending on the side pairing transformation. One has to be slightly careful in situations where the attaching regions are being identified via an orientation preserving diffeomorphism, the reason being that if we have a knotted 2-handle that passes over the 1-handle and we push it through the 1-handle, we find that the knotted part of the 2-handle changes to its mirror. However, if all 2-handles present have components that are unknotted then pushing any 2-handle through a 1-handle will not in anyway change the 2-handle. As we will see later we are in precisely the situation where all the 2-handles are unknotted. At this stage it is hard to get a good idea of how these 1-handles sit in 3-space, we will soon show a better way to think of these 1-handles that will be very useful in the second part of this thesis.

In order to see what a 2-handle looks like in the above picture we first need to understand how

equivalence classes of codimension 2 sides arise. Recall that two codimension 1 sides intersect if the centre vector of the spheres defining the sides have one entry the same, and the other entry in different positions. For example the side $S_{(+1,+1,0,0)}$ intersects $S_{(+1,0,+1,0)}$ because they both have a $+1$ in the first position and the second non-zero co-ordinates are in different positions. On the other hand the side $S_{(+1,+1,0,0)}$ does not intersect $S_{(0,0,-1,+1)}$ as their non-zero co-ordinates are in different positions. Also, $S_{(+1,+1,0,0)}$ does not intersect $S_{(-1,0,0,-1)}$ because the first entry of each have different signs. Once we know which codimension 1 sides intersect, we find an equivalence class by simply applying side pairing transformations to the intersection. For example, we know that $S_{(+1,+1,0,0)}$ intersects $S_{(+1,0,+1,0)}$, which using the above table we can write as $A \cap C$, we then apply the transformation a and find that $A \cap C$ goes to $A' \cap D$. We can then apply d and we find that we end up at $A' \cap D'$. We continue in this way until we cycle back to $A \cap C$. Once we end up back at $A \cap C$ we know we have found an equivalence class. The full equivalence class for $A \cap C$ is:

$$A \cap C \xrightarrow{a} A' \cap D \xrightarrow{d} A' \cap D' \xrightarrow{a^{-1}} A \cap C' \xrightarrow{c^{-1}} A \cap C \ .$$

Note that if a pairs A with A' then a^{-1} is the transformation that pairs A' with A. Continuing in this fashion we can work out all codimension 2 equivalence classes, the following table gives all 24 such classes.

1.	$A \cap C \xrightarrow{a} A' \cap D \xrightarrow{d} A' \cap D' \xrightarrow{a^{-1}} A \cap C' \xrightarrow{c^{-1}} A \cap C$
2.	$A \cap G \xrightarrow{a} A' \cap G' \xrightarrow{g^{-1}} B \cap G \xrightarrow{b} B' \cap G' \xrightarrow{g^{-1}} A \cap G$
3.	$A \cap H \xrightarrow{a} A' \cap H' \xrightarrow{h^{-1}} B \cap H \xrightarrow{b} B' \cap H' \xrightarrow{h^{-1}} A \cap H$
4.	$A \cap E \xrightarrow{a} A' \cap E \xrightarrow{e} B \cap E' \xrightarrow{b} B' \cap E' \xrightarrow{e^{-1}} A \cap E$
5.	$A \cap F \xrightarrow{a} A' \cap F \xrightarrow{f} B \cap F' \xrightarrow{b} B' \cap F' \xrightarrow{f^{-1}} A \cap F$
6.	$A \cap I \xrightarrow{a} A' \cap I \xrightarrow{i} B \cap I' \xrightarrow{b} B' \cap I' \xrightarrow{i^{-1}} A \cap I$
7.	$A \cap J \xrightarrow{a} A' \cap J \xrightarrow{j} B \cap J' \xrightarrow{b} B' \cap J' \xrightarrow{j^{-1}} A \cap J$
8.	$B \cap C \xrightarrow{b} B' \cap D \xrightarrow{d} B' \cap D' \xrightarrow{b^{-1}} B \cap C' \xrightarrow{c^{-1}} B \cap C$
9.	$C \cap G \xrightarrow{c} C' \cap G \xrightarrow{g} D \cap G' \xrightarrow{d} D' \cap G' \xrightarrow{g^{-1}} C \cap G$
10.	$C \cap H \xrightarrow{c} C' \cap H \xrightarrow{h} D \cap H' \xrightarrow{d} D' \cap H' \xrightarrow{h^{-1}} C \cap H$
11.	$C \cap E \xrightarrow{c} C' \cap F \xrightarrow{f} D \cap F' \xrightarrow{d} D' \cap E' \xrightarrow{e^{-1}} C \cap E$
12.	$C \cap F' \xrightarrow{c} C' \cap E' \xrightarrow{e^{-1}} D \cap E \xrightarrow{d} D' \cap F \xrightarrow{f} C \cap F'$
13.	$C \cap K \xrightarrow{c} C' \cap L \xrightarrow{l} C' \cap L' \xrightarrow{c^{-1}} C \cap K' \xrightarrow{k^{-1}} C \cap K$
14.	$D \cap K \xrightarrow{d} D' \cap L \xrightarrow{l} D' \cap L' \xrightarrow{d^{-1}} D \cap K' \xrightarrow{k^{-1}} D \cap K$
15.	$G \cap I \xrightarrow{g} G' \cap J' \xrightarrow{j^{-1}} H \cap J \xrightarrow{h} H' \cap I' \xrightarrow{i^{-1}} G \cap I$
16.	$G \cap J' \xrightarrow{g} G' \cap I \xrightarrow{i} H \cap I' \xrightarrow{h} H' \cap J \xrightarrow{j} G \cap J'$
17.	$G \cap K \xrightarrow{g} G' \cap L \xrightarrow{l} H' \cap L' \xrightarrow{h^{-1}} H \cap K' \xrightarrow{k^{-1}} G \cap K$
18.	$G \cap L \xrightarrow{g} G' \cap K \xrightarrow{k} H' \cap K' \xrightarrow{h^{-1}} H \cap L' \xrightarrow{l^{-1}} G \cap L$
19.	$E \cap I \xrightarrow{e} E' \cap J' \xrightarrow{j^{-1}} F \cap J \xrightarrow{f} F' \cap I' \xrightarrow{i^{-1}} E \cap I$
20.	$E \cap J \xrightarrow{e} E' \cap I' \xrightarrow{i^{-1}} F \cap I \xrightarrow{f} F' \cap J' \xrightarrow{j^{-1}} E \cap J$
21.	$E \cap K \xrightarrow{e} E' \cap L \xrightarrow{l} E' \cap L' \xrightarrow{e^{-1}} E \cap K' \xrightarrow{k^{-1}} E \cap K$
22.	$F \cap L \xrightarrow{f} F' \cap K \xrightarrow{k} F' \cap K' \xrightarrow{f^{-1}} F \cap L' \xrightarrow{l^{-1}} F \cap L$
23.	$I \cap K \xrightarrow{i} I' \cap K' \xrightarrow{k^{-1}} J' \cap K \xrightarrow{j^{-1}} J \cap K' \xrightarrow{k^{-1}} I \cap K$
24.	$I \cap L \xrightarrow{i} I' \cap L' \xrightarrow{l^{-1}} J' \cap L \xrightarrow{j^{-1}} J \cap L' \xrightarrow{l^{-1}} I \cap L$

The following picture shows the 2 handle given by the equivalence

$$A \cap C \xrightarrow{a} A' \cap D \xrightarrow{d} A' \cap D' \xrightarrow{a^{-1}} A \cap C' \xrightarrow{c^{-1}} A \cap C$$

the green edges and their blue vertices outline how the class looks in the whole handle decomposition.

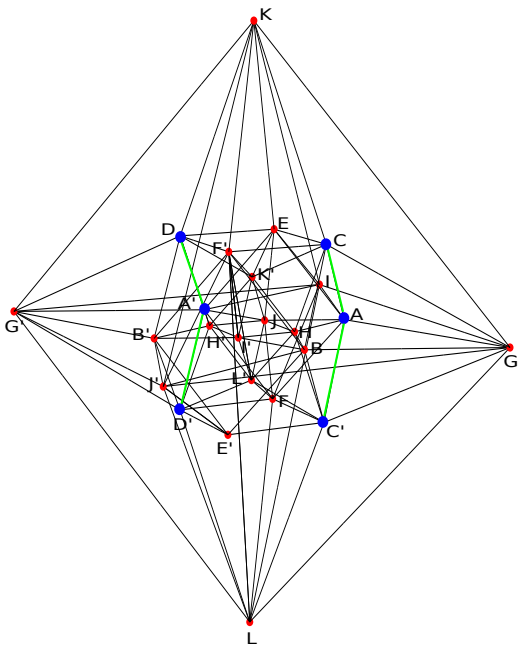

Let us give another picture of a 2 handle, this time we take the 2-handle corresponding to the class

$$C \cap E \xrightarrow{c} C' \cap F \xrightarrow{f} D \cap F' \xrightarrow{d} D' \cap E' \xrightarrow{e^{-1}} C \cap E$$

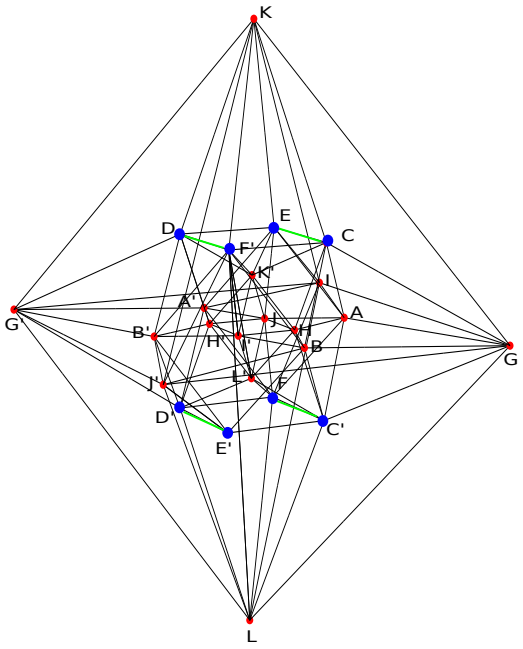

In total there are twenty four 2-handles and it is clear that drawing each 2-handle in a picture like the above would be very cumbersome. Also, drawing all of them together in one picture proves to be a very difficult task, and even when one manages to do so it turns out to be very hard to see which bits of 2-handles belong to which equivalence class. In order to overcome

these management issues of the 2-handles observe that if we split $\mathbb{R}^3$ into the $x-y$, $x-z$ and $y-z$ planes, then all of the 1-handles will lie in these planes. For example the 1-handles $A-A'$ and $B-B'$ lie in the $x-y$ plane, $C-C'$ and $D-D'$ lie in the $x-z$ plane, $E-E'$ and $F-F'$ lie in the $y-z$ plane. Some 1-handles will lie in the intersection of these planes, for example $I-I'$ lies in both the $x-y$ and $y-z$ planes. Exactly which plane (or planes) each 1-handle lies in can be found by simply looking at the table above showing the co-ordinates of the 1-handles. Due to the fact that each 1-handle lies in at least one of three 2-planes, it turns out that many of the 2-handles will lie in one of these three 2-planes. The upshot of all of this is that if we split $\mathbb{R}^3$ into these three 2-planes, we can then visualise the various 2-handles in each 2-plane separately. Unfortunately this hinges on the fact that every 2-handle resides on one of these three 2-planes, and this is not true. It turns out that there are always six 2-handles which will not lie in any one of the $x-y$, $x-z$ or $y-z$ planes. Therefore what we have to do is draw these six special 2-handles in a separate diagram, this means to show the structure of the 2-handles for each of the Ratcliffe-Tschantz manifolds we will draw four diagrams. Three diagrams will consist of those 2-handles lying in the $x-y$, $x-z$, $y-z$ planes and one more diagram showing the six special 2-handles that do not lie in any of these three 2-planes.

The following picture shows those 2-handles of manifold no. 3 that lie in the $x-y$ plane. We have drawn the 1-handles as 3-balls now as we have enough space to do so.

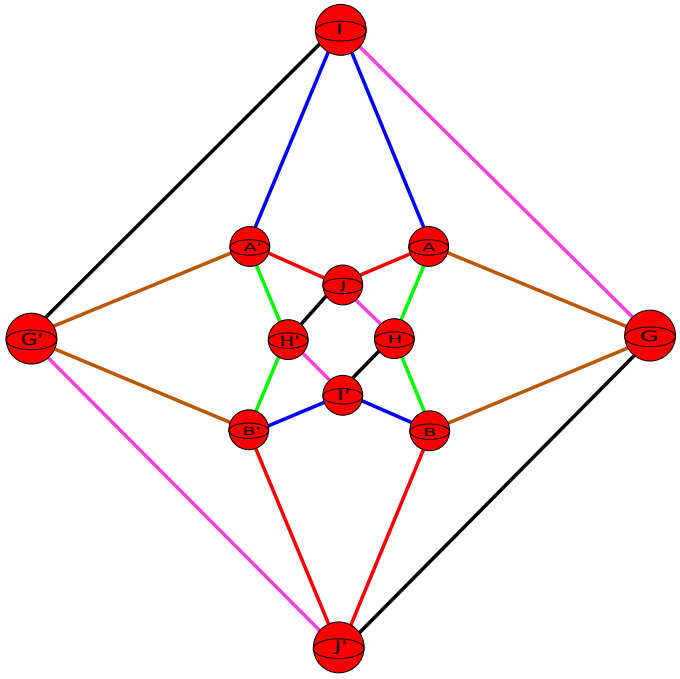

The 2-handles have been colour coded to make it easier to see which bits of 2-handle correspond to which 2-handle.

The following table shows which 2-handle corresponds to which colour:

colour	equivalence class
green	$A \cap H \xrightarrow{a} A' \cap H' \xrightarrow{h^{-1}} B \cap H \xrightarrow{b} B' \cap H' \xrightarrow{h^{-1}} A \cap H$
red	$A \cap J \xrightarrow{a} A' \cap J \xrightarrow{j} B \cap J' \xrightarrow{b} B' \cap J' \xrightarrow{j^{-1}} A \cap J$
brown	$A \cap G \xrightarrow{a} A' \cap G' \xrightarrow{g^{-1}} B \cap G \xrightarrow{b} B' \cap G' \xrightarrow{g^{-1}} A \cap G$
blue	$A \cap I \xrightarrow{a} A' \cap I \xrightarrow{i} B \cap I' \xrightarrow{b} B' \cap I' \xrightarrow{i^{-1}} A \cap I$
pink	$G \cap I \xrightarrow{g} G' \cap J' \xrightarrow{j^{-1}} H \cap J \xrightarrow{h} H' \cap I' \xrightarrow{i^{-1}} G \cap I$
black	$G \cap J' \xrightarrow{g} G' \cap I \xrightarrow{i} H \cap I' \xrightarrow{h} H' \cap J \xrightarrow{j} G \cap J'$

The following picture shows those 2-handles that lie in the $x - z$ plane, with the table after it telling you which 2-handle corresponds to which colour.

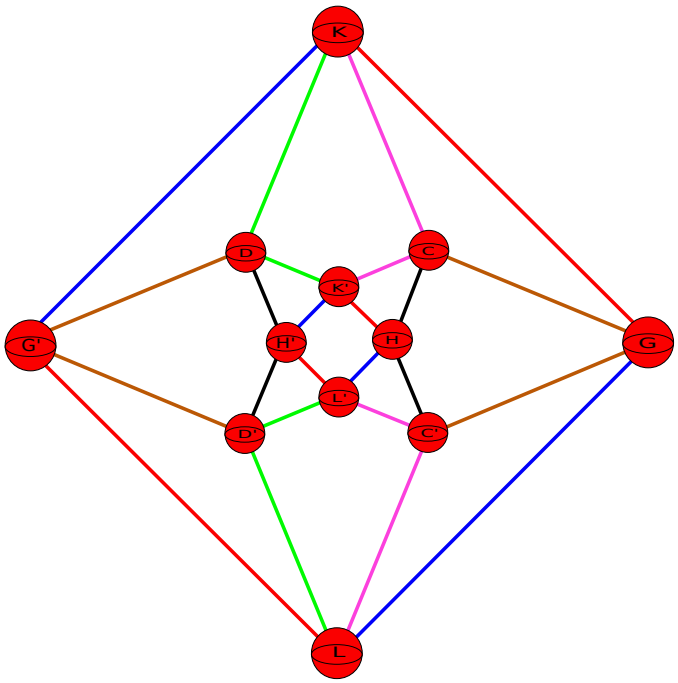

colour	equivalence class
green	$D \cap K \xrightarrow{d} D' \cap L \xrightarrow{l} D' \cap L' \xrightarrow{d^{-1}} D \cap K' \xrightarrow{k^{-1}} D \cap K$
red	$G \cap K \xrightarrow{g} G' \cap L \xrightarrow{l} H' \cap L' \xrightarrow{h^{-1}} H \cap K' \xrightarrow{k^{-1}} G \cap K$
brown	$C \cap G \xrightarrow{c} C' \cap G \xrightarrow{g} D \cap G' \xrightarrow{d} D' \cap G' \xrightarrow{g^{-1}} C \cap G$
blue	$G \cap L \xrightarrow{g} G' \cap K \xrightarrow{k} H' \cap K' \xrightarrow{h^{-1}} H \cap L' \xrightarrow{l^{-1}} G \cap L$
pink	$C \cap K \xrightarrow{c} C' \cap L \xrightarrow{l} C' \cap L' \xrightarrow{c^{-1}} C \cap K' \xrightarrow{k^{-1}} C \cap K$
black	$C \cap H \xrightarrow{c} C' \cap H \xrightarrow{h} D \cap H' \xrightarrow{d} D' \cap H' \xrightarrow{h^{-1}} C \cap H$

The following picture shows those 2-handles that lie in the $y-z$ plane.

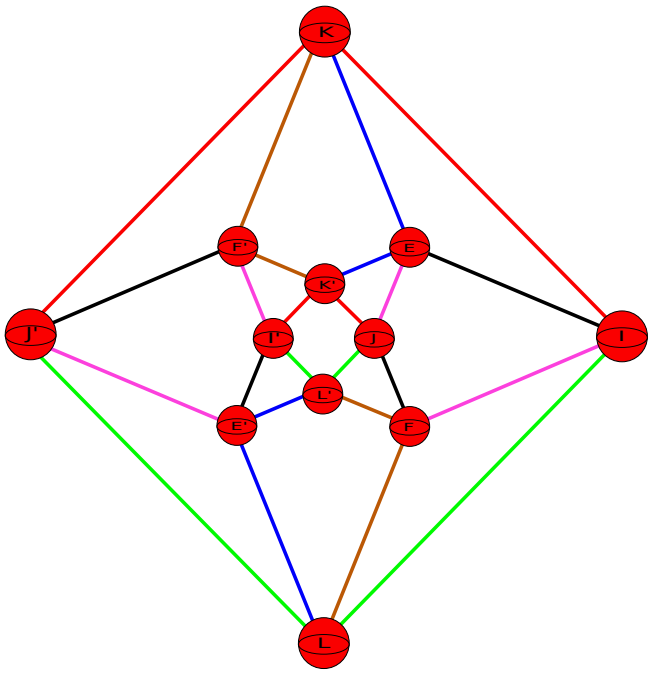

colour	equivalence class
green	$I \cap L \xrightarrow{i} I' \cap L' \xrightarrow{l^{-1}} J' \cap L \xrightarrow{j^{-1}} J \cap L' \xrightarrow{l^{-1}} I \cap L$
red	$I \cap K \xrightarrow{i} I' \cap K' \xrightarrow{k^{-1}} J' \cap K \xrightarrow{j^{-1}} J \cap K' \xrightarrow{k^{-1}} I \cap K$
brown	$F \cap L \xrightarrow{f} F' \cap K \xrightarrow{k} F' \cap K' \xrightarrow{f^{-1}} F \cap L' \xrightarrow{l^{-1}} F \cap L$
blue	$E \cap K \xrightarrow{e} E' \cap L \xrightarrow{l} E' \cap L' \xrightarrow{e^{-1}} E \cap K' \xrightarrow{k^{-1}} E \cap K$
pink	$E \cap J \xrightarrow{e} E' \cap I' \xrightarrow{i^{-1}} F \cap I \xrightarrow{f} F' \cap J' \xrightarrow{j^{-1}} E \cap J$
black	$E \cap I \xrightarrow{e} E' \cap J' \xrightarrow{j^{-1}} F \cap J \xrightarrow{f} F' \cap I' \xrightarrow{i^{-1}} E \cap I$

The final diagram shows a picture of those six 2-handles that do not lie in any one of the $x-y$, $x-z$, $y-z$ planes.

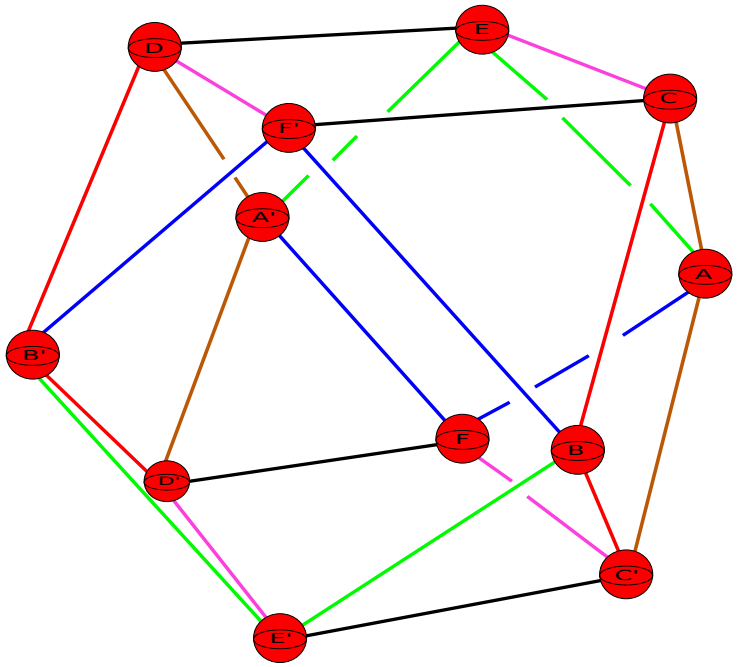

colour	equivalence class
green	$A \cap E \xrightarrow{a} A' \cap E \xrightarrow{e} B \cap E' \xrightarrow{b} B' \cap E' \xrightarrow{e^{-1}} A \cap E$
red	$B \cap C \xrightarrow{b} B' \cap D \xrightarrow{d} B' \cap D' \xrightarrow{b^{-1}} B \cap C' \xrightarrow{c^{-1}} B \cap C$
brown	$A \cap C \xrightarrow{a} A' \cap D \xrightarrow{d} A' \cap D' \xrightarrow{a^{-1}} A \cap C' \xrightarrow{c^{-1}} A \cap C$
blue	$A \cap F \xrightarrow{a} A' \cap F \xrightarrow{f} B \cap F' \xrightarrow{b} B' \cap F' \xrightarrow{f^{-1}} A \cap F$
pink	$C \cap E \xrightarrow{c} C' \cap F \xrightarrow{f} D \cap F' \xrightarrow{d} D' \cap E' \xrightarrow{e^{-1}} C \cap E$
black	$C \cap F' \xrightarrow{c} C' \cap E' \xrightarrow{e^{-1}} D \cap E \xrightarrow{d} D' \cap F \xrightarrow{f} C \cap F'$

The above four diagrams showing the various 2-handles constitutes a complete Kirby diagram for manifold no. 3, and every Ratcliffe-Tschantz manifold has a Kirby diagram that can be visualised by four similar diagrams.

The 3-handles can be found in a similar way, the starting point is to work out all codimension 3 equivalence classes. A codimension 3 side is obtained by intersecting three distinct codimension 1 sides. We already know that two codimension 1 sides intersect if the centre co-ordinates defining the associated spheres have a common non-zero entry in the same position, and the other non-zero entry are in different positions. Three codimension 1 sides have non-empty intersection if any pair of sides from the three sides have non-empty intersection. We then find an equivalence class as in the codimension 2 case, take such a non-empty intersection and apply side pairing transformations until you cycle back to the original intersection of the three sides.

Doing this for all codimension 3 sides gives us all the equivalence classes, which in turn gives us all the 3-handles.

The following table shows all the codimension 3 equivalence classes, there are twelve in total and each class contains eight sides.

1.	$A \cap C \cap E \xrightarrow{a} A' \cap D \cap E \xrightarrow{e} B \cap C' \cap E' \xrightarrow{b} B' \cap D' \cap E' \xrightarrow{d^{-1}} B' \cap D \cap F' \xrightarrow{b^{-1}} B \cap C \cap F' \xrightarrow{f^{-1}} A' \cap D' \cap F \xrightarrow{a^{-1}} A \cap C' \cap F$
2.	$A \cap C \cap G \xrightarrow{a} A' \cap D \cap G' \xrightarrow{g^{-1}} B \cap C' \cap G \xrightarrow{b} B' \cap D' \cap G' \xrightarrow{d^{-1}} B' \cap D \cap G' \xrightarrow{b^{-1}} B \cap C \cap G \xrightarrow{g} A' \cap D' \cap G' \xrightarrow{a^{-1}} A \cap C' \cap G$
3.	$A \cap C \cap H \xrightarrow{a} A' \cap D \cap H' \xrightarrow{h^{-1}} B \cap C' \cap H \xrightarrow{b} B' \cap D' \cap H' \xrightarrow{d^{-1}} B' \cap D \cap H' \xrightarrow{b^{-1}} B \cap C \cap H \xrightarrow{h} A' \cap D' \cap H' \xrightarrow{a^{-1}} A \cap C' \cap H$
4.	$A \cap E \cap I \xrightarrow{a} A' \cap E \cap I \xrightarrow{i} B \cap F' \cap I' \xrightarrow{b} B' \cap F' \cap I' \xrightarrow{f^{-1}} A \cap F \cap J \xrightarrow{a} A' \cap F \cap J \xrightarrow{j} B \cap E' \cap J' \xrightarrow{b} B' \cap E' \cap J'$
5.	$A \cap E \cap J \xrightarrow{a} A' \cap E \cap J \xrightarrow{j} B \cap F' \cap J' \xrightarrow{b} B' \cap F' \cap J' \xrightarrow{f^{-1}} A \cap F \cap I \xrightarrow{a} A' \cap F \cap I \xrightarrow{i} B \cap E' \cap I' \xrightarrow{b} B' \cap E' \cap I'$
6.	$A \cap G \cap I \xrightarrow{a} A' \cap G' \cap I \xrightarrow{i} B \cap H \cap I' \xrightarrow{b} B' \cap H' \cap I' \xrightarrow{h^{-1}} A \cap H \cap J \xrightarrow{a} A' \cap H' \cap J \xrightarrow{j} B \cap G \cap J' \xrightarrow{b} B' \cap G' \cap J'$
7.	$C \cap E \cap K \xrightarrow{c} C' \cap F \cap L \xrightarrow{l} C' \cap F \cap L' \xrightarrow{c^{-1}} C \cap E \cap K' \xrightarrow{e} D' \cap E' \cap L' \xrightarrow{d^{-1}} D \cap F' \cap K' \xrightarrow{k^{-1}} D \cap F' \cap K \xrightarrow{d} D' \cap E' \cap L$
8.	$C \cap F' \cap K \xrightarrow{c} C' \cap E' \cap L \xrightarrow{l} C' \cap E' \cap L' \xrightarrow{c^{-1}} C \cap F' \cap K' \xrightarrow{f^{-1}} D' \cap F \cap L' \xrightarrow{d^{-1}} D \cap E \cap K' \xrightarrow{k^{-1}} D \cap E \cap K \xrightarrow{d} D' \cap F \cap L$
9.	$C \cap G \cap K \xrightarrow{c} C' \cap G \cap L \xrightarrow{l} C' \cap H \cap L' \xrightarrow{c^{-1}} C \cap H \cap K' \xrightarrow{h} D' \cap H' \cap L' \xrightarrow{d^{-1}} D \cap H' \cap K' \xrightarrow{k^{-1}} D \cap G' \cap K \xrightarrow{d} D' \cap G' \cap L$
10.	$E \cap I \cap K \xrightarrow{e} E' \cap J' \cap L \xrightarrow{l} E' \cap I' \cap L' \xrightarrow{e^{-1}} E \cap J \cap K' \xrightarrow{j} F' \cap J' \cap K \xrightarrow{f^{-1}} F \cap I \cap L \xrightarrow{l} F \cap J \cap L' \xrightarrow{f} F' \cap I' \cap K'$
11.	$G \cap I \cap K \xrightarrow{g} G' \cap J' \cap L \xrightarrow{l} H' \cap I' \cap L' \xrightarrow{h^{-1}} H \cap J \cap K' \xrightarrow{j} G' \cap J' \cap K \xrightarrow{g^{-1}} G \cap I \cap L \xrightarrow{l} H \cap J \cap L' \xrightarrow{h} H' \cap I' \cap K'$
12.	$G \cap J' \cap K \xrightarrow{g} G' \cap I \cap L \xrightarrow{l} H' \cap J \cap L' \xrightarrow{h^{-1}} H \cap I' \cap K' \xrightarrow{i^{-1}} G' \cap I \cap K \xrightarrow{g^{-1}} G \cap J' \cap L \xrightarrow{l} H \cap I' \cap L' \xrightarrow{h} H' \cap J \cap K'$

As each class contains eight elements we find that each 3-handle will consist of eight triangles.

The following picture shows the 3-handle corresponding to the class:

$$A \cap C \cap E \xrightarrow{a} A' \cap D \cap E \xrightarrow{e} B \cap C' \cap E' \xrightarrow{b} B' \cap D' \cap E' \xrightarrow{d^{-1}} B' \cap D \cap F' \xrightarrow{b^{-1}} B \cap C \cap F' \xrightarrow{f^{-1}} A' \cap D' \cap F \xrightarrow{a^{-1}} A \cap C' \cap F$$

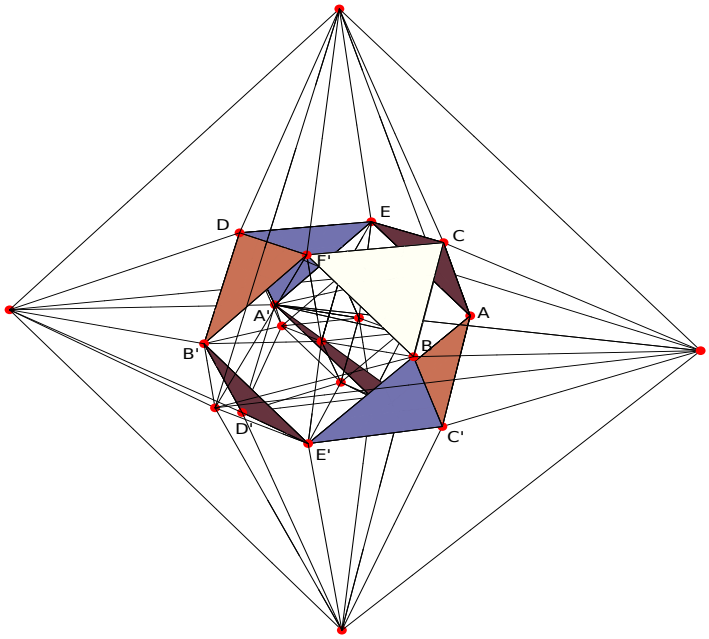

We have used a few colours to colour the triangles in the above picture to make it easier for the reader to see exactly where each triangle lies. The totality of all eight triangles represents one 3-handle.

The following picture shows the 3-handle corresponding to the class:

$$A \cap C \cap G \xrightarrow{a} A' \cap D \cap G' \xrightarrow{g^{-1}} B \cap C' \cap G \xrightarrow{b} B' \cap D' \cap G' \xrightarrow{d^{-1}} B' \cap D \cap G' \xrightarrow{b^{-1}} B \cap C \cap G \xrightarrow{g} A' \cap D' \cap G' \xrightarrow{a^{-1}} A \cap C' \cap G$$

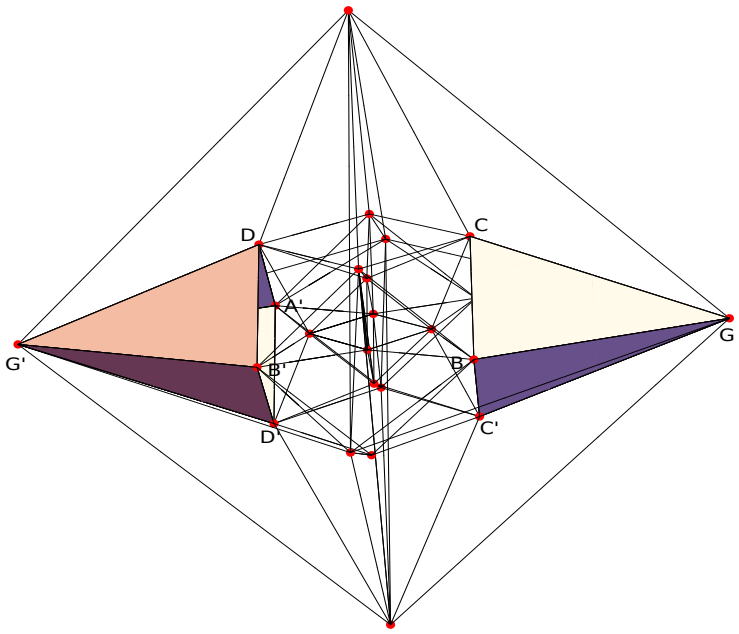

In the above picture we cannot see all components of the 3-handle, the bit of handle corresponding to $A \cap C \cap G$ lies behind $B \cap C \cap G$, and the bit corresponding to $A \cap C' \cap G$ lies behind $B \cap C' \cap G$.

The following picture shows the 3-handle corresponding to the class:

$$A \cap C \cap H \xrightarrow{a} A' \cap D \cap H' \xrightarrow{h^{-1}} B \cap C' \cap H \xrightarrow{b} B' \cap D' \cap H' \xrightarrow{d^{-1}} B' \cap D \cap H' \xrightarrow{b^{-1}} B \cap C \cap H \xrightarrow{h} A' \cap D' \cap H' \xrightarrow{a^{-1}} A \cap C' \cap H$$

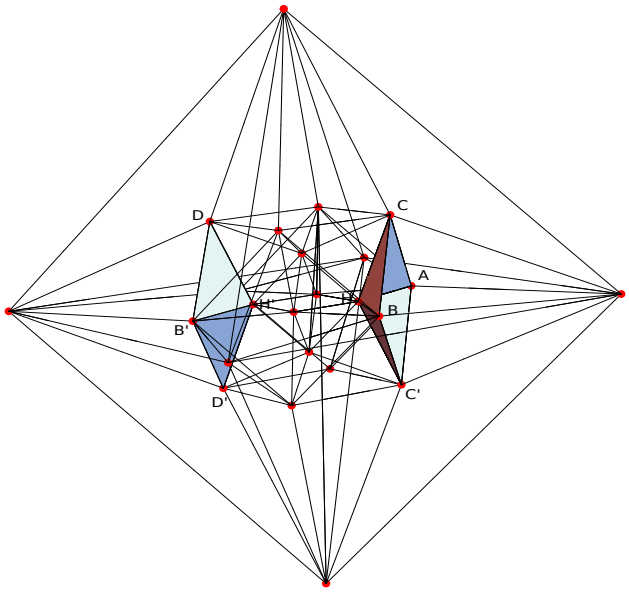

The triangles corresponding to $A' \cap D \cap H'$ and $A' \cap D' \cap H'$ lie behind $B' \cap D \cap H'$ and $B' \cap D' \cap H'$ respectively, and hence cannot be seen in the above picture. The above pictures of the first three 3-handles show that they do not lie in any one of the $x-y$, $x-z$ or $y-z$ planes. In general only three 3-handles will lie in any one of the $x-y$, $x-z$ or $y-z$ planes. For manifold no. 3 the 3-handles corresponding to orbits of $A \cap G \cap I$, $C \cap G \cap K$ and $E \cap I \cap K$ (numbers 6, 9 and 10 in the above table) all lie in the $x-y$, $x-z$ and $y-z$ planes respectively

The following picture shows the 3-handle corresponding to the class determined by $A \cap G \cap I$.

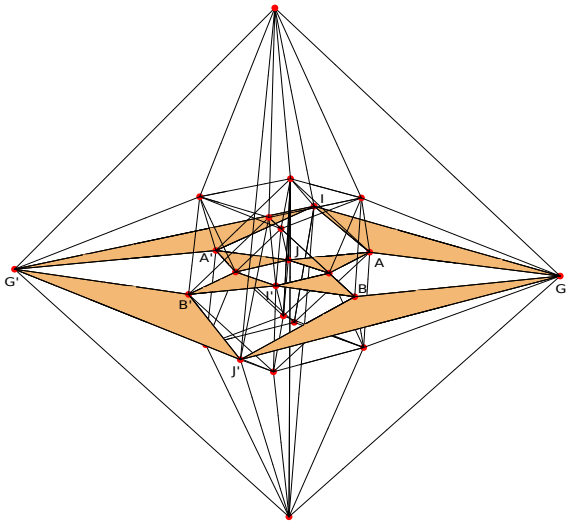

In summary we have shown the handle structure of the 4-manifold numbered 3 in the Ratcliffe-Tschantz census (see table 1.1), furthermore we have explicitly shown how the 2-handle structure

can be clearly visualised via a Kirby diagram consisting of four diagrams. When we consider boundary fillings these diagrams will prove to be invaluable. Let us mention that the choice of the orientable manifold numbered 3 was completely arbitrary, one can obtain similar handle structures for any of the orientable manifolds, the associated Kirby diagram describing the 2-handle structure can also be clearly visualised through four separate diagrams.

All the manifolds in table 1.1 are orientable, however most of the Ratcliffe-Tschantz manifolds are non-orientable and one can ask whether we can obtain Kirby diagrams in a similar fashion for all of them. The procedure is exactly analogous to the orientable case, for the sake of completeness we give one non-orientable example.

Towards the beginning of their paper, Ratcliffe and Tschantz make special mention of one particular non-orientable manifold. They say "quite surprisingly, there is a congruence two 24-cell manifold with an even larger symmetry group of order 320. This manifold has the largest symmetry group among all the congruence two 24-cell manifolds. If one equates beauty with symmetry, then this manifold is the most beautiful congruence two 24-cell manifold" (see p. 102, second last paragraph in [17]). By "congruence two 24-cell manifold" they mean one of the Ratcliffe-Tschantz manifolds. The most beautiful manifold they speak of is numbered 1011 in the census, we believe such a comment gives enough incentive to investigate this manifold from the handle decomposition viewpoint out of the possible 1149 choices. Therefore we start by describing, as in the case of manifold no. 3, its handle decomposition.

The side pairing code for manifold 1011 is **14FF28**, decoding this we obtain the explicit transformations:

$$S_{(+1,+1,0,0)} \xrightarrow[k_{(-1,+1,+1,+1)}]{a} S_{(-1,+1,0,0)} \qquad S_{(+1,-1,0,0)} \xrightarrow[k_{(-1,+1,+1,+1)}]{b} S_{(-1,-1,0,0)}$$

$$S_{(+1,0,+1,0)} \xrightarrow[k_{(+1,+1,-1,+1)}]{c} S_{(+1,0,-1,0)} \qquad S_{(-1,0,+1,0)} \xrightarrow[k_{(+1,+1,-1,+1)}]{d} S_{(-1,0,-1,0)}$$

$$S_{(0,+1,+1,0)} \xrightarrow[k_{(-1,-1,-1,-1)}]{e} S_{(0,-1,-1,0)} \qquad S_{(0,+1,-1,0)} \xrightarrow[k_{(-1,-1,-1,-1)}]{f} S_{(0,-1,+1,0)}$$

$$S_{(+1,0,0,+1)} \xrightarrow[k_{(-1,-1,-1,-1)}]{g} S_{(-1,0,0,-1)} \qquad S_{(+1,0,0,-1)} \xrightarrow[k_{(-1,-1,-1,-1)}]{h} S_{(-1,0,0,+1)}$$

$$S_{(0,+1,0,+1)} \xrightarrow[k_{(+1,-1,+1,+1)}]{i} S_{(0,-1,0,+1)} \qquad S_{(0,+1,0,-1)} \xrightarrow[k_{(+1,-1,+1,+1)}]{j} S_{(0,-1,0,-1)}$$

$$S_{(0,0,+1,+1)} \xrightarrow[k_{(+1,+1,+1,-1)}]{k} S_{(0,0,+1,-1)} \qquad S_{(0,0,-1,+1)} \xrightarrow[k_{(+1,+1,+1,-1)}]{l} S_{(0,0,-1,-1)} \ .$$

The labelling of the 1-handles and their co-ordinates in $\mathbb{R}^3$ is shown in the following table:

A	S_{++00}	$(\frac{1}{\sqrt{2}}, \frac{1}{\sqrt{2}}, 0)$	A'	S_{-+00}	$(\frac{-1}{\sqrt{2}}, \frac{1}{\sqrt{2}}, 0)$
B	S_{+-00}	$(\frac{1}{\sqrt{2}}, \frac{-1}{\sqrt{2}}, 0)$	B'	S_{--00}	$(\frac{-1}{\sqrt{2}}, \frac{-1}{\sqrt{2}}, 0)$
C	S_{+0+0}	$(\frac{1}{\sqrt{2}}, 0, \frac{1}{\sqrt{2}})$	C'	S_{+0-0}	$(\frac{1}{\sqrt{2}}, 0, \frac{-1}{\sqrt{2}})$
D	S_{-0+0}	$(\frac{-1}{\sqrt{2}}, 0, \frac{1}{\sqrt{2}})$	D'	S_{-0-0}	$(\frac{-1}{\sqrt{2}}, 0, \frac{-1}{\sqrt{2}})$
E	S_{0++0}	$(0, \frac{1}{\sqrt{2}}, \frac{1}{\sqrt{2}})$	E'	S_{0--0}	$(0, \frac{-1}{\sqrt{2}}, \frac{-1}{\sqrt{2}})$
F	S_{0+-0}	$(0, \frac{1}{\sqrt{2}}, \frac{-1}{\sqrt{2}})$	F'	S_{0-+0}	$(0, \frac{-1}{\sqrt{2}}, \frac{1}{\sqrt{2}})$
G	S_{+00+}	$(1+\sqrt{2}, 0, 0)$	G'	S_{-00-}	$(1-\sqrt{2}, 0, 0)$
H	S_{+00-}	$(-1+\sqrt{2}, 0, 0)$	H'	S_{-00+}	$(-1-\sqrt{2}, 0, 0)$
I	S_{0+0+}	$(0, 1+\sqrt{2}, 0)$	I'	S_{0-0+}	$(0, -1-\sqrt{2}, 0)$
J	S_{0+0-}	$(0, -1+\sqrt{2}, 0)$	J'	S_{0-0-}	$(0, 1-\sqrt{2}, 0)$
K	S_{00++}	$(0, 0, 1+\sqrt{2})$	K'	S_{00+-}	$(0, 0, -1+\sqrt{2})$
L	S_{00-+}	$(0, 0, -1-\sqrt{2})$	L'	S_{00--}	$(0, 0, 1-\sqrt{2})$

The twenty four equivalence classes of 2 handles is given in the following table with identifying transformations.

1.	$A \cap C \xrightarrow{a} A' \cap D \xrightarrow{d} A' \cap D' \xrightarrow{a^{-1}} A \cap C' \xrightarrow{c^{-1}} A \cap C$
2.	$A \cap G \xrightarrow{a} A' \cap H' \xrightarrow{h^{-1}} B \cap H \xrightarrow{b} B' \cap G' \xrightarrow{g^{-1}} A \cap G$
3.	$A \cap H \xrightarrow{a} A' \cap G' \xrightarrow{g^{-1}} B \cap G \xrightarrow{b} B' \cap H' \xrightarrow{h^{-1}} A \cap H$
4.	$A \cap E \xrightarrow{a} A' \cap E \xrightarrow{e} B \cap E' \xrightarrow{b} B' \cap E' \xrightarrow{e^{-1}} A \cap E$
5.	$A \cap F \xrightarrow{a} A' \cap F \xrightarrow{f} B \cap F' \xrightarrow{b} B' \cap F' \xrightarrow{f^{-1}} A \cap F$
6.	$A \cap I \xrightarrow{a} A' \cap I \xrightarrow{i} B' \cap i' \xrightarrow{b^{-1}} B \cap I' \xrightarrow{i^{-1}} A \cap I$
7.	$A \cap J \xrightarrow{a} A' \cap J \xrightarrow{j} B' \cap J' \xrightarrow{b^{-1}} B \cap J' \xrightarrow{j^{-1}} A \cap J$
8.	$B \cap C \xrightarrow{b} B' \cap D \xrightarrow{d} B' \cap D' \xrightarrow{b^{-1}} B \cap C' \xrightarrow{c^{-1}} B \cap C$
9.	$C \cap G \xrightarrow{c} C' \cap G \xrightarrow{g} D \cap G' \xrightarrow{d} D' \cap G' \xrightarrow{g^{-1}} C \cap G$
10.	$C \cap H \xrightarrow{c} C' \cap H \xrightarrow{h} D \cap H' \xrightarrow{d} D' \cap H' \xrightarrow{h^{-1}} C \cap H$
11.	$C \cap E \xrightarrow{c} C' \cap F \xrightarrow{f} D \cap F' \xrightarrow{d} D' \cap E' \xrightarrow{e^{-1}} C \cap E$
12.	$C \cap F' \xrightarrow{c} C' \cap E' \xrightarrow{e^{-1}} D \cap E \xrightarrow{d} D' \cap F \xrightarrow{f} C \cap F'$
13.	$C \cap K \xrightarrow{c} C' \cap L \xrightarrow{l} C' \cap L' \xrightarrow{c^{-1}} C \cap K' \xrightarrow{k^{-1}} C \cap K$
14.	$D \cap K \xrightarrow{d} D' \cap L \xrightarrow{l} D' \cap L' \xrightarrow{d^{-1}} D \cap K' \xrightarrow{k^{-1}} D \cap K$
15.	$G \cap I \xrightarrow{g} G' \cap J' \xrightarrow{j^{-1}} G' \cap J \xrightarrow{g^{-1}} G \cap I' \xrightarrow{i^{-1}} G \cap I$
16.	$G \cap K \xrightarrow{g} G' \cap L' \xrightarrow{l^{-1}} H' \cap L \xrightarrow{h^{-1}} H \cap K' \xrightarrow{k^{-1}} G \cap K$
17.	$G \cap L \xrightarrow{g} G' \cap K' \xrightarrow{k^{-1}} H' \cap K \xrightarrow{h^{-1}} H \cap L' \xrightarrow{l^{-1}} G \cap L$
18.	$H \cap J \xrightarrow{h} H' \cap I' \xrightarrow{i^{-1}} H' \cap I \xrightarrow{h^{-1}} H \cap J' \xrightarrow{j^{-1}} H \cap J$
19.	$E \cap I \xrightarrow{e} E' \cap J' \xrightarrow{j^{-1}} F \cap J \xrightarrow{f} F' \cap I' \xrightarrow{i^{-1}} E \cap I$
20.	$E \cap J \xrightarrow{e} E' \cap I' \xrightarrow{i^{-1}} F \cap I \xrightarrow{f} F' \cap J' \xrightarrow{j^{-1}} E \cap J$
21.	$E \cap K \xrightarrow{e} E' \cap L' \xrightarrow{l^{-1}} E' \cap L \xrightarrow{e^{-1}} E \cap K' \xrightarrow{k^{-1}} E \cap K$
22.	$F \cap L \xrightarrow{f} F' \cap K' \xrightarrow{k^{-1}} F' \cap K \xrightarrow{f^{-1}} F \cap L' \xrightarrow{l^{-1}} F \cap L$
23.	$I \cap K \xrightarrow{i} I' \cap K \xrightarrow{k} J' \cap K' \xrightarrow{j^{-1}} J \cap K' \xrightarrow{k^{-1}} I \cap K$
24.	$I \cap L \xrightarrow{i} I' \cap L \xrightarrow{l} J' \cap L' \xrightarrow{j^{-1}} J \cap L' \xrightarrow{l^{-1}} I \cap L$

The following picture shows those 2-handles lying in the $x - y$ plane, with the table following explaining the colour coding.

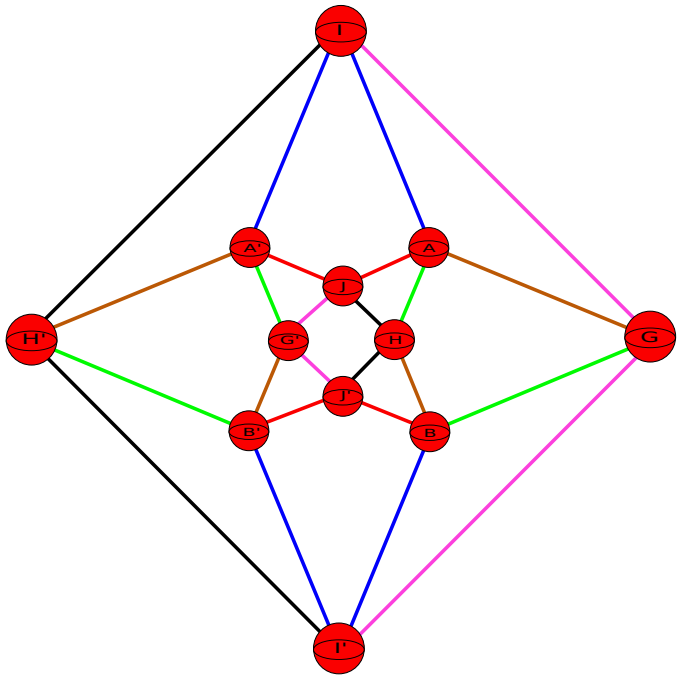

colour	equivalence class
green	$A \cap H \xrightarrow{a} A' \cap G' \xrightarrow{g^{-1}} B \cap G \xrightarrow{b} B' \cap H' \xrightarrow{h^{-1}} A \cap H$
red	$A \cap J \xrightarrow{a} A' \cap J \xrightarrow{j} B' \cap J' \xrightarrow{b^{-1}} B \cap J' \xrightarrow{j^{-1}} A \cap J$
brown	$A \cap G \xrightarrow{a} A' \cap H' \xrightarrow{h^{-1}} B \cap H \xrightarrow{b} B' \cap G' \xrightarrow{g^{-1}} A \cap G$
blue	$A \cap I \xrightarrow{a} A' \cap I \xrightarrow{i} B' \cap I' \xrightarrow{b^{-1}} B \cap I' \xrightarrow{i^{-1}} A \cap I$
pink	$G \cap I \xrightarrow{g} G' \cap J' \xrightarrow{j^{-1}} G' \cap J \xrightarrow{g^{-1}} G \cap I' \xrightarrow{i^{-1}} G \cap I$
black	$H \cap J \xrightarrow{h} H' \cap I' \xrightarrow{i^{-1}} H' \cap I \xrightarrow{h^{-1}} H \cap J' \xrightarrow{j^{-1}} H \cap J$

The 2-handles that lie in the $x - z$ plane can be seen in the following picture.

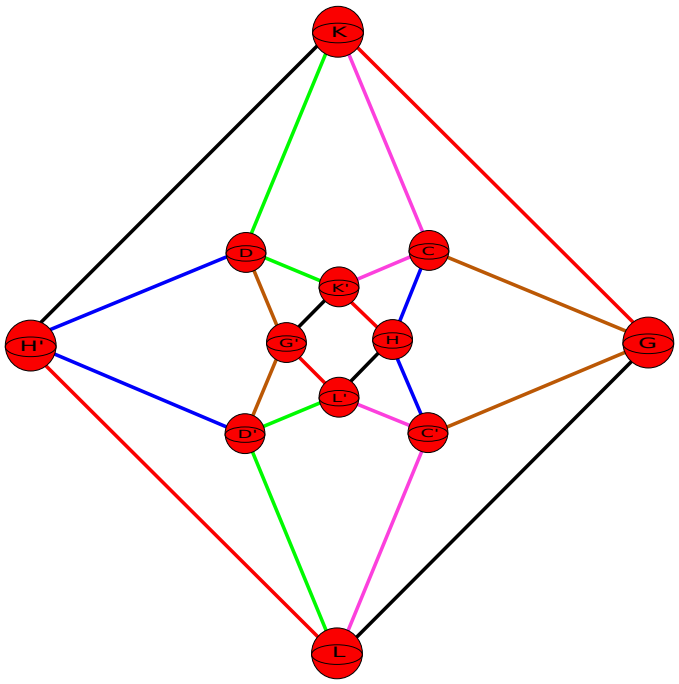

colour	equivalence class
green	$D \cap K \xrightarrow{d} D' \cap L \xrightarrow{l} D' \cap L' \xrightarrow{d^{-1}} D \cap K' \xrightarrow{k^{-1}} D \cap K$
red	$G \cap K \xrightarrow{g} G' \cap L' \xrightarrow{l^{-1}} H' \cap L \xrightarrow{h^{-1}} H \cap K' \xrightarrow{k^{-1}} G \cap K$
brown	$C \cap G \xrightarrow{c} C' \cap G \xrightarrow{g} D \cap G' \xrightarrow{d} D' \cap G' \xrightarrow{g^{-1}} C \cap G$
blue	$C \cap H \xrightarrow{c} C' \cap H \xrightarrow{h} D \cap H' \xrightarrow{d} D' \cap H' \xrightarrow{h^{-1}} C \cap H$
pink	$C \cap K \xrightarrow{c} C' \cap L \xrightarrow{l} C' \cap L' \xrightarrow{c^{-1}} C \cap K' \xrightarrow{k^{-1}} C \cap K$
black	$G \cap L \xrightarrow{g} G' \cap K' \xrightarrow{k^{-1}} H' \cap K \xrightarrow{h^{-1}} H \cap L' \xrightarrow{l^{-1}} G \cap L$

The 2-handles that lie in the $y - z$ plane can be seen in the following picture.

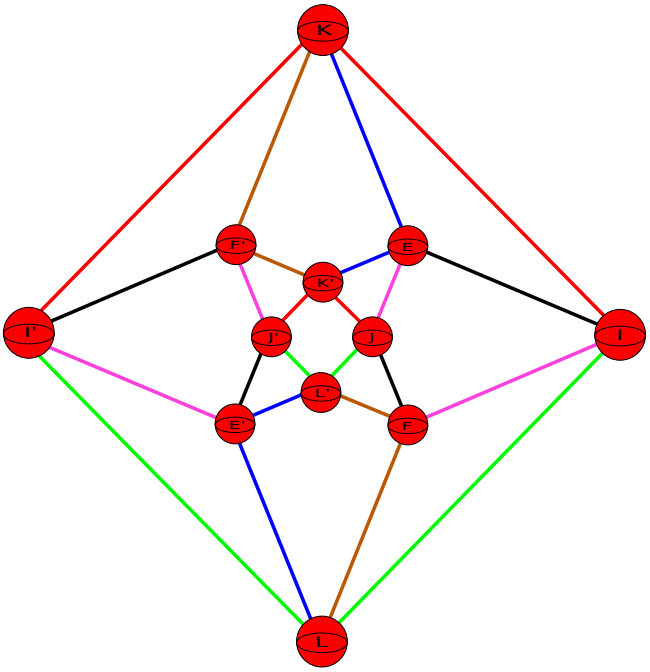

colour	equivalence class
green	$I \cap L \xrightarrow{i} I' \cap L \xrightarrow{l} J' \cap L' \xrightarrow{j^{-1}} J \cap L' \xrightarrow{l^{-1}} I \cap L$
red	$I \cap K \xrightarrow{i} I' \cap K \xrightarrow{k} J' \cap K' \xrightarrow{j^{-1}} J \cap K' \xrightarrow{k^{-1}} I \cap K$
brown	$F \cap L \xrightarrow{f} F' \cap K' \xrightarrow{k^{-1}} F' \cap K \xrightarrow{f^{-1}} F \cap L' \xrightarrow{l^{-1}} F \cap L$
blue	$E \cap K \xrightarrow{e} E' \cap L' \xrightarrow{l^{-1}} E' \cap L \xrightarrow{e^{-1}} E \cap K' \xrightarrow{k^{-1}} E \cap K$
pink	$E \cap J \xrightarrow{e} E' \cap I' \xrightarrow{i^{-1}} F \cap I \xrightarrow{f} F' \cap J' \xrightarrow{j^{-1}} E \cap J$
black	$E \cap I \xrightarrow{e} E' \cap J' \xrightarrow{j^{-1}} F \cap J \xrightarrow{f} F' \cap I' \xrightarrow{i^{-1}} E \cap I$

Finally, the 2-handles that do not lie in any one of the above three planes can be seen in the following picture.

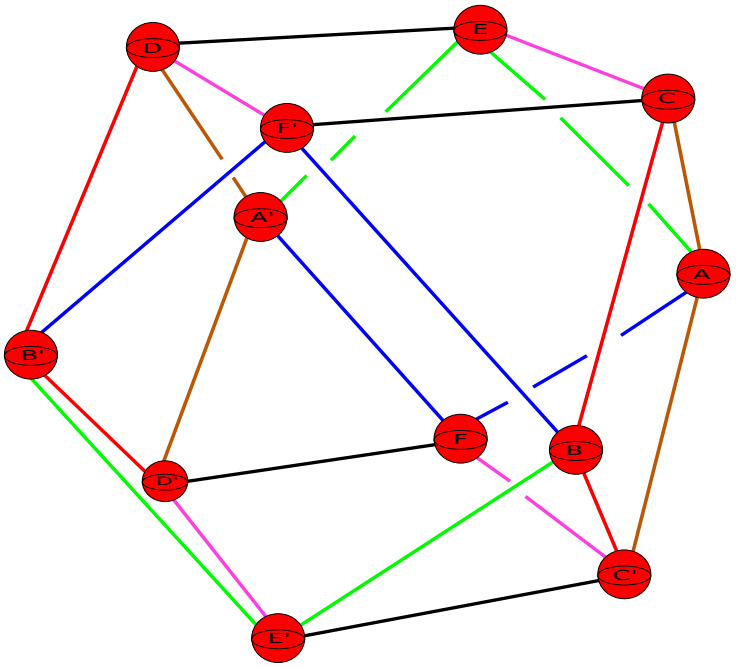

colour	equivalence class
green	$A \cap E \xrightarrow{a} A' \cap E \xrightarrow{e} B \cap E' \xrightarrow{b} B' \cap E' \xrightarrow{e^{-1}} A \cap E$
red	$B \cap C \xrightarrow{b} B' \cap D \xrightarrow{d} B' \cap D' \xrightarrow{b^{-1}} B \cap C' \xrightarrow{c^{-1}} B \cap C$
brown	$A \cap C \xrightarrow{a} A' \cap D \xrightarrow{d} A' \cap D' \xrightarrow{a^{-1}} A \cap C' \xrightarrow{c^{-1}} A \cap C$
blue	$A \cap F \xrightarrow{a} A' \cap F \xrightarrow{f} B \cap F' \xrightarrow{b} B' \cap F' \xrightarrow{f^{-1}} A \cap F$
pink	$C \cap E \xrightarrow{c} C' \cap F \xrightarrow{f} D \cap F' \xrightarrow{d} D' \cap E' \xrightarrow{e^{-1}} C \cap E$
black	$C \cap F' \xrightarrow{c} C' \cap E' \xrightarrow{e^{-1}} D \cap E \xrightarrow{d} D' \cap F \xrightarrow{f} C \cap F'$

1.4 The planar framing of the 2-handles

A 2-handle in a 4-manifold is, by definition, simply a copy of $D^2 \times D^2$ and is attached along a copy of $S^1 \times D^2$. We can think of the attaching data of a 2-handle to consist of two items:

- The attaching circle given by an embedding of $S^1 \times \{0\}$ in the 4-manifold, which is a copy of a knot in the one handle body structure.
- A trivialisation of the normal bundle to the knot coming from the fact that we also have the D^2 factor to take in to account.

When drawing the attaching region of a 2-handle in a Kirby diagram, the general practise is to draw the attaching circle as some knot and then give the information of the trivialisation of the normal bundle to the attaching circle in some external way. The trivialisation of the normal bundle becomes important when one wants to carry out handle slides/cancellations. In the case that the attaching circle of the 2-handle does not run over any 1-handles this is easy to do. Namely, the attaching circle is just a knot in some region of $\mathbb{R}^3$ and the trivialisation of the associated normal bundle is given by an integer, called the *framing number*. The reason why the trivialisation of the normal bundle corresponds to an integer is essentially because one can measure how twisted the normal bundle is by taking a parallel curve to the attaching circle and counting (with sign) how many times it wraps around the attaching circle. One make this intuition rigorous by using the fact that a trivialisation of the normal bundle of the attaching circle of such a 2-handle corresponds to an element of $\pi_1(O(2)) \cong \mathbb{Z}$, after one makes a choice of which element in $\pi_1(O(2))$ corresponds to zero in $\mathbb{Z}$, for this explanation see [8] p.117.
In the general case, the attaching circle of a 2-handle may comprise of several components, consisting of arcs, with each component running over a 1-handle. In this situation one has to be careful about how one encodes the trivialisation of the normal bundle. A natural instinct might be to try and mimic the above case, where our 2-handle did not run across any 1-handles. However one must be very careful in trying to carry this process out, in general such a generalisation of the *framing number* is only well-defined modulo 2 (see [8] p.120 and [1] p.6-7). There are quite a few ways to overcome these technicalities, we will not bother going in to the details of the various ways. Rather, we will keep track of the trivialisation of the normal bundle to our 2-handles by defining what we call a *planar framing*. This will be sufficient for our purposes, especially when we start carrying out handle slides/cancellations.

The following discussion will be valid for any one of the Ratcliffe-Tschantz manifolds. In the next chapter we will be carrying out various handle slides/cancellations associated to a filling of manifold 1011. In view of this we will explain how to keep track of the normal bundle data associated to the attaching circles of the 2-handles of manifold 1011.

To start with we need to explicitly understand what the attaching maps for the attaching spheres of the 1-handles are. We are going to start by giving a description of what the attaching map for the 1-handle A, A' looks like, this description will then provide us with an explicit formula for computing the attaching map for all other 1-handles. The 1-handle A, A' has attaching spheres consisting of one sphere centred at $(\frac{1}{\sqrt{2}}, \frac{1}{\sqrt{2}}, 0)$, denoted by A and another centred at $(\frac{-1}{\sqrt{2}}, \frac{1}{\sqrt{2}}, 0)$, denoted by A'. Recall that the way we obtained the 1-handles in $\mathbb{R}^3$ was to identify each side of the 24-cell with a unique point on S^3 and then use stereographic projection to map this point to a point in $\mathbb{R}^3$. Therefore, if we take a sphere of small radius about $(\frac{1}{\sqrt{2}}, \frac{1}{\sqrt{2}}, 0)$, applying the inverse stereographic projection map we will obtain a small sphere centred about

the point $(\frac{1}{\sqrt{2}}, \frac{1}{\sqrt{2}}, 0, 0)$ and contained in S^3. The line through $(0,0,0,0)$ and $(\frac{1}{\sqrt{2}}, \frac{1}{\sqrt{2}}, 0, 0)$ meets the sphere $S_{(+1,+1,0,0)}$ in a unique point, which we call a_0.

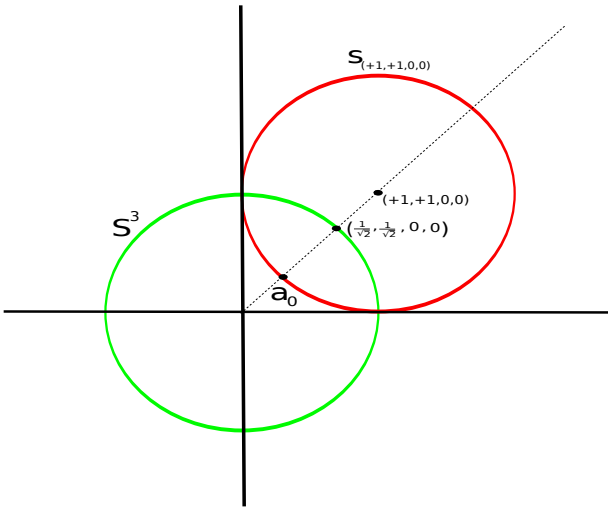

The sphere of small radius centred at $(\frac{1}{\sqrt{2}}, \frac{1}{\sqrt{2}}, 0, 0)$ can then be projected to a sphere of small radius about a_0. When we apply the transformation $a = rk_{(-1,+1,+1,+1)}$, the small sphere about a_0 will get mapped to a small sphere about a point a_1 on the side $S_{(-1,+1,0,0)}$. The point a_1 is given by the intersection of the line through $(0,0,0,0)$ and $(-\frac{1}{\sqrt{2}}, \frac{1}{\sqrt{2}}, 0, 0)$ with the sphere $S_{(-1,+1,0,0)}$. Observe that when applying a the r-part is reflection in the image side, hence does not affect the small sphere about a_0 and contained in $S_{(+1,+1,0,0)}$. We then radially project this small sphere about a_1 to obtain a small sphere about $(-\frac{1}{\sqrt{2}}, \frac{1}{\sqrt{2}}, 0, 0)$ and contained in S^3. Finally, applying the stereographic projection map we end up with a small sphere about the point $(-\frac{1}{\sqrt{2}}, \frac{1}{\sqrt{2}}, 0)$.

In summary, we started with a small sphere centred about $(\frac{1}{\sqrt{2}}, \frac{1}{\sqrt{2}}, 0)$ in $\mathbb{R}^3$, corresponding to the side A, applied a diffeomorphism and obtained another sphere centred about $(-\frac{1}{\sqrt{2}}, \frac{1}{\sqrt{2}}, 0)$ in $\mathbb{R}^3$. This sphere corresponds to the side A'. Note that the sphere centred at $(\frac{1}{\sqrt{2}}, \frac{1}{\sqrt{2}}, 0)$, corresponding to A, may have radius different from that of the image sphere centred at $(-\frac{1}{\sqrt{2}}, \frac{1}{\sqrt{2}}, 0)$, corresponding to A'.

If we let $\phi : S^3 \to \mathbb{R}^3 \cup \{\infty\}$ denote stereographic projection, it is not hard to see that the above diffeomorphism from the attaching sphere corresponding to A to the attaching sphere corresponding to A' is given by

$$\phi \circ k_{(-1,1,1,1)} \circ \phi^{-1}.$$

This argument works for all 1-handles to show that the diffeomorphism that identifies the attaching spheres is given by

$$\phi \circ k \circ \phi^{-1}$$

where k denotes the k-part of the transformation pairing the sides in question.

Using the above formula for the diffeomorphism we can explicitly work out how the attaching spheres of the 1-handles are identified. We give the explicit details for the 1-handle A, A'. In this case the k-part is $k_{(-1,1,1,1)}$, we then need to work out $\phi \circ k_{(-1,1,1,1)} \circ \phi^{-1}$. It is easy to compute this explicitly to obtain

$$\phi \circ k_{(-1,1,1,1)} \circ \phi^{-1}(x, y, z) = (-x, y, z).$$

Therefore the attaching sphere corresponding to A, which is a sphere of small radius about $(\frac{1}{\sqrt{2}}, \frac{1}{\sqrt{2}}, 0)$ is identified to the attaching sphere corresponding to A', which is a sphere centred about $(-\frac{1}{\sqrt{2}}, \frac{1}{\sqrt{2}}, 0)$ via the reflection $(x, y, z) \mapsto (-x, y, z)$.

We can carry out such computations for all 1-handles, the following table tells you exactly what the identifying diffeomorphism is in each case.

1-handle	Identifying diffeomorphism
A, A' & B, B'	$(x, y, z) \mapsto (-x, y, z)$
C, C' & D, D'	$(x, y, z) \mapsto (x, y, -z)$
E, E' & F, F'	$(x, y, z) \mapsto \left(-\frac{x}{x^2+y^2+z^2}, -\frac{y}{x^2+y^2+z^2}, -\frac{z}{x^2+y^2+z^2} \right)$
G, G' & H, H'	$(x, y, z) \mapsto \left(-\frac{x}{x^2+y^2+z^2}, -\frac{y}{x^2+y^2+z^2}, -\frac{z}{x^2+y^2+z^2} \right)$
I, I' & J, J'	$(x, y, z) \mapsto (x, -y, z)$
K, K' & L, L'	$(x, y, z) \mapsto \left(\frac{x}{x^2+y^2+z^2}, \frac{y}{x^2+y^2+z^2}, \frac{z}{x^2+y^2+z^2} \right)$

From the table you can see that all attaching spheres of 1-handles are identified by either a reflection or by a composition of a collections of reflections together with an inversion in S^2.

Now that we know exactly how the attaching spheres of each 1-handle are identified we can deal with the problem of understanding the normal bundle data associated to each 2-handle. We

can split the 2-handles in to two groups, those that lie in the $x-y$, $x-z$ or $y-z$ planes, and the other six that do not all lie in any one of these planes. When carrying out a handle slide of a 2-handle over another 2-handle one has to pick a parallel curve to the 2-handle, the handle slide is then done by carrying out a type of band sum (see [8] p.139 for details). It is in this regard that the trivialisation of the normal bundle of a 2-handle component becomes important as it tells us how the parallel curve looks in our diagram. Therefore we need to consider two situations, how a trivialisation for the normal bundle of those 2-handles lying in the $x-y$, $x-z$ or $y-z$ planes looks, and then how a trivialisation for the normal bundle for the six 2-handles that do not lie in any one of these planes looks.

We start with the case of those 2-handles lying in the $x-y$, $x-z$ or $y-z$ planes. The discussion is the same for each plane so we focus on the $x-y$ plane. Each 2-handle has four components consisting of straight line segments. Fix any 2-handle in the $x-y$ plane, we can then take a parallel straight line segment to one component of the 2-handle and chase it around. What we find is that because the attaching circle of this 2-handle is confined to the $x-y$ plane any parallel curve must also be confined to the $x-y$ plane. What this tells us is that the trivialisation of the normal bundle of a component of such a 2-handle is one that does not "twist" out of the $x-y$ plane i.e. it is confined to the $x-y$ plane. This argument shows that all the 2-handles that reside in one of the $x-y$, $x-z$ or $y-z$ planes have components whose normal bundles are trivialised in a similar manner, in particular this implies that any such parallel curve to such a 2-handle must remain confined to such a plane, and hence cannot twist around any component of the 2-handle in any way. It thus follows that if we were to carry out a handle slide within one of these planes then the resulting 2-handle will also be confined to this plane.

The next case to consider is that of the six 2-handles that do not all lie in the $x-y$, $x-z$ or $y-z$ planes. What we need to do is understand how a parallel curve behaves to each such 2-handle. It is here that it becomes vital that we explicitly know how the attaching spheres associated to each 1-handle are being identified, this is because we are going to take a parallel segment and then follow it along the 2-handle keeping track of how it emerges out of attaching spheres of 1-handles. Let us give the details in the case of the pink 2-handle. We start by taking a parallel curve to the pink 2-handle at the point shown in the following diagram. We take a parallel curve just below the pink 2-handle component running from C to E, shown as a black dashed line.

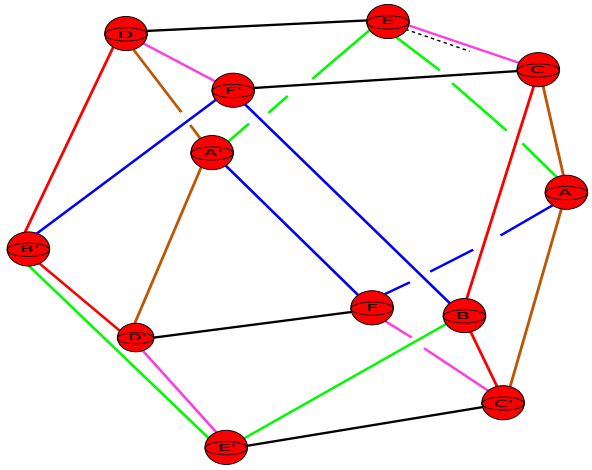

When this parallel curve hits E it comes back out of E', we need to work out exactly where it comes out of E'. Recall from the above we know that the diffeomorphism that identifies the attaching sphere of E to that of E' is given by

$$(x, y, z) \mapsto \left(-\frac{x}{x^2+y^2+z^2}, -\frac{y}{x^2+y^2+z^2}, -\frac{z}{x^2+y^2+z^2} \right)$$

which is a composition of an inversion in the unit sphere centred at the origin together with the antipodal map. First of all, the pink 2-handle component that goes into E comes out of E' in the following way.

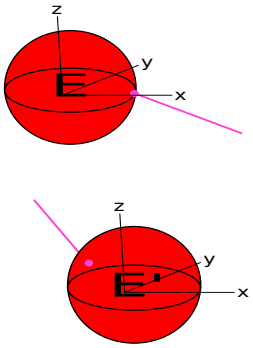

We have put axes at each centre point of each sphere so that the reader knows which directions are positive. To see how we get this diagram, just observe that the point at which the pink 2-handle component hits E can be written as $(r, \frac{1}{\sqrt{2}}, \frac{1}{\sqrt{2}})$, where r is the radius of the attaching sphere (some small number, which we do not need to explicitly know). This point lies outside of the unit sphere $S^2 \subseteq \mathbb{R}^2$. If we apply the inversion map

$$(x, y, z) \mapsto (\frac{x}{x^2+y^2+z^2}, \frac{y}{x^2+y^2+z^2}, \frac{z}{x^2+y^2+z^2})$$

The point $(r, \frac{1}{\sqrt{2}}, \frac{1}{\sqrt{2}})$ will get mapped to $(\frac{r}{r^2+1}, \frac{1}{\sqrt{2}(r^2+1)}, \frac{1}{\sqrt{2}(r^2+1)})$, which lies inside the unit sphere S^2. In fact, the attaching sphere E centred at $(0, \frac{1}{\sqrt{2}}, \frac{1}{\sqrt{2}})$ will map to a sphere under the

inversion map. One can carry out some simple computations to work out that the image sphere will have centre $(0, \frac{1}{\sqrt{2}(1-r^2)}, \frac{1}{\sqrt{2}(1-r^2)})$ and have radius $R := \frac{r}{1-r^2}$. The following diagram shows the image of $(r, \frac{1}{\sqrt{2}}, \frac{1}{\sqrt{2}})$ under the inversion map.

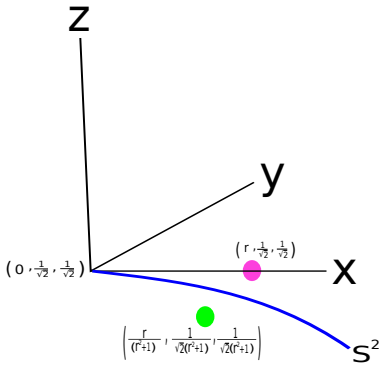

The green point represents the image, and the blue curve represents a piece of S^2 that is intersecting the attaching sphere E. If we now apply the antipodal map to the above green point $(\frac{r}{r^2+1}, \frac{1}{\sqrt{2}(r^2+1)}, \frac{1}{\sqrt{2}(r^2+1)})$ we can see that we will get a point in E' that will look like what we had before (see two diagram above).

We now want to carry out the same analysis for a piece of a parallel curve that hits the attaching sphere E. We start by choosing our component of parallel curve to lie directly below the pink 2-handle component. The following diagram shows a close up of this

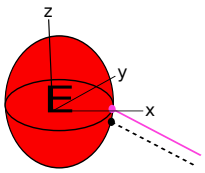

We choose the parallel curve so that it hits the attaching sphere at a point with co-ordinates of the form $(r-\gamma, \frac{1}{\sqrt{2}}, \frac{1}{\sqrt{2}}-\delta)$, where γ and δ are small so that $(r-\gamma, \frac{1}{\sqrt{2}}, \frac{1}{\sqrt{2}}-\delta)$ lies outside of S^2 (i.e. has norm greater than one). When we apply inversion in S^2 the point $(r-\gamma, \frac{1}{\sqrt{2}}, \frac{1}{\sqrt{2}}-\delta)$ will map to $\left(\frac{r-\gamma}{(r-\gamma)^2+\frac{1}{2}+(\frac{1}{\sqrt{2}}-\delta)^2}, \frac{1}{\sqrt{2}} \cdot \frac{r-\gamma}{(r-\gamma)^2+\frac{1}{2}+(\frac{1}{\sqrt{2}}-\delta)^2}, (\frac{1}{\sqrt{2}}-\delta) \cdot \frac{r-\gamma}{(r-\gamma)^2+\frac{1}{2}+(\frac{1}{\sqrt{2}}-\delta)^2}\right)$. The following diagram shows the images of these points under inversion in S^2.

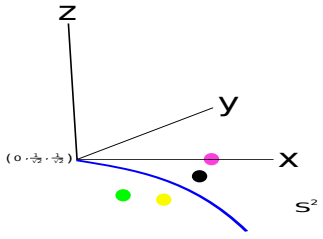

The pink and green points are the same points as before, the black point is $(r-\gamma, \frac{1}{\sqrt{2}}, \frac{1}{\sqrt{2}}-\delta)$, and the yellow point represents the image of the black point under the inversion map. We then apply the antipodal map to find the complete image of the black point. The following diagram shows this image, together with how the parallel curve comes out of E'. The point to take away is that the parallel curve comes out of E' lying a bit below the pink 2-handle component.

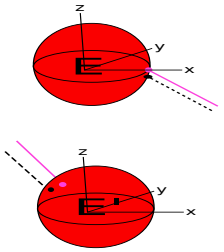

The pink 2-handle component then runs and hits the attaching sphere D', along with the parallel curve this looks like.

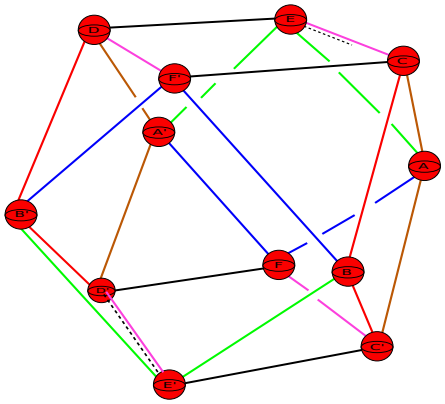

The attaching map for the 1-handle D, D' is given by the reflection $(x, y, z) \mapsto (x, y, -z)$, and in this case it easy to see how the parallel curve component comes out of D. The parallel curve will run slightly above the pink 2-handle component.

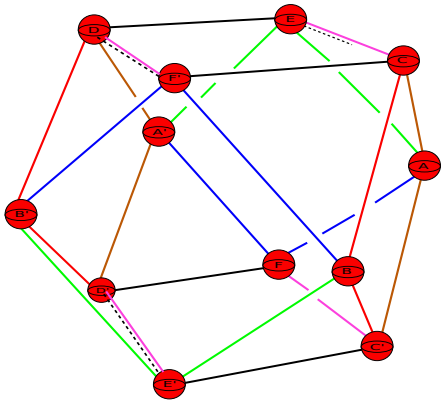

The attaching map for F, F' is the same as the attaching map for E, E', and in order to see how the parallel curve component comes out of F we need to perform a similar sort of analysis as we did for when we tried to understand how it came out of E'. As the details are exactly analogous to what we did for E, E' we won't give the details. The parallel curve comes out a little above the pink 2-handle component as shown in the following diagram.

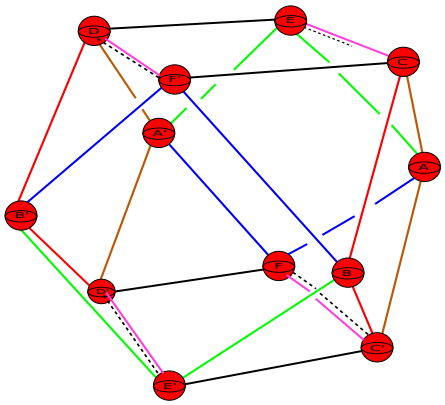

Finally, the attaching map for C, C' is the same as that of D, D', namely the reflection $(x, y, z) \mapsto (x, y, -z)$. It is easy to see that under this map the parallel curve component comes out of C just below the pink 2-handle component and joins up with where our parallel component initially started going in to E. The following picture shows this.

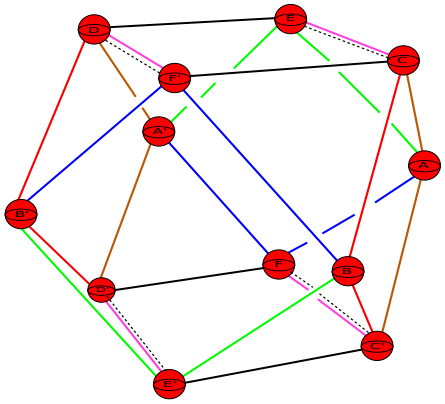

What we have seen is that when we take a parallel curve to the pink 2-handle component and follow it around, nowhere does it cross over the pink 2-handle. In some sense a parallel curve behaves as if the pink 2-handle was confined to a 2-plane. Another way to think of this is that the normal bundle can be given by taking a normal vector to each straight line segment comprising a 2-handle and then using the Euclidean connection, given by the Euclidean dot product, to parallel transport the normal vector along the 2-handle segment. This viewpoint makes it clear that these 2-handles have parallel curves that behave very similar to the 2-handles

that lie in the $x-y$, $x-z$ or $y-z$ planes. Due to this we say that each 2-handle contained in the Kirby diagram of manifold 1011 has a *planar framing*. The word *planar* is used to remind the reader that the parallel curves are behaving as if they were lying in a single 2-plane. Using the fact that the 2-handles in this diagram are given by a planar framing we will find that any handle slide we carry out in this diagram can be done in a very simple manner, just as if the 2-handle we were sliding over lay in one of the $x-y$, $x-z$ or $y-z$ planes.

Although we have focused on manifold 1011 a similar sort of analysis can be applied to show that any one of the Ratcliffe-Tschantz manifolds has a Kirby diagram where all the 2-handles have this *planar framing* type behaviour.

Chapter 2

Elementary Moves and Boundary Fillings

The primary aim of this chapter is to construct an explicit example of a smooth 4-manifold that admits a hyperbolic link complement and whose diffeomorphism type we can characterise. We will start by explaining how the Euclidean structure on each cusp of a Ratcliffe-Tschantz manifold can be understood through an analysis of how a horospherical neighbourhood about an ideal vertex changes as we apply various side pairing transformations. This will then allow us to explicitly construct a fundamental domain for each cusp. We then move on to showing how we can view each cusp in the Kirby diagram we constructed in the previous chapter, and how we can fill in these cusps in a standard way to obtain a closed 4-manifold. In the final section, we show using the theory of Kirby calculus how to obtain an explicit example of a smooth four dimensional hyperbolic link complement in a smooth standard S^4.

2.1 Parabolic transformations and the Euclidean structure of a cusp

In this section we are going to explain how to compute parabolic transformations associated to each cusp component. We are going to focus on the 5-cusped orientable manifolds and the 5-cusped non-orientable manifolds. This means that the methods we employ in this section will be primarily with these manifolds in our viewpoint. The same techniques can be employed to compute parabolic transformations for the 6-cusped manifolds with the only modification needed to do with equivalence classes of ideal vertices. As all the examples we consider will be 5-cusped we will not worry about this modification for the 6-cusped manifolds.

Recall that the 24-cell P has twenty four ideal vertices, eight of the form $(\pm 1, 0, 0, 0)$, $(0, \pm 1, 0, 0)$, $(0, 0, \pm 1, 0)$, $(0, 0, 0, \pm 1)$ and sixteen of the form $(\pm 1/2, \pm 1/2, \pm 1/2, \pm 1/2)$. When we apply any group of side pairing transformations defining any one of the 5-cusped Ratcliffe-Tschantz

manifolds we find that the ideal vertices split into five equivalence classes. We have four of the form:

$$\{(1,0,0,0),(-1,0,0,0)\},\{(0,1,0,0),(0,-1,0,0)\},$$

$$\{(0,0,1,0),(0,0,-1,0)\},\{(0,0,0,1),(0,0,0,-1)\}$$

and one of the form:

$$\{(\pm 1/2,\pm 1/2,\pm 1/2,\pm 1/2)\}.$$

In order to compute the parabolic isometries associated to these five cusps we need to look at horospherical neighbourhoods about each ideal vertex. Recall that given any ideal vertex of the form $(\pm 1,0,0,0)$, $(0,\pm 1,0,0)$, $(0,0,\pm 1,0)$, $(0,0,0,\pm 1)$, such a vertex lies on a given side S if the centre vector of the sphere defining the side has an equal non-zero entry in the same position as the vertex. For example the ideal vertex $(-1,0,0,0)$ lies on the side $S_{(-1,0,0,1)}$ but not on the side $S_{(1,0,0,1)}$ or on the side $S_{(0,1,1,0)}$. Any ideal vertex of the form $(\pm 1/2,\pm 1/2,\pm 1/2,\pm 1/2)$ lies on a side S if the non-zero entries of the centre of the sphere defining the side have the same sign as the non-zero entries in the same position of the ideal vertex. For example the ideal vertex $(1/2,1/2,-1/2,1/2)$ lies on the side $S_{(+1,0,-1,0)}$ but not on the side $S_{(-1,+1,0,0)}$.

The above recollection shows us that each ideal vertex lies on precisely six sides. Since each side of the 24-cell P intersects precisely four other sides, and does so at right angles, we find that a horospherical neighbourhood of any of the ideal vertices is a rectangular box. From this fact it follows that for each of the equivalence classes

$$\{(1,0,0,0),(-1,0,0,0)\},\{(0,1,0,0),(0,-1,0,0)\},$$

$$\{(0,0,1,0),(0,0,-1,0)\},\{(0,0,0,1),(0,0,0,-1)\}$$

the associated boundary cusp will have fundamental domain consisting of two rectangular boxes. For example, if we take the vertex class $\{(1,0,0,0),(-1,0,0,0)\}$ then we can think of a fundamental domain for the associated cusp cross section as a horospherical neighbourhood about the ideal vertex $(1,0,0,0)$ together with a horospherical neighbourhood about the ideal vertex $(-1,0,0,0)$. Similarly for the class $\{(\pm 1/2,\pm 1/2,\pm 1/2,\pm 1/2)\}$, we can think of the boundary cusp cross section as coming from sixteen rectangular boxes, each one corresponding to a horospherical neighbourhood about an ideal vertex making up the equivalence class. In order to understand the structure of these cusp cross sections we need to understand the parabolic isometries associated to them. Through the general theory of non-compact hyperbolic manifolds of finite volume we know that the stabiliser subgroup of an ideal vertex induces the Euclidean structure on the cusp cross section. The way one generally sees this is to observe that if one takes a horospherical neighbourhood about an ideal vertex, then the stabiliser subgroup acts as a group of Euclidean affine transformations on this neighbourhood. Viewing this neighbourhood as a copy of $\mathbb{R}^3$ one observes that the quotient via the action of the stabiliser subgroup

is a Euclidean 3-manifold, the one corresponding to the cusp cross section (the reader who is not familiar with this material can consult [3] Thm.D.3.3, p.145). In order to compute the stabiliser subgroup one can take a horospherical neighbourhood about an ideal vertex and see how it transforms under the side pairing transformations associated to the sides making up the horospherical neighbourhood. We are going to give explicit examples of how to do this shortly. Before we do this let us remind the reader that the Euclidean structure associated to each of the five (or six) cusps is given in the Ratcliffe-Tschantz census under the column headed **LT**. A quick glance at the census shows that many of the manifolds in the census have very different cusp structures, this means that in general one needs to carry out such computations for the particular manifolds they are interested in. That being said, the general principle of how to compute the cusp structures works for all the Ratcliffe-Tschantz manifolds, and is in fact a standard technique from the theory of non-compact hyperbolic manifolds of finite volume.

As promised we are going to give a calculation of the cusp structure for a particular manifold using horospherical neighbourhoods as described above. Since we have already dealt with aspects of manifold no. 3 we choose to use it again. For the convenience of the reader we recall its basic construction. The side pairing code for manifold no. 3 is **1477B8**, decoding this gives the following side pairing transformations:

$$S_{(+1,+1,0,0)} \xrightarrow[k_{(-1,+1,+1,+1)}]{a} S_{(-1,+1,0,0)} \qquad S_{(+1,-1,0,0)} \xrightarrow[k_{(-1,+1,+1,+1)}]{b} S_{(-1,-1,0,0)}$$

$$S_{(+1,0,+1,0)} \xrightarrow[k_{(+1,+1,-1,+1)}]{c} S_{(+1,0,-1,0)} \qquad S_{(-1,0,+1,0)} \xrightarrow[k_{(+1,+1,-1,+1)}]{d} S_{(-1,0,-1,0)}$$

$$S_{(0,+1,+1,0)} \xrightarrow[k_{(-1,-1,-1,+1)}]{e} S_{(0,-1,-1,0)} \qquad S_{(0,+1,-1,0)} \xrightarrow[k_{(-1,-1,-1,+1)}]{f} S_{(0,-1,+1,0)}$$

$$S_{(+1,0,0,+1)} \xrightarrow[k_{(-1,-1,-1,+1)}]{g} S_{(-1,0,0,+1)} \qquad S_{(+1,0,0,-1)} \xrightarrow[k_{(-1,-1,-1,+1)}]{h} S_{(-1,0,0,-1)}$$

$$S_{(0,+1,0,+1)} \xrightarrow[k_{(-1,-1,+1,-1)}]{i} S_{(0,-1,0,-1)} \qquad S_{(0,+1,0,-1)} \xrightarrow[k_{(-1,-1,+1,-1)}]{j} S_{(0,-1,0,+1)}$$

$$S_{(0,0,+1,+1)} \xrightarrow[k_{(+1,+1,+1,-1)}]{k} S_{(0,0,+1,-1)} \qquad S_{(0,0,-1,+1)} \xrightarrow[k_{(+1,+1,+1,-1)}]{l} S_{(0,0,-1,-1)} \ .$$

The labelling of the sides is given in the following table:

A	$S_{(+1,+1,0,0)}$	$(\frac{1}{\sqrt{2}}, \frac{1}{\sqrt{2}}, 0)$	A'	$S_{(-1,+1,0,0)}$	$(\frac{-1}{\sqrt{2}}, \frac{1}{\sqrt{2}}, 0)$
B	$S_{(+1,-1,0,0)}$	$(\frac{1}{\sqrt{2}}, \frac{-1}{\sqrt{2}}, 0)$	B'	$S_{(-1,-1,0,0)}$	$(\frac{-1}{\sqrt{2}}, \frac{-1}{\sqrt{2}}, 0)$
C	$S_{(+1,0,+1,0)}$	$(\frac{1}{\sqrt{2}}, 0, \frac{1}{\sqrt{2}})$	C'	$S_{(+1,0,-1,0)}$	$(\frac{1}{\sqrt{2}}, 0, \frac{-1}{\sqrt{2}})$
D	$S_{(-1,0,+1,0)}$	$(\frac{-1}{\sqrt{2}}, 0, \frac{1}{\sqrt{2}})$	D'	$S_{(-1,0,-1,0)}$	$(\frac{-1}{\sqrt{2}}, 0, \frac{-1}{\sqrt{2}})$
E	$S_{(0,+1,+1,0)}$	$(0, \frac{1}{\sqrt{2}}, \frac{1}{\sqrt{2}})$	E'	$S_{(0,-1,-1,0)}$	$(0, \frac{-1}{\sqrt{2}}, \frac{-1}{\sqrt{2}})$
F	$S_{(0,+1,-1,0)}$	$(0, \frac{1}{\sqrt{2}}, \frac{-1}{\sqrt{2}})$	F'	$S_{(0,-1,+1,0)}$	$(0, \frac{-1}{\sqrt{2}}, \frac{1}{\sqrt{2}})$
G	$S_{(+1,0,0,+1)}$	$(1+\sqrt{2}, 0, 0)$	G'	$S_{(-1,0,0,-1)}$	$(1-\sqrt{2}, 0, 0)$
H	$S_{(+1,0,0,-1)}$	$(-1+\sqrt{2}, 0, 0)$	H'	$S_{(-1,0,0,+1)}$	$(-1-\sqrt{2}, 0, 0)$
I	$S_{(0,+1,0,+1)}$	$(0, 1+\sqrt{2}, 0)$	I'	$S_{(0,-1,0,+1)}$	$(0, -1-\sqrt{2}, 0)$
J	$S_{(0,+1,0,-1)}$	$(0, -1+\sqrt{2}, 0)$	J'	$S_{(0,-1,0,-1)}$	$(0, 1-\sqrt{2}, 0)$
K	$S_{(0,0,+1,+1)}$	$(0, 0, 1+\sqrt{2})$	K'	$S_{(0,0,+1,-1)}$	$(0, 0, -1+\sqrt{2})$
L	$S_{(0,0,-1,+1)}$	$(0, 0, -1-\sqrt{2})$	L'	$S_{(0,0,-1,-1)}$	$(0, 0, 1-\sqrt{2})$

Consider the equivalence class of ideal vertices $\{(1,0,0,0), (-1,0,0,0)\}$, if we start with the ideal vertex $(1,0,0,0)$ then by the above discussion it is easy to see that it lies on the sides A, B, C, C', G and H. The vertex $(1,0,0,0)$ can be thought of as the unit basis vector e_1 in $\mathbb{R}^4$, a horospherical neighbourhood represented by pieces of the sides A, B, C, C', G and H can then be thought of as a rectangular box in $\mathbb{R}^3$ (viewed as an orthogonal hyperplane to e_1). The orientation of the orthogonal copy of $\mathbb{R}^3$ will always be taken to be:

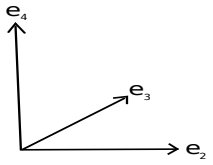

The horospherical neighbourhood will then look like:

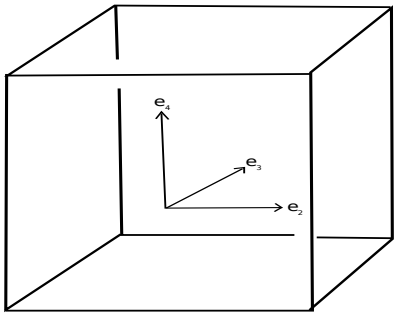

As the side A is defined via the sphere $S_{(+1,+1,0,0)}$ with centre vector $(+1,+1,0,0)$ we see that its intersection with a horospherical neighbourhood about $(1,0,0,0)$ can be thought of as a plane centred at $(x,0,0)$ (here the three co-ordinates are (e_2, e_3, e_4)), where $x \in \mathbb{R}$, and parallel to the plane defined by the equation $e_2 = 0$. The actual value of x is unimportant, it depends on where exactly we form our horospherical neighbourhood about $(1,0,0,0)$, which in turn

comes down to how high up into the horoball about $(1,0,0,0)$ we are. The side B is defined via the sphere $S_{(+1,-1,0,0)}$ with centre vector $(+1,-1,0,0)$, its intersection with a horospherical neighbourhood about $(1,0,0,0)$ can be thought of as a plane centred at $(-x,0,0)$ and parallel to the plane defined by the equation $e_2 = 0$. The side C is defined by the sphere $S_{(+1,0,+1,0)}$ with centre vector $(+1,+1,0,0)$, similar reasoning to the above shows that its intersection with a horospherical neighbourhood about the ideal vertex $(1,0,0,0)$ can be viewed as a plane centred at $(0,y,0)$, where $y \in \mathbb{R}$, parallel to the plane $e_3 = 0$. The side C' can be viewed as a plane centred at $(0,-y,0)$ parallel to the plane $e_3 = 0$. The side G is defined by the sphere $S_{(+1,0,0,+1)}$ with centre vector $(+1,0,0,+1)$, intersecting it with a horospherical neighbourhood about the ideal vertex $(1,0,0,0)$ we obtain a plane centred at $(0,0,z)$, where $z \in \mathbb{R}$ and parallel to the plane $e_4 = 0$. The side H can be viewed as a plane centred at $(0,0,-z)$ parallel to the plane $e_4 = 0$. Using this description we can label the above rectangular box, which represents a horospherical neighbourhood based at $(1,0,0,0)$, as follows:

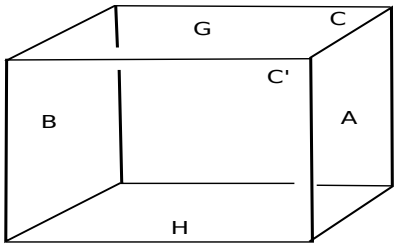

The equivalence class corresponding to the ideal vertex $(+1,0,0,0)$ also contains the ideal vertex $(-1,0,0,0)$, therefore in order to describe the parabolic isometries giving rise to the cusp corresponding to this class we need to describe a horospherical neighbourhood about $(-1,0,0,0)$. The procedure is exactly analogous to what we did above. However, for this vertex we are going to orient the orthogonal copy of $\mathbb{R}^3$ to the vertex $(-1,0,0,0)$ as follows:

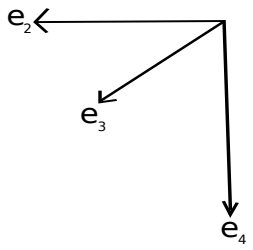

The reason for this choice will become apparent shortly, for now let us observe that it leads to the following labelling of a horospherical neighbourhood:

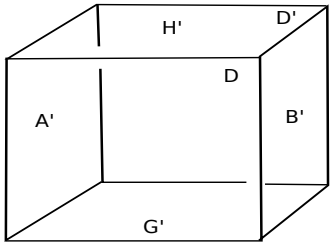

A fundamental domain for a cross section of the cusp corresponding to the above ideal vertex equivalence class consists of these two rectangular boxes.

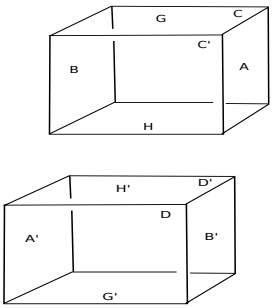

We can see that when we apply the transformation h the bottom face of the top box gets joined to the top face of the bottom box. In principle the bottom face of the top box has four different ways it can be joined to the top face of the bottom box. However, observe that when applying the transformation h, the side B maps to A', side A maps to B', side C maps to D', and side C' maps to D. This means we can visualise a fundamental domain as a rectangular box with sides labelled as follows:

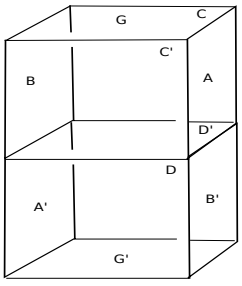

This is why we chose to orient the orthogonal copy of $\mathbb{R}^3$ to the ideal vertex $(-1,0,0,0)$ the way we did. We then see that the top face of the rectangular box will be identified to the bottom face of the rectangular box by the parabolic transformation $g^{-1}h$ (note that $g^{-1}h$ fixes the ideal vertex $(1,0,0,0)$, hence is clearly an element of the stabiliser subgroup of the ideal vertex $(1,0,0,0)$). Similarly the front face will be identified to the back face via the transformation c

(note one could also take the transformation d, they both act in the same way). Finally, the identification of the face on the right side with the left side is done by the transformation $a^{-1}h$, this is because the top right A get identified to the bottom left A', and the bottom right B' gets identified to the top left B. Thus what we see that is happening is that the top face is being identified to the bottom face via a translation, the front face is being identified to the back face via a translation, but the side faces are being identified by a "twist" (also called a screw parabolic transformation). This tells us that the stabiliser subgroup associated to the vertex equivalence class $\{(1,0,0,0),(-1,0,0,0)\}$ is generated by the three transformations $\langle c, g^{-1}h, a^{-1}h\rangle$. Put another way the parabolic subgroup associated to the vertex class $\{(1,0,0,0),(-1,0,0,0)\}$ is the subgroup $\langle c, g^{-1}h, a^{-1}h\rangle$.

Once one has understood the parabolic subgroup associated to a cusp, one can try to understand how the Euclidean structure on the cusp cross section comes about. For a general non-compact hyperbolic manifold of finite volume this can be a difficult task, the reason being that in order to work out the Euclidean structure on the cross section one needs a solid understanding of how elements of the associated parabolic subgroup act as Euclidean transformations on a horospherical neighbourhood. For the Ratcliffe-Tschantz manifolds the action of the parabolic subgroup on a horospherical neighbourhood can be completely understood due to some nice symmetry of the 24-cell, and the fact that the side pairing transformations are very easy to describe.

Continuing with the above example, we outline how to describe the Euclidean structure on a cusp cross section associated to the ideal vertex class $\{(1,0,0,0),(-1,0,0,0)\}$. We already know that the associated parabolic subgroup is given by $\langle c, g^{-1}h, a^{-1}h\rangle$, we want to understand how these transformations act on a horospherical neighbourhood centred about $(1,0,0,0)$. A Euclidean transformation on $\mathbb{R}^3$ is just an affine transformation of the form:

$$x \mapsto \Lambda \cdot x + v$$

where $\Lambda \in O(3)$ and $v \in \mathbb{R}^3$. For each of the transformations $c, g^{-1}h, a^{-1}h$ we want to understand what the matrix Λ looks like, and what the translation vector v looks like. Each side pairing transformation consists of two components, a k-part and an r-part, the k-part is given by a diagonal matrix, hence its action on the copy of $\mathbb{R}^3$ is easy to understand. The r-part consists of reflection in the image side of the k-part, in this case its action on $\mathbb{R}^3$ is also easy to understand, this is because, as was mentioned before, the intersection of the sides that the ideal vertex $(1,0,0,0)$ lies on with a horospherical neighbourhood can be thought as the box (remember our orientation convention):

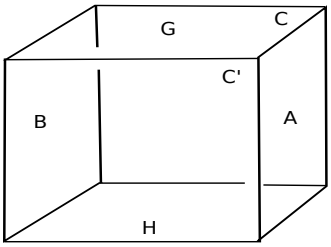

Since the sides intersect the horospherical neighbourhood in planes parallel to the e_2-e_3, e_2-e_4 and e_3-e_4 planes we see that the r-part is an affine transformation with Λ-matrix corresponding to one of reflections in the e_2-e_3, e_2-e_4 or e_3-e_4 planes. For example suppose we take the side pairing transformation c. From the picture above we see that the part of the side C' that intersects the horospherical neighbourhood can be thought of as a plane parallel to the plane $e_3=0$ and centred at the point $(0,-y,0)$.

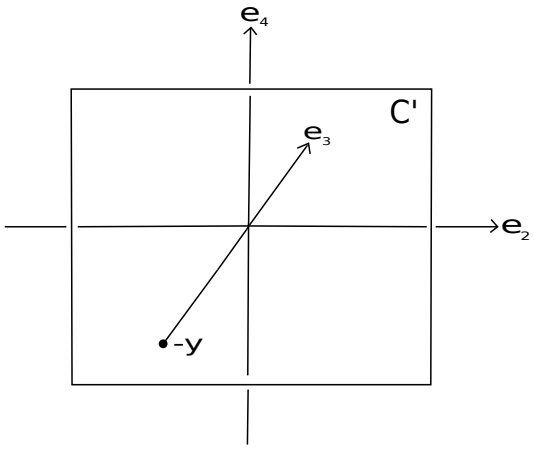

This tells us that the r-part of the transformation c, which remember is reflection in the side C', is a reflection in this plane. But it is easy to see that such a reflection is the affine transformation:

$$w \mapsto \begin{pmatrix} 1 & 0 & 0 \\ 0 & -1 & 0 \\ 0 & 0 & 1 \end{pmatrix} \cdot w + \begin{pmatrix} 0 \\ -2y \\ 0 \end{pmatrix}$$

The k-part of the transformation c is given by the matrix:

$$\begin{pmatrix} 1 & 0 & 0 & 0 \\ 0 & 1 & 0 & 0 \\ 0 & 0 & -1 & 0 \\ 0 & 0 & 0 & 1 \end{pmatrix}$$

whose action on the horospherical neighbourhood (which we are viewing as a copy of $\mathbb{R}^3$) is

given by the matrix:

$$\begin{pmatrix} 1 & 0 & 0 \\ 0 & -1 & 0 \\ 0 & 0 & 1 \end{pmatrix}$$

Therefore the action of the transformation c on this horospherical neighbourhood being the composition of the k-part and the r-part, is given by the transformation:

$$w \mapsto \begin{pmatrix} 1 & 0 & 0 \\ 0 & -1 & 0 \\ 0 & 0 & 1 \end{pmatrix} \begin{pmatrix} 1 & 0 & 0 \\ 0 & -1 & 0 \\ 0 & 0 & 1 \end{pmatrix} \cdot w + \begin{pmatrix} 0 \\ -2y \\ 0 \end{pmatrix} = w + \begin{pmatrix} 0 \\ -2y \\ 0 \end{pmatrix}$$

This tells us that the Euclidean transformation that corresponds to the action of c on a horospherical neighbourhood about $(1, 0, 0, 0)$ is nothing more than a translation by the vector $(0, -2y, 0)$.

We can apply the same techniques to understand the action of the parabolic transformation $g^{-1}h$ on the horospherical neighbourhood. In this case we need to understand the k and r-parts of two transformations, g^{-1} and h.

The k-part of the transformation h is given by the matrix:

$$\begin{pmatrix} -1 & 0 & 0 & 0 \\ 0 & -1 & 0 & 0 \\ 0 & 0 & -1 & 0 \\ 0 & 0 & 0 & 1 \end{pmatrix}$$

The side H' is parallel to the plane $e_4 = 0$ and centred at the vector $(0, 0, -z)$. Therefore the r-part of the transformation h is given by the affine transformation:

$$w \mapsto \begin{pmatrix} 1 & 0 & 0 \\ 0 & 1 & 0 \\ 0 & 0 & -1 \end{pmatrix} \cdot w + \begin{pmatrix} 0 \\ 0 \\ -2z \end{pmatrix}$$

The k-part of the transformation g^{-1} is the same is that of h, the r-part is given by reflection in the plane defined by the side G. The associated plane is parallel to the plane $e_4 = 0$ and centred at the point $(0, 0, z)$. Therefore the r-part for g^{-1} is given by the affine transformation:

$$w \mapsto \begin{pmatrix} 1 & 0 & 0 \\ 0 & 1 & 0 \\ 0 & 0 & -1 \end{pmatrix} \cdot w + \begin{pmatrix} 0 \\ 0 \\ 2z \end{pmatrix}$$

The composition $g^{-1}h$ consists of the two k-parts one from g^{-1} and one from h, as these are both equal they simply give the identity. Therefore to understand $g^{-1}h$ as an affine transformation we need only understand the composition of the r-parts of h and g^{-1}. This is easy to calculate:

$$w \mapsto \begin{pmatrix} 1 & 0 & 0 \\ 0 & 1 & 0 \\ 0 & 0 & -1 \end{pmatrix} \left(\begin{pmatrix} 1 & 0 & 0 \\ 0 & 1 & 0 \\ 0 & 0 & -1 \end{pmatrix} \cdot w + \begin{pmatrix} 0 \\ 0 \\ -2z \end{pmatrix} \right) + \begin{pmatrix} 0 \\ 0 \\ 2z \end{pmatrix}$$

which is the affine transformation:

$$w \mapsto x + \begin{pmatrix} 0 \\ 0 \\ 4z \end{pmatrix}$$

Finally, let us work out how the parabolic transformation $a^{-1}h$ behaves as a Euclidean transformation on a horospherical neighbourhood. The k-parts of h and a^{-1} are given by the following matrices:

$$\begin{pmatrix} -1 & 0 & 0 & 0 \\ 0 & -1 & 0 & 0 \\ 0 & 0 & -1 & 0 \\ 0 & 0 & 0 & 1 \end{pmatrix}, \begin{pmatrix} -1 & 0 & 0 & 0 \\ 0 & 1 & 0 & 0 \\ 0 & 0 & 1 & 0 \\ 0 & 0 & 0 & 1 \end{pmatrix}$$

We have already computed the r-part of h, as for the r-part of a^{-1} observe that the side A is parallel to the $e_2 = 0$ plane, and centred at the vector $(x, 0, 0)$. Reflection in this plane is given by the affine transformation:

$$w \mapsto \begin{pmatrix} -1 & 0 & 0 \\ 0 & 1 & 0 \\ 0 & 0 & 1 \end{pmatrix} \cdot w + \begin{pmatrix} 2x \\ 0 \\ 0 \end{pmatrix}$$

The composition $a^{-1}h$ is then given by the affine transformation:

$$w \mapsto \begin{pmatrix} -1 & 0 & 0 \\ 0 & 1 & 0 \\ 0 & 0 & 1 \end{pmatrix} \left(\left(\begin{pmatrix} -1 & 0 & 0 \\ 0 & -1 & 0 \\ 0 & 0 & -1 \end{pmatrix} \cdot w + \begin{pmatrix} 0 \\ 0 \\ -2z \end{pmatrix} \right) + \begin{pmatrix} 2x \\ 0 \\ 0 \end{pmatrix} \right.$$

which when we expand out we obtain:

$$\begin{pmatrix} 1 & 0 & 0 \\ 0 & -1 & 0 \\ 0 & 0 & -1 \end{pmatrix} \cdot w + \begin{pmatrix} 2x \\ 0 \\ -2z \end{pmatrix}$$

The reader will recall that before we started showing how to compute the action of these parabolic isometries on a horospherical neighbourhood, we showed how a cusp cross section arises through a fundamental domain consisting of two rectangular boxes. We went on to say that the right and left sides of this fundamental domain (which were being identified by the parabolic transformation $a^{-1}h$) were identified via a "twist". The reader who was not content with the use of the word "twist" at that time should now be at ease, for the "twisting" we speak of is given by the matrix

$$\begin{pmatrix} 1 & 0 & 0 \\ 0 & -1 & 0 \\ 0 & 0 & -1 \end{pmatrix}$$

in the above formula for the affine transformation associated to the parabolic isometry $a^{-1}h$.

In summary, we have shown that the parabolic subgroup corresponding to the ideal vertex equivalence class $\{(1, 0, 0, 0), (-1, 0, 0, 0)\}$ is given by the group $\langle c, g^{-1}h, a^{-1}h \rangle$. Furthermore, for each of these parabolic isometries we have shown how they act on a horospherical neighbourhood as a Euclidean transformation. The following table summarises this information

Parabolic isometry	Affine transformation
c	$\begin{pmatrix} 1 & 0 & 0 \\ 0 & 1 & 0 \\ 0 & 0 & 1 \end{pmatrix}, \begin{pmatrix} 0 \\ -2y \\ 0 \end{pmatrix}$
$g^{-1}h$	$\begin{pmatrix} 1 & 0 & 0 \\ 0 & 1 & 0 \\ 0 & 0 & 1 \end{pmatrix}, \begin{pmatrix} 0 \\ 0 \\ 4z \end{pmatrix}$
$a^{-1}h$	$\begin{pmatrix} 1 & 0 & 0 \\ 0 & -1 & 0 \\ 0 & 0 & -1 \end{pmatrix}, \begin{pmatrix} 2x \\ 0 \\ -2z \end{pmatrix}$

where in the second column the matrix is in $O(3)$ and the vector corresponds to the translation vector.

The information presented above is enough for one to obtain the Euclidean structure of the cusp corresponding to the class $\{(1,0,0,0),(-1,0,0,0)\}$. Using the classification of orientable compact Euclidean 3-manifolds (see [22] Thm.3.5.5, p.117) we see that this cusp has type B (see table 1. column headed **LT**) using the Hantzsche-Wendt notation or type $\mathcal{G}_2$ using Wolf's notation.

One can carry out an analogous procedure to work out generators for the parabolic subgroups corresponding to the other ideal vertex equivalence classes and their corresponding affine transformations. The only slight difference is that when dealing with the class $\{(\pm 1/2, \pm 1/2, \pm 1/2, \pm 1/2)\}$ one has to take sixteen boxes to form a fundamental domain. Also, computing the associated affine transformations in this case is slightly harder as one does not have such a nice parameterisation of horospherical neighbourhoods as in the case for the other equivalence classes. We will not need explicit formulas for the corresponding affine transformations, hence will not bother the reader with an explanation of how to find them in this situation. For the sake of completeness we have included the following table showing the end results of the above computations for all other ideal vertex equivalence classes.

Ideal vertex class	Generators for stabiliser subgroup	Affine transformations	Euclidean structure
$\{(1,0,0,0),(-1,0,0,0)\}$	c	$\begin{pmatrix}1&0&0\\0&1&0\\0&0&1\end{pmatrix}, \begin{pmatrix}0\\-2y\\0\end{pmatrix}$	**B** ($\mathcal{G}_2$)
	$g^{-1}h$	$\begin{pmatrix}1&0&0\\0&1&0\\0&0&1\end{pmatrix}, \begin{pmatrix}0\\0\\4z\end{pmatrix}$	
	$a^{-1}h$	$\begin{pmatrix}1&0&0\\0&-1&0\\0&0&-1\end{pmatrix}, \begin{pmatrix}2x\\0\\-2z\end{pmatrix}$	
$\{(0,1,0,0),(0,-1,0,0)\}$	a	$\begin{pmatrix}1&0&0\\0&1&0\\0&0&1\end{pmatrix}, \begin{pmatrix}-2x\\0\\0\end{pmatrix}$	**A** ($\mathcal{G}_1$)
	$e^{-1}f$	$\begin{pmatrix}1&0&0\\0&1&0\\0&0&1\end{pmatrix}, \begin{pmatrix}0\\4y\\0\end{pmatrix}$	
	$e^{-1}i$	$\begin{pmatrix}1&0&0\\0&1&0\\0&0&1\end{pmatrix}, \begin{pmatrix}0\\2y\\-2z\end{pmatrix}$	
$\{(0,0,1,0),(0,0,-1,0)\}$	k	$\begin{pmatrix}1&0&0\\0&1&0\\0&0&1\end{pmatrix}, \begin{pmatrix}0\\0\\-2z\end{pmatrix}$	**A** ($\mathcal{G}_1$)
	$d^{-1}c$	$\begin{pmatrix}1&0&0\\0&1&0\\0&0&1\end{pmatrix}, \begin{pmatrix}4x\\0\\0\end{pmatrix}$	
	$e^{-1}c$	$\begin{pmatrix}1&0&0\\0&1&0\\0&0&1\end{pmatrix}, \begin{pmatrix}0\\2y\\-2z\end{pmatrix}$	
$\{(0,0,0,1),(0,0,0,-1)\}$	g	$\begin{pmatrix}1&0&0\\0&-1&0\\0&0&-1\end{pmatrix}, \begin{pmatrix}-2x\\0\\0\end{pmatrix}$	**F** ($\mathcal{G}_6$)
	$k^{-1}l$	$\begin{pmatrix}1&0&0\\0&1&0\\0&0&1\end{pmatrix}, \begin{pmatrix}0\\0\\4z\end{pmatrix}$	
	$i^{-1}l$	$\begin{pmatrix}-1&0&0\\0&1&0\\0&0&-1\end{pmatrix}, \begin{pmatrix}0\\-2y\\2z\end{pmatrix}$	
$\{(\pm1/2,\pm1/2,\pm1/2,\pm1/2)\}$	$e^{-1}g$	$\begin{pmatrix}1&0&0\\0&1&0\\0&0&1\end{pmatrix}, \begin{pmatrix}0\\-4y\\0\end{pmatrix}$	**B** ($\mathcal{G}_2$)
	$a^{-1}k^{-1}ak$	$\begin{pmatrix}1&0&0\\0&1&0\\0&0&1\end{pmatrix}, \begin{pmatrix}8x\\0\\0\end{pmatrix}$	
	$a^{-1}k^{-1}j^{-1}b^{-1}fc$	$\begin{pmatrix}-1&0&0\\0&-1&0\\0&0&1\end{pmatrix}, \begin{pmatrix}-2x\\-2y\\-4z\end{pmatrix}$	

We point out that if we order the ideal vertices according to our table above then we see that the Euclidean structures on the associated cusps are given by **BAAFB**. However, if we go to manifolds no.3 in the Ratcliffe-Tschantz census we see that under the column headed **LT** the Euclidean structure on the cusps is given by **AABBF**. This is because they chose to write out

the Euclidean structures in alphabetical order, as opposed to any ordering on the ideal vertices.

The Euclidean structure on each cusp is found by an appeal to the classification theorem of compact connected orientable flat 3-dimensional Riemannian manifolds (see [22] Thm.3.5.5, p.117). One simply needs to identify the linear holonomy group, and one can do this from the computations of the associated affine transformations. The matrices of each generator (when viewed as an affine transformation on a horospherical neighbourhood) generate the linear holonomy group. For example, consider the first entry in the above table, we see that two of the generators have the identity matrix as their $O(3)$ component, when viewed as an affine transformation, and one of the generators has $\begin{pmatrix} 1 & 0 & 0 \\ 0 & -1 & 0 \\ 0 & 0 & -1 \end{pmatrix}$ as its $O(3)$ component. Therefore the linear holonomy group is generated by $\begin{pmatrix} 1 & 0 & 0 \\ 0 & -1 & 0 \\ 0 & 0 & -1 \end{pmatrix}$, which has order 2. This implies the linear holonomy group associated to this cusp is $\mathbb{Z}_2$. Using the classification theorem (see [22] Thm.3.5.5, p.117) we see that it corresponds to a Euclidean structure of type **B** (or $\mathcal{G}_2$ in Wolf's notation).

Observe that from the table above we see that each stabiliser subgroup corresponding to a cusp has a translation as one of its generators when viewed as an affine transformation. This means that each cross section of any of these cusps can be viewed as an S^1-fibre bundle over some compact 2-manifold. In other words, if we let E denote a Euclidean 3-manifold arising as the cusp cross section of manifold no.3 then we obtain an S^1-fibre bundle:

$$E \to S$$

where S is some compact (possibly non-orientable) closed surface. We can then fill in each S^1-fibre by a disk D^2, obtaining a D^2-bundle

$$\pi : \widetilde{E} \to S.$$

It is not hard to see that the boundary of $\widetilde{E}$ is precisely the Euclidean 3-manifold E. The 4-manifold $\widetilde{E}$ has a nice handle decomposition coming from the handle decomposition of the surface S. S is a compact surface, hence can be given a handle decomposition consisting of one 0-handle, n 1-handles ($n = 2 - \chi(S)$), and one 2-handle (see [8] p.131 last paragraph). The k-handles of $\widetilde{E}$ are given by preimages under π of k-handles of B (see [8] p.131 last paragraph). This means that $\widetilde{E}$ has a handle decomposition consisting of one 0-handle, n 1-handles and one 2-handle.

If we then take horoball neighbourhoods about each cusp of manifold no.3 then chop them off we are left with a 4-manifold that has five boundary components consisting of the Euclidean 3-manifolds in the above table. As explained above each of these 3-manifold boundary components bounds a 4-manifold that is a disk bundle over some compact surface. Denoting these five 4-manifolds by $\widetilde{\mathbf{B}}$, $\widetilde{\mathbf{A}}$, $\widetilde{\mathbf{A}}$, $\widetilde{\mathbf{F}}$, $\widetilde{\mathbf{B}}$, corresponding to the labelling we gave the 3-manifolds in the

above table, we see that we can glue each of these 4-manifolds to their corresponding boundary component in manifold no.3, obtaining a closed 4-manifold. On the level of Kirby diagrams this gluing procedure is done by taking the Kirby diagram for manifold no.3 and adding one 2-handle, n 3-handles and one 4-handle (see [1] chap.3, p.35).

We mention that this "filling in" of boundary components works for any of the Ratcliffe-Tschantz manifolds. Once we have "filled in" these boundary components we obtain a closed 4-manifold, we can then try and apply certain handle slides/cancellations to try and reduce the Kirby diagram of this "filled in" manifold. The hope is that we can reduce it to the Kirby diagram of a familiar closed 4-manifold that we can explicitly identify. Provided we are successful in this reduction process, we would have then found an explicit four dimensional hyperbolic link complement. Before we go on to describe the "elementary moves" we will be using so as to reduce the Kirby diagram of a filled in manifold we will give the parabolic information corresponding to manifold 1011 as this will be our first example of a link complement that we can explicitly identify.

Ideal vertex class	Generators for stabiliser subgroup	Affine transformations	Euclidean structure
$\{(1,0,0,0),(-1,0,0,0)\}$	c	$\begin{pmatrix}1&0&0\\0&1&0\\0&0&1\end{pmatrix}, \begin{pmatrix}0\\-2y\\0\end{pmatrix}$	$\mathbf{G}$ $(\mathcal{B}_1)$
	$a^{-1}b$	$\begin{pmatrix}1&0&0\\0&1&0\\0&0&1\end{pmatrix}, \begin{pmatrix}4x\\0\\0\end{pmatrix}$	
	$a^{-1}g$	$\begin{pmatrix}1&0&0\\0&-1&0\\0&0&1\end{pmatrix}, \begin{pmatrix}2x\\0\\-2z\end{pmatrix}$	
$\{(0,1,0,0),(0,-1,0,0)\}$	a	$\begin{pmatrix}1&0&0\\0&1&0\\0&0&1\end{pmatrix}, \begin{pmatrix}-2x\\0\\0\end{pmatrix}$	$\mathbf{G}$ $(\mathcal{B}_1)$
	$e^{-1}f$	$\begin{pmatrix}1&0&0\\0&1&0\\0&0&1\end{pmatrix}, \begin{pmatrix}0\\4y\\0\end{pmatrix}$	
	$e^{-1}i$	$\begin{pmatrix}-1&0&0\\0&1&0\\0&0&1\end{pmatrix}, \begin{pmatrix}0\\2y\\-2z\end{pmatrix}$	
$\{(0,0,1,0),(0,0,-1,0)\}$	k	$\begin{pmatrix}1&0&0\\0&1&0\\0&0&1\end{pmatrix}, \begin{pmatrix}0\\0\\-2z\end{pmatrix}$	$\mathbf{G}$ $(\mathcal{B}_1)$
	$c^{-1}d$	$\begin{pmatrix}1&0&0\\0&1&0\\0&0&1\end{pmatrix}, \begin{pmatrix}4x\\0\\0\end{pmatrix}$	
	$c^{-1}e$	$\begin{pmatrix}1&0&0\\0&1&0\\0&0&-1\end{pmatrix}, \begin{pmatrix}2x\\-2y\\0\end{pmatrix}$	
$\{(0,0,0,1),(0,0,0,-1)\}$	j	$\begin{pmatrix}1&0&0\\0&1&0\\0&0&1\end{pmatrix}, \begin{pmatrix}0\\-2y\\0\end{pmatrix}$	$\mathbf{G}$ $(\mathcal{B}_1)$
	$g^{-1}h^{-1}$	$\begin{pmatrix}1&0&0\\0&1&0\\0&0&1\end{pmatrix}, \begin{pmatrix}4x\\0\\0\end{pmatrix}$	
	$g^{-1}k$	$\begin{pmatrix}1&0&0\\0&-1&0\\0&0&1\end{pmatrix}, \begin{pmatrix}2x\\0\\-2z\end{pmatrix}$	
$\{(\pm1/2,\pm1/2,\pm1/2,\pm1/2)\}$	$e^{-1}g$	$\begin{pmatrix}1&0&0\\0&1&0\\0&0&1\end{pmatrix}, \begin{pmatrix}0\\-4y\\0\end{pmatrix}$	$\mathbf{G}$ $(\mathcal{B}_1)$
	$a^{-1}k^{-1}ak$	$\begin{pmatrix}1&0&0\\0&1&0\\0&0&1\end{pmatrix}, \begin{pmatrix}8x\\0\\0\end{pmatrix}$	
	$a^{-1}k^{-1}j^{-1}fc$	$\begin{pmatrix}1&0&0\\0&-1&0\\0&0&1\end{pmatrix}, \begin{pmatrix}-4x\\2y\\-4z\end{pmatrix}$	

2.2 Elementary Moves

In this section we are going to show how to reduce the Kirby diagram of a filled in Ratcliffe-Tschantz manifold, which we take to mean filling in the boundary components, using a combi-

nation of handle slides and cancellations, which we call elementary moves.

We have already understood the Euclidean 3-manifolds that arise as the boundary components of manifold no. 3, they are of the form **B**, **A**, **A**, **F**, **B**, and each is the boundary of the 4-manifold which we denoted by $\widetilde{\mathbf{B}}$, $\widetilde{\mathbf{A}}$, $\widetilde{\mathbf{A}}$, $\widetilde{\mathbf{F}}$, $\widetilde{\mathbf{B}}$ respectively. We also saw that a handle structure of any of these 4-manifolds consisted of one 0-handle, n 1-handles and a unique 2-handle. When we glue any of these 4-manifolds to their 3-manifold boundary component in manifold no. 3 (i.e. doing a boundary filling) we need to add one 4-handle, n 3-handles and one 2-handle to the handle decomposition of manifold no. 3. This means that on the level of our Kirby diagram we need to show where the added 2-handle goes.

Recall that the handle decomposition of manifold no. 3 can be viewed via the four following diagrams:

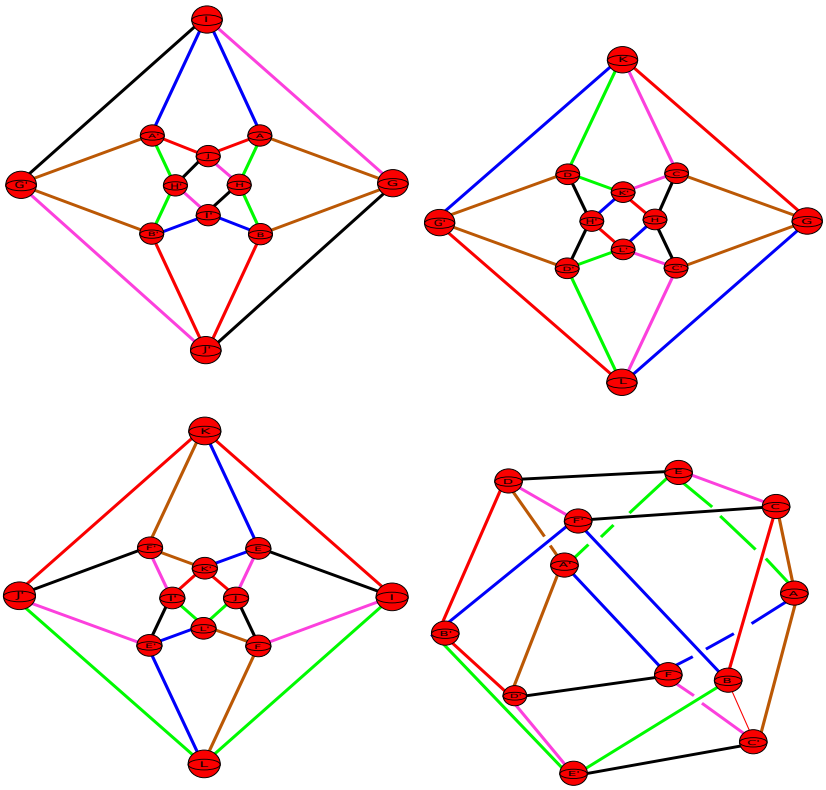

The top two diagrams show those handles lying in the $x-y$ and $x-z$ planes respectively, the bottom left those which lie in the $y-z$ plane and the bottom right those 2-handles that do not all lie in a single two plane.

Consider the boundary component given by the code **A** (or $\mathcal{G}_1$ in Wolf's notation), this is the 3-torus and it bounds the solid 4-manifold $S^1 \times S^1 \times D^2$. When we glue in the solid 3-torus we need to add one 4-handle, two 3-handles (as the Euler characteristic of $T^2 = 0$) and one 2-handle. If we go back to the table outlining the generators of each parabolic subgroup

corresponding to each boundary component, we see that the first boundary component labelled **A** has a generator given by the translation a. This means that algebraically the translation a represents an S^1-fibre of the boundary component. Therefore when we glue in a solid torus to this boundary component we can do so along the S^1-fibre corresponding to the translation a. Algebraically this means we are killing the transformation a, hence the 2-handle we are attaching must be a straight line segment running between $A - A'$ once. As the 1-handle $A - A'$ lies in the $x - y$ plane we draw this 2-handle as a dashed line segment lying in the $x - y$ plane, it must also be added to the diagram showing the six 2-handles that do not all lie in a single 2-plane.

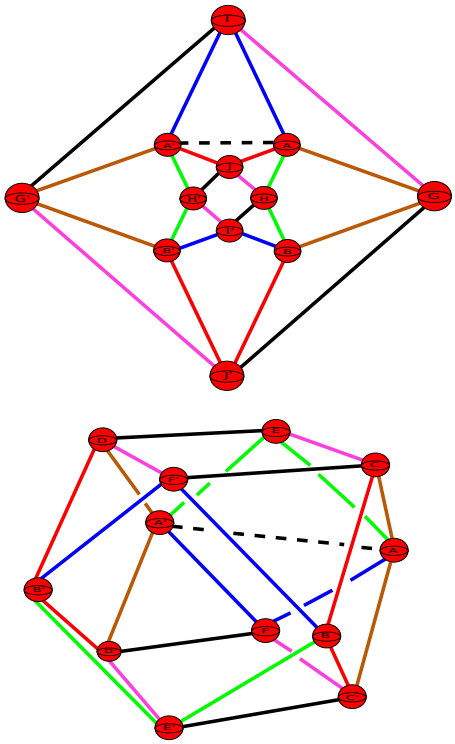

There are two subtle points we need to address with this gluing procedure. First of all, we did not explain how the normal bundle to the added 2-handle looks in the Kirby diagram. In order to understand this one must carry out a similar analysis as was done when trying to understand how the normal bundles of the 2-handles in the Kirby diagram look like (see end of previous chapter). The point is that these added 2-handles will, most of the time, lie in a single plane, hence the trivialisation of their normal bundle is easy to understand. When the added 2-handle does not lie in a single plane we will find that it has a planar framing, in other words a parallel curve to the 2-handle behaves as if the added 2-handle was lying in a plane. The second point to address has to do with how exactly we know where to put the added 2-handle in our Kirby diagram. In the above diagram the added 2-handle lies in the $x - y$ plane, just before the diagram we said that we can draw this 2-handle as a straight line running between A, A' in the $x - y$ plane because both A and A' lie in the $x - y$ plane. The question is, why

is this the right place for the added 2-handle? The basic idea of why this is the right place has to do with how the fundamental domain of this boundary component looks. It consists of two rectangular boxes, one coming from the ideal vertex $(0,1,0,0)$, and another coming from $(0,-1,0,0)$. The rectangular box centred at $(0,1,0,0)$ has two of its sides being A and A' and the S^1-fibre that we are filling along corresponds to a straight line joining A and A'. When we formed the Kirby diagram we did so by taking the dual polyhedron to the 24-cell P, when we do this the rectangular boxes will look like octahedrons in the Kirby diagram, as the dual of a rectangular box is an octahedron. The point is that we can then go to our Kirby diagram find the associated dual octahedron, and then identify the corresponding S^1-fibre as a straight line running between some 1-handles. If we do this for the above mentioned boundary component we find that the added 2-handle does indeed lie where we have drawn it in the above diagram. This explanation may seem convoluted, but for now we insist the reader to not pay too much attention to it as the primary aim of this section is to explain the "elementary moves" we will be using to reduce a Kirby diagram, and we don't want the reader to get bogged down with some minor details. In the next section we will deal with an explicit example, and give full details of exactly how the dual octahedra look like in the Kirby diagram, which in turn will tell us exactly how the added 2-handles look like, and how they should be added.

Coming back to the above diagram we can see that the added 2-handle only passes over $A-A'$ once, in other words the attaching sphere of the added 2-handle transversely intersects the belt sphere of the 1-handle $A-A'$ once. This means this 1-handle and 2-handle pair form a cancelling pair and can be erased from the diagram. Any other 2-handles that pass over the 1-handle $A-A'$ must first be slid over the added 2-handle, and then we can erase the pair of handles from the diagram. Observe that because all the added 2-handles, coming from boundary fillings, are unknotted and have parallel curves that do not twist around the 2-handle in any way (i.e. they are planar framed), whenever we slide 2-handles over them nothing non-trivial will happen, making the sliding process very straightforward. This standard handle cancellation move is the **first elementary move** we will be using to try and reduce our Kirby diagram. Let us show how the diagram in the $x-y$ plane changes when we carry out such a cancellation.

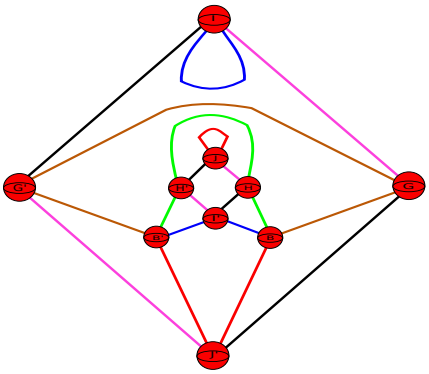

After this cancellation has taken place we can see that a few 2-handles have slid into new positions. In particular notice how the blue 2-handle has a component that now loops back into I, similarly the red 2-handle has a component that loops back into J.

The **second elementary move** we will be making use of is to push such 2-handles through the 1-handle piece they loop back into. For example if we consider the component of the blue 2-handle that loops back into I, we see that we can push it through I to come out as a component that loops back into I'.

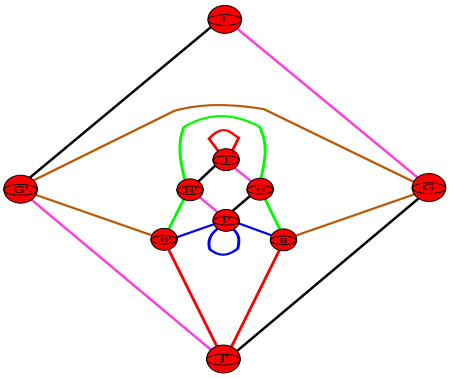

We can then slide the blue 2-handle off I', giving a blue 2-handle that runs between $B - B'$ once.

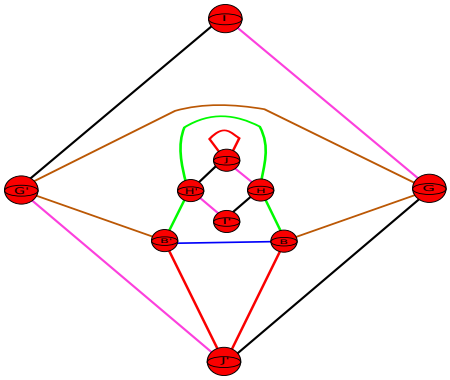

We can also carry out the same move for the component of the red 2-handle that loops back into J:

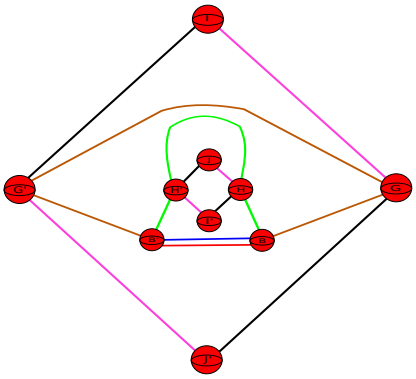

In the above move it is very important that we have that the 2-handle we are pushing through being unknotted. This is because some of our 1-handles are being identified via orientation preserving diffeomorphisms, hence pushing 2-handles through will cause bits of knots to get mirrored, however if the 2-handles are all unknotted then one does not have to worry about such minor technicalities.

We now have a blue 2-handle and a red 2-handle passing over the 1-handle $B - B'$ once. The **third elementary move** we will be making use of can be described as follows. We can cancel the 1-handle $B - B'$ using the blue 2-handle that now runs over it once, in so doing the red 2-handle will form an unknotted circle:

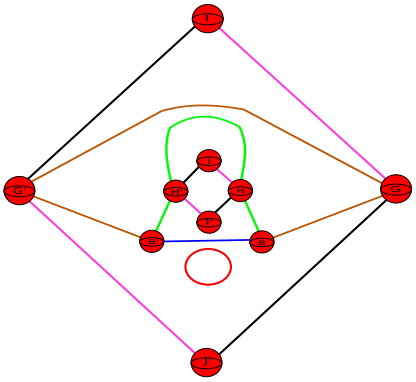

Note that this unknotted circle now has a well-defined notion of a framing number. You can see that because the 2-handles in the $x-y$ plane all have parallel curves that do not twist around them in any way the unknotted circle must have framing zero. This unknotted circle then cancels a 3-handle and can be deleted from the diagram, a proof of this fact can be found in [8] prop.5.1.9, p.148.

The three moves described above will be heavily used in various situations in the sections to come, this is why we took the time to explain each one carefully. On top of this we will carry out various handle slides, as all our 2-handle are unknotted and have a planar framing the handle slides we carry out will always be straightforward. If at any point we exploit the use of a non-trivial move we will take the time to carefully explain how one proceeds.

Filling in the boundary components of any one of the Ratcliffe-Tschantz manifolds produces a compact 4-manifold (possibly non-orientable) for which we know how to build a Kirby diagram for. Using the elementary moves outlined above one can try and reduce the Kirby diagram of this smooth 4-manifold, the hope is that after sufficiently many reductions the end Kirby diagram is that of a compact smooth 4-manifold that we can identify. This gives a way of trying to identify which compact smooth 4-manifolds have smooth complements that are given by the Ratcliffe-Tschantz manifolds, and in turn allows one to obtain explicit examples of smooth hyperbolic link complements. In general this proves to be a very difficult task, the reason being is that we have at least twenty four 2-handles to deal with and we view many of them in certain 2-planes. The added 2-handles (coming from filling boundary components) will in general pass through some of these 2-planes giving rise to intersection points that have to be carefully tracked when carrying out various elementary moves. In the next section we will give an explicit example of a situation in which we can identify the filled in 4-manifold up to diffeomorphism.

2.3 An explicit example: Manifold 1011

In this section we will show that the double cover of the Ratcliffe-Tschantz manifold numbered 1011 is a smooth complement in the standard smooth 4-sphere. In other words if we perform a boundary filling, as described in the previous section, on the orientable double cover of manifold 1011 we get a closed smooth 4-manifold that is diffeomorphic to S^4.

For the remainder of this section we are going to denote the manifold numbered 1011 in the Ratcliffe-Tschantz census by M. We remind the reader of the structure of the Kirby diagram for M:

The following picture shows those 2-handles lying in the $x - y$ plane, with the table following explaining the colour coding.

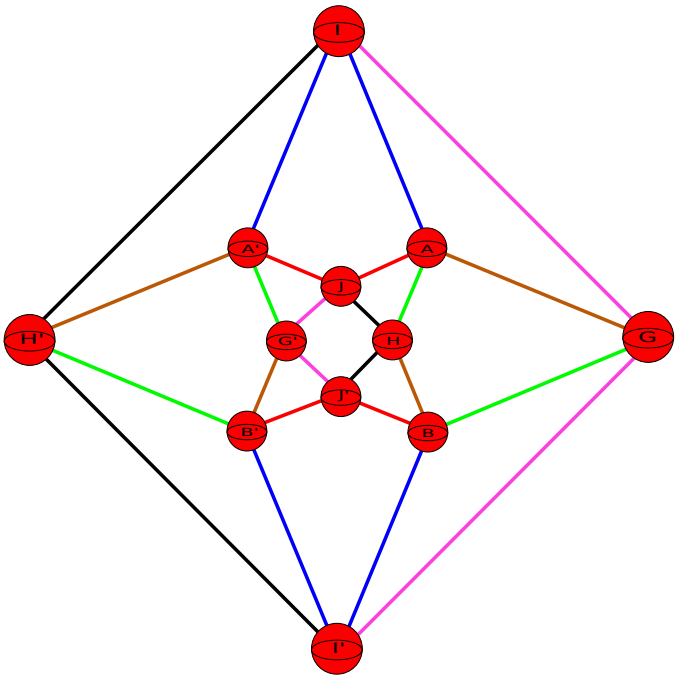

colour	equivalence class
green	$A \cap H \xrightarrow{a} A' \cap G' \xrightarrow{g^{-1}} B \cap G \xrightarrow{b} B' \cap H' \xrightarrow{h^{-1}} A \cap H$
red	$A \cap J \xrightarrow{a} A' \cap J \xrightarrow{j} B' \cap J' \xrightarrow{b^{-1}} B \cap J' \xrightarrow{j^{-1}} A \cap J$
brown	$A \cap G \xrightarrow{a} A' \cap H' \xrightarrow{h^{-1}} B \cap H \xrightarrow{b} B' \cap G' \xrightarrow{g^{-1}} A \cap G$
blue	$A \cap I \xrightarrow{a} A' \cap I \xrightarrow{i} B' \cap i' \xrightarrow{b^{-1}} B \cap I' \xrightarrow{i^{-1}} A \cap I$
pink	$G \cap I \xrightarrow{g} G' \cap J' \xrightarrow{j^{-1}} G' \cap J \xrightarrow{g^{-1}} G \cap I' \xrightarrow{i^{-1}} G \cap I$
black	$H \cap J \xrightarrow{h} H' \cap I' \xrightarrow{i^{-1}} H' \cap I \xrightarrow{h^{-1}} H \cap J' \xrightarrow{j^{-1}} H \cap J$

The 2-handles that lie in the $x - z$ plane can be seen in the following picture.

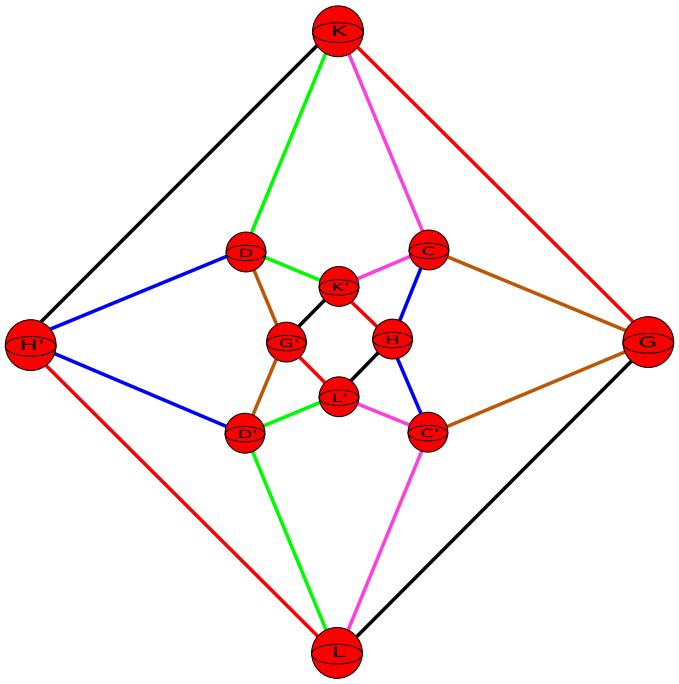

colour	equivalence class
green	$D \cap K \xrightarrow{d} D' \cap L \xrightarrow{l} D' \cap L' \xrightarrow{d^{-1}} D \cap K' \xrightarrow{k^{-1}} D \cap K$
red	$G \cap K \xrightarrow{g} G' \cap L' \xrightarrow{l^{-1}} H' \cap L \xrightarrow{h^{-1}} H \cap K' \xrightarrow{k^{-1}} G \cap K$
brown	$C \cap G \xrightarrow{c} C' \cap G \xrightarrow{g} D \cap G' \xrightarrow{d} D' \cap G' \xrightarrow{g^{-1}} C \cap G$
blue	$C \cap H \xrightarrow{c} C' \cap H \xrightarrow{h} D \cap H' \xrightarrow{d} D' \cap H' \xrightarrow{h^{-1}} C \cap H$
pink	$C \cap K \xrightarrow{c} C' \cap L \xrightarrow{l} C' \cap L' \xrightarrow{c^{-1}} C \cap K' \xrightarrow{k^{-1}} C \cap K$
black	$G \cap L \xrightarrow{g} G' \cap K' \xrightarrow{k^{-1}} H' \cap K \xrightarrow{h^{-1}} H \cap L' \xrightarrow{l^{-1}} G \cap L$

The 2-handles that lie in the $y - z$ plane can be seen in the following picture.

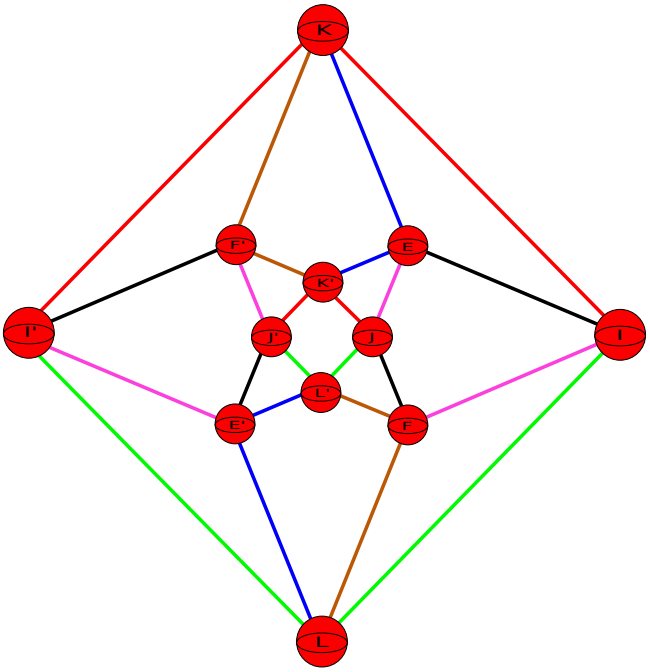

colour	equivalence class
green	$I \cap L \xrightarrow{i} I' \cap L \xrightarrow{l} J' \cap L' \xrightarrow{j^{-1}} J \cap L' \xrightarrow{l^{-1}} I \cap L$
red	$I \cap K \xrightarrow{i} I' \cap K \xrightarrow{k} J' \cap K' \xrightarrow{j^{-1}} J \cap K' \xrightarrow{k^{-1}} I \cap K$
brown	$F \cap L \xrightarrow{f} F' \cap K' \xrightarrow{k^{-1}} F' \cap K \xrightarrow{f^{-1}} F \cap L' \xrightarrow{l^{-1}} F \cap L$
blue	$E \cap K \xrightarrow{e} E' \cap L' \xrightarrow{l^{-1}} E' \cap L \xrightarrow{e^{-1}} E \cap K' \xrightarrow{k^{-1}} E \cap K$
pink	$E \cap J \xrightarrow{e} E' \cap I' \xrightarrow{i^{-1}} F \cap I \xrightarrow{f} F' \cap J' \xrightarrow{j^{-1}} E \cap J$
black	$E \cap I \xrightarrow{e} E' \cap J' \xrightarrow{j^{-1}} F \cap J \xrightarrow{f} F' \cap I' \xrightarrow{i^{-1}} E \cap I$

Finally, the 2-handles that do not lie in any one of the above three planes can be seen in the following picture.

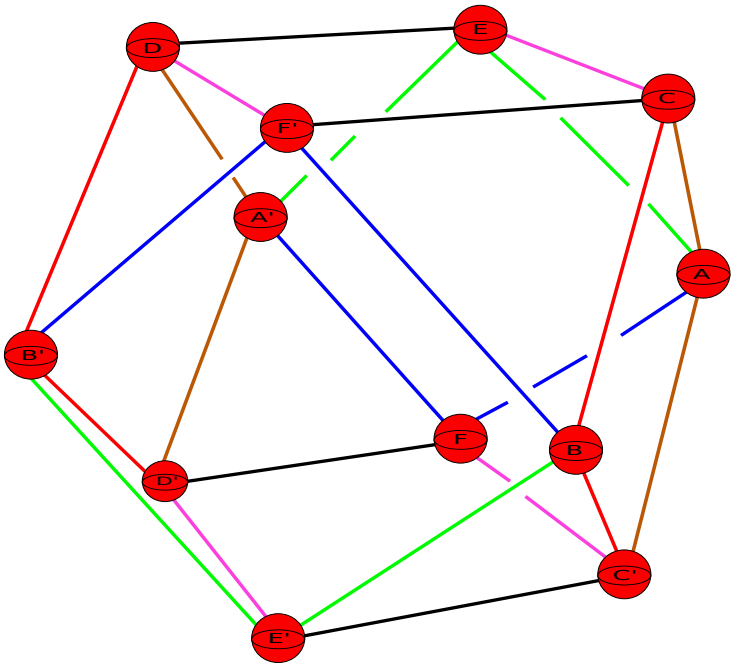

colour	equivalence class
green	$A \cap E \xrightarrow{a} A' \cap E \xrightarrow{e} B \cap E' \xrightarrow{b} B' \cap E' \xrightarrow{e^{-1}} A \cap E$
red	$B \cap C \xrightarrow{b} B' \cap D \xrightarrow{d} B' \cap D' \xrightarrow{b^{-1}} B \cap C' \xrightarrow{c^{-1}} B \cap C$
brown	$A \cap C \xrightarrow{a} A' \cap D \xrightarrow{d} A' \cap D' \xrightarrow{a^{-1}} A \cap C' \xrightarrow{c^{-1}} A \cap C$
blue	$A \cap F \xrightarrow{a} A' \cap F \xrightarrow{f} B \cap F' \xrightarrow{b} B' \cap F' \xrightarrow{f^{-1}} A \cap F$
pink	$C \cap E \xrightarrow{c} C' \cap F \xrightarrow{f} D \cap F' \xrightarrow{d} D' \cap E' \xrightarrow{e^{-1}} C \cap E$
black	$C \cap F' \xrightarrow{c} C' \cap E' \xrightarrow{e^{-1}} D \cap E \xrightarrow{d} D' \cap F \xrightarrow{f} C \cap F'$

Recall the manifold M is non-orientable and has five cusps each of which has the type $\mathbf{G}$ (or in Wolf's notation type $\mathcal{B}_1$). We denote the 4-manifold that bounds this 3-manifold by $\widetilde{\mathbf{G}}$, remember this is the associated disc bundle to $\mathbf{G}$. We need to choose a translation in each parabolic subgroup that is going to correspond to an S^1-fibre which we will fill in. We have already shown the parabolic information corresponding to each cusp in the table at the end of section 2.1. From that table the reader can see that we can take the first generator associated to each stabiliser subgroup as the translation corresponding to an S^1-fibre. That is, we take the transformations c, a, k, j and $e^{-1}g$. We are going to fill in each of these five S^1-fibres by gluing in the manifold $\widetilde{\mathbf{G}}$, on the level of the above Kirby diagrams we need to show where the added 2-handles go.

In order to understand where these added 2-handles will go in our Kirby diagram let us go

back and see how we obtained these parabolic translations. The idea was to take each ideal vertex then take a horospherical neighbourhood about each of these vertices, and then by applying various isometries we could work out the parabolic translations. For example when we took the ideal vertex $\{(1,0,0,0)\}$ we found that its equivalence class consisted of two points $\{(1,0,0,0),(-1,0,0,0)\}$, and hence a fundamental domain for the parabolic subgroup corresponding to this class were two rectangular boxes, one centred at the ideal vertex $(1,0,0,0)$ and one centred at $(-1,0,0,0)$. The rectangular box around the ideal vertex $(1,0,0,0)$ took the form:

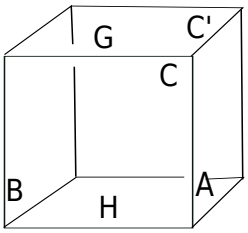

We then found that the isometry c was a parabolic translation in the parabolic subgroup corresponding to the class $\{(1,0,0,0),(-1,0,0,0)\}$. When we formed the handle decomposition of the 24-cell what we were really doing was taking a dual cell structure. This means that if we take the dual of the above box we will be getting that part of the fundamental domain in the handle decomposition of the 24-cell. As the dual of a rectangular box is an octahedron, taking the dual of the above box gives:

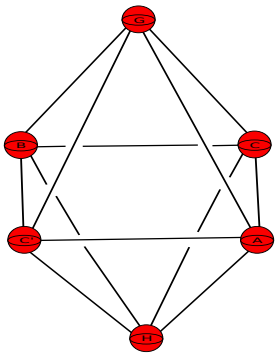

Filling in the S^1-fibre of the associated boundary component involves attaching a 2-handle from C to C'. In our Kirby diagram this involves drawing an attaching circle between C and C' in our octahedron. Note that the S^1-fibre is identified in the fundamental domain by a straight line joining side C to side C' and running inside the rectangular box making up the fundamental domain. Therefore, in our Kirby diagram the added 2-handle, representing a filling of the S^1-fibre corresponding to the translation c, will be a straight line running from C to C' and

contained in the dual octahedron.

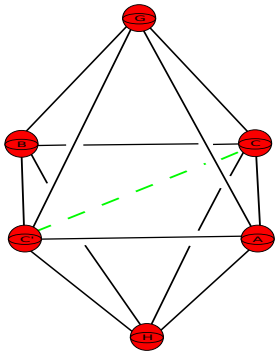

We can also see how this looks in part of our ambient handle decomposition diagram. Recall, the coordinates of C, C', A, B, G and H are:

A	$S_{(+1,+1,0,0)}$	$(\frac{1}{\sqrt{2}}, \frac{1}{\sqrt{2}}, 0)$	B	$S_{(+1,-1,0,0)}$	$(\frac{1}{\sqrt{2}}, \frac{-1}{\sqrt{2}}, 0)$
C	$S_{(+1,0,+1,0)}$	$(\frac{1}{\sqrt{2}}, 0, \frac{1}{\sqrt{2}})$	C'	$S_{(+1,0,-1,0)}$	$(\frac{1}{\sqrt{2}}, 0, \frac{-1}{\sqrt{2}})$
G	$S_{(+1,0,0,+1)}$	$(1+\sqrt{2}, 0, 0)$	H	$S_{(+1,0,0,-1)}$	$(-1+\sqrt{2}, 0, 0)$

The following shows a picture of this octahedron (in purple) in part of the ambient handle decomposition diagram.

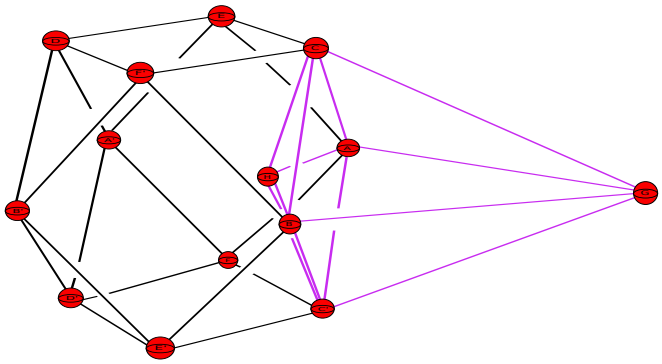

The filling of $C - C'$ can be seen in the following picture, with the attaching circle of the 2-handle we are using to do the filling being shown in green. You can clearly see that it lies in the $x - z$ plane.

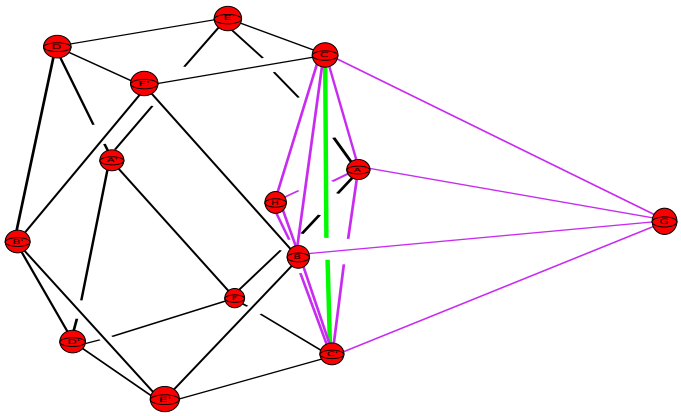

We can do the same for all the other fillings we are going to carry out. The reader should keep in mind that each attaching circle of an added 2-handle, corresponding to a filling, comes from a straight line joining two sides of the rectangular box making up the fundamental domain of the boundary component we are filling.

If we consider the ideal vertex $\{(0,1,0,0)\}$ we saw that its equivalence class consisted of the two vertices $\{(0,1,0,0),(0,-1,0,0)\}$. The horosphere about the vertex $\{(0,1,0,0)\}$ looks like:

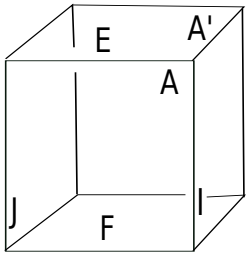

Taking the dual gives the following octahedron:

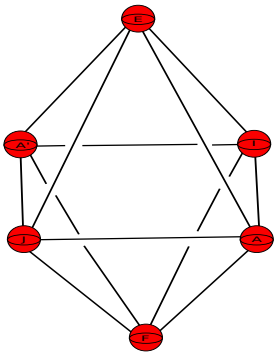

Filling in the S^1 fibre of the associated boundary component involves attaching a 2-handle from A to A' in the following way.

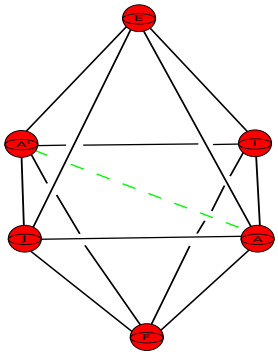

A picture of this dual octahedron in part of the three dimensional handle decomposition diagram is shown in the following picture, with the octahedron given by the purple edges.

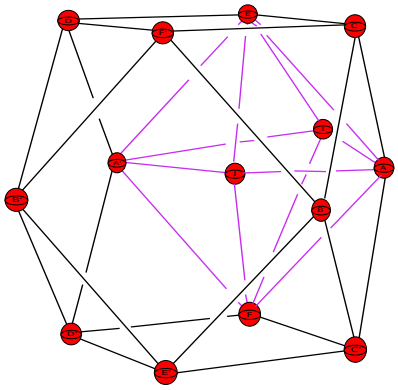

The filling of $A - A'$ can be seen in the following picture, with the added 2-handle in green. One can clearly see that it lies in the $x - y$ plane, and does not interfere with the other 2-handles.

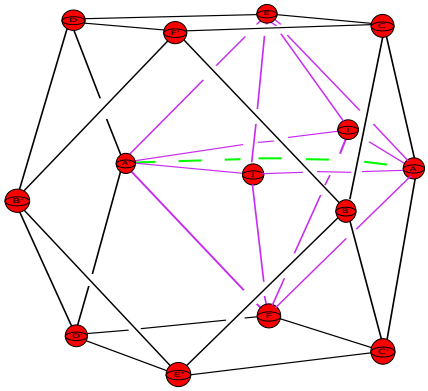

For the ideal vertex $(0, 0, 1, 0)$ we found that the equivalence class was $\{(0, 0, 1, 0), (0, 0, -1, 0)\}$, the horosphere about the vertex $(0, 0, 1, 0)$ looks like:

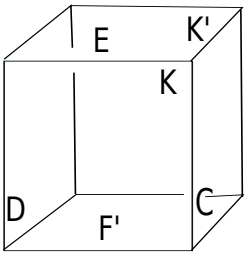

The dual octahedron then takes the form:

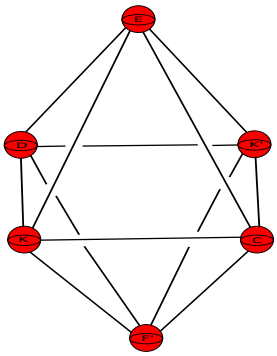

Filling in the S^1 fibre of the associated boundary component involves attaching a 2-handle from K to K', and in this case we take the following attaching circle.

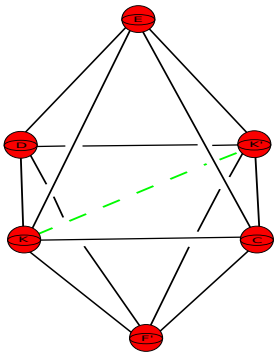

A picture of this dual octahedron in part of the handle decomposition is shown in the following picture, with the octahedron given by the purple edges

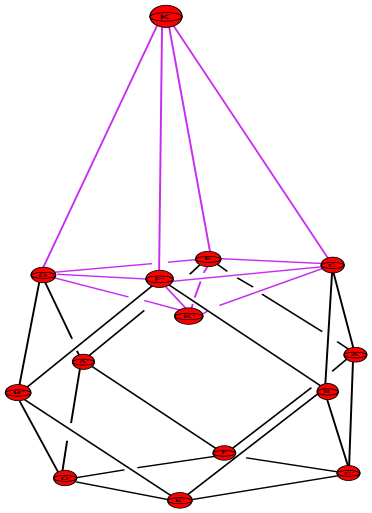

The attaching circle of the 2-handle we are attaching is shown in the following picture, it is clear that this 2-handle lies in the $x-z$ and $y-z$ planes, and does not interfere with any of the other 2-handles.

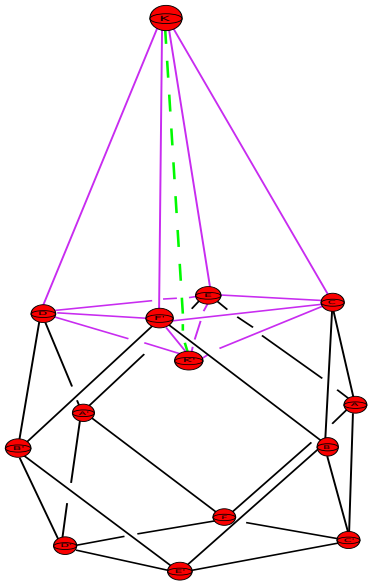

For the vertex class $\{(0,0,0,1),(0,0,0,-1)\}$ we found that the isometry j was a parabolic translation. In this case we need to look at the horosphere about the ideal vertex $(0,0,0,-1)$.

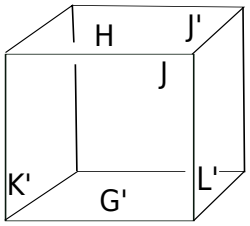

The dual octahedron is then given by

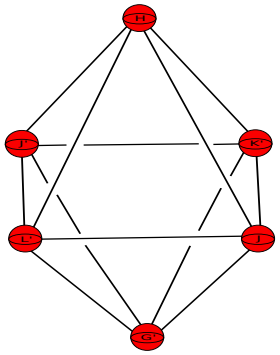

and the added 2-handle can be seen in the following picture.

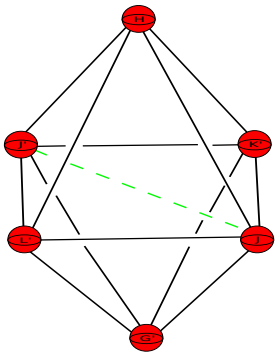

A picture of this dual octahedron in part of the handle decomposition is shown in the following picture, with the octahedron given by the purple edges.

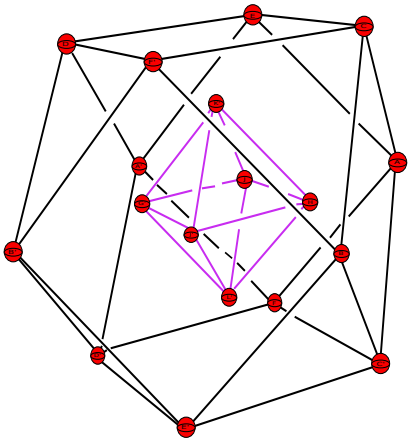

The attaching circle of the 2-handle we are attaching is shown in the following picture, it is clear that this 2-handle lies in the $x-y$ and $y-z$ planes, and does not interfere with any of the other 2-handles.

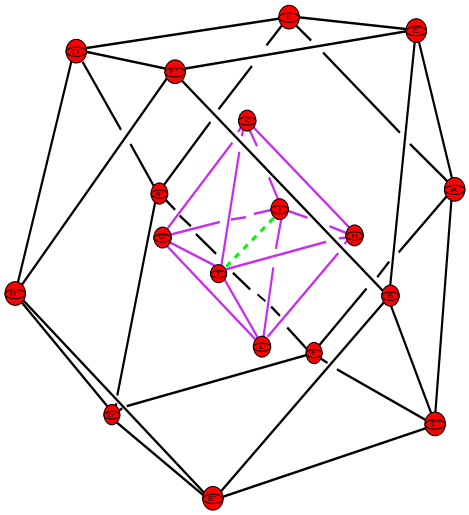

The final vertex class to consider consists of the ideal vertices $\{(\pm 1/2, \pm 1/2, \pm 1/2, \pm 1/2)\}$. In this case we found that the isometry $e^{-1}g$ corresponded to a parabolic translation. Therefore, when we fill the fibre corresponding to this isometry we need to add a 2-handle component from E to G and one from E' to G'. In this case we need to consider two horospheres, the one about the vertex $(1/2, 1/2, 1/2, 1/2)$ and the one about the vertex $(-1/2, -1/2, -1/2, -1/2)$. Both these horosphere are shown in the following picture, the one on the left corresponding to $(1/2, 1/2, 1/2, 1/2)$.

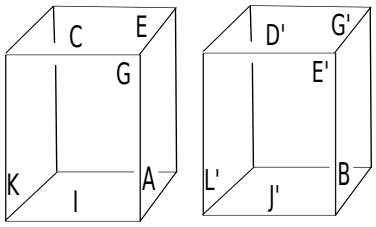

The dual octahedrons are then given by:

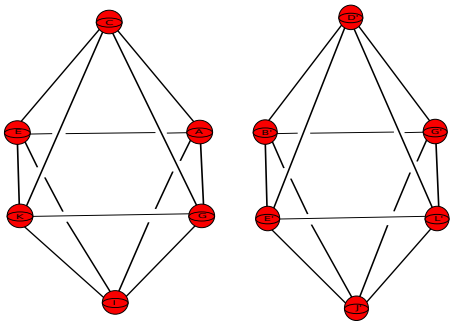

The following shows a three dimensional picture of the first octahedron above.

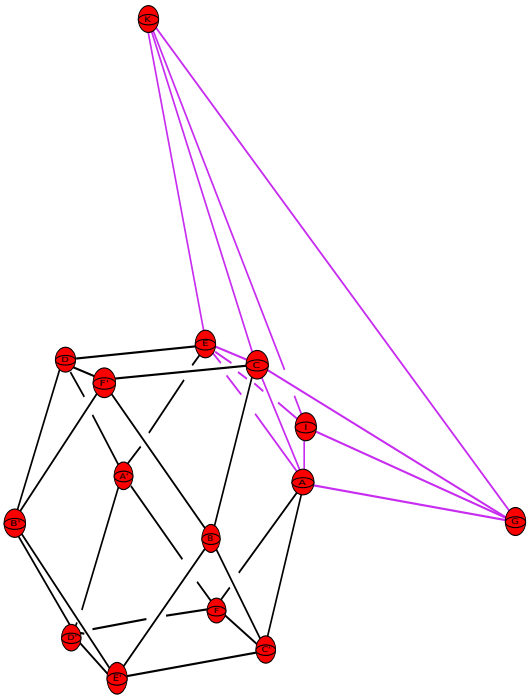

The 2-handle that we are going to add has one component running from E to G, and can be seen in the following diagram. The reader should note that we have drawn the added component as a curved arc when it really should be a straight line running from E to G. The reason for drawing it as a curved arc is simply because it is easier to view in the diagram, the reader should really picture this as a straight line.

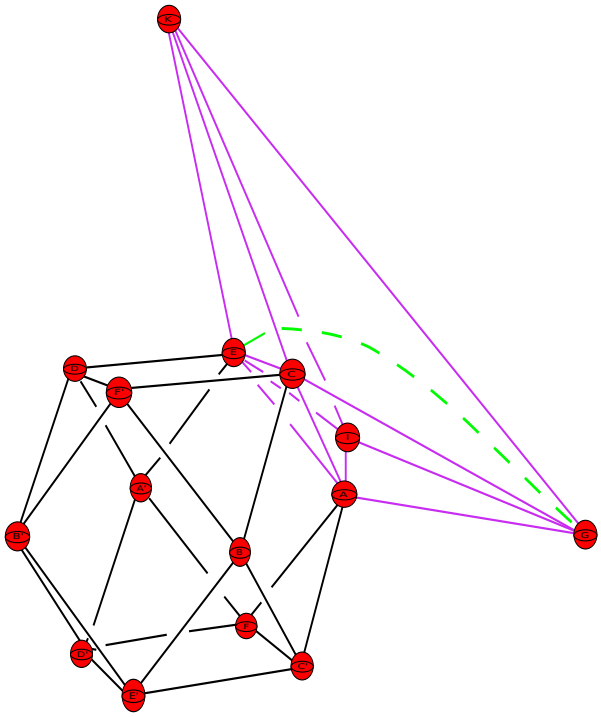

Observe that the added component falls outside of the diagrams showing the $x-y$, $x-z$, $y-z$ planes and the diagrams showing the six 2-handles that do not all lie in a single 2-plane. Due to this, any handle cancellation/slides we do which take place in the $x-y$, $x-z$ and $y-z$ planes or the diagram corresponding to the six 2-handles that do not all lie in a single 2-plane, will not interfere with this added 2-handle component running from E to G.

The following shows a three dimensional picture of the second octahedron above

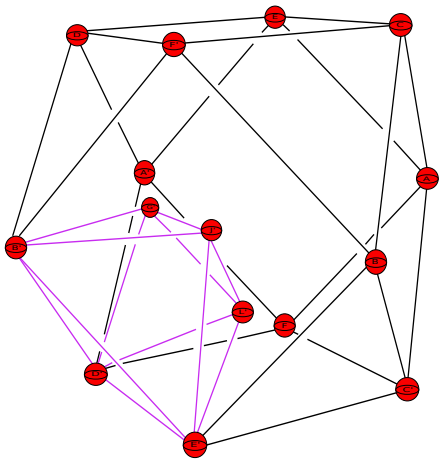

The 2-handle component that we are adding runs from E' to G' and can be seen in the following diagram:

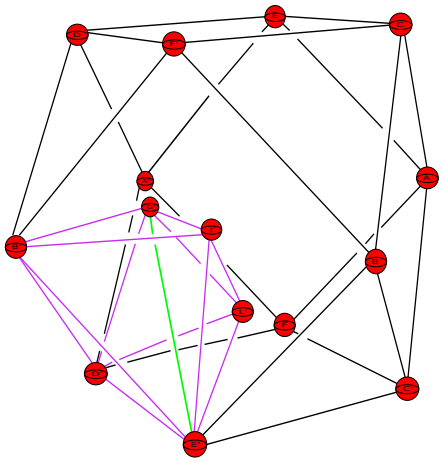

In this case the added 2-handle runs inside the diagram corresponding to the six 2-handles that do not all lie in a single 2-plane. However, it does not lie in any of the planes $x-y$, $x-z$ or $y-z$. Furthermore, all the handle cancellations/slides we do to begin with will not interfere with this 2-handle.

The following picture shows the Kirby diagrams with the added attaching circle of the added

2-handles that pass over $A - A'$, $J - J'$, $K - K'$ and $C - C'$, they are the black dashed lines. We note that these 2-handles pass over the 1-handles in question once. Also, the added 2-handle running between $C - C'$ in the $x - z$ plane is drawn as a curved arc, as opposed to a straight line, purely for ease of viewing.

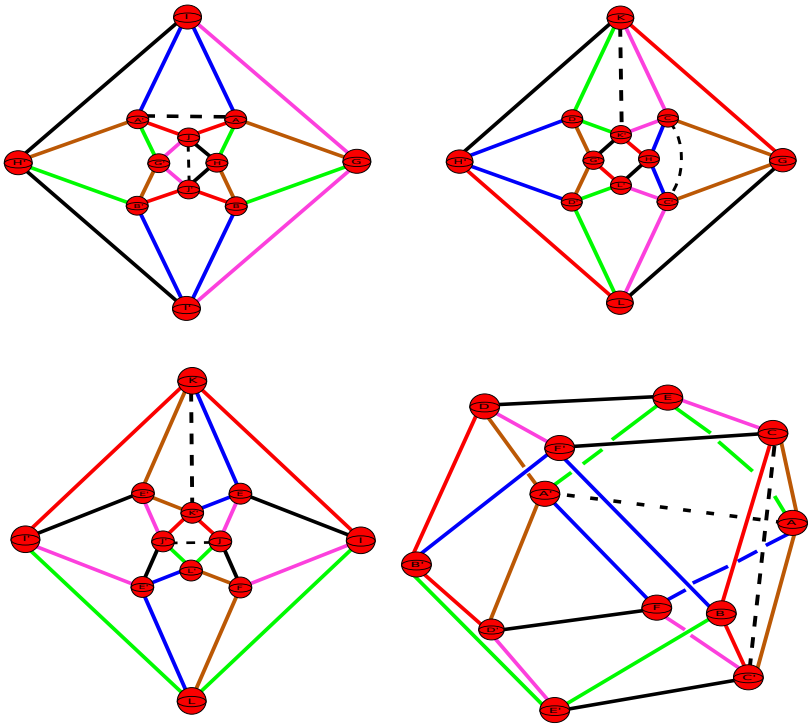

The added 2-handle that runs from E to G and E' to G' are shown in the following picture.

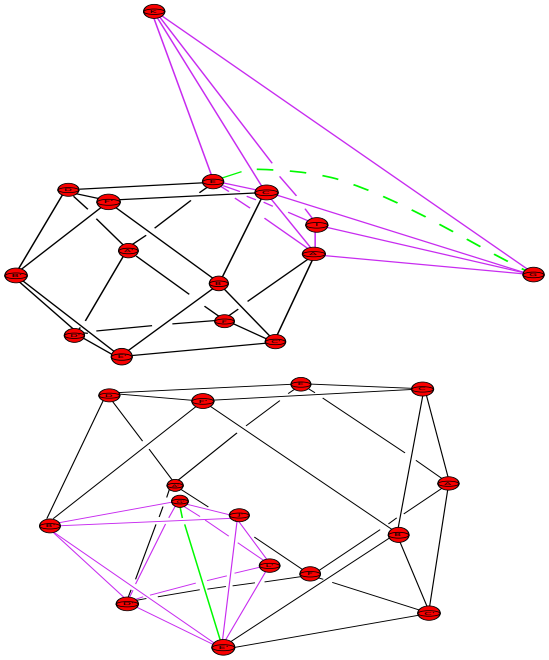

The above shows the Kirby diagram associated to the smooth closed 4-manifold that is obtained

from filling in the boundary components of M. Recall that at the end of the last chapter we explained how the 2-handles associated to the Kirby diagram of M had what we called a planar framing. This had the feature that whenever we took a parallel curve to such a 2-handle it would never cross over the 2-handle. We want to briefly show that the same feature is possessed by the added 2-handles making up the closed boundary filling of M.

The first four added 2-handles all lie in at least one single 2-plane, it is easy to check that a parallel curve to such a 2-handle cannot cross over the 2-handle in any way, and lies in the same plane. We will show this for the added 2-handle that runs between A, A'. This added 2-handle lies in the $x-y$ plane, we take a parallel curve just above it that is going into A, and that also lies in the $x-y$ plane. It is shown as the orange curve going into A in the following diagram.

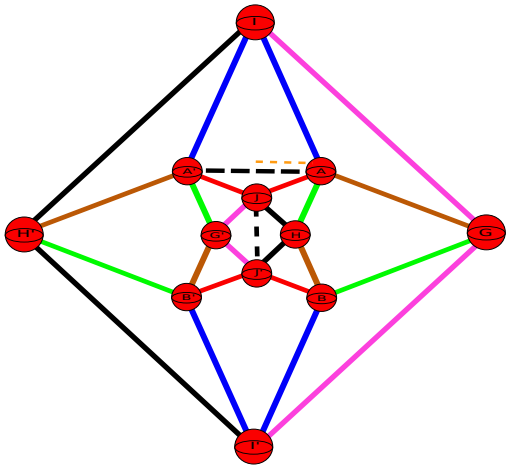

The attaching map for A, A' is given by the reflection $(x, y, z) \mapsto (-x, y, z)$, it is therefore clear that when the parallel curve goes into A it comes out of A' also above the added 2-handle. The following diagram shows what the parallel curve looks like.

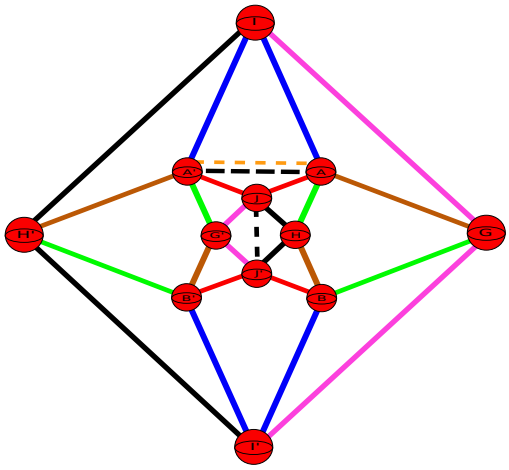

We see that a parallel curve to the added 2-handle running between A, A' does not at any point

cross over the added 2-handle. A similar argument for the added 2-handles running between C, C', J, J', K, K' shows that these added 2-handles have parallel curves behaving in a similar way.

Let us show that the added 2-handle running from E to G and from E' to G' has parallel curve exhibiting a similar behaviour. We start by taking a parallel curve component to the piece going into E, we choose the parallel curve component to lie just above this added 2-handle piece. The following picture shows the added 2-handle (corresponding to the boundary filling) in green, and the parallel curve component in orange. Remember that we are drawing the added 2-handle component, in green, as a curved arc purely for ease of viewing. The reader should really think of this as a straight line running from E to G. Due to this we have had to draw the parallel curve as a curved arc, again the reader should think of this as a straight line running into E and that is parallel to what should be a straight line running between E and G.

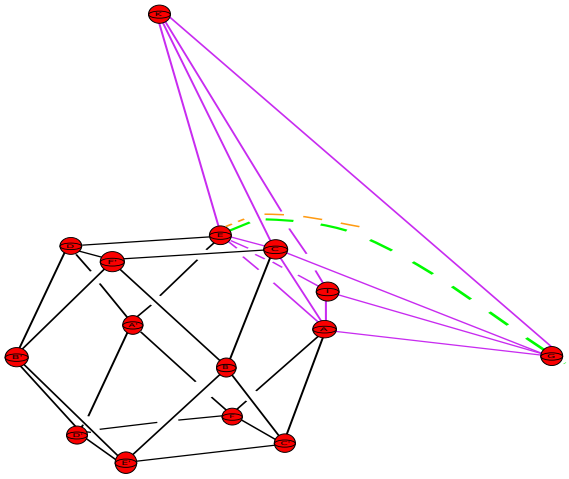

The attaching map for E, E' was given by the composition of the inversion in S^2 followed by the antipodal map. A rough computation, similar to what we did when analysing 2-handles in the diagram corresponding to those six 2-handles that did not all lie in a single plane (see end of previous chapter) shows that the orange parallel curve comes out of E' slightly above the added green 2-handle.

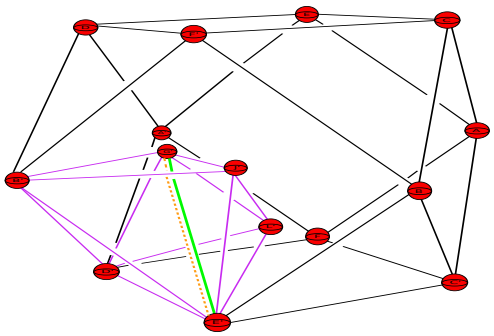

The attaching map for G, G' is the same as the one for E, E', and a little rough analysis shows that when the parallel curve comes out of G' it does so just above the added green 2-handle.

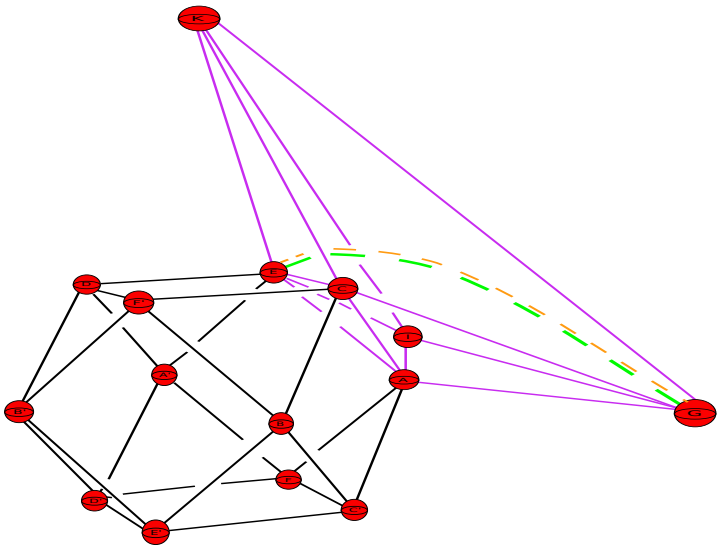

We thus see that the parallel curve never crosses over the added 2-handle, and in this regard has a planar framing. The importance of this observation is that the closed filled in manifold, obtained from filling in the boundary of M, has a Kirby diagram with every 2-handle having a planar framing is that it allows us to carry out handle slides in a very straight forward manner. In particular, for those 2-handles that reside in the diagram corresponding to the six 2-handles that do not all lie in a single plane the handle slides can be carried out as if these 2-handles were all lying in a single 2-plane.

There is one technicality to do with the **second elementary move** we described in section 2.2. This was the handle slide that involved pushing a component of 2-handle through one attaching sphere of a 1-handle so that it came out of the second attaching sphere. When we described this handle slide, we showed how it took place in the case that the 2-handles were all residing in a single 2-plane. In this situation it was straightforward to understand how the 2-handle component behaved as it went through one attaching sphere and then out the other. We also want to carry out such handle slides in the diagram corresponding to the six 2-handles that do not all lie in a single 2-plane. In this case one has to be a bit careful, the reason being that if the attaching map identifying the attaching spheres is some "wild" diffeomorphism then it may well be the case that when we push a component of 2-handle through one attaching sphere it could come out the other in a very non-trivial way. The point is that for all the Kirby diagrams we consider this will never be a problem as the attaching maps between attaching spheres are very straightforward. Let us explain this in a bit more detail.

Suppose we have a 1-handle S, S' and we have a component of a 2-handle that goes in to S, as

shown in the following diagram.

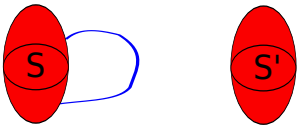

We can then push the blue 2-handle component through S so that it comes out of S'. What we are really doing when we carry out such a move is we are isotoping the blue curve onto the attaching sphere S, producing a curve on S. For example, the following diagram shows one such isotopy in which the blue 2-handle component has been moved to give a curve on the attaching sphere S.

Now, we have an attaching map from S to S', which is some diffeomorphism identifying the spheres. Therefore, the blue curve on S will map to some image curve on S', once we understand how this image curve on S' looks we can then understand what the blue 2-handle component looks like after we have pushed it through S. It is at this point that one must be very careful, for the attaching map identifying S to S' could be some "wild" diffeomorphism, which in turn may map the blue curve on S to some curve on S' that winds around S' several times. If there are other bits of 2-handle coming out of S', then this image curve could wrap around some of these other bits of 2-handle, and this is precisely why it is important to know what the attaching map between the attaching spheres is. In our case all attaching maps are reflections or compositions of reflections with inversion in S^2, therefore it is a straightforward process to work out what a 2-handle component looks like when we push it through a 1-handle.

We give an explicit example of this sort of computation. Consider the diagram consisting of the six 2-handles that did not all lie in a single plane together with the added 2-handle running from A to A', corresponding to a filling of a boundary component.

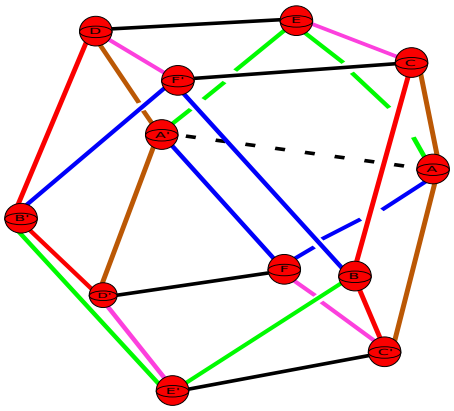

When we use the added 2-handle running between A and A' (black dashed line) to cancel A, A' the green 2-handle component moves in to the following position.

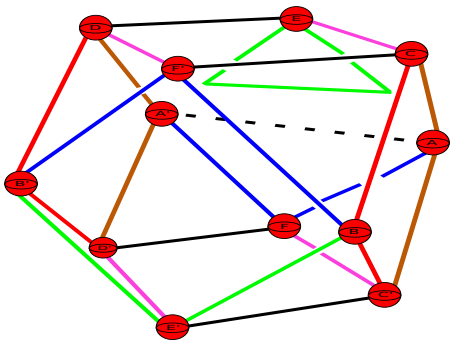

We can then slide this green 2-handle component through E so that it comes out of E'. To start with this involves isotoping the green curve looping back into E to the following curve on E.

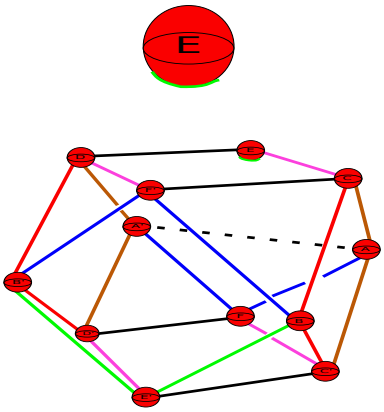

We have shown a close up of the curve on E and how it looks in the whole diagram. The curve sits in a plane parallel to the x-z plane

If we want to push it through so that it comes out of E' we need to understand what the attaching map for E, E' is. Observe that there are other 2-handles that are hitting E', we have a pink and black 2-handle component in the above diagram, but E' also sits in the y-z plane, and there are blue, black and pink 2-handle components in that plane meeting E' (see diagram showing 2-handles in the y-z plane). Therefore it is possible that when we send the green curve on E, using the attaching map of E, E', we could end up with an image curve on E' that winds around some of these other 2-handle components meeting E'.

In this situation we know exactly how E is identified to E', we showed that the identifying map was given by

$$(x, y, z) \mapsto \left(-\frac{x}{x^2+y^2+z^2}, -\frac{y}{x^2+y^2+z^2}, -\frac{z}{x^2+y^2+z^2} \right)$$

which is the composition of the inversion in S^2 followed by the antipodal map. Recall that the attaching sphere corresponding to E is a sphere (of some small arbitrary radius) centred at the point $(0, \frac{1}{\sqrt{2}}, \frac{1}{\sqrt{2}})$. The green curve on E lies inside S^2:

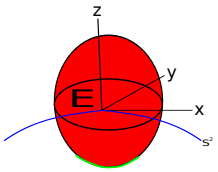

When we apply the inversion map it will map to a curve outside of S^2. The following diagram shows what it looks like when we apply the inversion map.

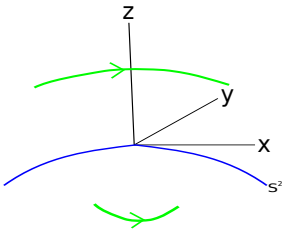

We then apply the antipodal map to get the following curve on E'.

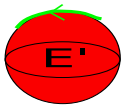

In the whole diagram we then see that the image of the green curve, which was residing on E, under the attaching map from E to E' looks like:

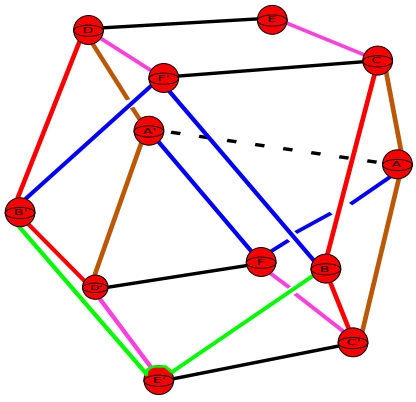

Thus, what we are able to conclude is that when we push the original green curve through E it comes out of E' in straightforward manner, and does not "wind around" any of the other 2-handle components meeting E'. We can then proceed to push the green 2-handle component

off E' to obtain a green 2-handle component passing over B, B' once and that does not interfere with any of the other 2-handles

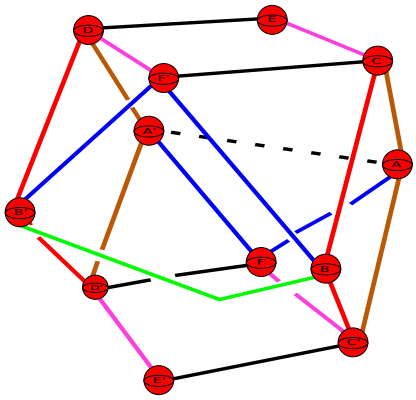

In general we will carry out several moves where we push a 2-handle component through the attaching sphere of a 1-handle. As all our attaching maps are reflections or reflections composed with inversion in S^2, we will find that we will never be in a situation where the curve on one attaching sphere is pushed to a curve in the image attaching sphere in such a way that it winds around other bits of 2-handle.

Before we proceed to doing some handle cancellations we remark that some of these added 2-handles will intersect some of the other planes. For example consider the added 2-handle that runs between $C - C'$, as the co-ordinate of $C = (\frac{1}{\sqrt{2}}, 0, \frac{1}{\sqrt{2}})$ and $C' = (\frac{1}{\sqrt{2}}, 0, \frac{-1}{\sqrt{2}})$, we can see that in the bottom right picture above, this 2-handle must intersect the $x - y$ plane. We have drawn this intersection point as a black dot in the top left picture below. Similarly the added 2-handle that runs over $A - A'$ intersects the $y - z$ plane in a point, and this has been drawn as a black dot in the bottom left picture below. Finally, the 2-handle passing over $J - J'$ intersects the $x - z$ plane in a point, and this can be seen as a black dot in the top right picture below.

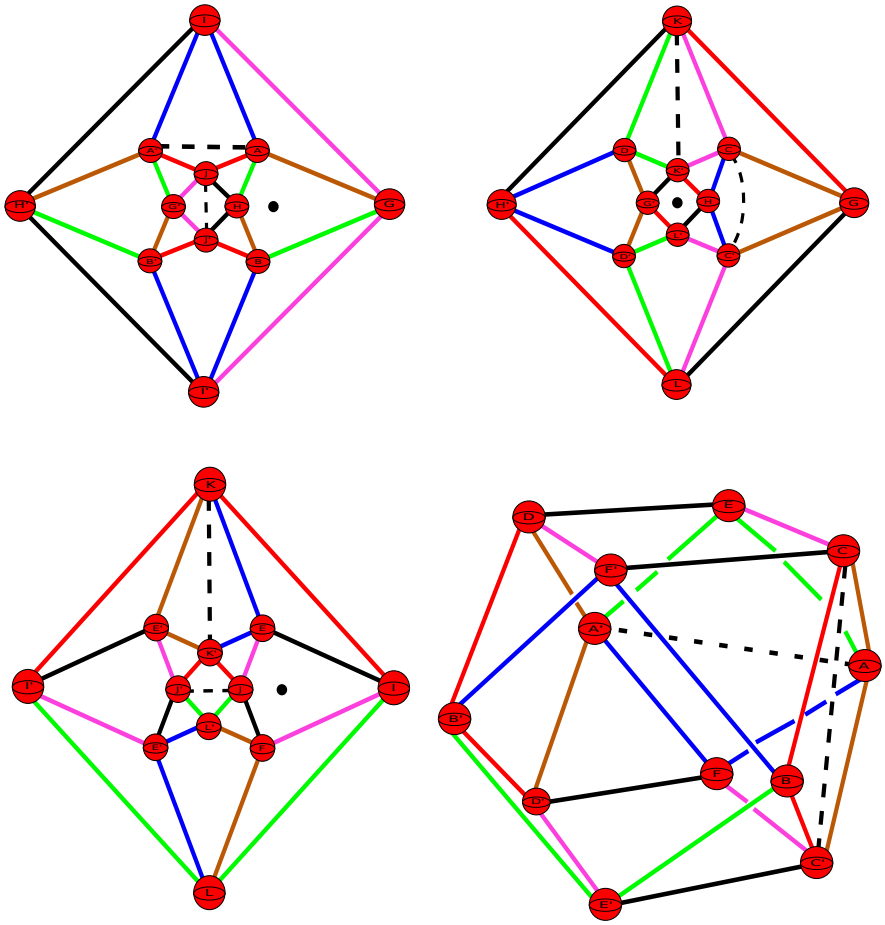

When we start cancelling handles and doing handle slides we have to be careful that we do not cut through any of the other 2-handles for then we would be doing an "illegal" move, and that if one of our 2-handles goes around another, then a handle slide on one may cause the other to change position and we have to keep track of this. It turns out that none of this really creates any problems as all our moves are primarily done in the planes in question, and it can be clearly seen that they do not tangle around any of the added 2-handles that intersect these planes.

The above discussion may seem confusing so we go through a few handle cancellations in detail to make our point.

The added 2-handles corresponding to boundary fillings pass over a 1-handle once and hence form a handle cancellation pair, therefore we may cancel them from our diagram. We recall that if we have a handle cancelling pair that does not meet any other 2-handles in a Kirby diagram then we can simply delete them from the diagram. However, if there are some 2-handles that pass over the 1-handle that we are cancelling, we must push those 2-handles through the 2-handle that is cancelling the 1-handle.

We start by cancelling $A - A'$ (the reader should compare this with the first elementary move

we showed in the previous section) using the added 2-handle that passes over it once. This only affects the 2-handles in the $x-y$ plane and the six extra 2-handles that do not lie in any one plane. The following pictures show the Kirby diagrams of these handles once we have done the cancellation.

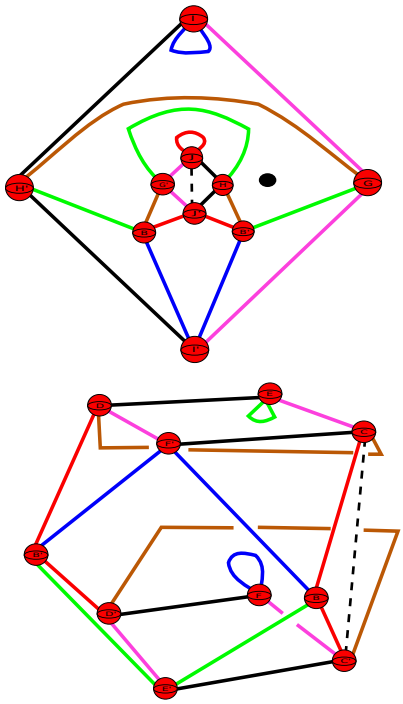

Recall that this 2-handle that we just used to cancel $A-A'$ intersected the $y-z$ plane, hence when we use it to cancel $A-A'$ we will introduce new intersection points in the $y-z$ plane, and it is important to keep track of these new intersection points.

We start by giving an analysis of what happens when we cancel $A-A'$ from the $x-y$ plane. First of all, the cancellation from the $x-y$ plane introduces some new 2-handles in the $x-y$ plane. We have the blue 2-handle that starts at I and loops back into I. This creates an intersection point in the $y-z$ plane close to I, you can see it as the black dot in the following diagram:

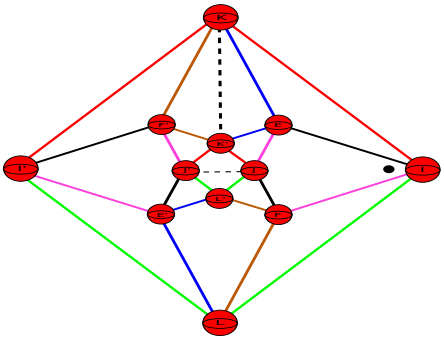

We also have the new brown 2-handle in the $x-y$ plane that goes between G and H', this creates a second intersection point with the $y-z$ plane:

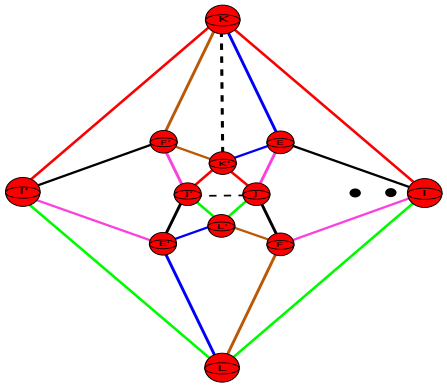

Remaining in the $x-y$ plane we also have the new green 2-handle that passes between G' and H, this introduces a third intersection point in the $y-z$ plane.

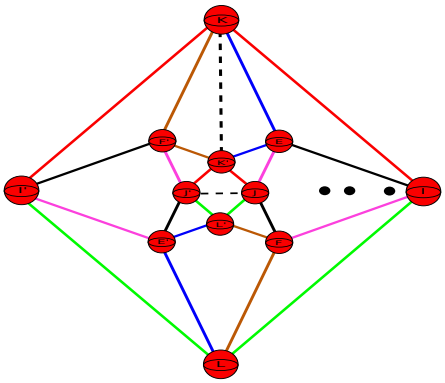

Finally, we have the red 2-handle that starts at J and loops back into it, this gives a fourth intersection point.

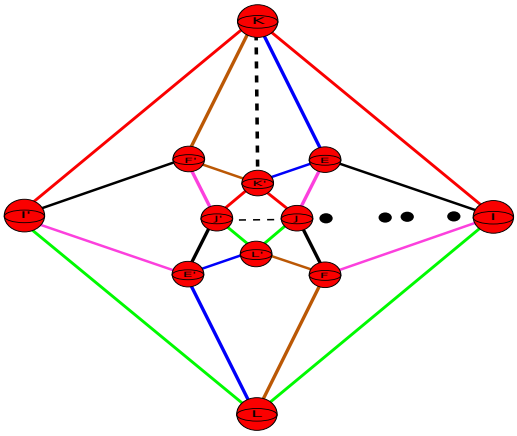

In total we obtain four new intersection points from cancelling $A - A'$ from the $x - y$ plane. However we are not done yet, there will also be some intersection points arising from the cancellation of $A - A'$ from the diagram containing the six 2-handles that do not all lie in any 2-plane.

The analysis of this situation is exactly analogous to what we did above. We start with the green 2-handle that starts at E and loops back into it. This gives an intersection point in the $y - z$ plane near E as shown in the following diagram.

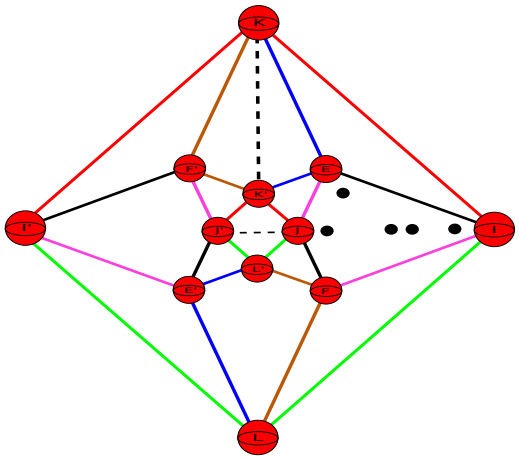

The brown 2-handle that runs between C and D gives an intersection point that looks like:

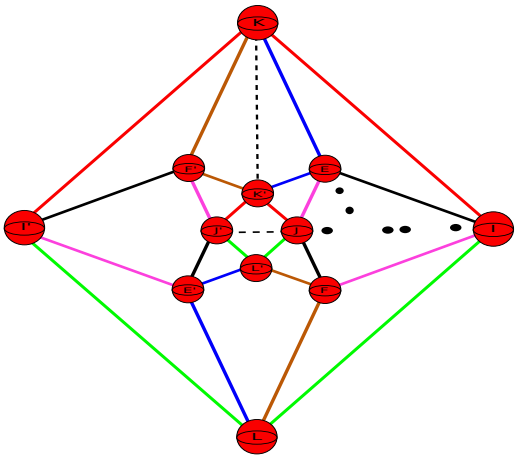

There is also the brown 2-handle that runs between C' and D', this gives a point of intersection that looks like:

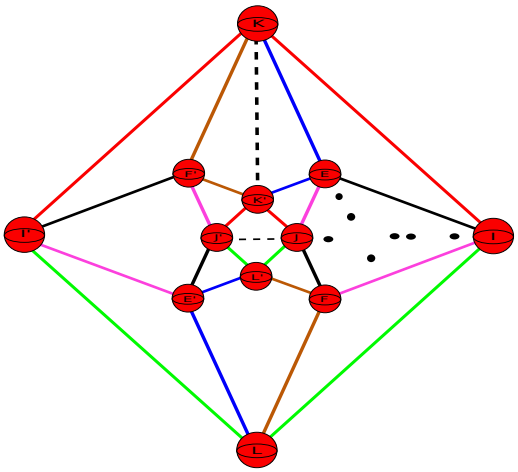

Finally, we have the 2-handle that starts at F and loops back into it, it gives an intersection point near F:

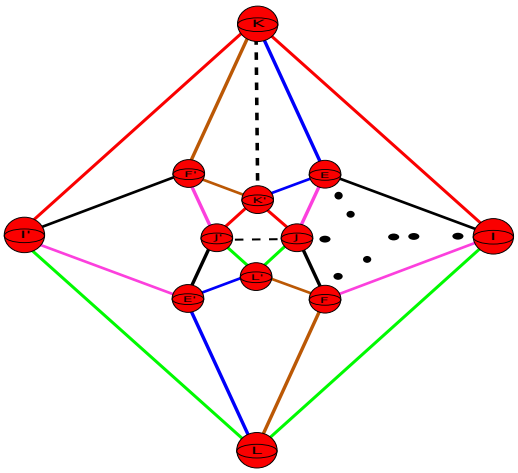

In total we get 8 new intersection points, to make things easier we want to keep track of how each intersection came about. Namely, we want to keep track of which 2-handle in which diagram gave us a particular intersection point. To do this we will introduce a simple coding system that will allow us to keep track of where these points of intersection are coming from. Each intersection point will be labelled with either four letters or two letters. In the case of four letters, the first two will tell us that the intersection point is coming from the $x-y$, $x-z$ or $y-z$ planes, and the next two letters will tell us the 1-handles that the 2-handle causing the intersection point is passing between, the actual 2-handle will be clear from context. In the case of a two letter code, we are to interpret that the 2-handle causing the intersection point is coming from the diagram representing the six 2-handles that do not all lie in a single 2-plane. The two letters denote the two 1-handles that this 2-handle passes over, again the actual 2-handle in question will be clear from the context.

At times it will be difficult for us to show the labels of all intersection points in the whole diagram simply because there may be too many intersection points and not enough space. In these instances we will always show two diagrams, a whole diagram with unlabelled points of intersection and a close up diagram of the labelled intersection points. It will be easy to tell which point corresponds to which point in the two diagrams.

It is time to show an explicit example of what exactly we mean by this code, and how exactly it looks. The following picture shows the $y-z$ plane with a black dot near I labelled **XY_II**, the first two letters being XY tell us that the 2-handle giving this point of intersection is coming from the $x-y$ plane, the second two letters are II and this tells us that the 2-handle in the $x-y$ plane is starting at I and looping back into I.

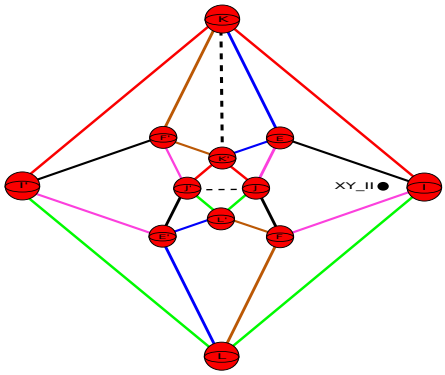

This is precisely the point of intersection we talked about above which arose through cancelling $A-A'$ in the $x-y$ plane, and we showed a picture of it previously. There were also many other intersection points (remember there were 8 in total!), as another example the following picture shows a labelled intersection point coming from cancelling $A-A'$ in the diagram corresponding to the six 2-handles that do not all lie in a single 2-plane. The labelling consists of just two letters, which immediately tells us that the 2-handle contributing this point of intersection is coming from the diagram corresponding to the six 2-handles that do not all lie in a single 2-plane. The two letters are CD, which tell us that the 2-handle in question is running between the 1-handle C and the 1-handle D.

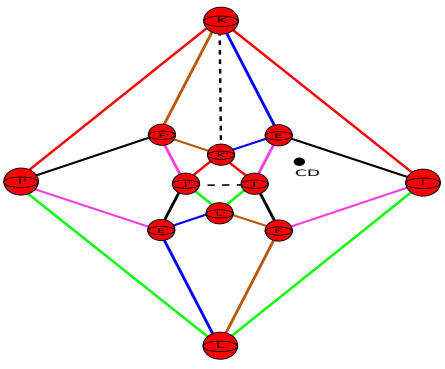

When we cancelled $A - A'$ we saw that there were a total of 8 new points of intersection. The following shows a close up of all these points of intersection with their corresponding labels.

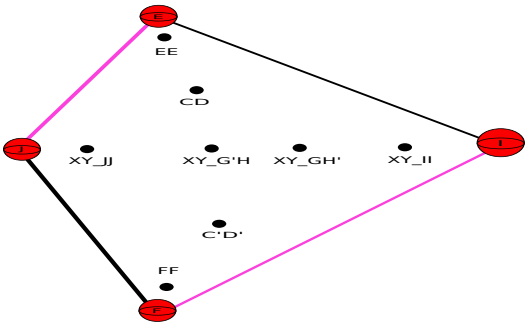

So far we have done one handle cancellation, and in some detail explained how we get extra points of intersection. The following picture shows what we have done.

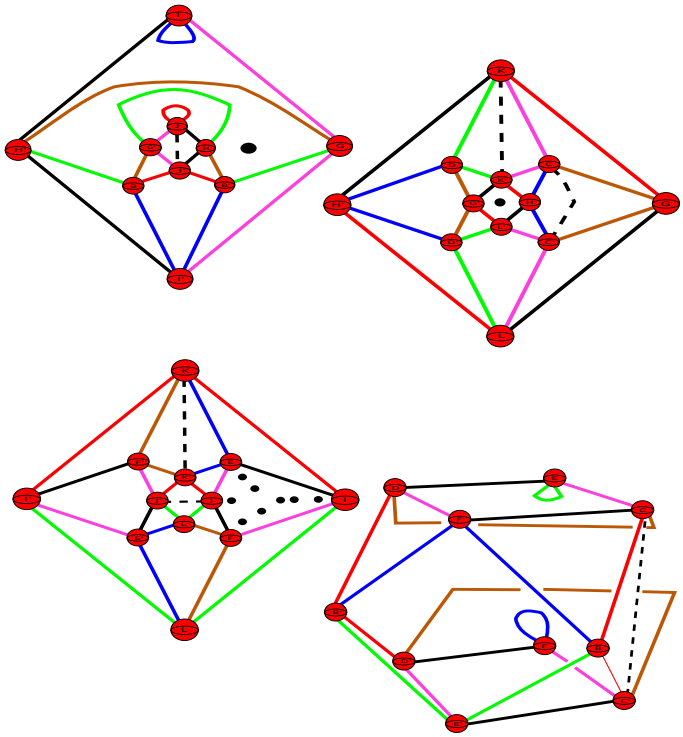

In the top left diagram we have a 2-handle, corresponding to (the one in blue)

$$A \cap I \xrightarrow{a} A' \cap I \xrightarrow{i} B' \cap i' \xrightarrow{b^{-1}} B \cap I' \xrightarrow{i^{-1}} A \cap I$$

which has a component that loops back into I. In the above picture this is the blue arc at the top meeting I twice. We can then slide it over the 1-handle $I - I'$ to give a 2-handle that meets $B - B'$ once.

There is also a second handle slide we can do in the $x - y$ plane. Namely, we have the 2-handle

in red that starts at J and loops back into it. We can then slide it over the 1-handle $J - J'$ to give a 2-handle in red that also meets $B - B'$ once.

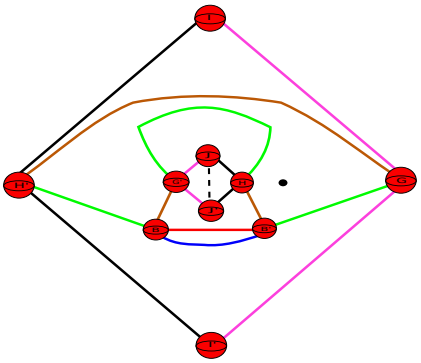

In carrying out these two handle slides the intersection points labelled **XY_II** and **XY_JJ** in the $y - z$ plane will disappear. However, in the $x - y$ plane the 2-handle (in blue) that meets $B - B'$ once will give a point of intersection in the $y - z$ plane in the region bounded by the 1-handles I', F', J' and E' and the 2-handles that run between them, and the red 2-handle that meets $B - B'$ will also give an intersection point in the $y - z$ plane in the region bounded by the 1-handles I', F', J', E' and the 2-handles that run between them.

The picture below shows these new intersection points along with the other intersection points that we have encountered so far. The two diagrams at the bottom of the picture show close ups of the regions that these intersection points lie in and the labels of the intersection points.

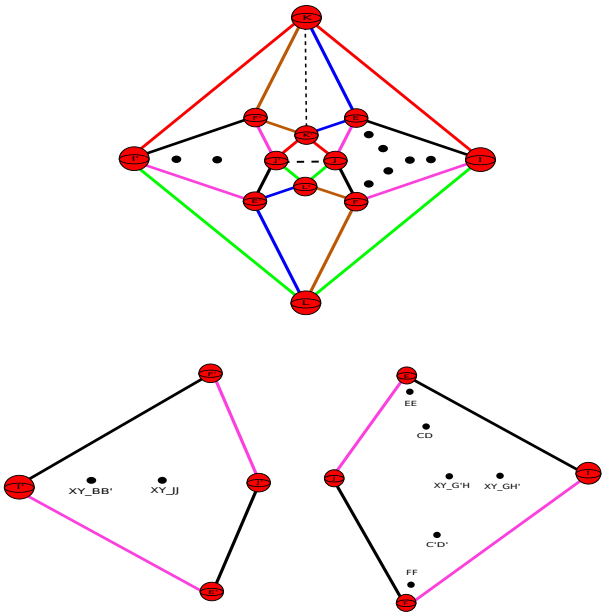

We can also carry out two handle slides in the diagram consisting of the 2-handles that do not all lie in a single 2-plane. We can slide the green 2-handle that starts and ends at E through E

and then off E' to obtain a 2-handle that meets $B - B'$ once. Similarly we can slide the blue 2-handle that starts and ends at F through F and then off F' to give another 2-handle that meets $B - B'$ once.

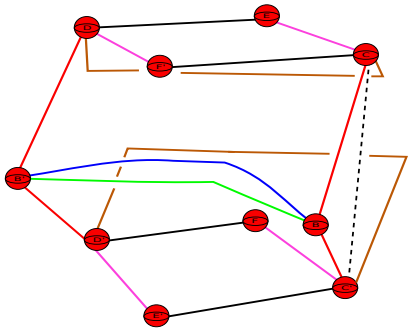

These handle slides that we have carried out have not interfered with the added 2-handles running from E to G and E' to G'. In the case of the added 2-handle that runs between E and G this is easy to see as it lies outside of the diagrams for which these handle cancellations and slides are being done. In the case of the 2-handle that runs between E' and G' it is also easy to see, using some three dimensional insight, that none of the cancellations and slides we have done so far affect the handle. The following picture shows how this 2-handle sits after we have carried out the above cancellations and slides, it is drawn in yellow. The picture is supposed to give the reader some insight in to why it is the case that carrying out the above cancellations and slides does not affect the added 2-handle that runs between E' and G'.

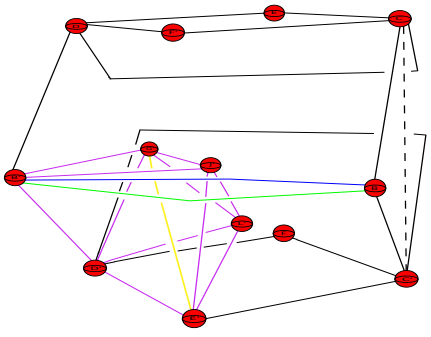

The two handle slides just carried out above will cause the intersection points in the $y - z$ plane labelled **EE** and **FF** to disappear, but the two new 2-handles between $B - B'$, that arose through these handle slides, will give two new points of intersection in the $y - z$ plane in the region bounded by I', F', J', E' and the 2-handles that run between them.

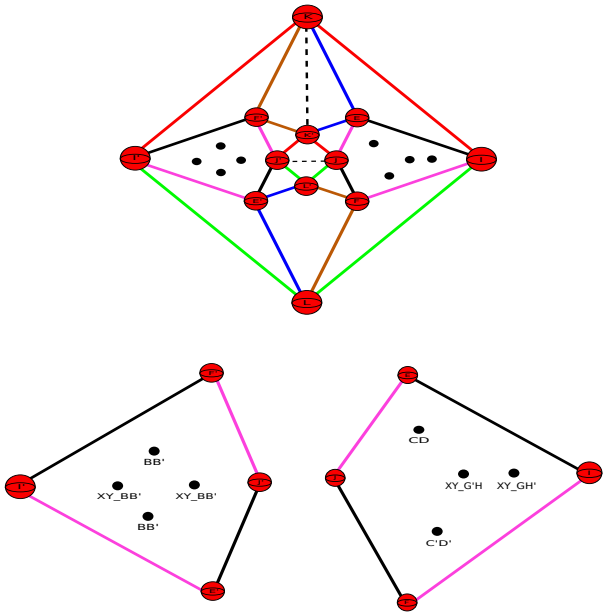

The following picture shows the end result of cancelling $A - A'$, along with the various handle slides we under took after this cancellation

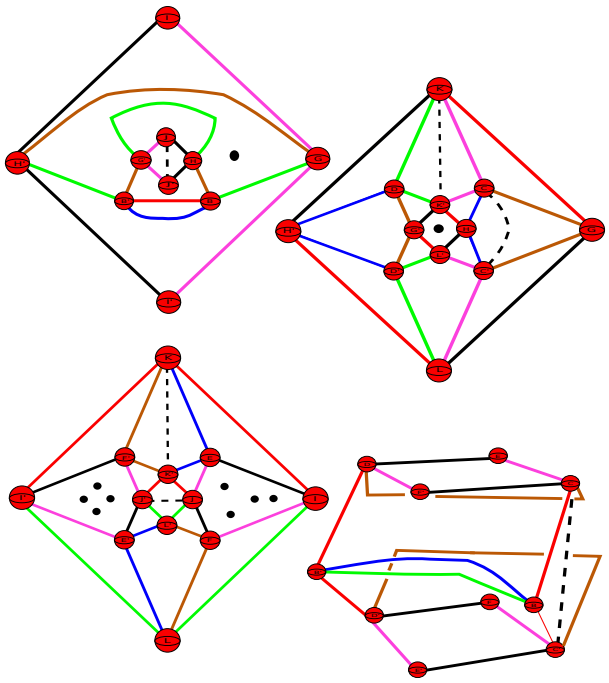

and the picture below shows how the added 2-handles running between E and G, and E' and G' sit in our Kirby diagram so far.

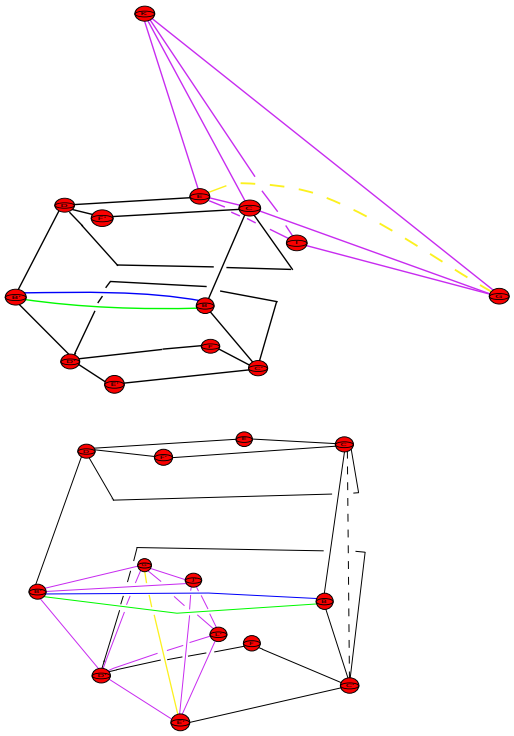

We now cancel $K - K'$, in this case only the 2-handles in the $x - z$ and $y - z$ planes change.

The following picture shows how the Kirby diagrams change after we have carried out this cancellation.

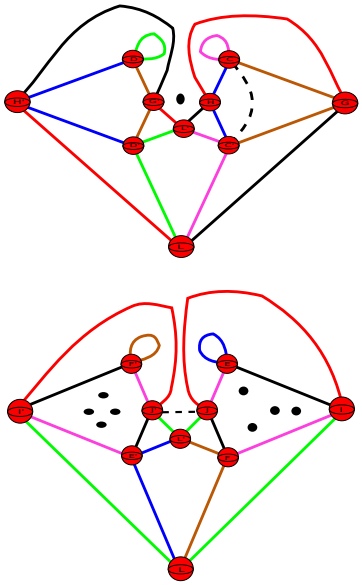

At this point one can ask if cancelling $K - K'$ has introduced any new intersection points in any of the other diagrams ? The only candidate is the $x - y$ plane. In this case it is easy to see that no intersection points are created. Let us give a brief explanation of why this is the case. Start with the $x - z$ plane, this meets the $x - y$ plane along a straight line that passes

through the one handles H', G', H and G. In the following picture you can see this line as the horizontal yellow line through H', G', H and G, where the top diagram is that of the $x-y$ plane, and the bottom diagram is that of the $x-z$.

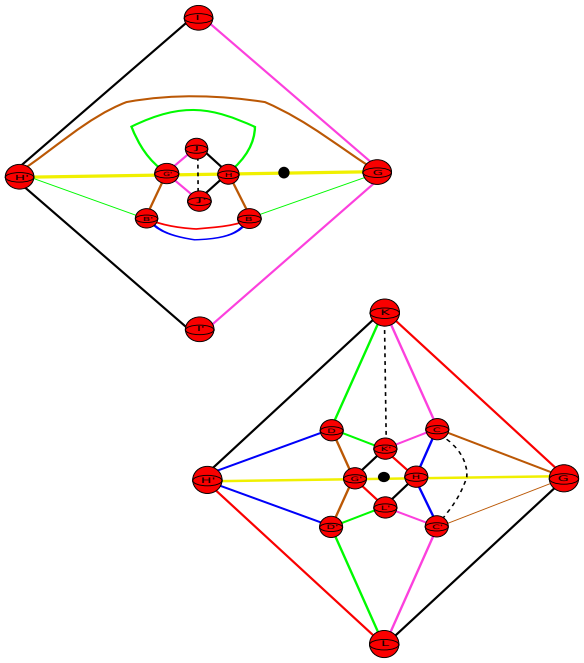

When we cancel $K-K'$ from the $x-z$ plane it is easy to see that none of the cancellations interfere with the yellow line, meaning that in cancelling $K-K'$ from the $x-z$ plane none of the 2-handles that emerge from this cancellation cross the yellow line. This means none of these 2-handles contribute to any intersection points in the $x-y$ plane.

In the case of the $y-z$ plane we have that it intersects the $x-y$ plane along a vertical line through I', J', J and I, as shown in the following picture.

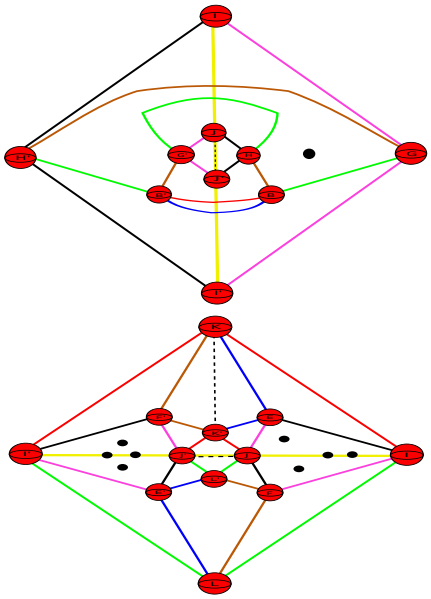

In this case you can also clearly see that when we cancel $K - K'$ from the $y - z$ plane none of the new 2-handles that emerge from this cancellation cross the horizontal yellow line in the $y - z$ plane. This means none of these 2-handles intersect the $x - y$ plane, and hence we do not get any points of intersection from cancelling $K - K'$ from the $y - z$ plane.

Coming back to the pictures of the $x - z$ and $y - z$ planes, after cancelling $K - K'$ we see that we can do some handle slides. First of all, in the $x - z$ plane we have a green 2-handle that starts at D and loops back into it, and a pink 2-handle that starts at C and loops back into it. We can slide the green 2-handle through D to D' and then off D' to give a 2-handle meeting $L - L'$ once. We can do the same with the pink 2-handle to get another 2-handle meeting $L - L'$ once.

In the case of the $y - z$ plane we have the red 2-handle that starts at F' and loops back into it, and we have the blue 2-handle that starts at E and loops back into it. We can then slide these (just as we did above) to give two 2-handles that meet $L - L'$ once.

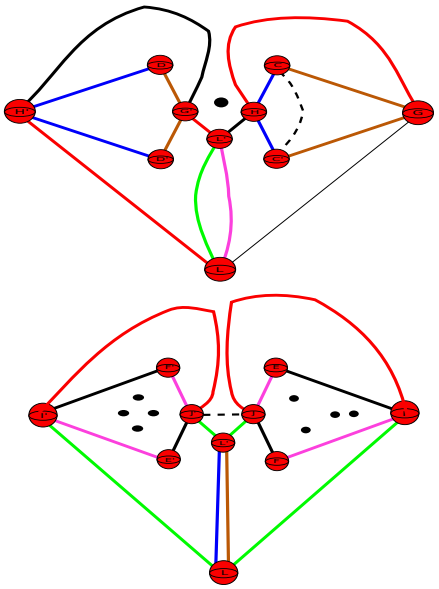

Observe that in carrying out these handle slides we have not added any new points of intersection to the $x - y$ plane. For example the two handle slides we did in the $x - z$ plane gave us two 2-handles that met $L - L'$ once. These two 2-handles do not cross the intersection line of the $x - y$ plane with the $x - z$ plane, hence these new 2-handles cannot intersect the $x - y$ plane. A similar analysis for the handle slides in the $y - z$ plane shows that they do not add any points of intersection as well.

It is clear that in cancelling the 1-handle $K - K'$ we have introduced no new intersection points in the other diagrams. For example when we cancelled $K - K'$ in the $x - z$ plane, we introduced a 2-handle that loops back in to C, it is the pink 2-handle in the first cancellation diagram. This 2-handle does not introduce any intersection points in the $x - y$ plane because C lies above the

$x-y$ plane. Similarly we also introduced a 2-handle that goes from H to G, it is drawn as the red 2-handle in the picture above. This 2-handle also does not create any points of intersection with the $x-y$ plane. A similar analysis shows that when we first cancel $K-K'$ none of the new 2-handles formed create any new intersection points.

We then proceeded to doing some handle slides, and we can ask whether these handle slides create any new intersection points. It turns out that they do not, and one can easily see this by simply thinking of what happens in a 3-dimensional picture. Let us give an explicit analysis of this, we will work with the $y-z$ plane and the 2-handle that loops back in to E, it is drawn in blue in the first picture showing what happens when we cancel $K-K'$ (see the picture before the three above pictures). We push this 2-handle through $E-E'$ to get a 2-handle meeting $L-L'$, note that E', L' and L all lie below the $x-y$ plane. Hence when we push this 2-handle through $E-E'$ to give a 2-handle between $L-L'$ we create no intersection points with the $x-y$ plane. Similarly, this new 2-handle does not create any intersection points with the $x-z$ plane.

So far we have filled in two boundary components of the manifold M corresponding to the fibres given by the isometries a and k. We then carried out various handle cancellations and handle slides. The following picture puts all that we have done so far together.

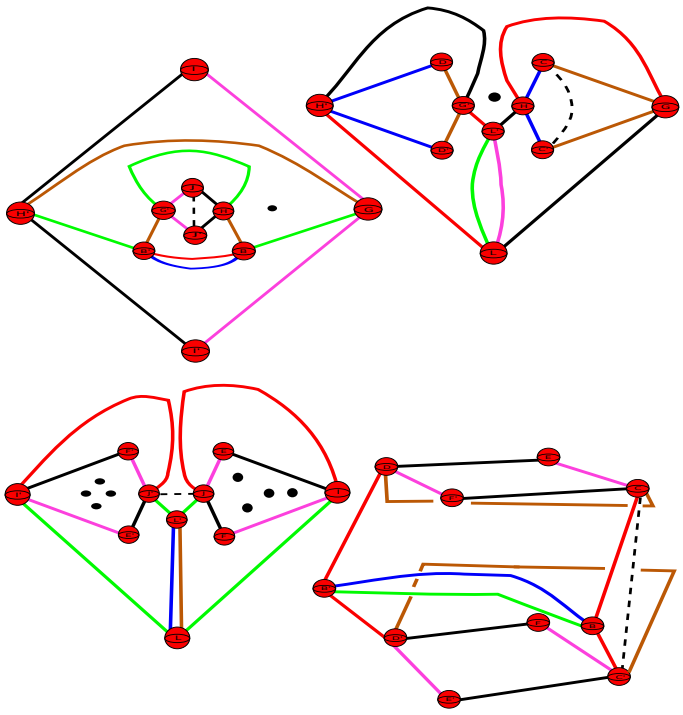

The labelling of the intersection points are shown in the following diagram. The top two diagrams show close ups of the regions around the intersection points in the $x-y$ and $x-z$ planes respectively (viewing from left to right). The bottom two diagrams show close ups of

the intersection points in the $y-z$ plane.

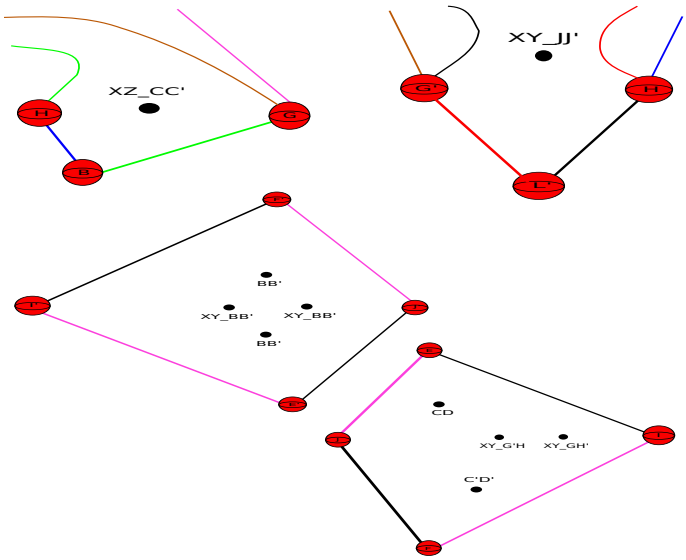

The next step is to cancel $J-J'$, this cancellation will only affect the $x-y$ and $y-z$ planes. The diagrams on the right correspond to sliding the obvious handles in the left picture over 1-handles and then off them to obtain 2-handles that only meet certain 1-handles once. For example in cancelling $J-J'$ from the $x-y$ plane we obtain a pink 2-handle that starts at G' and loops back into it (see the top left diagram in the picture below), we can then slide this through G' and off G to obtain a pink 2-handle that meets $I-I'$ once (see the top right diagram in the picture below).

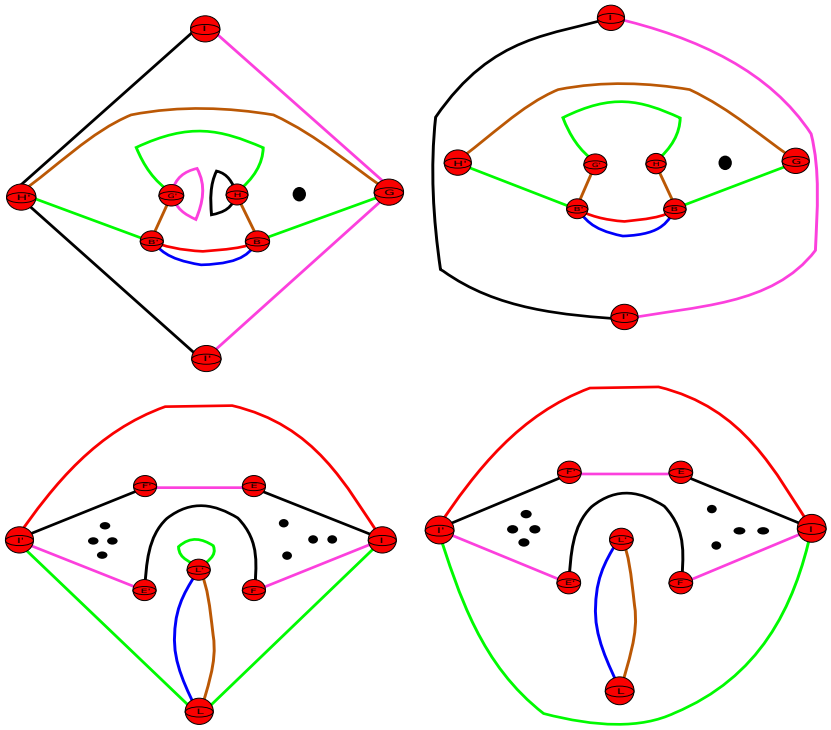

When we first cancel $J - J'$ in the $x - y$ plane we introduce some new 2-handles, namely the one in pink that loops back into G' and the one in black that does the same with H. These two 2-handles create two new points of intersection with the $x - z$ plane:

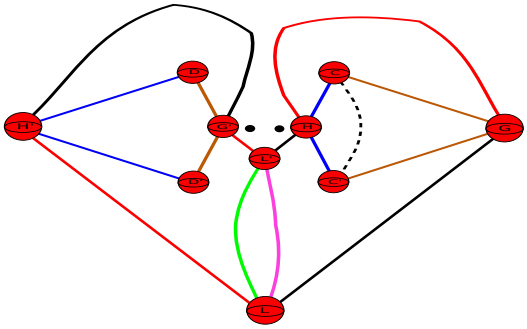

When we cancel $J - J'$ in the $y - z$ plane we introduce a 2-handle between $I - I'$, $E - F'$, $E' - F$, and one that loops back into L'. These four 2-handles each create intersection points with $x - z$ plane as well, you can see them as the four vertical black dots:

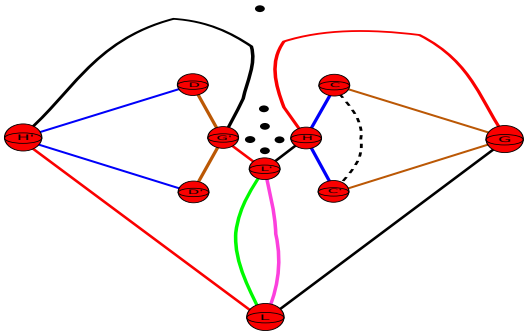

The labelling of these 6 new intersection points is given in the following picture.

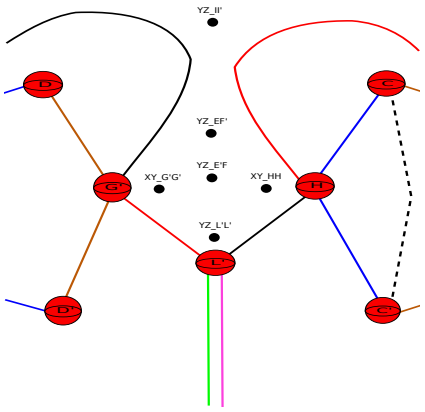

After cancelling $J - J'$ we carried out some some handles slides. In the $x - y$ plane we slid the new 2-handle that starts at G' and loops back into it (the one in pink) through G' and then off G to give a 2-handle that passes over $I - I'$ once. This will cause the intersection point in the $x - z$ plane, labelled **XY_G'G'**, to disappear. However, a new intersection point will arise

corresponding to the new 2-handle that passes over $I - I'$ once. This new intersection point is shown in the following diagram as the black dot to the right of G, you can also see that the intersection point labelled **XY_G'G'** is no longer in the picture.

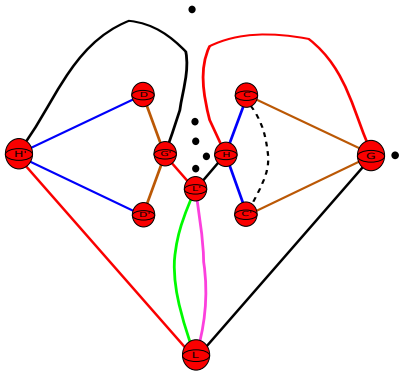

The other handle slide we did in the $x - y$ plane was to take the black 2-handle that starts at H and loops back into it and slide it through H and then off H' to give a new 2-handle that passes over $I - I'$ once. This handle slide causes the intersection point labelled **XY_HH** to disappear with a new intersection point appearing to the left of H' (viewed in the $x - z$ plane).

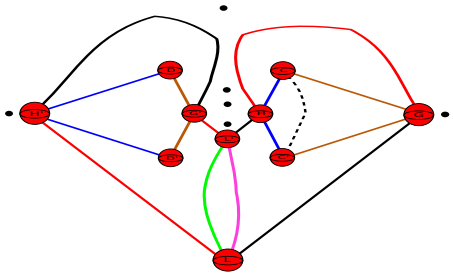

We also carried out one handle slide in the $y - z$ plane. This handle slide corresponded to taking the green 2-handle that starts at L' and loops back into it, pushing it through L' so it comes out at L, and then sliding it off to give a new 2-handle that passes over $I - I'$ once. This causes the intersection point labelled **YZ_L'L'** to disappear, with a new intersection point just below L to appear. The following picture shows this new intersection point and all the others with their corresponding label.

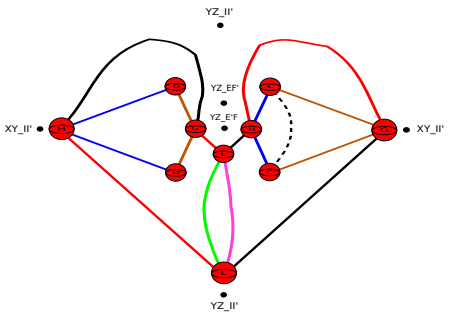

If we put everything we have done so far we get the following:

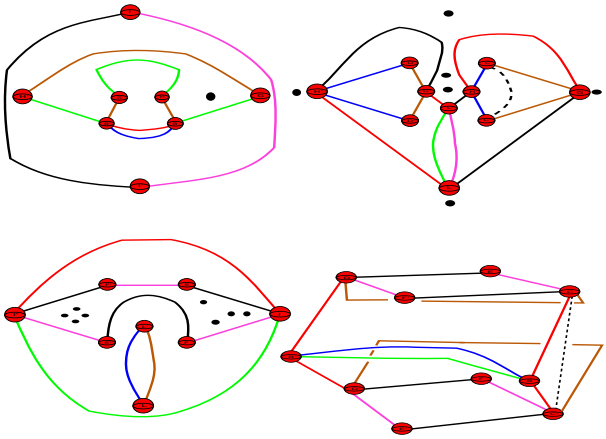

The pictures showing how the added 2-handle running between E and G, and E' and G' is the same as before.

We move on to cancelling $C - C'$, this will only affect the $x - z$ plane and the six 2-handles not lying in any one plane.

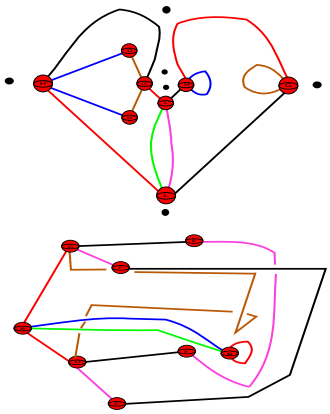

Recall that the added 2-handle that passed between $C - C'$ (the one we just used above to cancel $C - C'$) intersected the $x - y$ plane. Therefore the above handle cancellation will give rise to some points of intersection in the $x - y$ plane. We take the time to explain how these points of intersection look like.

Start with the $x - z$ plane, when we cancel $C - C'$ we got two new 2-handles one in blue which starts at H and loops back into it, and one in brown that starts at G and loops back into it. These will give two new intersection points in the $x - y$ plane, as shown below:

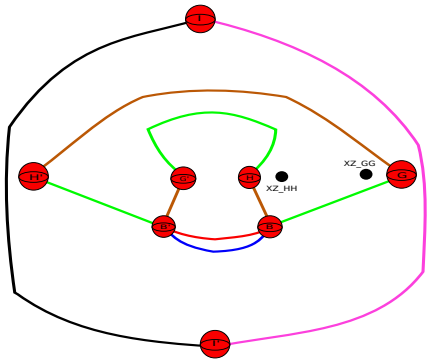

Moving to the case of the six 2-handles that did not all lie in a single 2-plane, we see that we get four new points of intersection. First of all, we have the red 2-handle that starts and ends at B. Secondly, we have the black 2-handle that runs from E' to F' and the pink 2-handle that runs from F to E. Finally, we have the brown 2-handle that runs from D to D'. All four of these 2-handles give four points of intersection in the $x-y$ plane. The following picture show these points of intersections in the $x-y$ plane, with the bottom diagram being a close up showing the labelling of these intersection points.

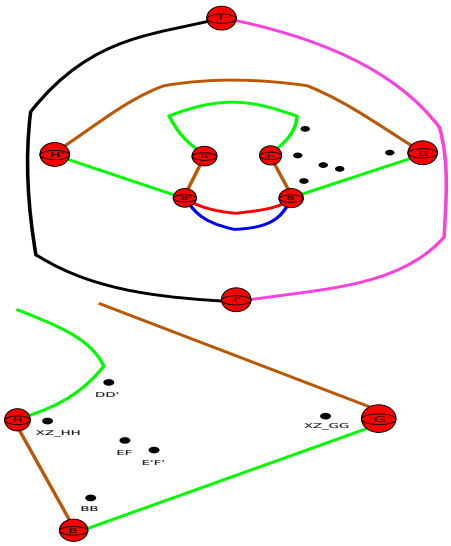

We also have to deal with the points of intersection in the $y-z$ plane. We have two points of intersection labelled **C'D'** and **CD**, when we cancel $C-C'$ from the diagram that consisted of the six 2-handles that did not all lie in a single 2-plane the part of the brown 2-handle component running from C' to D' and the part running from C to D join together to give a brown 2-handle running from D to D'. Thus in the $y-z$ plane we will still see two points of intersection but their labelling will be **DD'** because this new brown 2-handle running from D to D' intersects the $y-z$ plane in two distinct points.

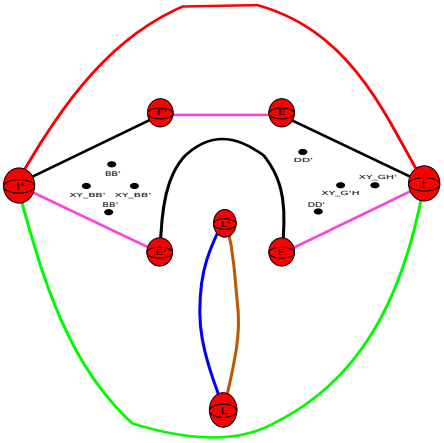

We can then carry out three handle slides. In the $x-z$ plane we can slide the blue 2-handle that starts and ends at H through H and then off H' to give a blue 2-handle between $D-D'$. Similarly, we can slide the red 2-handle that starts and ends at G off G' to give a red 2-handle that meets $D-D'$ once. Finally, in the diagram corresponding to the six 2-handles that did not all lie in a single 2-plane, we have the red 2-handle that starts and ends at B. We can slide it off B' to give a red 2-handle meeting $D-D'$ once.

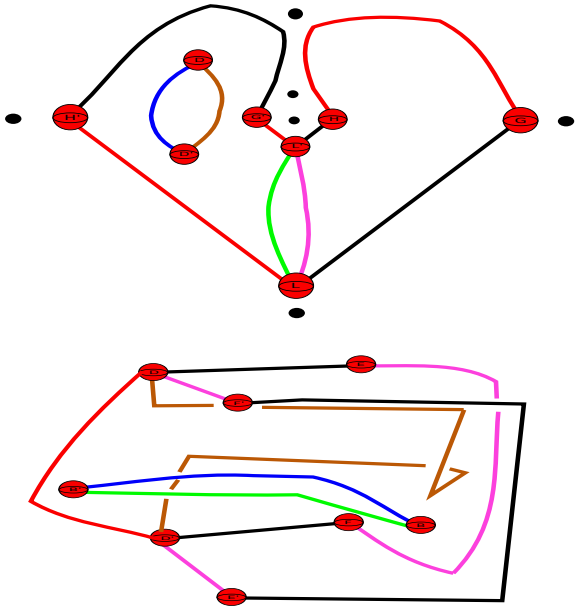

The first two handle slides we undertook will cause the points of intersection labelled **XZ_HH** and **XZ_GG** to disappear from the $x-y$ plane, however we will get two new points of intersection coming from the new 2-handles that run between $D-D'$, these are shown in the picture below with labelling **XZ_DD'**. The second handle slide we undertook will cause the point of intersection labelled **BB** to disappear, but the new 2-handle that we obtained running from D

to D' will give a new intersection point labelled **DD'**. These new points of intersection can be seen in the picture below.

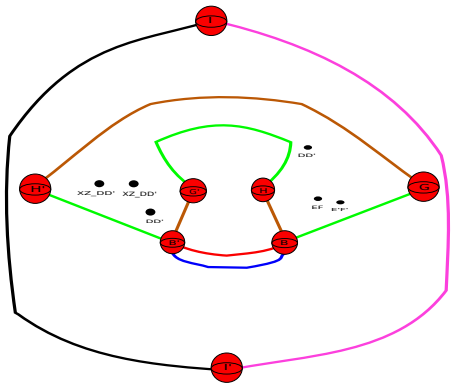

These handle slides do not affect the $y-z$ plane.

So far we have we have cancelled the 1-handles $A-A'$, $K-K'$, $J-J'$ and $C-C'$, the result of all these cancellations and various handle slides are shown in the picture below along with points of intersections that arise when we cancel/slide handles.

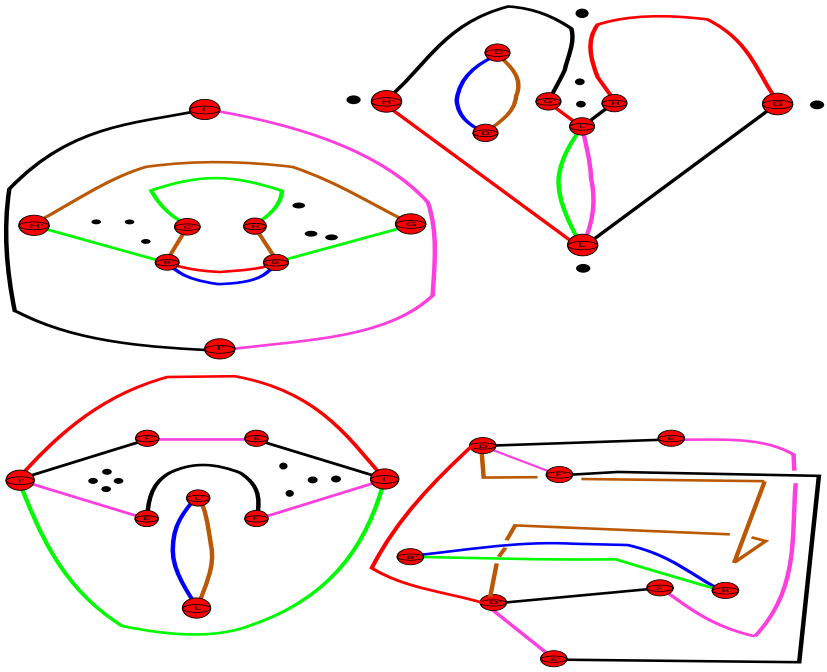

It is clear that none of the handle cancellations and slides we have done so far have interfered with the added 2-handles running from E to G and E' to G'. This will be the case for many of the handle cancellations and slides we do in the following, and because of this we will often omit drawing the 2-handles between E to G and E' to G'. However, it is recommended that the reader keep a mental image of these two 2-handles so as to help convince themselves that none of the handle cancellations/slides we carry out do indeed affect these two 2-handles.

In the above picture you can see several 2-handles that pass over certain 1-handles only once. For example, if we look at the $x-y$ plane we can see that there is a red 2-handle and a blue 2-handle that passes between the 1-handle $B-B'$ once, hence we may use either of these to cancel $B-B'$.

Cancelling $B-B'$ only affects the handle diagram in the $x-y$ plane and the diagram corresponding to the six 2-handles not lying in any one plane.

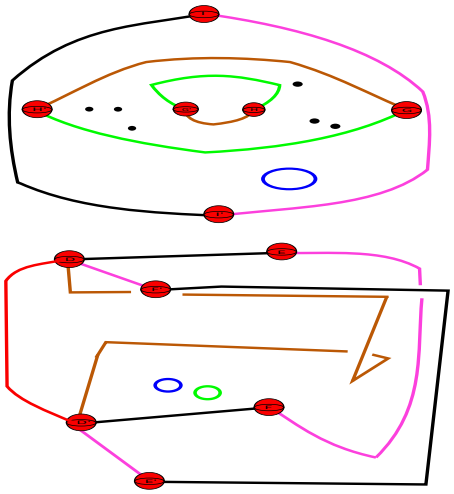

The unknotted circles in the above picture denote 2-handles not meeting any 1-handles and have zero framing. Hence they can be used to cancel a 3-handle, and so we may simply erase them from the diagram (recall elementary move number 3, which we outlined in the previous section).

Recall that the 2-handles running between B and B' gave points of intersection in the $y-z$ plane. To remind the reader the picture below shows all the points of intersection in the $y-z$ plane.

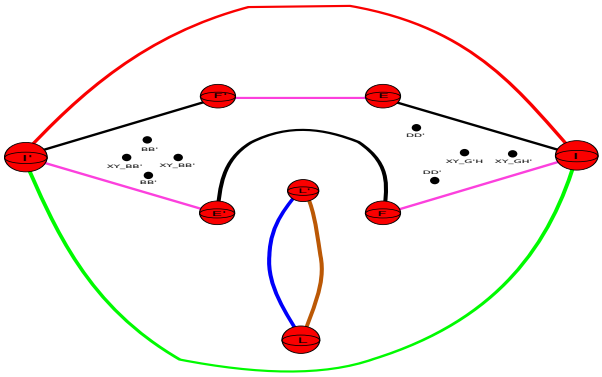

When we cancel $B-B'$ from the $x-y$ plane using the red 2-handle, the intersection point corresponding to this 2-handle in the $y-z$ plane will disappear. However, a new one corre-

sponding to the green 2-handle running from G to H' will appear, and one corresponding to the brown 2-handle running from G' to H will appear. The blue 2-handle running between B and B' (still staying in the $x-y$ plane) also corresponds to an intersection point in the $y-z$ plane, when we cancel $B-B'$ this 2-handle forms a closed loop with framing 0. It then gives a point of intersection in the $y-z$ plane, however since the framing of this 2-handle is 0 it cancels a 3-handle, and so we can simply delete it from our diagram. This means that we can simply delete the corresponding point of intersection from the $y-z$ plane. Similarly, when we cancelled $B-B'$ from the diagram that consisted of the 2-handles that did not all lie in a single 2-plane we obtained two 2-handles, one in blue and the other in green which are loops with zero framing. Hence they each cancel a 3-handle respectively and can be deleted from the diagram. This means that the points of intersection they give in the $y-z$ plane can be deleted.

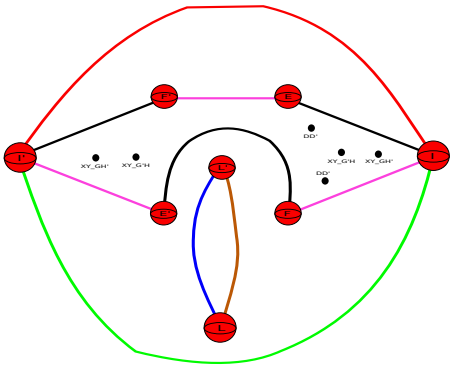

Observe that there are two points of intersection labelled **XY_GH'**, and another two labelled **XY_G'H**. It is easy to work out which one corresponds to which 2-handle in the $x-y$ plane. For example, the point of intersection between E', I' and F' labelled **XY_GH'** corresponds to the green 2-handle running between G and H' in the $x-y$ plane, and the point of intersection labelled **XY_GH'** between E, I and F corresponds to the brown 2-handle running between G and H' in the $x-y$ plane.

Before we show how all diagrams look like after the cancellation of $B-B'$, we want to go back to the diagram that corresponded to the six 2-handles that did not all lie in a single 2-plane.

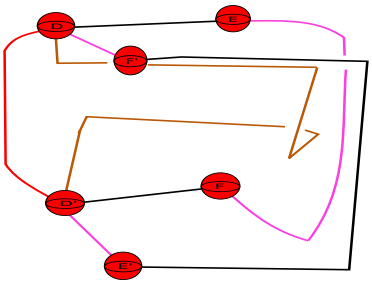

Look at the brown 2-handle that runs between D and D'. We were going to do an isotopy that moves this 2-handle into a different position. When carrying out such an isotopy we have to be careful that we do not pass through any other 2-handles. Therefore in order to do this in a correct manner we need to keep track of the intersection points with the other planes.

We are going to push the brown 2-handle in the following direction:

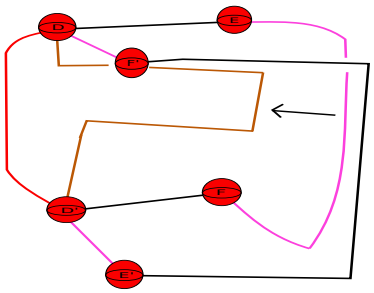

This will cause the brown 2-handle (over time) to move in the following way:

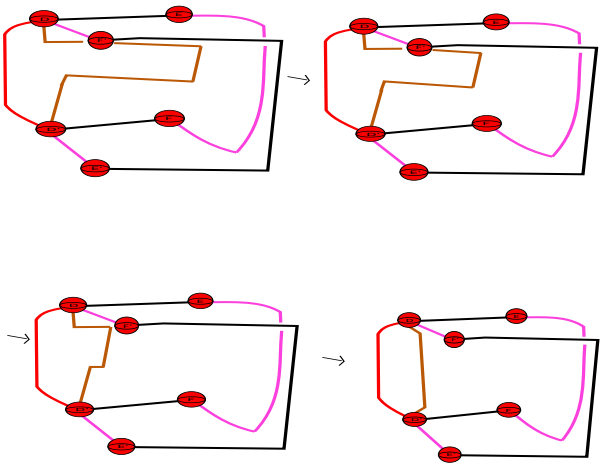

During this moving of the brown 2-handle the intersection point corresponding to this 2-handle in the $x - y$ plane also moves, and the trajectory it takes looks like:

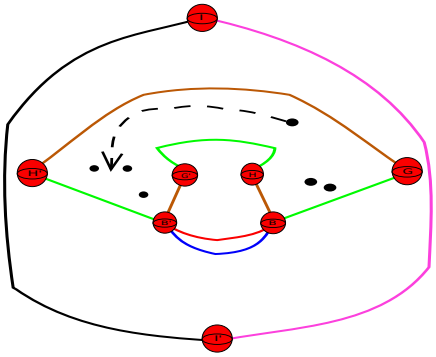

Observe that so far, in moving the brown 2-handle we have not passed through any of the other 2-handles, this is because in the $x-y$ plane we have kept track of how the intersection point has moved. In the $x-z$ plane there is nothing to check as the brown 2-handle that we are moving does not intersect this plane. Finally, in the case of the $y-z$ plane we have that this 2-handle intersects it in two points, thus in carrying out this isotopy of the 2-handle in question there will definitely be some change in the $y-z$ plane. In order to understand what goes on observe that when we continue to move the 2-handle in the direction shown above we will come to a stage where a vertical arc of this 2-handle will lie in the $y-z$ plane. Thus when we look at the $y-z$ plane we will see an arc between the two points of intersection corresponding to this brown 2-handle. The following picture shows this arc in the $y-z$ plane.

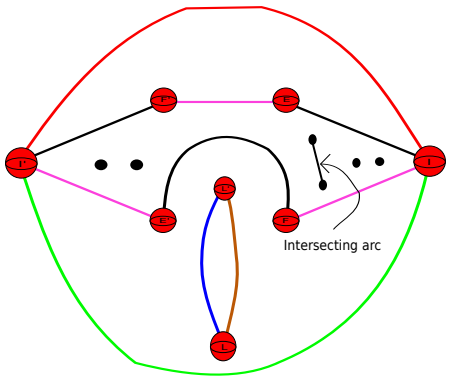

As we continue to move this 2-handle in the direction indicated we will see this arc in the $y-z$ plane disappear along with the original two points of intersection that this 2-handle gave.

The final position of this 2-handle is shown in the following picture, with the bottom diagram showing the final position of the intersection point in the $x-y$ plane.

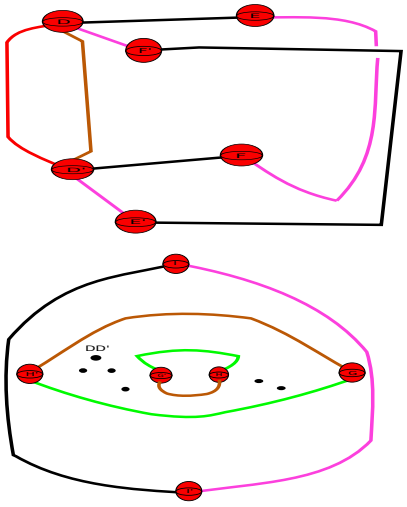

The following picture shows all diagrams so far, notice that two points of intersection in the

$y - z$ plane have disappeared.

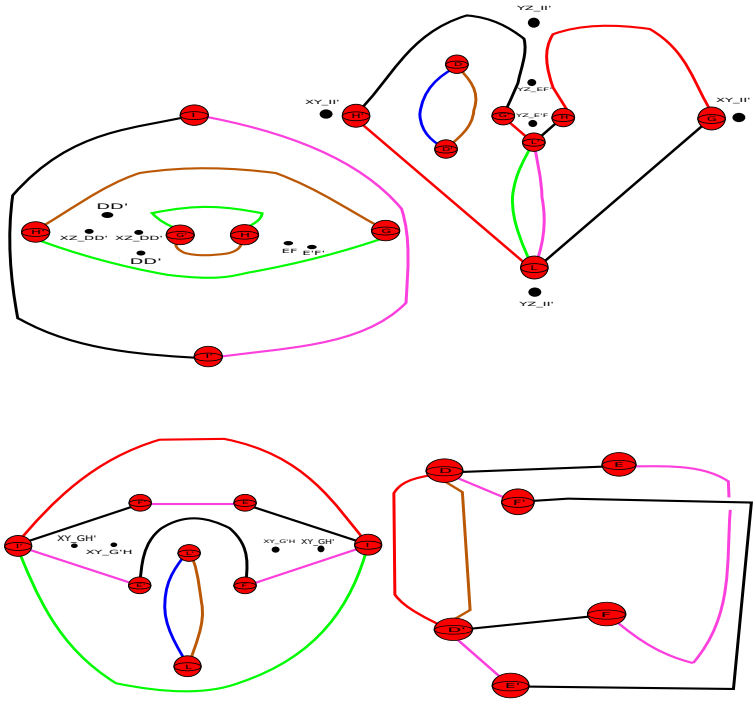

We are going to move on to cancelling $D - D'$. In this case we have a few options in regard to which 2-handle we use to carry out the cancellation. In the $x - z$ plane we have the choice of the brown and blue 2-handles that pass between $D - D'$ once, and in the diagram that corresponded to the six 2-handles that did not all lie in a single 2-plane, we have the choice of the red and brown 2-handle that passes between $D - D'$ once. We will choose the red 2-handle in the diagram that corresponds to the six 2-handles that did not all lie in a single 2-plane.

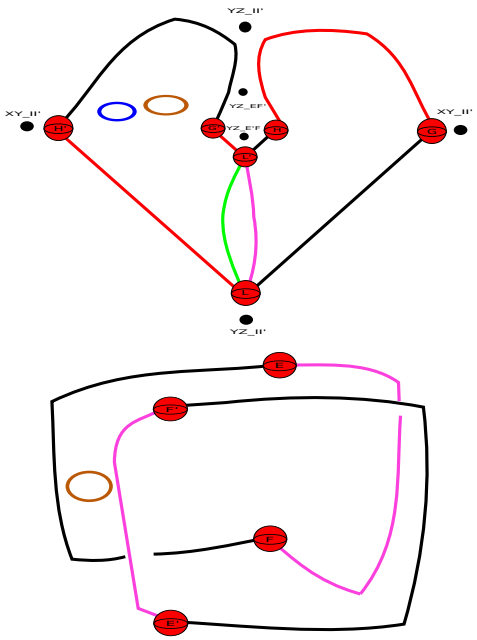

Observe that after cancelling $D - D'$ all the 2-handles that passed between $D - D'$ become loops with framing 0. We can see two in the $x - z$ plane, one in blue and the other in brown, and we can see one brown one in the other diagram. As all these two handles have framing 0 we know that they form a cancellation pair with a 3-handle, and hence we can erase them from our diagram. In doing so we will see the intersection points in the $x - y$ plane labelled **XZ_DD'** and **DD'** disappear, but we will get two new ones corresponding to the pink 2-handle running from E' to F' and the black 2-handle running from E to F, both in the diagram that corresponds to the six 2-handles that did not all lie in a single 2-plane.

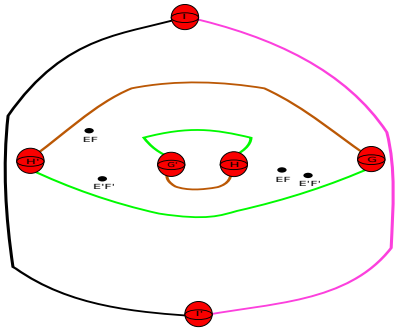

All diagrams look like:

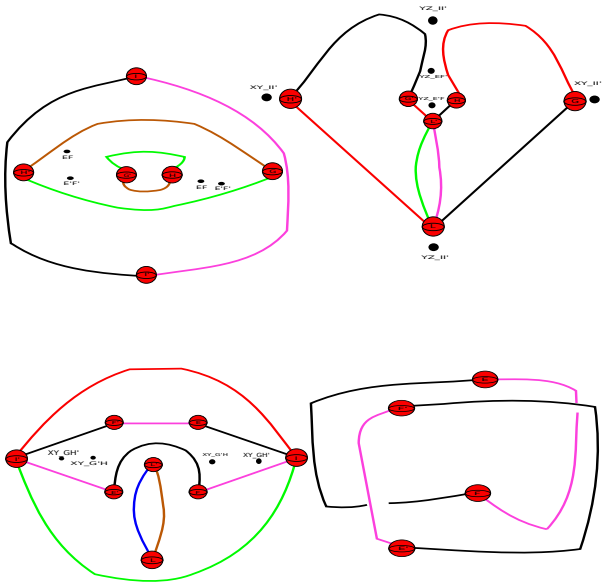

Let us remark that the cancellations and slides we have done so far have not interfered in any way with the two added 2-handles that run from E to G and E' to G'.

We move on to cancelling $L - L'$ using the green 2-handle in the $x - z$ plane. This cancellation only affects the diagrams in the $x - z$ and $y - z$ planes.

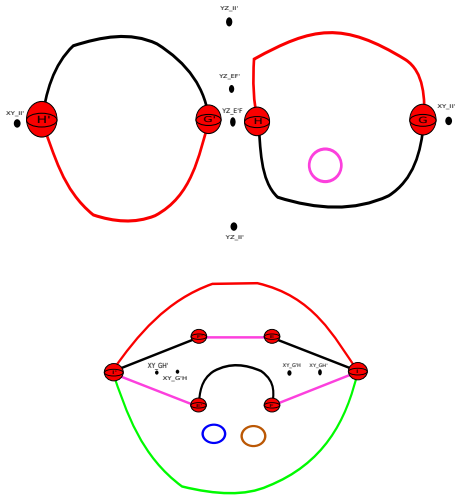

In undertaking this cancellation we obtain three 2-handles that become loops which carry framing number 0, these will then cancel a 3-handle and hence we can simply erase them from our diagrams.

Note that as none of the 2-handles that ran between $L - L'$ intersected any of the other planes, the points of intersection in the various planes do not change. Furthermore it is easy to see that cancelling $L - L'$ does not cause the added 2-handles that run from E to G and E' to G' to change.

We can then cancel $I - I'$ using the red 2-handle that lies in the $y - z$ plane.

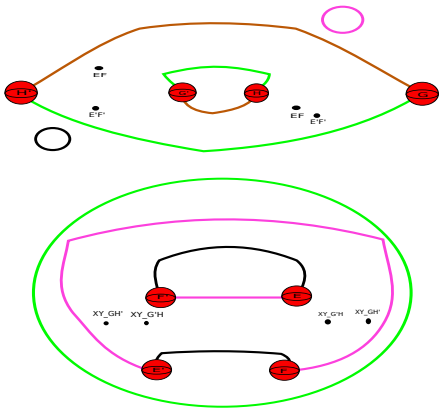

We obtain three 2-handles that are loops with framing 0, which we can simply erase from the diagrams. As for the intersection points, the only plane we have to worry about is the $x - z$ plane. The intersection points labelled **XY_II'** disappear and nothing new takes their place. The points of intersection labelled **YZ_II'** also disappear, but we get two new points of intersection at the top of the $y - z$ plane corresponding to the black 2-handle in the $y - z$ plane that runs between E and F' and the pink 2-handle in the $y - z$ plane that runs between E' and F. The labelling of these points of intersection are **YZ_EF'** and **YZ_E'F** respectively.

The following picture shows the diagrams so far with labelled points of intersection. The first diagram represents the $x-y$ plane, the one below it is the $x-z$ plane, and the next two diagrams are the $y-z$ plane and the diagram that corresponded to the six 2-handles that did not all lie in a single plane.

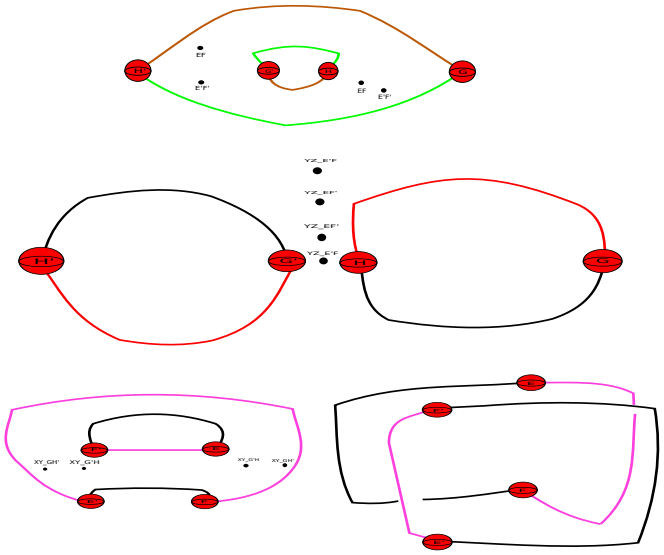

We can isotope the pink 2-handle in the $y-z$ plane joining E' to F, so that it does not enclose the 1-handles E and F'. The isotopy moves the 2-handle in the direction of the x-axis. The following picture shows the direction in which we move this 2-handle.

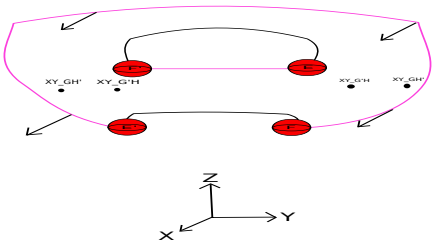

It is easy to see that in moving this 2-handle in this direction, we do not pass through any of the other 2-handles, hence it is a well defined isotopy. The final position of this 2-handle can be seen in the following picture.

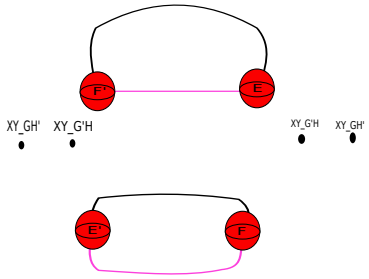

We can also isotope the 2-handles in the diagram that corresponded to the six 2-handles that did not all lie in a single plane to get:

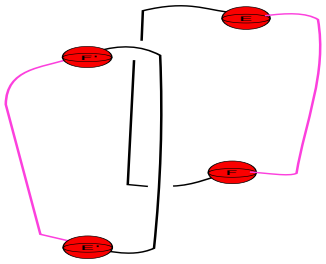

The 2-handles now lie in planes parallel to the $x - z$ plane.

We observe that this will cause the points of intersection in the $x - y$ plane to move into the following position:

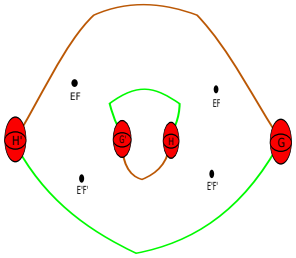

We can now put everything together to give a picture in 3-space. Remember the co-ordinates of the 1-handles H, H', G, G' and E, E', F, F' are given as:

E	$S_{(0,+1,+1,0)}$	$(0, \frac{1}{\sqrt{2}}, \frac{1}{\sqrt{2}})$	E'	$S_{(0,-1,-1,0)}$	$(0, \frac{-1}{\sqrt{2}}, \frac{-1}{\sqrt{2}})$
F	$S_{(0,+1,-1,0)}$	$(0, \frac{1}{\sqrt{2}}, \frac{-1}{\sqrt{2}})$	F'	$S_{(0,-1,+1,0)}$	$(0, \frac{-1}{\sqrt{2}}, \frac{1}{\sqrt{2}})$
G	$S_{(+1,0,0,+1)}$	$(1+\sqrt{2}, 0, 0)$	G'	$S_{(-1,0,0,-1)}$	$(1-\sqrt{2}, 0, 0)$
H	$S_{(+1,0,0,-1)}$	$(-1+\sqrt{2}, 0, 0)$	H'	$S_{(-1,0,0,+1)}$	$(-1-\sqrt{2}, 0, 0)$

The following picture shows a diagram of these 1-handles in 3-space along with the various 2-handles that run between them.

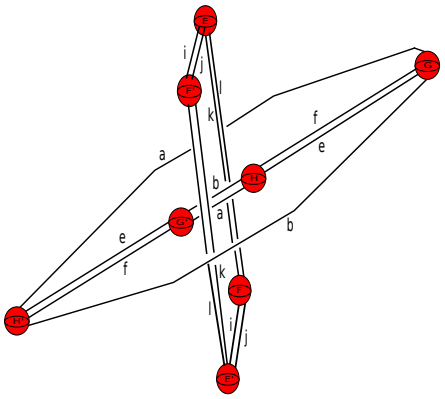

Observe that in the top diagram the 2-handle denoted by e passes over the 1-handle $H - H'$ once, hence they form a cancelling pair, and the cancellation can be done in the $x - y$ plane without affecting any of the other 2-handles.

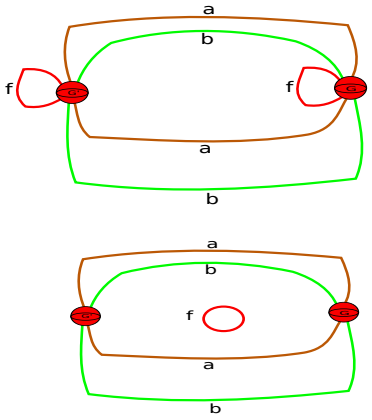

The 2-handles denoted by f then cancels a 3-handle and can be erased from the diagram.

In our 3-space picture we then have:

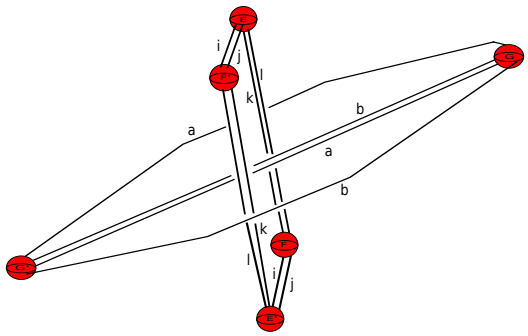

The 2-handle denoted k runs over $F - F'$ once, and hence we can use it to cancel $F - F'$. This cancellation can be done in the $y - z$ plane without affecting the other 2-handles.

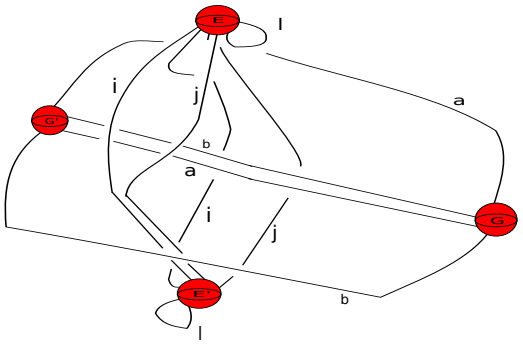

The 2-handle l slides off $E - E'$ and cancels a 3-handle, we are then left with:

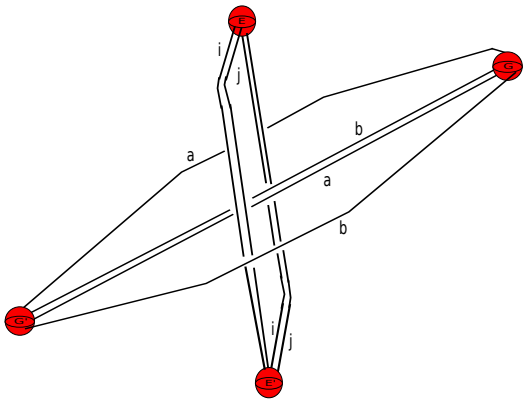

We can then slide the 2-handle denoted j along i to obtain a 2-handle that has one component looping back into E and another into E'. We can push either component through the attaching sphere it loops back into obtaining an unknot with framing zero. This then cancels a 3-handle and can be deleted from the diagram.

Recall we still have not dealt with the 2-handle that corresponds to filling in the last boundary component. This is represented by $e^{-1}g$, which corresponds to attaching a 2-handle component from E to G, and then one from E' to G'. So far the handle cancellations and slides we have done have not affected these two components, and hence it suffices to put them in now.

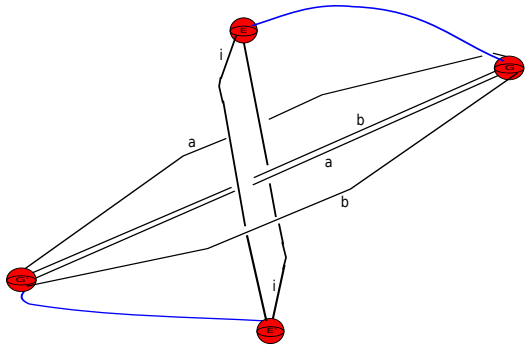

We can then use them to cancel $G - G'$:

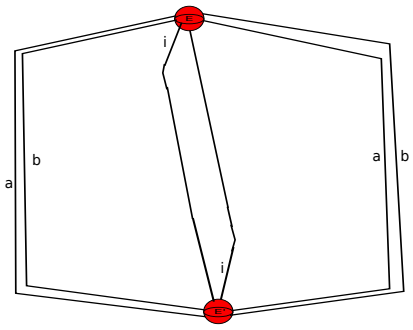

At this point one can perform a handle slide, one can slide the 2-handle labelled b along a the

end result is that b will have two components, one that loops back into E and one that loops back into E'. We can then push one component through the attaching sphere it loops back into obtaining an unknot with zero framing. This cancels with a 3-handle and can be erased from the diagram. We are then left with the same diagram as above with only the 2-handles labelled a and i remaining.

The fundamental group of this manifold is clearly $\mathbb{Z}_2$. We want to take the double cover of the above 4-manifold to get a simply connected 4-manifold. Let us denote the above 4-manifold by Y, then we want to form the double cover $X \to Y$. More precisely using the Kirby diagram of Y obtained above, we want to obtain a Kirby diagram of X. In order to do this we proceed as follows. First of all since Y has only one 1-handle we can identity the 1-skeleton of Y with $S^1 \times D^3$. As X is a cyclic double cover we have that the 1-skeleton of Y is 2-fold covered in the obvious way. I.e. the 1-skeleton of X is $S^1 \times D^3$ and this double covers $S^1 \times D^3$ (corresponding to the 1-skeleton of Y) in the usual way. Each of the remaining handles of Y lift to two copies of that handle in X. There is a subtle issue in what we have said so far, namely we did not say how the data determining the trivialisation of the normal bundle to each 2-handle lift to the double cover. In our case this is not a problem as all our 2-handles have a planar framing, and so when we lift them we still get 2-handles with a planar framing (i.e. parallel curves do not twist around). In the general case one only has to observe that a choice of trivialisation on each normal bundle to each knot (representing a 2-handle) lifts to that trivialisation on each lifted knot, and changing the trivialisation to the normal bundle of a 2-handle in Y by one twist causes the trivialisation on each lifted knot to change by one twist, hence we know how to lift any choice of trivialisation. Focusing on our case we make an important observation, the 2-handles in our manifold Y do not twist around each other in any way, hence when we lift them to X we can focus on their lifts separately. In our situation we have two 2-handles denoted a and i. When we lift each one, we will get two 2-handles each passing the lifted 1-handle once. As none of them twist around each other we use any lifted one to cancel the lifted 1-handle, leaving us with three unknot's with framing zero. Each of these then cancels a 3-handle, and we see that the manifold we are left with is S^4. The boundary components of manifold 1011 where given by the non-orientable closed flat 3-manifold labelled **G** ($\mathcal{B}_1$ in Wolf's notation). Appealing to the classification of closed flat 3-manifolds we know that the orientable double cover of **G** is the flat 3-manifold given by **A** ($\mathcal{G}_1$ in Wolf's notation), which is the 3-torus.

Thus we have proved the following theorem:

Theorem 2.3.1. *There exists a collection L of five linked tori embedded in a standard smooth S^4 such that the complement $S^4 - L$ admits a finite volume hyperbolic geometry.*

We should mention that D. Ivanšić proves in his paper [10] (see thm.4.3, p.18) that there exists a system of five linked 3-tori embedded in a smooth manifold X that is homeomorphic to S^4

such that $X - L$ admits a finite volume hyperbolic geometry. The manifold he uses to construct X is also manifold 1011. However, he does not prove that X is diffeomorphic to S^4 and in particular does not consider constructions to do with Kirby diagrams and the Kirby calculus

Chapter 3

A hyperbolic link complement in a standard smooth $S^2 \times S^2$

In this chapter we construct a smooth hyperbolic link complement in a standard smooth $S^2 \times S^2$. We follow the general procedure outlined in the previous chapter, the only difference being that we will work with a Kirby diagram associated to the double cover of a non-orientable Ratcliffe-Tschantz manifold. Due to this we begin the chapter with an explanation of how to construct a Kirby diagram for the orientable double cover associated to any of the Ratcliffe-Tschantz manifolds. We then end the chapter by proving, using the methods of Kirby calculus, that a boundary filling of the orientable double cover of manifold no. 35 has a double cover that is diffeomorphic to $S^2 \times S^2$.

3.1 How to construct the orientable double cover

The main aim of this section is to show the reader how, given a presentation of the fundamental group of a non-orientable Ratcliffe-Tschantz manifold, we can obtain a presentation of the orientable double cover. We will then put this technique to use in the next section for a particular example, showing the reader how to obtain a Kirby diagram for the orientable double cover.

The principle technique in extracting a presentation for the orientable double cover is a easy case of the *Reidemeister-Schreier* rewriting process. Fix a non-orientable Ratcliffe-Tschantz manifold, which from here on in we denote by M. We know that the orientable double cover of M, denoted $\widetilde{M}$, corresponds to an index 2 subgroup of $\pi_1(M)$. In fact if we let

$$\phi : \pi_1(M) \to \mathbb{Z}_2$$

denote the homomorphism that sends the orientation preserving isometries, making up M, to 1 and the orientation reversing isometries to -1. Then we have that $ker(\phi) = \pi_1(\widetilde{M})$, and it is clear that $\pi_1(\widetilde{M})$ is an index 2 subgroup of $\pi_1(M)$.

Given a group G and a finite index subgroup H of G we remind the reader of the definition of a transversal to H in G.

Definition 3.1.1. A transversal to H in G is a subset T of G such that

$$G = \bigcup_{t \in T} H \cdot t$$

In our case it is easy to find a transversal, we simply take any orientation reversing isometry, making up M, call it α. Then it should be clear that the set $\{1, \alpha\}$ is a transversal to $\pi_1(\widetilde{M})$ in $\pi_1(M)$. Now, let us fix the finite presentation of $\pi_1(M) = \langle X|R\rangle$, recall that the set X is given by the side pairing transformations that make up M. Let $\psi : \pi_1(M) \to T$ be the map that the sends an element $x \in \pi_1(M)$ to its coset representative. In our case the definition of ψ can be given explicitly in the form:

- $\psi(x) = 1$ if x is orientation preserving.
- $\psi(x) = \alpha$ if x is orientation reversing.

Let $\rho : \pi_1(M) \to \pi_1(\widetilde{M})$ be defined by $\pi(x) = x \cdot \psi(x)^{-1}$. In our case the definition of ρ can also be explicitly written in the form:

- $\rho(x) = x$ if x is orientation preserving
- $\rho(x) = x \cdot \alpha^{-1}$ if x is orientation reversing

We then have the following theorem.

Theorem 3.1.2 (Reidemeister-Schreier rewriting process)**.** *A presentation of $\pi_1(\widetilde{M})$ is given by $\langle X'|R'\rangle$, where*

$$X' = \{\rho(tx) \neq 1 | t \in T \text{ and } x \in X\}$$

$$R' = \{xrx^{-1} | x \in X \text{ and } r \in R\}$$

and the word xrx^{-1} is written in terms of elements of X'.

We would like to remind the reader that the above theorem is actually a very special case of the general rewriting process. As we only need the case of an index two subgroup (since we are dealing with orientable double covers) we thought it best to restrict to this simple case. For the proof of the theorem (and its general form) we refer the reader to [12] p.106.

3.2 Example: Double cover of Manifold 35

We start by giving the side pairing information for manifold 35, which we will denote by M.

The side pairing code for this manifold is **146928**. The explicit side pairings are given as:

$$S_{(+1,+1,0,0)} \xrightarrow[k_{(-1,+1,+1,+1)}]{a} S_{(-1,+1,0,0)} \qquad S_{(+1,-1,0,0)} \xrightarrow[k_{(-1,+1,+1,+1)}]{b} S_{(-1,-1,0,0)}$$

$$S_{(+1,0,+1,0)} \xrightarrow[k_{(+1,+1,-1,+1)}]{c} S_{(+1,0,-1,0)} \qquad S_{(-1,0,+1,0)} \xrightarrow[k_{(+1,+1,-1,+1)}]{d} S_{(-1,0,-1,0)}$$

$$S_{(0,+1,+1,0)} \xrightarrow[k_{(+1,-1,-1,+1)}]{e} S_{(0,-1,-1,0)} \qquad S_{(0,+1,-1,0)} \xrightarrow[k_{(+1,-1,-1,+1)}]{f} S_{(0,-1,+1,0)}$$

$$S_{(+1,0,0,+1)} \xrightarrow[k_{(-1,+1,+1,-1)}]{g} S_{(-1,0,0,-1)} \qquad S_{(+1,0,0,-1)} \xrightarrow[k_{(-1,+1,+1,-1)}]{h} S_{(-1,0,0,+1)}$$

$$S_{(0,+1,0,+1)} \xrightarrow[k_{(+1,-1,+1,+1)}]{i} S_{(0,-1,0,+1)} \qquad S_{(0,+1,0,-1)} \xrightarrow[k_{(+1,-1,+1,+1)}]{j} S_{(0,-1,0,-1)}$$

$$S_{(0,0,+1,+1)} \xrightarrow[k_{(+1,+1,+1,-1)}]{k} S_{(0,0,+1,-1)} \qquad S_{(0,0,-1,+1)} \xrightarrow[k_{(+1,+1,+1,-1)}]{l} S_{(0,0,-1,-1)} \ .$$

The labelling of the sides of this manifold are given in the following table:

A	$S_{(+1,+1,0,0)}$	$(\frac{1}{\sqrt{2}}, \frac{1}{\sqrt{2}}, 0)$	A'	$S_{(-1,+1,0,0)}$	$(\frac{-1}{\sqrt{2}}, \frac{1}{\sqrt{2}}, 0)$
B	$S_{(+1,-1,0,0)}$	$(\frac{1}{\sqrt{2}}, \frac{-1}{\sqrt{2}}, 0)$	B'	$S_{(-1,-1,0,0)}$	$(\frac{-1}{\sqrt{2}}, \frac{-1}{\sqrt{2}}, 0)$
C	$S_{(+1,0,+1,0)}$	$(\frac{1}{\sqrt{2}}, 0, \frac{1}{\sqrt{2}})$	C'	$S_{(+1,0,-1,0)}$	$(\frac{1}{\sqrt{2}}, 0, \frac{-1}{\sqrt{2}})$
D	$S_{(-1,0,+1,0)}$	$(\frac{-1}{\sqrt{2}}, 0, \frac{1}{\sqrt{2}})$	D'	$S_{(-1,0,-1,0)}$	$(\frac{-1}{\sqrt{2}}, 0, \frac{-1}{\sqrt{2}})$
E	$S_{(0,+1,+1,0)}$	$(0, \frac{1}{\sqrt{2}}, \frac{1}{\sqrt{2}})$	E'	$S_{(0,-1,-1,0)}$	$(0, \frac{-1}{\sqrt{2}}, \frac{-1}{\sqrt{2}})$
F	$S_{(0,+1,-1,0)}$	$(0, \frac{1}{\sqrt{2}}, \frac{-1}{\sqrt{2}})$	F'	$S_{(0,-1,+1,0)}$	$(0, \frac{-1}{\sqrt{2}}, \frac{1}{\sqrt{2}})$
G	$S_{(+1,0,0,+1)}$	$(1+\sqrt{2}, 0, 0)$	G'	$S_{(-1,0,0,-1)}$	$(1-\sqrt{2}, 0, 0)$
H	$S_{(+1,0,0,-1)}$	$(-1+\sqrt{2}, 0, 0)$	H'	$S_{(-1,0,0,+1)}$	$(-1-\sqrt{2}, 0, 0)$
I	$S_{(0,+1,0,+1)}$	$(0, 1+\sqrt{2}, 0)$	I'	$S_{(0,-1,0,+1)}$	$(0, -1-\sqrt{2}, 0)$
J	$S_{(0,+1,0,-1)}$	$(0, -1+\sqrt{2}, 0)$	J'	$S_{(0,-1,0,-1)}$	$(0, 1-\sqrt{2}, 0)$
K	$S_{(0,0,+1,+1)}$	$(0, 0, 1+\sqrt{2})$	K'	$S_{(0,0,+1,-1)}$	$(0, 0, -1+\sqrt{2})$
L	$S_{(0,0,-1,+1}$	$(0, 0, -1-\sqrt{2})$	L'	$S_{(0,0,-1,-1)}$	$(0, 0, 1-\sqrt{2})$

The twenty four 2-handles are given in the following table:

1.	$A \cap C \xrightarrow{a} A' \cap D \xrightarrow{d} A' \cap D' \xrightarrow{a^{-1}} A \cap C' \xrightarrow{c^{-1}} A \cap C$
2.	$A \cap E \xrightarrow{a} A' \cap E \xrightarrow{e} B' \cap E' \xrightarrow{b^{-1}} B \cap E' \xrightarrow{e^{-1}} A \cap E$
3.	$A \cap F \xrightarrow{a} A' \cap F \xrightarrow{f} B' \cap F' \xrightarrow{b^{-1}} B \cap F' \xrightarrow{f^{-1}} A \cap F$
4.	$A \cap G \xrightarrow{a} A' \cap H' \xrightarrow{h^{-1}} A \cap H \xrightarrow{a} A' \cap G' \xrightarrow{g^{-1}} A \cap G$
5.	$A \cap I \xrightarrow{a} A' \cap I \xrightarrow{i} B' \cap I' \xrightarrow{b^{-1}} B \cap I' \xrightarrow{i^{-1}} A \cap I$
6.	$A \cap J \xrightarrow{a} A' \cap J \xrightarrow{j} B' \cap J' \xrightarrow{b^{-1}} B \cap J' \xrightarrow{j^{-1}} A \cap J$
7.	$B \cap C \xrightarrow{b} B' \cap D \xrightarrow{d} B' \cap D' \xrightarrow{b^{-1}} B \cap C' \xrightarrow{c^{-1}} B \cap C$
8.	$B \cap G \xrightarrow{b} B' \cap H' \xrightarrow{h^{-1}} B \cap H \xrightarrow{b} B' \cap G' \xrightarrow{g^{-1}} B \cap G$
9.	$C \cap E \xrightarrow{c} C' \cap F \xrightarrow{f} C \cap F' \xrightarrow{c} C' \cap E' \xrightarrow{e^{-1}} C \cap E$
10.	$C \cap G \xrightarrow{c} C' \cap G \xrightarrow{g} D' \cap G' \xrightarrow{d^{-1}} D \cap G' \xrightarrow{g^{-1}} C \cap G$
11.	$C \cap H \xrightarrow{c} C' \cap H \xrightarrow{h} D' \cap H' \xrightarrow{d^{-1}} D \cap H' \xrightarrow{h^{-1}} C \cap H$
12.	$C \cap K \xrightarrow{c} C' \cap L \xrightarrow{l} C' \cap L' \xrightarrow{c^{-1}} C \cap K' \xrightarrow{k^{-1}} C \cap K$
13	$D \cap E \xrightarrow{d} D' \cap F \xrightarrow{f} D \cap F' \xrightarrow{d} D' \cap E' \xrightarrow{e^{-1}} D \cap E$
14.	$D \cap K \xrightarrow{d} D' \cap L \xrightarrow{l} D' \cap L' \xrightarrow{d^{-1}} D \cap K' \xrightarrow{k^{-1}} D \cap K$
15.	$E \cap I \xrightarrow{e} E' \cap I' \xrightarrow{i^{-1}} F \cap I \xrightarrow{f} F' \cap I' \xrightarrow{i^{-1}} E \cap I$
16.	$E \cap J \xrightarrow{e} E' \cap J' \xrightarrow{j^{-1}} F \cap J \xrightarrow{f} F' \cap J' \xrightarrow{j^{-1}} E \cap J$
17.	$E \cap K \xrightarrow{e} E' \cap L \xrightarrow{l} E' \cap L' \xrightarrow{e^{-1}} E \cap K' \xrightarrow{k^{-1}} E \cap K$
18.	$F \cap L \xrightarrow{f} F' \cap K \xrightarrow{k} F' \cap K' \xrightarrow{f^{-1}} F \cap L' \xrightarrow{l^{-1}} F \cap L$
19.	$G \cap I \xrightarrow{g} G' \cap J \xrightarrow{j} G' \cap J' \xrightarrow{g^{-1}} G \cap I' \xrightarrow{i^{-1}} G \cap I$
20.	$G \cap K \xrightarrow{g} G' \cap K' \xrightarrow{k^{-1}} H' \cap K \xrightarrow{h^{-1}} H \cap K' \xrightarrow{k^{-1}} G \cap I'$
21.	$G \cap L \xrightarrow{g} G' \cap L' \xrightarrow{l^{-1}} H' \cap L \xrightarrow{h^{-1}} H \cap L' \xrightarrow{l^{-1}} G \cap L$
22.	$H \cap J \xrightarrow{h} H' \cap I \xrightarrow{i} H' \cap I' \xrightarrow{h^{-1}} H \cap J' \xrightarrow{j^{-1}} H \cap J$
23.	$I \cap K \xrightarrow{i} I' \cap K \xrightarrow{k} J' \cap K' \xrightarrow{j^{-1}} J \cap K' \xrightarrow{k^{-1}} I \cap K$
24.	$I \cap L \xrightarrow{i} I' \cap L \xrightarrow{l} J' \cap L' \xrightarrow{j^{-1}} J \cap L' \xrightarrow{l^{-1}} J \cap L$

The manifold has five cusps with associated boundary components having code **GGGGH** (or in *Wolf's* notation $\mathcal{B}_1\mathcal{B}_1\mathcal{B}_1\mathcal{B}_1\mathcal{B}_2$). One can resort to the standard procedure of working out parabolic subgroups associated to each cusp, and then pick out those generators that are translations. We will not give the details of the explicit computations of the parabolic subgroups associated to each cusp, the method is exactly analogous to what we have done previously. Instead, we simply give the following table which outlines the translations we will be filling along.

Ideal vertex	Filling translation
$\{(1,0,0,0),(-1,0,0,0)\}$	c
$\{(0,1,0,0),(0,-1,0,0)\}$	a
$\{(0,0,1,0),(0,0,-1,0)\}$	k
$\{(0,0,0,1),(0,0,0,-1)\}$	i
$\{(\pm 1/2,\pm 1/2,\pm 1/2,\pm 1/2)\}$	$e^{-1}heh^{-1}$

Filling along the boundary components corresponding to these five cusps via the above translations, algebraically corresponds to adding the translations as relations to the fundamental group of manifold 35. It is easy to see that a presentation for the fundamental group of manifold 35 is obtained by taking generators corresponding to pairs of sides of P, and relations given by the 24 codimension 2 equivalence classes. Therefore a presentation for the filling is obtained by adding the relations $c = a = k = i = e^{-1}heh^{-1} = 1$. One can then simplify the presentation to obtain $\langle e, g | e^2, g^2, ege^{-1}g^{-1}\rangle$ (one can do this computation by hand, although it is rather tedious. An easier approach is to use a computer program, for example using **Magma** one can input the presentation of the group and then use the **ReduceGenerators** command to obtain the simplification), thereby concluding that the filled in manifold as fundamental group $\mathbb{Z}_2 \times \mathbb{Z}_2$. It is then clear that the orientable double cover has fundamental group $\mathbb{Z}_2$. If we denote the orientable double cover by $\widetilde{M}$, then we have that its universal cover is a two fold covering, which we will denote by $\widetilde{M}_2$. All the Ratcliffe-Tschantz manifolds have Euler characteristic 1, this implies that $\widetilde{M}_2$ has Euler characteristic 4. Appealing to the classification theorems of *Donaldson* and *Freedman* we can conclude that the homeomorphism type of $\widetilde{M}_2$ is determined by one of the three manifolds $S^2 \times S^2$, $\mathbb{CP}^2 \# \mathbb{CP}^2$ or $\overline{\mathbb{CP}^2} \# \overline{\mathbb{CP}^2}$. In fact using the theory of spin structures one can conclude that $\widetilde{M}_2$ must be homeomorphic to $S^2 \times S^2$. Unfortunately, one cannot conclude anything about the diffeomorphism type of $\widetilde{M}_2$, in fact it is unknown if $S^2 \times S^2$ admits a unique smooth structure so at this point we cannot rule out the case that we are getting an exotic copy of $S^2 \times S^2$. In order to understand the diffeomorphism type of $\widetilde{M}_2$ we will, as we have been doing all along, resort to the Kirby calculus. We will construct a Kirby diagram for the orientable double cover $\widetilde{M}$, then apply various elementary moves to simplify the diagram, then take the double cover of this simplified diagram and conclude that $\widetilde{M}_2$ is in fact diffeomorphic to $S^2 \times S^2$.

The starting point to obtaining a Kirby diagram of the double cover is to identify the orientation preserving isometries and those that are orientation reversing. Recall, any side pairing transformation is written as the composition rk, where r is reflection in the image side and k is a diagonal matrix. It is clear that r is orientation reversing (since it is a reflection in a hyperplane), therefore we can conclude the orientation preserving isometries are those whose k-part has an odd number of -1's, and the orientation reversing isometries are those that have

an even number of -1's. We then find that the orientation preserving isometries are given by a, b, c, d, i, k, and the orientation reversing isometries are given by e, f, g, h.

From section 3.1, we know that a fundamental domain for the orientable double cover consists of two copies of the 24-cell P attached along a codimension one side corresponding to one of the orientation reversing isometries. If we take the orientation reversing isometry g^{-1}, then we can think of the fundamental domain of the orientable double cover to consist of the union $P \cup g^{-1} \cdot P$. In order to understand how we obtain the double cover from $P \cup g^{-1} \cdot P$, we need to work out what the side pairing transformations are i.e. which side gets paired to which side. Before we do this, let us comment on a thought that has possibly crossed the readers mind. Why did we pick g^{-1} as opposed to g ? The reason for this will become apparent soon, but for now let us just say that it turns out to make ones life much easier when drawing Kirby diagrams if one chooses g^{-1} over g. Appealing to the theory outlined in section 3.1 we find that if we fix a side pairing transformation $\phi : S \to S'$, we have two cases to consider. First, if ϕ is orientation preserving we find that:

$$S \xrightarrow{\phi} S' \text{ and } g^{-1}S \xrightarrow{g^{-1}\phi g} g^{-1}S'$$

and if ϕ is orientation reversing, then:

$$S \xrightarrow{g^{-1}\phi} g^{-1}S' \text{ and } g^{-1}S \xrightarrow{\phi g} S' .$$

From here it is easy to work out what the side pairing transformation for the orientable double cover are.

$$A \xrightarrow{a} A' \qquad g^{-1}A \xrightarrow{g^{-1}ag} g^{-1}A' \qquad\qquad B \xrightarrow{b} B' \qquad g^{-1}B \xrightarrow{g^{-1}bg} g^{-1}B'$$

$$C \xrightarrow{c} C' \qquad g^{-1}C \xrightarrow{g^{-1}cg} g^{-1}C' \qquad\qquad D \xrightarrow{d} D' \qquad g^{-1}D \xrightarrow{g^{-1}dg} g^{-1}D'$$

$$E \xrightarrow{g^{-1}e} g^{-1}E' \qquad g^{-1}E \xrightarrow{eg} E' \qquad\qquad F \xrightarrow{g^{-1}f} g^{-1}F' \qquad g^{-1}F \xrightarrow{fg} F'$$

$$G \xrightarrow{g^{-1}g} g^{-1}G' \qquad g^{-1}G \xrightarrow{gg} G' \qquad\qquad H \xrightarrow{g^{-1}h} g^{-1}H' \qquad g^{-1}H \xrightarrow{hg} H'$$

$$I \xrightarrow{i} I' \qquad g^{-1}I \xrightarrow{g^{-1}ig} g^{-1}I' \qquad\qquad J \xrightarrow{j} J' \qquad g^{-1}J \xrightarrow{g^{-1}jg} g^{-1}J'$$

$$K \xrightarrow{k} K' \qquad g^{-1}K \xrightarrow{g^{-1}kg} g^{-1}K' \qquad\qquad L \xrightarrow{l} L' \qquad g^{-1}L \xrightarrow{g^{-1}lg} g^{-1}L'$$

The next step is to work out equivalence classes of codimension 2 sides, this is done in the usual way. One simply takes a codimension 2 side and applies side pairing transformations until one cycles back to the original codimension 2 side. Recall that a codimension 2 side is given by the intersection of two distinct codimension 1 sides. We already know which codimension 1 sides in P intersect, applying the transformation g^{-1} then tells us which codimension 1 sides intersect in $g^{-1}P$. In total we obtain forty eight distinct equivalence classes, with each class containing precisely four distinct codimension 2 sides. The following table collects together all forty eight equivalence classes.

1.	$A \cap C \xrightarrow{a} A' \cap D \xrightarrow{d} A' \cap D' \xrightarrow{a^{-1}} A \cap C' \xrightarrow{c^{-1}} A \cap C$
2.	$A \cap E \xrightarrow{a} A' \cap E \xrightarrow{g^{-1}e} g^{-1}B' \cap g^{-1}E' \xrightarrow{(g^{-1}bg)^{-1}} g^{-1}B \cap g^{-1}E' \xrightarrow{(g^{-1}e)^{-1}} A \cap E$
3.	$A \cap F \xrightarrow{a} A' \cap F \xrightarrow{g^{-1}f} g^{-1}B' \cap g^{-1}F' \xrightarrow{(g^{-1}bg)^{-1}} g^{-1}B \cap g^{-1}F' \xrightarrow{(g^{-1}f)^{-1}} A \cap F$
4.	$A \cap G \xrightarrow{a} A' \cap H' \xrightarrow{(hg)^{-1}} g^{-1}A \cap g^{-1}H \xrightarrow{g^{-1}ag} g^{-1}A' \cap g^{-1}G' \xrightarrow{(g^{-1}g)^{-1}} A \cap G$
5.	$A \cap I \xrightarrow{a} A' \cap I \xrightarrow{i} B' \cap I' \xrightarrow{b^{-1}} B \cap I' \xrightarrow{i^{-1}} A \cap I$
6.	$A \cap J \xrightarrow{a} A' \cap J \xrightarrow{j} B' \cap J' \xrightarrow{b^{-1}} B \cap J' \xrightarrow{j^{-1}} A \cap J$
7.	$B \cap C \xrightarrow{b} B' \cap D \xrightarrow{d} B' \cap D' \xrightarrow{b^{-1}} B \cap C' \xrightarrow{c^{-1}} B \cap C$
8.	$B \cap G \xrightarrow{b} B' \cap H' \xrightarrow{(hg)^{-1}} g^{-1}B \cap g^{-1}H \xrightarrow{g^{-1}bg} g^{-1}B' \cap g^{-1}G' \xrightarrow{(g^{-1}g)^{-1}} B \cap G$
9.	$C \cap E \xrightarrow{c} C' \cap F \xrightarrow{g^{-1}f} g^{-1}C \cap g^{-1}F' \xrightarrow{g^{-1}cg} g^{-1}C' \cap g^{-1}E' \xrightarrow{(g^{-1}e)^{-1}} C \cap E$
10.	$C \cap G \xrightarrow{c} C' \cap G \xrightarrow{g^{-1}g} g^{-1}D' \cap g^{-1}G' \xrightarrow{(g^{-1}dg)^{-1}} g^{-1}D \cap g^{-1}G' \xrightarrow{(g^{-1}g)^{-1}} C \cap G$
11.	$C \cap H \xrightarrow{c} C' \cap H \xrightarrow{g^{-1}h} g^{-1}D' \cap g^{-1}H' \xrightarrow{(g^{-1}dg)^{-1}} g^{-1}D \cap g^{-1}H' \xrightarrow{(g^{-1}h)^{-1}} C \cap H$
12.	$C \cap K \xrightarrow{c} C' \cap L \xrightarrow{l} C' \cap L' \xrightarrow{c^{-1}} C \cap K' \xrightarrow{k^{-1}} C \cap K$
13	$D \cap E \xrightarrow{d} D' \cap F \xrightarrow{g^{-1}f} g^{-1}D \cap g^{-1}F' \xrightarrow{g^{-1}dg} g^{-1}D' \cap g^{-1}E' \xrightarrow{(g^{-1}e)^{-1}} D \cap E$
14.	$D \cap K \xrightarrow{d} D' \cap L \xrightarrow{l} D' \cap L' \xrightarrow{d^{-1}} D \cap K' \xrightarrow{k^{-1}} D \cap K$
15.	$E \cap I \xrightarrow{g^{-1}e} g^{-1}E' \cap g^{-1}I' \xrightarrow{(g^{-1}ig)^{-1}} g^{-1}F \cap g^{-1}I \xrightarrow{fg} F' \cap I' \xrightarrow{i^{-1}} E \cap I$
16.	$E \cap J \xrightarrow{g^{-1}e} g^{-1}E' \cap g^{-1}J' \xrightarrow{(g^{-1}jg)^{-1}} g^{-1}F \cap g^{-1}J \xrightarrow{fg} F' \cap J' \xrightarrow{j^{-1}} E \cap J$
17.	$E \cap K \xrightarrow{g^{-1}e} g^{-1}E' \cap g^{-1}L \xrightarrow{g^{-1}lg} g^{-1}E' \cap g^{-1}L' \xrightarrow{(g^{-1}e)^{-1}} E \cap K' \xrightarrow{k^{-1}} E \cap K$
18.	$F \cap L \xrightarrow{g^{-1}f} g^{-1}F' \cap g^{-1}K \xrightarrow{g^{-1}kg} g^{-1}F' \cap g^{-1}K' \xrightarrow{(g^{-1}f)^{-1}} F \cap L' \xrightarrow{l^{-1}} F \cap L$
19.	$G \cap I \xrightarrow{g^{-1}g} g^{-1}G' \cap g^{-1}J \xrightarrow{g^{-1}jg} g^{-1}G' \cap g^{-1}J' \xrightarrow{(g^{-1}g)^{-1}} G \cap I' \xrightarrow{i^{-1}} G \cap I$
20.	$G \cap K \xrightarrow{g^{-1}g} g^{-1}G' \cap g^{-1}K' \xrightarrow{(g^{-1}kg)^{-1}} g^{-1}H' \cap g^{-1}K \xrightarrow{(g^{-1}h)^{-1}} H \cap K' \xrightarrow{k^{-1}} G \cap K$
21.	$G \cap L \xrightarrow{g^{-1}g} g^{-1}G' \cap g^{-1}L' \xrightarrow{(g^{-1}lg)^{-1}} g^{-1}H' \cap g^{-1}L \xrightarrow{(g^{-1}h)^{-1}} H \cap L' \xrightarrow{l^{-1}} G \cap L$
22.	$H \cap J \xrightarrow{g^{-1}h} g^{-1}H' \cap g^{-1}I \xrightarrow{g^{-1}ig} g^{-1}H' \cap g^{-1}I' \xrightarrow{(g^{-1}h)^{-1}} H \cap J' \xrightarrow{j^{-1}} H \cap J$
23.	$I \cap K \xrightarrow{i} I' \cap K \xrightarrow{k} J' \cap K' \xrightarrow{j^{-1}} J \cap K' \xrightarrow{k^{-1}} I \cap K$
24.	$I \cap L \xrightarrow{i} I' \cap L \xrightarrow{l} J' \cap L' \xrightarrow{j^{-1}} J \cap L' \xrightarrow{l^{-1}} I \cap L$

25.	$g^{-1}A \cap g^{-1}C \xrightarrow{g^{-1}ag} g^{-1}A' \cap g^{-1}D \xrightarrow{g^{-1}dg} g^{-1}A' \cap g^{-1}D' \xrightarrow{(g^{-1}ag)^{-1}} g^{-1}A \cap g^{-1}C' \xrightarrow{(g^{-1}cg)^{-1}} g^{-1}A \cap g^{-1}C$
26.	$g^{-1}A \cap g^{-1}E \xrightarrow{g^{-1}ag} g^{-1}A' \cap g^{-1}E \xrightarrow{eg} B' \cap E' \xrightarrow{b^{-1}} B \cap E' \xrightarrow{(eg)^{-1}} g^{-1}A \cap g^{-1}E$
27.	$g^{-1}A \cap g^{-1}F \xrightarrow{g^{-1}ag} g^{-1}A' \cap g^{-1}F \xrightarrow{fg} B' \cap F' \xrightarrow{b^{-1}} B \cap F' \xrightarrow{(fg)^{-1}} g^{-1}A \cap g^{-1}F$
28.	$g^{-1}A \cap g^{-1}G \xrightarrow{g^{-1}ag} g^{-1}A' \cap g^{-1}H' \xrightarrow{(g^{-1}h)^{-1}} A \cap H \xrightarrow{a} A' \cap G' \xrightarrow{(gg)^{-1}} gA \cap gG$
29.	$g^{-1}A \cap g^{-1}I \xrightarrow{g^{-1}ag} g^{-1}A' \cap g^{-1}I \xrightarrow{g^{-1}ig} g^{-1}B' \cap g^{-1}I' \xrightarrow{(g^{-1}bg)^{-1}} g^{-1}B \cap g^{-1}I' \xrightarrow{(g^{-1}ig)^{-1}} g^{-1}A \cap g^{-1}I$
30.	$g^{-1}A \cap g^{-1}J \xrightarrow{g^{-1}ag} g^{-1}A' \cap g^{-1}J \xrightarrow{g^{-1}jg} g^{-1}B' \cap g^{-1}J' \xrightarrow{(g^{-1}bg)^{-1}} g^{-1}B \cap g^{-1}J' \xrightarrow{(g^{-1}jg)^{-1}} g^{-1}A \cap g^{-1}J$
31.	$g^{-1}B \cap g^{-1}C \xrightarrow{g^{-1}bg} g^{-1}B' \cap g^{-1}D \xrightarrow{g^{-1}dg} g^{-1}B' \cap g^{-1}D' \xrightarrow{(g^{-1}bg)^{-1}} g^{-1}B \cap g^{-1}C' \xrightarrow{(g^{-1}cg)^{-1}} g^{-1}B \cap g^{-1}C$
32.	$g^{-1}B \cap g^{-1}G \xrightarrow{g^{-1}bg} g^{-1}B' \cap g^{-1}H' \xrightarrow{(g^{-1}h)^{-1}} B \cap H \xrightarrow{b} B' \cap G' \xrightarrow{(gg)^{-1}} g^{-1}B \cap g^{-1}G$
33.	$g^{-1}C \cap g^{-1}E \xrightarrow{g^{-1}cg} g^{-1}C' \cap g^{-1}F \xrightarrow{fg} C \cap F' \xrightarrow{c} C' \cap E' \xrightarrow{(eg)^{-1}} g^{-1}C \cap g^{-1}E$
34.	$g^{-1}C \cap g^{-1}G \xrightarrow{g^{-1}cg} g^{-1}C' \cap g^{-1}G \xrightarrow{gg} D' \cap G' \xrightarrow{d^{-1}} D \cap G' \xrightarrow{(gg)^{-1}} g^{-1}C \cap g^{-1}G$
35.	$g^{-1}C \cap g^{-1}H \xrightarrow{g^{-1}cg} g^{-1}C' \cap g^{-1}H \xrightarrow{hg} D' \cap H' \xrightarrow{d^{-1}} D \cap H' \xrightarrow{(hg)^{-1}} g^{-1}C \cap g^{-1}H$
36.	$g^{-1}C \cap g^{-1}K \xrightarrow{g^{-1}cg} g^{-1}C' \cap g^{-1}L \xrightarrow{g^{-1}lg} g^{-1}C' \cap g^{-1}L' \xrightarrow{(g^{-1}cg)^{-1}} g^{-1}C \cap g^{-1}K' \xrightarrow{(g^{-1}kg)^{-1}} g^{-1}C \cap g^{-1}K$
37.	$g^{-1}D \cap g^{-1}E \xrightarrow{g^{-1}dg} g^{-1}D' \cap g^{-1}F \xrightarrow{fg} D \cap F' \xrightarrow{d} D' \cap E' \xrightarrow{(eg)^{-1}} g^{-1}D \cap g^{-1}E$
38.	$g^{-1}D \cap g^{-1}K \xrightarrow{g^{-1}dg} g^{-1}D' \cap g^{-1}L \xrightarrow{g^{-1}lg} g^{-1}D' \cap g^{-1}L' \xrightarrow{(g^{-1}dg)^{-1}} g^{-1}D \cap g^{-1}K' \xrightarrow{(g^{-1}kg)^{-1}} g^{-1}D \cap g^{-1}K$
39.	$g^{-1}E \cap g^{-1}I \xrightarrow{eg} E' \cap I' \xrightarrow{i^{-1}} F \cap I \xrightarrow{g^{-1}f} g^{-1}F' \cap g^{-1}I' \xrightarrow{(g^{-1}ig)^{-1}} g^{-1}E \cap g^{-1}I$
40.	$g^{-1}E \cap g^{-1}J \xrightarrow{eg} E' \cap J' \xrightarrow{j^{-1}} F \cap J \xrightarrow{g^{-1}f} g^{-1}F' \cap g^{-1}J' \xrightarrow{(g^{-1}jg)^{-1}} g^{-1}E \cap g^{-1}J$
41.	$g^{-1}E \cap g^{-1}K \xrightarrow{eg} E' \cap L \xrightarrow{l} E' \cap L' \xrightarrow{(eg)^{-1}} g^{-1}E \cap g^{-1}K' \xrightarrow{(g^{-1}kg)^{-1}} g^{-1}E \cap g^{-1}K$
42.	$g^{-1}F \cap g^{-1}L \xrightarrow{fg} F' \cap K \xrightarrow{k} F' \cap K' \xrightarrow{(fg)^{-1}} g^{-1}F \cap g^{-1}L' \xrightarrow{(g^{-1}lg)^{-1}} g^{-1}F \cap g^{-1}L$
43.	$g^{-1}G \cap g^{-1}I \xrightarrow{gg} G' \cap J \xrightarrow{j} G' \cap J' \xrightarrow{(gg)^{-1}} g^{-1}G \cap g^{-1}I' \xrightarrow{(g^{-1}ig)^{-1}} g^{-1}G \cap g^{-1}I$
44.	$g^{-1}G \cap g^{-1}K \xrightarrow{gg} G' \cap K' \xrightarrow{k^{-1}} H' \cap K \xrightarrow{hg} g^{-1}H \cap g^{-1}K' \xrightarrow{(g^{-1}kg)^{-1}} g^{-1}G \cap g^{-1}K$
45.	$g^{-1}G \cap g^{-1}L \xrightarrow{gg} G' \cap L' \xrightarrow{l^{-1}} H' \cap L \xrightarrow{(hg)^{-1}} g^{-1}H \cap g^{-1}L' \xrightarrow{(g^{-1}lg)^{-1}} g^{-1}G \cap g^{-1}L$
46.	$g^{-1}H \cap g^{-1}J \xrightarrow{hg} H' \cap I \xrightarrow{i} H' \cap I' \xrightarrow{hg} g^{-1}H \cap g^{-1}J' \xrightarrow{(g^{-1}jg)^{-1}} g^{-1}H \cap g^{-1}J$
47.	$g^{-1}I \cap g^{-1}K \xrightarrow{g^{-1}ig} g^{-1}I' \cap g^{-1}K \xrightarrow{g^{-1}kg} g^{-1}J' \cap g^{-1}K' \xrightarrow{(g^{-1}jg)^{-1}} g^{-1}J \cap g^{-1}K' \xrightarrow{(g^{-1}kg)^{-1}} g^{-1}I \cap g^{-1}K$
48.	$g^{-1}I \cap g^{-1}L \xrightarrow{g^{-1}ig} g^{-1}I' \cap g^{-1}L \xrightarrow{g^{-1}lg} g^{-1}J' \cap g^{-1}L' \xrightarrow{(g^{-1}jg)^{-1}} g^{-1}J \cap g^{-1}L' \xrightarrow{(g^{-1}lg)^{-1}} g^{-1}I \cap g^{-1}L$

As was mentioned earlier, a fundamental domain for the orientable double cover $\widetilde{M}$ consists of two copies of P obtained by taking the standard copy of P (as we have described earlier) and transforming it across the side G via the transformation g^{-1} to obtain another copy of P on the other side of G. The union of these two copies of P joined along the side G constitutes a fundamental domain for $\widetilde{M}$. Recall that the side G corresponds to the sphere with centre $(1,0,0,1)$, and in the handle decomposition the side G corresponds to the point $(1+\sqrt{2},0,0)$. Then since the transformation $g^{-1} = k_{(-1,1,1,-1)}r$, where r is now reflection in the side G, we can think of that part of the Kirby diagram of $\widetilde{M}$ coming from the $g^{-1}P$ piece as being obtained by taking the part coming from P, applying the transformation $k_{(-1,1,1,-1)}$ to each component of a 1-handle pair, and then reflecting along a plane parallel to the plane $y = z = 0$ and lying on the right side of $(1+\sqrt{2},0,0)$, this reflection along a plane parallel to the plane $y = z = 0$

corresponds to the r part of the transformation g^{-1}. Note that the exact centre of the plane parallel to $y = z = 0$ is not important, for example we can take the centre to be given by the vector $(3, 0, 0)$ (as long as it lies to the right of $(1 + \sqrt{2}, 0, 0)$). From here it is easy to see how a Kirby diagram for $\widetilde{M}$ will look like. It will consist of the usual Kirby diagram corresponding to M, and then to the right of that part of the one handle labelled G it will consist of a diagram obtained by taking the diagram corresponding to M, applying the transformation $k_{(-1,1,1,-1)}$, and then reflecting through a plane parallel to $y = z = 0$ and centred at $(3, 0, 0)$, in other words we take the diagram corresponding to M and then apply the transformation g^{-1}. Recall that whenever we drew a Kirby diagram of a Ratcliffe-Tschantz manifold we would split the total diagram into four diagrams, three such diagrams would correspond to those 2-handles that lie in the x-y, x-z and y-z planes, and one more diagram corresponded to those 2-handles that did not all lie in such a plane, there were always six such 2-handles. We can similarly decompose the Kirby diagram of $\widetilde{M}$ into a collection of four such diagrams. The difference in this case is that each diagram will have have two components, one coming from that part of the fundamental domain corresponding to P, and another coming from that part corresponding to $g^{-1}P$.

It is time to show the reader how these diagrams look like. Previously, each diagram would show six 2-handles with each 2-handle being shown in a particular colour. The situation now is that each diagram will have twelve 2-handles, hence we will need twelve colours to distinguish each 2-handle. So as to avoid confusion right from the start we have included the following table which shows precisely the colours we will be using.

Orange	
Brown	
Turquoise	
Yellow	
Dark Green	
Light Green	
Green	
Pink	
Grey	
Red	
Blue	
Black	

In the following diagrams, for each side S we denote the component of the 1-handle corresponding to $g^{-1}S$ by $S-$. There are in total twenty four 1-handles.

The following diagram shows that part of the Kirby diagram contained in the x-y plane, with

the table following outlining the colouring of the 2-handle.

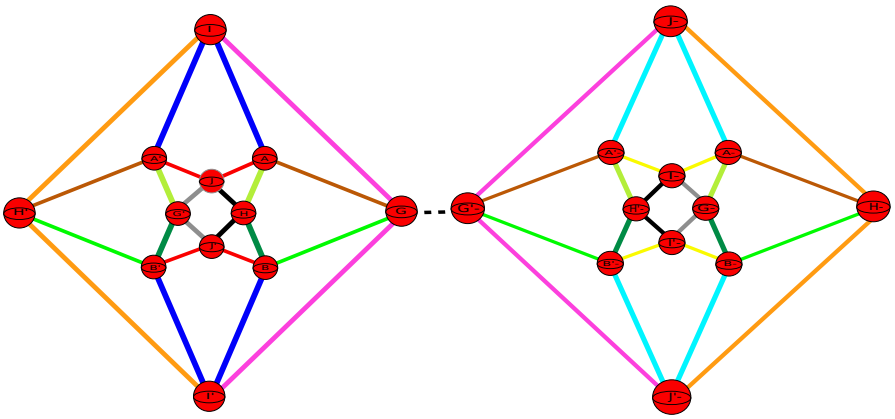

Colour	Equivalence class
Orange	$g^{-1}H \cap g^{-1}J \xrightarrow{hg} H' \cap I \xrightarrow{i} H' \cap I' \xrightarrow{hg} g^{-1}H \cap g^{-1}J' \xrightarrow{(g^{-1}jg)^{-1}} g^{-1}H \cap g^{-1}J$
Brown	$A \cap G \xrightarrow{a} A' \cap H' \xrightarrow{(hg)^{-1}} g^{-1}A \cap g^{-1}H \xrightarrow{g^{-1}ag} g^{-1}A' \cap g^{-1}G' \xrightarrow{(g^{-1}g)^{-1}} A \cap G$
Turquoise	$g^{-1}A \cap g^{-1}J \xrightarrow{g^{-1}ag} g^{-1}A' \cap g^{-1}J \xrightarrow{g^{-1}jg} g^{-1}B' \cap g^{-1}J' \xrightarrow{(g^{-1}bg)^{-1}} g^{-1}B \cap g^{-1}J' \xrightarrow{(g^{-1}jg)^{-1}} g^{-1}A \cap g^{-1}J$
Yellow	$g^{-1}A \cap g^{-1}I \xrightarrow{g^{-1}ag} g^{-1}A' \cap g^{-1}I \xrightarrow{g^{-1}ig} g^{-1}B' \cap g^{-1}I' \xrightarrow{(g^{-1}bg)^{-1}} g^{-1}B \cap g^{-1}I' \xrightarrow{(g^{-1}ig)^{-1}} g^{-1}A \cap g^{-1}I$
Dark Green	$g^{-1}B \cap g^{-1}G \xrightarrow{g^{-1}bg} g^{-1}B' \cap g^{-1}H' \xrightarrow{(g^{-1}h)^{-1}} B \cap H \xrightarrow{b} B' \cap G' \xrightarrow{(gg)^{-1}} g^{-1}B \cap g^{-1}G$
Light Green	$g^{-1}A \cap g^{-1}G \xrightarrow{g^{-1}ag} g^{-1}A' \cap g^{-1}H' \xrightarrow{(g^{-1}h)^{-1}} A \cap H \xrightarrow{a} A' \cap G' \xrightarrow{(gg)^{-1}} gA \cap gG$
Green	$B \cap G \xrightarrow{b} B' \cap H' \xrightarrow{(hg)^{-1}} g^{-1}B \cap g^{-1}H \xrightarrow{g^{-1}bg} g^{-1}B' \cap g^{-1}G' \xrightarrow{(g^{-1}g)^{-1}} B \cap G$
Pink	$G \cap I \xrightarrow{g^{-1}g} g^{-1}G' \cap g^{-1}J \xrightarrow{g^{-1}jg} g^{-1}G' \cap g^{-1}J' \xrightarrow{(g^{-1}g)^{-1}} G \cap I' \xrightarrow{i^{-1}} G \cap I$
Grey	$g^{-1}G \cap g^{-1}I \xrightarrow{gg} G' \cap J \xrightarrow{j} G' \cap J' \xrightarrow{(gg)^{-1}} g^{-1}G \cap g^{-1}I' \xrightarrow{(g^{-1}ig)^{-1}} g^{-1}G \cap g^{-1}I$
Red	$A \cap J \xrightarrow{a} A' \cap J \xrightarrow{j} B' \cap J' \xrightarrow{b^{-1}} B \cap J' \xrightarrow{j^{-1}} A \cap J$
Blue	$A \cap I \xrightarrow{a} A' \cap I \xrightarrow{i} B' \cap I' \xrightarrow{b^{-1}} B \cap I' \xrightarrow{i^{-1}} A \cap I$
Black	$H \cap J \xrightarrow{g^{-1}h} g^{-1}H' \cap g^{-1}I \xrightarrow{g^{-1}ig} g^{-1}H' \cap g^{-1}I' \xrightarrow{(g^{-1}h)^{-1}} H \cap J' \xrightarrow{j^{-1}} H \cap J$

We can see two sets of 1-handles, there are those on the right of G and those on the left. Just to make sure the reader understands exactly how this diagram is being formed, let us explain why the 1-handle component $A-$ sits where it does. The 1-handle component $A-$ corresponds to the side $g^{-1}A$, the transformation g^{-1} consists of two parts the r-part, which is reflection through the side G and the k-part given by the diagonal matrix whose diagonal is $(-1,+1,+1,-1)$. The side A can be identified with its centre vector given by $(1,1,0,0)$, which after mapping to $\mathbb{R}^3$ is identified by the co-ordinate $(1/\sqrt{2}, 1/\sqrt{2}, 0)$. Applying the k matrix to this vector we obtain the vector $(-1,1,0,0)$, this tells us that the k part of the transformation maps the 1-handle component A to A'. We still need to deal with the r-part, since the side G has corresponding 1-handle component in $\mathbb{R}^3$ with centre $(1+\sqrt{2},0,0)$, and the r-part is reflection through the side G, we see that we need to reflect each centre co-ordinate corresponding to each 1-handle component through a plane parallel to the $y=z=0$ plane centred at the point $(3,0,0)$ (any centre vector to the right of G will do). From here it should be clear that applying k to A

followed by reflection in the plane parallel to $y = z = 0$ and centred at $(3, 0, 0)$ gives us the point where $A-$ is in the above diagram. The reader can check for him/her-self that the images of all the other 1-handle components are in the places they are shown in the diagram.

The fundamental domain for $\widetilde{M}$ consists of two copies of M joined together at the side G, therefore the total polyhedron that constitutes the fundamental domain will not contain the side G and its image $g^{-1}G'$ as these two sides have been identified. This means that in the Kirby diagram associated to $\widetilde{M}$ we need to kill the 1-handle pair $G - G'-$, we do this by adding a 2-handle whose attaching circle runs over the 1-handle $G - G'-$ once. It can be seen as the dotted line running from G to $G'-$ in the above diagram, we have chosen to add this 2-handle so that its attaching circle lies in the x-y and x-z planes.

We move on to show that part of the Kirby diagram that is contained in the x-z plane, the table that follows the diagram shows which 2-handle corresponds to which colour.

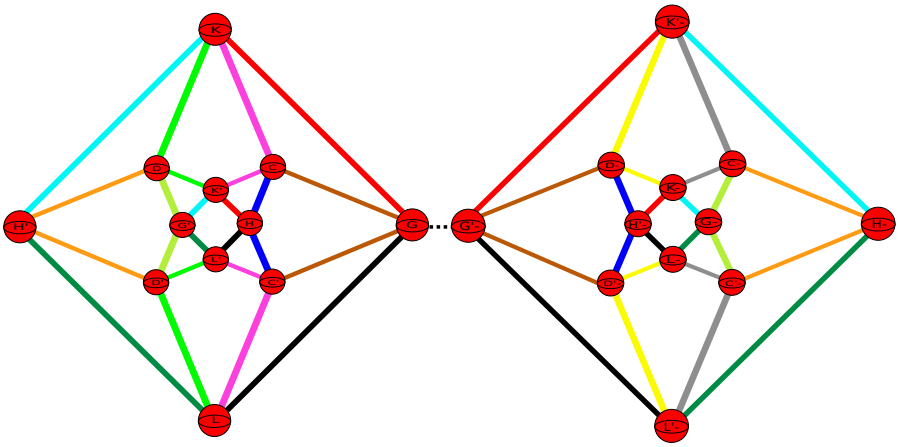

Colour	**Equivalence class**
Orange	$g^{-1}C \cap g^{-1}H \xrightarrow{g^{-1}cg} g^{-1}C' \cap g^{-1}H \xrightarrow{hg} D' \cap H' \xrightarrow{d^{-1}} D \cap H' \xrightarrow{(hg)^{-1}} g^{-1}C \cap g^{-1}H$
Brown	$C \cap G \xrightarrow{c} C' \cap G \xrightarrow{g^{-1}g} g^{-1}D' \cap g^{-1}G' \xrightarrow{(g^{-1}dg)^{-1}} g^{-1}D \cap g^{-1}G' \xrightarrow{(g^{-1}g)^{-1}} C \cap G$
Turquoise	$g^{-1}G \cap g^{-1}K \xrightarrow{gg} G' \cap K' \xrightarrow{k^{-1}} H' \cap K \xrightarrow{hg} g^{-1}H \cap g^{-1}K' \xrightarrow{(g^{-1}kg)^{-1}} g^{-1}G \cap g^{-1}K$
Yellow	$g^{-1}D \cap g^{-1}K \xrightarrow{g^{-1}dg} g^{-1}D' \cap g^{-1}L \xrightarrow{g^{-1}lg} g^{-1}D' \cap g^{-1}L' \xrightarrow{(g^{-1}dg)^{-1}} g^{-1}D \cap g^{-1}K' \xrightarrow{(g^{-1}kg)^{-1}} g^{-1}D \cap g^{-1}K$
Dark Green	$g^{-1}G \cap g^{-1}L \xrightarrow{gg} G' \cap L' \xrightarrow{l^{-1}} H' \cap L \xrightarrow{(hg)^{-1}} g^{-1}H \cap g^{-1}L' \xrightarrow{(g^{-1}lg)^{-1}} g^{-1}G \cap g^{-1}L$
Light Green	$g^{-1}C \cap g^{-1}G \xrightarrow{g^{-1}cg} g^{-1}C' \cap g^{-1}G \xrightarrow{gg} D' \cap G' \xrightarrow{d^{-1}} D \cap G' \xrightarrow{(gg)^{-1}} g^{-1}C \cap g^{-1}G$
Green	$D \cap K \xrightarrow{d} D' \cap L \xrightarrow{l} D' \cap L' \xrightarrow{d^{-1}} D \cap K' \xrightarrow{k^{-1}} D \cap K$
Pink	$C \cap K \xrightarrow{c} C' \cap L \xrightarrow{l} C' \cap L' \xrightarrow{c^{-1}} C \cap K' \xrightarrow{k^{-1}} C \cap K$
Grey	$g^{-1}C \cap g^{-1}K \xrightarrow{g^{-1}cg} g^{-1}C' \cap g^{-1}L \xrightarrow{g^{-1}lg} g^{-1}C' \cap g^{-1}L' \xrightarrow{(g^{-1}cg)^{-1}} g^{-1}C \cap g^{-1}K' \xrightarrow{(g^{-1}kg)^{-1}} g^{-1}C \cap g^{-1}K$
Red	$G \cap K \xrightarrow{g^{-1}g} g^{-1}G' \cap g^{-1}K' \xrightarrow{(g^{-1}kg)^{-1}} g^{-1}H' \cap g^{-1}K \xrightarrow{(g^{-1}h)^{-1}} H \cap K' \xrightarrow{k^{-1}} G \cap K$
Blue	$C \cap H \xrightarrow{c} C' \cap H \xrightarrow{g^{-1}h} g^{-1}D' \cap g^{-1}H' \xrightarrow{(g^{-1}dg)^{-1}} g^{-1}D \cap g^{-1}H' \xrightarrow{(g^{-1}h)^{-1}} C \cap H$
Black	$G \cap L \xrightarrow{g^{-1}g} g^{-1}G' \cap g^{-1}L' \xrightarrow{(g^{-1}lg)^{-1}} g^{-1}H' \cap g^{-1}L \xrightarrow{(g^{-1}h)^{-1}} H \cap L' \xrightarrow{l^{-1}} G \cap L$

The part contained in the y-z plane is shown in the following diagram.

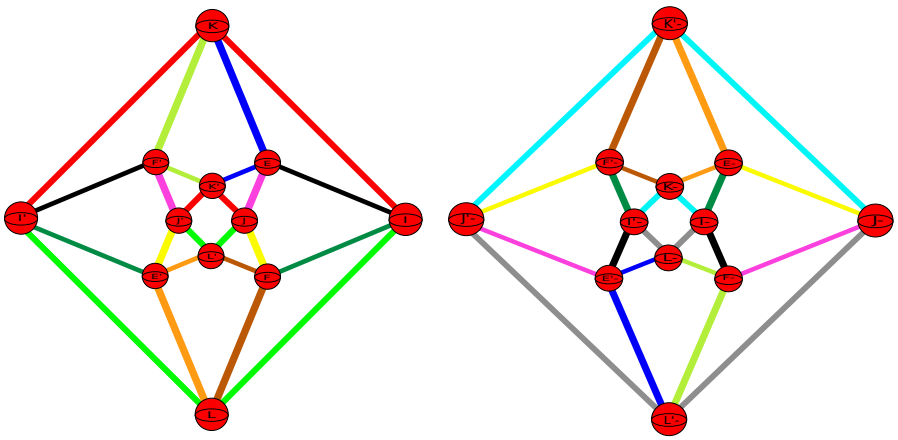

Colour	Equivalence class
Orange	$g^{-1}E \cap g^{-1}K \xrightarrow{eg} E' \cap L \xrightarrow{l} E' \cap L' \xrightarrow{(eg)^{-1}} g^{-1}E \cap g^{-1}K' \xrightarrow{(g^{-1}kg)^{-1}} g^{-1}E \cap g^{-1}K$
Brown	$F \cap L \xrightarrow{g^{-1}f} g^{-1}F' \cap g^{-1}K \xrightarrow{g^{-1}kg} g^{-1}F' \cap g^{-1}K' \xrightarrow{(g^{-1}f)^{-1}} F \cap L' \xrightarrow{l^{-1}} F \cap L$
Turquoise	$g^{-1}I \cap g^{-1}K \xrightarrow{g^{-1}ig} g^{-1}I' \cap g^{-1}K \xrightarrow{g^{-1}kg} g^{-1}J' \cap g^{-1}K' \xrightarrow{(g^{-1}jg)^{-1}} g^{-1}J \cap g^{-1}K' \xrightarrow{(g^{-1}kg)^{-1}} g^{-1}I \cap g^{-1}K$
Yellow	$g^{-1}E \cap g^{-1}J \xrightarrow{eg} E' \cap J' \xrightarrow{j^{-1}} F \cap J \xrightarrow{g^{-1}f} g^{-1}F' \cap g^{-1}J' \xrightarrow{(g^{-1}jg)^{-1}} g^{-1}E \cap g^{-1}J$
Dark Green	$g^{-1}E \cap g^{-1}I \xrightarrow{eg} E' \cap I' \xrightarrow{i^{-1}} F \cap I \xrightarrow{g^{-1}f} g^{-1}F' \cap g^{-1}I' \xrightarrow{(g^{-1}ig)^{-1}} g^{-1}E \cap g^{-1}I$
Light Green	$g^{-1}F \cap g^{-1}L \xrightarrow{fg} F' \cap K \xrightarrow{k} F' \cap K' \xrightarrow{(fg)^{-1}} g^{-1}F \cap g^{-1}L' \xrightarrow{(g^{-1}lg)^{-1}} g^{-1}F \cap g^{-1}L$
Green	$I \cap L \xrightarrow{i} I' \cap L \xrightarrow{l} J' \cap L' \xrightarrow{j^{-1}} J \cap L' \xrightarrow{l^{-1}} I \cap L$
Pink	$E \cap J \xrightarrow{g^{-1}e} g^{-1}E' \cap g^{-1}J' \xrightarrow{(g^{-1}jg)^{-1}} g^{-1}F \cap g^{-1}J \xrightarrow{fg} F' \cap J' \xrightarrow{j^{-1}} E \cap J$
Grey	$g^{-1}I \cap g^{-1}L \xrightarrow{g^{-1}ig} g^{-1}I' \cap g^{-1}L \xrightarrow{g^{-1}lg} g^{-1}J' \cap g^{-1}L' \xrightarrow{(g^{-1}jg)^{-1}} g^{-1}J \cap g^{-1}L' \xrightarrow{(g^{-1}lg)^{-1}} g^{-1}I \cap g^{-1}L$
Red	$I \cap K \xrightarrow{i} I' \cap K \xrightarrow{k} J' \cap K' \xrightarrow{j^{-1}} J \cap K' \xrightarrow{k^{-1}} I \cap K$
Blue	$E \cap K \xrightarrow{g^{-1}e} g^{-1}E' \cap g^{-1}L \xrightarrow{g^{-1}lg} g^{-1}E' \cap g^{-1}L' \xrightarrow{(g^{-1}e)^{-1}} E \cap K' \xrightarrow{k^{-1}} E \cap K$
Black	$E \cap I \xrightarrow{g^{-1}e} g^{-1}E' \cap g^{-1}I' \xrightarrow{(g^{-1}ig)^{-1}} g^{-1}F \cap g^{-1}I \xrightarrow{fg} F' \cap I' \xrightarrow{i^{-1}} E \cap I$

Finally, we have the 2-handles that do not all lie in one of the above planes. There are twelve in total, six coming from each copy of P contributing to the fundamental domain (two copies in total).

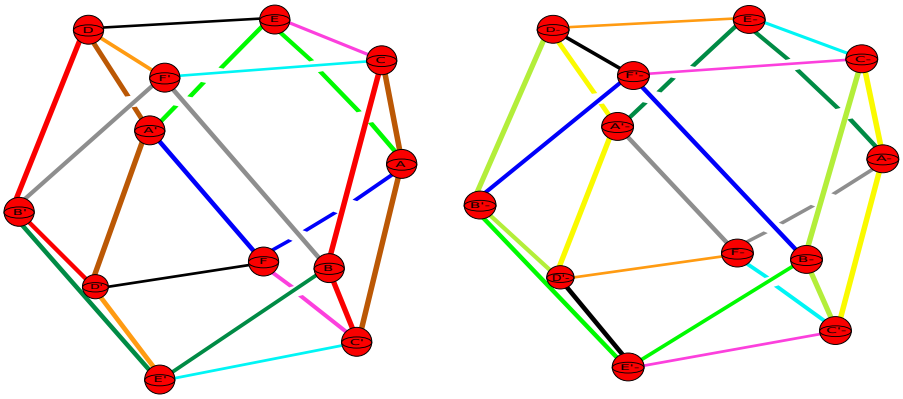

Colour	Equivalence class
Orange	$g^{-1}D \cap g^{-1}E \xrightarrow{g^{-1}dg} g^{-1}D' \cap g^{-1}F \xrightarrow{fg} D \cap F' \xrightarrow{d} D' \cap E' \xrightarrow{(eg)^{-1}} g^{-1}D \cap g^{-1}E$
Brown	$A \cap C \xrightarrow{a} A' \cap D \xrightarrow{d} A' \cap D' \xrightarrow{a^{-1}} A \cap C' \xrightarrow{c^{-1}} A \cap C$
Turquoise	$g^{-1}C \cap g^{-1}E \xrightarrow{g^{-1}cg} g^{-1}C' \cap g^{-1}F \xrightarrow{fg} C \cap F' \xrightarrow{c} C' \cap E' \xrightarrow{(eg)^{-1}} g^{-1}C \cap g^{-1}E$
Yellow	$g^{-1}A \cap g^{-1}C \xrightarrow{g^{-1}ag} g^{-1}A' \cap g^{-1}D \xrightarrow{g^{-1}dg} g^{-1}A' \cap g^{-1}D' \xrightarrow{(g^{-1}ag)^{-1}} g^{-1}A \cap g^{-1}C' \xrightarrow{(g^{-1}cg)^{-1}} g^{-1}A \cap g^{-1}C$
Dark Green	$g^{-1}A \cap g^{-1}E \xrightarrow{g^{-1}ag} g^{-1}A' \cap g^{-1}E \xrightarrow{eg} B' \cap E' \xrightarrow{b^{-1}} B \cap E' \xrightarrow{(eg)^{-1}} g^{-1}A \cap g^{-1}E$
Light Green	$g^{-1}B \cap g^{-1}C \xrightarrow{g^{-1}bg} g^{-1}B' \cap g^{-1}D \xrightarrow{g^{-1}dg} g^{-1}B' \cap g^{-1}D' \xrightarrow{(g^{-1}bg)^{-1}} g^{-1}B \cap g^{-1}C' \xrightarrow{(g^{-1}cg)^{-1}} g^{-1}B \cap g^{-1}C$
Green	$A \cap E \xrightarrow{a} A' \cap E \xrightarrow{g^{-1}e} g^{-1}B' \cap g^{-1}E' \xrightarrow{(g^{-1}bg)^{-1}} g^{-1}B \cap g^{-1}E' \xrightarrow{(g^{-1}e)^{-1}} A \cap E$
Pink	$C \cap E \xrightarrow{c} C' \cap F \xrightarrow{g^{-1}f} g^{-1}C \cap g^{-1}F' \xrightarrow{g^{-1}cg} g^{-1}C' \cap g^{-1}E' \xrightarrow{(g^{-1}e)^{-1}} C \cap E$
Grey	$g^{-1}A \cap g^{-1}F \xrightarrow{g^{-1}ag} g^{-1}A' \cap g^{-1}F \xrightarrow{fg} B' \cap F' \xrightarrow{b^{-1}} B \cap F' \xrightarrow{(fg)^{-1}} g^{-1}A \cap g^{-1}F$
Red	$B \cap C \xrightarrow{b} B' \cap D \xrightarrow{d} B' \cap D' \xrightarrow{b^{-1}} B \cap C' \xrightarrow{c^{-1}} B \cap C$
Blue	$A \cap F \xrightarrow{a} A' \cap F \xrightarrow{g^{-1}f} g^{-1}B' \cap g^{-1}F' \xrightarrow{(g^{-1}bg)^{-1}} g^{-1}B \cap g^{-1}F' \xrightarrow{(g^{-1}f)^{-1}} A \cap F$
Black	$D \cap E \xrightarrow{d} D' \cap F \xrightarrow{g^{-1}f} g^{-1}D \cap g^{-1}F' \xrightarrow{g^{-1}dg} g^{-1}D' \cap g^{-1}E' \xrightarrow{(g^{-1}e)^{-1}} D \cap E$

Recall that our primary interest is to study, via Kirby calculus, a boundary filling of the manifold M. Before we take this up in the next section, we mention that we have not yet explained how to obtain the 3-handles of the double cover. The procedure is exactly analogous to how we obtained the 3-handles in regard to the previous examples we have considered. We simply take three distinct codimension 1 sides with non-empty intersection, then apply side pairing transformations till we cycle back to the original intersection, this constitutes a 3-handle. As we will be dealing with closed 4-manifolds and hence do not have to worry about the 3 and 4-handles (this is due to a theorem of Laudenbach and Poénaru, see [8] p.116), we will not be showing tables of the 3-handles nor pictures of how they look like.

3.3 Boundary filling of the orientable double cover of Manifold 35.

In this section we are going to use elementary moves to reduce the Kirby diagram of $\widetilde{M}$, this will help us in identifying the diffeomorphism type of the double cover of $\widetilde{M}$. Recall that in the previous chapter we explained how all the 2-handles for a filling had a planar framing, furthermore we explained how the attaching maps being reflections or compositions of reflections with inversion in S^2 had the effect that when we pushed components of 2-handles through attaching spheres of 1-handles nothing "wild" could happen i.e. the 2-handle component being pushed through would not twist around the attaching sphere it came out of. These observations all hold true in the case of the orientable double cover of manifold 35, and in fact for all of the Ratcliffe-Tschantz manifolds. We will not go through the details of this as they are completely analogous to what we did in the previous chapter.

We already mentioned that the boundary type associated to each ideal vertex is given by the code **GGGGH** (or in *Wolf's* notation $\mathcal{B}_1\mathcal{B}_1\mathcal{B}_1\mathcal{B}_1\mathcal{B}_2$), each of these boundaries are themselves non-orientable, therefore in the orientable double cover they will lift to there own orientable double covers. We also mentioned that we computed a translation in each of the parabolic subgroups associated to each cusp, the translations we obtained were c, a, k, i and $e^{-1}heh^{-1}$. The first four translations are all given by orientation preserving transformations, hence in the double cover they correspond to translations in their respective boundary components. Therefore the associated filling of the corresponding boundary components in the Kirby diagram of $\widetilde{M}$ will consist of adding four 2-handles running over $C - C'$, $A - A'$, $K - K'$ and $I - I'$ once. The translation $e^{-1}heh^{-1}$ can be written as $e^{-1}heh^{-1} = (e^{-1}g)(g^{-1}h)(eg)(g^{-1}h^{-1})$, therefore the corresponding filling of the associated boundary component in $\widetilde{M}$ will involve adding a 2-handle with four components, one running from E to H, followed by one running from $H'-$ to $E-$, followed by one running from E' to H', and finally one running from $H-$ to $E'-$.

We move on to showing how the Kirby diagrams look with these added 2-handles. The following diagram shows the x-y plane, by considering a fundamental domain for the ideal vertex class $\{(0,0,0,1),(0,0,0,-1)\}$ we can replace the translation i with j, it will be much easier to use the transformation j when we apply elementary moves to the Kirby diagram, therefore we make this change from now itself. The reader should notice how the added 2-handles running over $A - A'$ and $J - J'$ lie completely in the x-y plane.

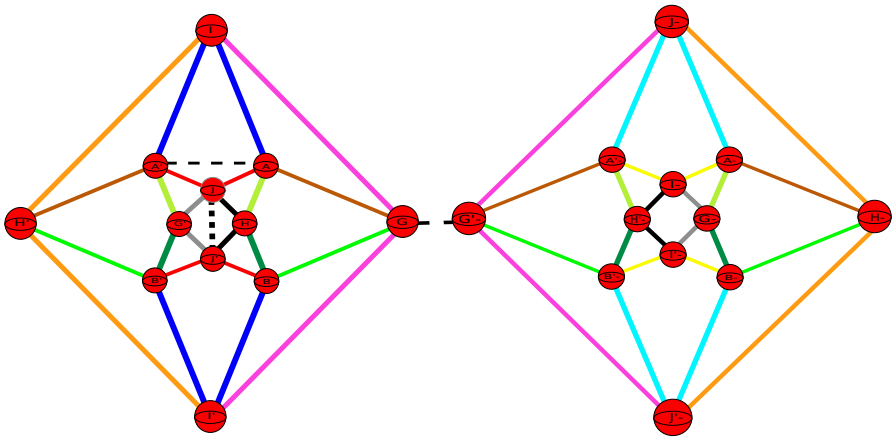

The following diagram shows the x-z plane, the reader should note how the added 2-handles running over $K - K'$ and $C - C'$ lie entirely in the x-z plane.

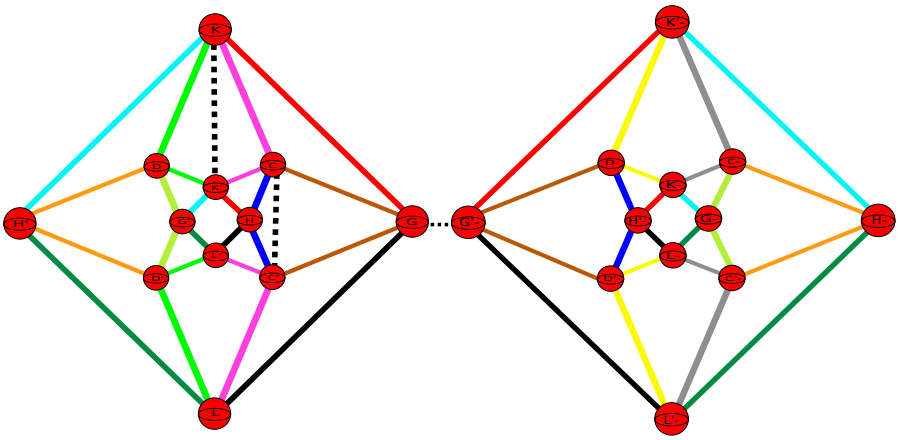

The following diagram shows a picture of the y-z plane, this plane also contains the added 2-handles running over $J - J'$ and $K - K'$.

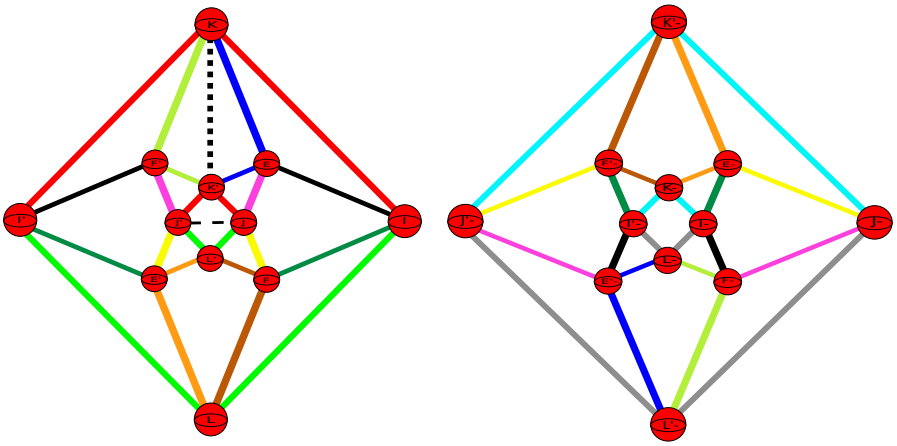

Finally, we have the twelve 2-handles that do not all lie in any one of the above planes.

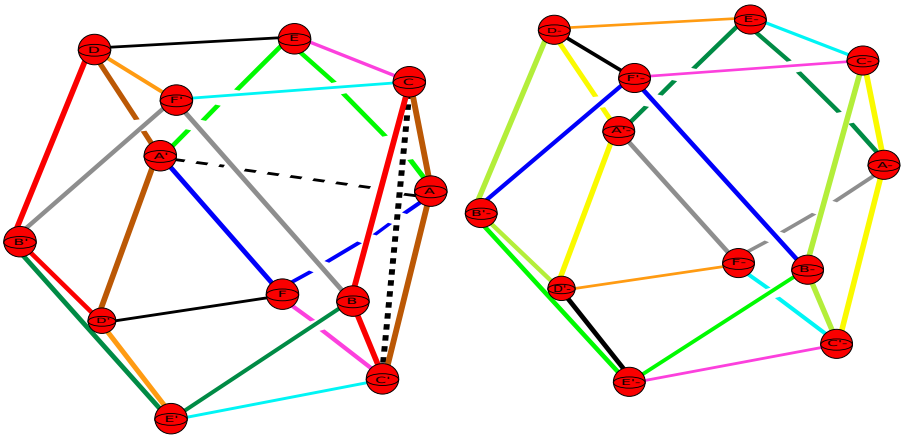

We have not shown the added 2-handle corresponding to the translation $e^{-1}h^{-1}eh$ that has components running from E to H, $H'-$ to $E-$, E' to H' and $H-$ to $E'-$. Two of the components, the ones running from E to H and E' to H', move from that part of the y-z plane corresponding to the piece of the Kirby diagram coming from P to the $x - y$ plane, hence they

run outside the four diagrams we have been showing. Due to this none of the elementary moves we carry out to begin with will affect these two components in any way. Similarly, the two components running from $H'-$ to $E-$ and $H-$ to $E'-$ move from that part of the y-z plane corresponding to the piece of the Kirby diagram coming from $g^{-1}P$ to the piece in the x-y plane, due to this they will also not be affected by any of the elementary moves to begin with. Therefore we will choose to leave this 2-handle out of our diagrams to start with, towards the end when we start doing handle slides that move between planes we will put this 2-handle back in so the reader can see exactly how it is affected.

We are now in the situation where we have various 2-handles that are running over 1-handles once, and hence we have various handle cancelling pairs. We want to start carrying out several of these cancellations, however we need to be a bit careful when we do so. A few of the 2-handles intersect the other planes, hence when carrying out cancellations/slides we must keep track of how these intersection points move. We remind the reader of our coding system that helps keep track of various intersection points. An intersection point in a diagram will be shown via a black dot, the dot will have a code next to it which is supposed to tell the reader which 2-handle is creating the point of intersection. The code will consist of either four characters or two characters, in the case that it consists of four characters the first two tell the reader from which plane the 2-handle, creating the intersection point, lies in. The second two characters tell us which 1-handles the 2-handle runs over, in situations where there are multiple 2-handles running over the 1-handles we will always make it apparent as to which 2-handle we are talking about. Finally, in the case that the code consists of just two letters we are to immediately take this to mean that the 2-handle creating the intersection point is residing in the diagram showing the twelve 2-handles that do not all lie in a single plane. The two characters of the code then tell us which 1-handles this 2-handle is running over.

The following shows pictures of the x-y, x-z and y-z planes respectively, with intersection points added

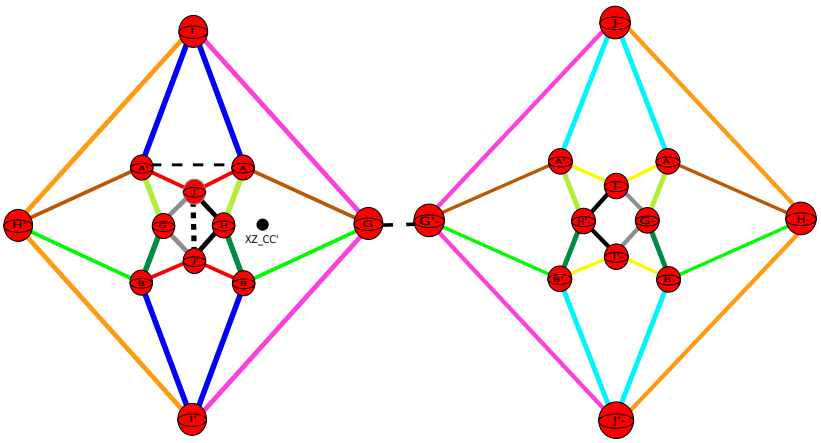

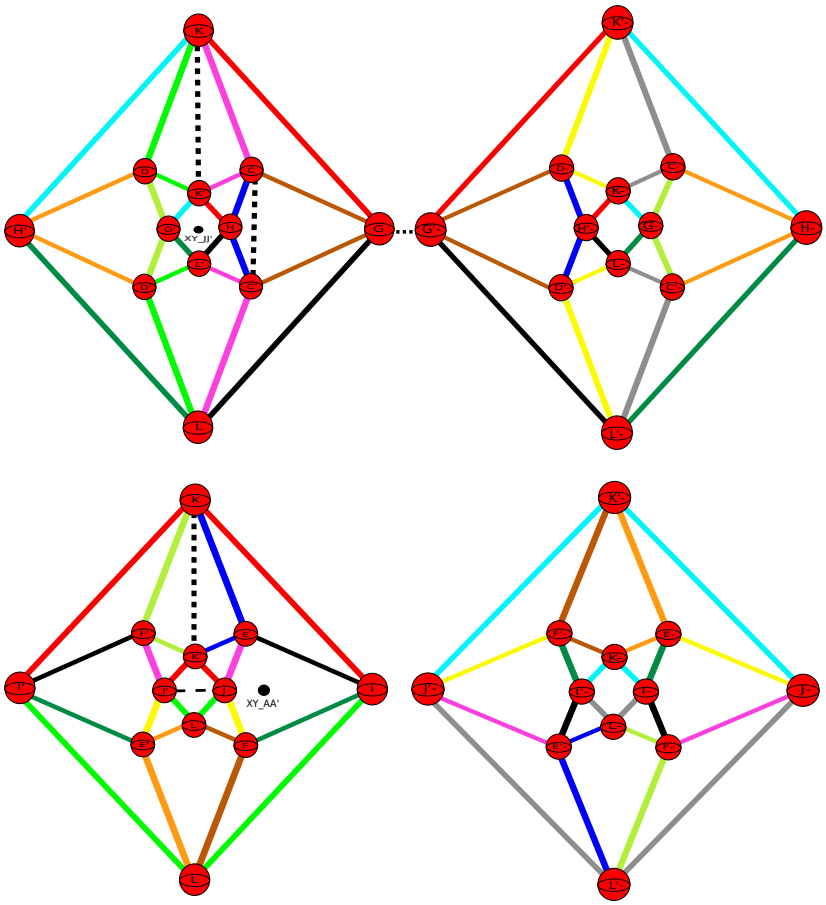

The first cancellation we are going to carry out is to cancel $G, G'-$ using the black dashed 2-handle in the x-y plane. This will only affect the diagrams in the x-y and x-y planes. The following shows how the diagram in the x-y plane changes.

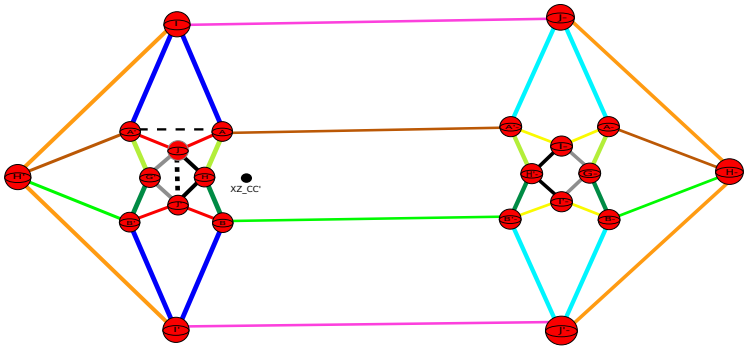

The diagram in the x-z plane changes as follows.

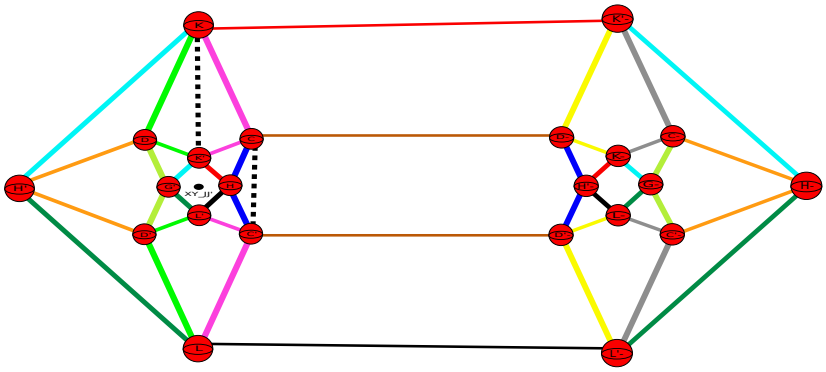

The next step we take is to cancel A, A' using the added 2-handle that runs over this 1-handle once. As this 2-handle resides in the x-y plane and the diagram showing the twelve 2-handles that do not all lie in a single plane, it is only these two diagrams that will be affected. However, the reader should keep in mind that this 2-handle creates a point of intersection with the y-z plane, hence there will be some changes to the y-z plane on the level of intersection points. The following picture shows how the x-y plane changes when we carry out this cancellation.

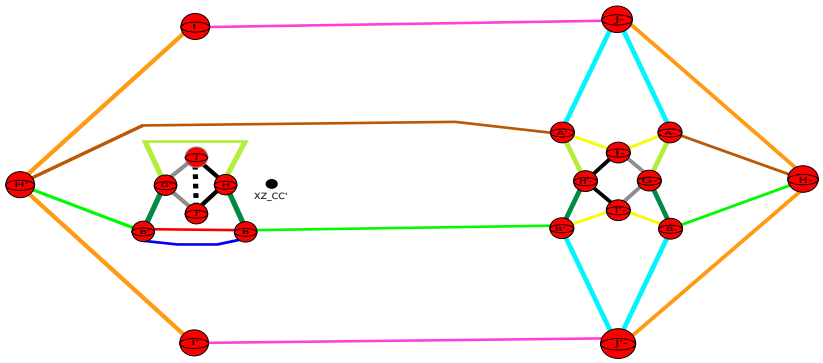

Observe that after carrying out the cancellation we have also carried out two handle slides. When we cancel A, A' we get a blue 2-handle component that loops back into I, we push this through I to come out of I', then slide the blue 2-handle off of I' to give a blue 2-handle running over B, B' once. We also get a red 2-handle component that loops back into J, we can perform an analogous slide to obtain a red 2-handle running over B, B' once. In general, when we carry out such handle cancellations we will also simultaneously carry out handle slides analogous to the one described above. It should be clear to the reader that we have carried out such handle slides.

The diagram corresponding to the twelve 2-handles that do not all lie in a single plane changes as follows.

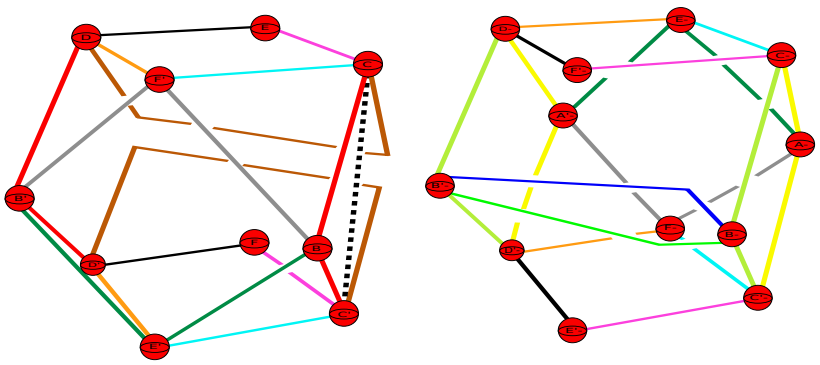

The reader should note that once again we have carried out some handle slides, when we cancel A, A' we obtain a blue 2-handle component that loops back into F, remember that in the double cover our 1-handle pair is $F, F'-$, therefore when we push this blue 2-handle component through F it will come out of $F'-$, then slide the blue 2-handle off of $F'-$ to obtain a blue 2-handle running over $B-, B'-$ once. Similarly when we cancel A, A' we get a green 2-handle component that loops into E, and since E is identified to $E'-$ this component can be pushed through to come out of $E'-$, we can then slide the green 2-handle into the position shown in the above picture.

The cancellation of A, A' with the added 2-handle that ran over it once causes the intersection point, in the y-z plane, labelled **XY_AA'** to disappear, with many new intersection points appearing. The following picture shows the y-z plane with the added intersection points coming from the above cancellation.

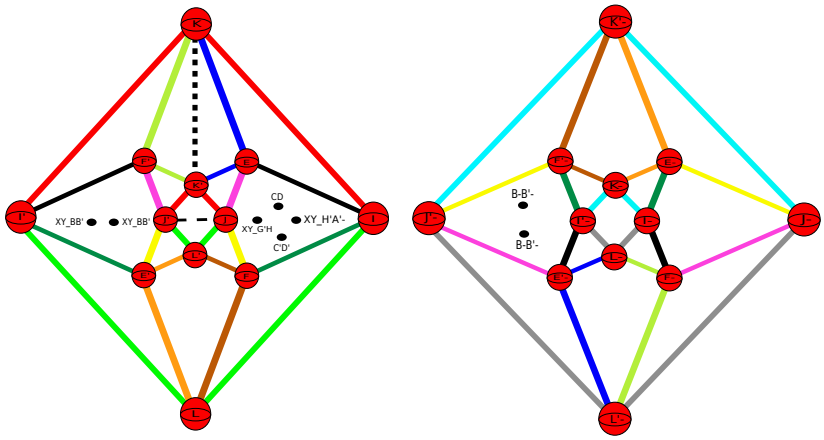

We move on to cancelling C, C' using the added 2-handle that passes over it once, and that resides in the x-z plane and the diagram corresponding to the twelve 2-handles that did not all lie in a single plane.

The x-z plane changes as follows:

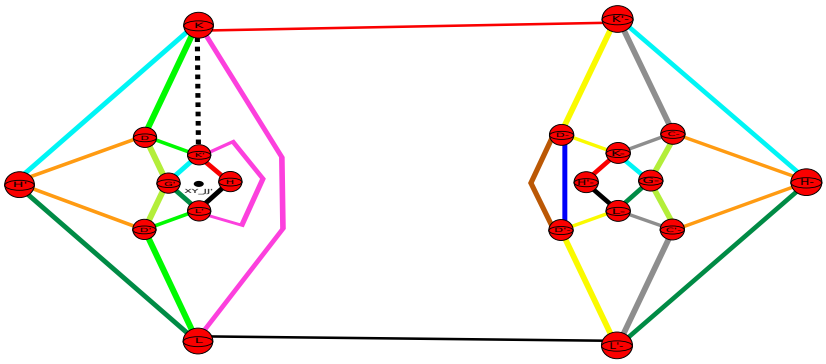

The reader should observe that we have also carried out a handle slide. Namely, we have pushed the blue 2-handle component that loops back into H through H and then slid it off of $H'-$ to get a blue 2-handle running over $D-, D'-$ once.

The diagram corresponding to the twelve 2-handles that did not all lie in a single plane changes to the following diagram.

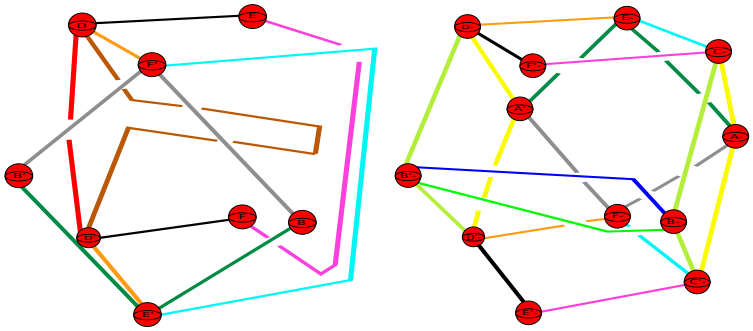

The 2-handle that was used to do the cancellation intersected the x-y plane, hence this point of intersection will disappear with some new ones coming in place of it. The following picture shows the coding of these new intersection points, it should be clear as to which components of 2-handle are creating the intersection points.

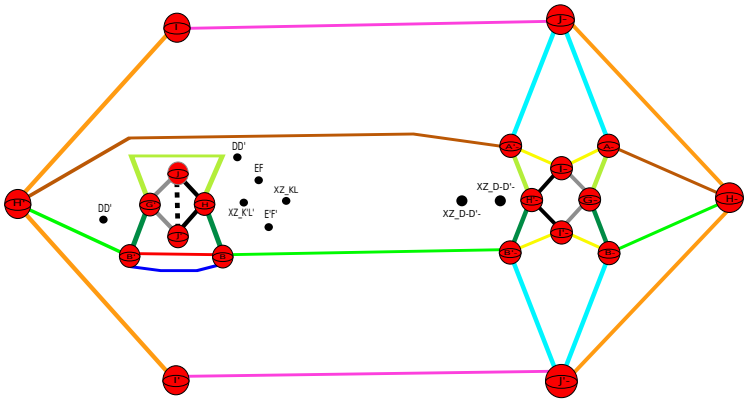

There were also points of intersection in the y-z plane created by the brown 2-handle component running from C to D and C' to D'. These will change as follows:

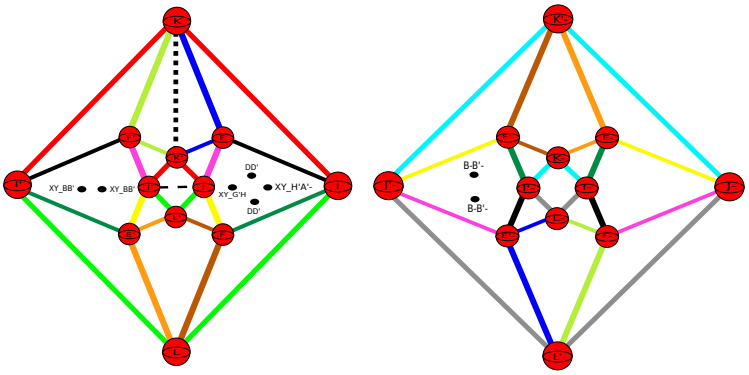

The next step we take is to cancel B, B' with the red 2-handle in the x-y plane. This cancellation will affect the x-y plane and the diagram corresponding to the twelve 2-handles that did not all lie in a single plane.

The following picture shows how the x-y plane changes after this cancellation has been carried out. The reader should observe that when we perform this cancellation using the red 2-handle, the blue 2-handle component slides to a zero framed unknot hence cancels a 3-handle and can be deleted from the diagram.

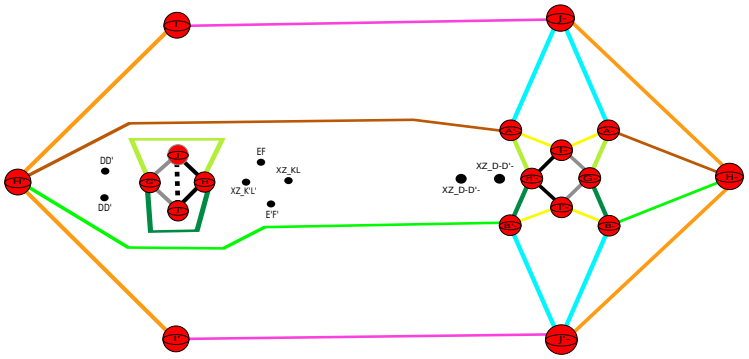

The following picture shows how the diagram corresponding to the twelve 2-handles that did not all lie in a single plane changes.

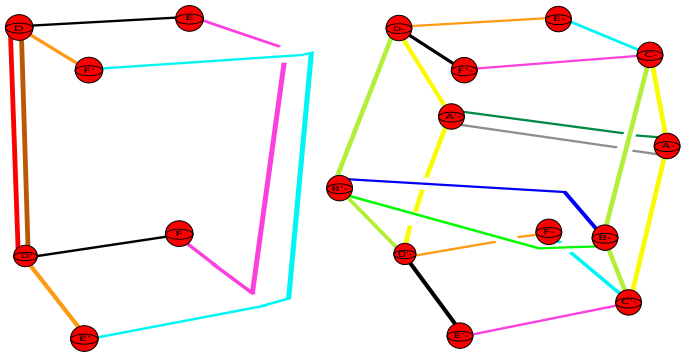

The astute reader would have noticed that in the picture above showing the x-y plane, the intersection point labelled **DD'** has moved from the right to the left. This is because when we

cancelled B, B' in the diagram corresponding to the twelve 2-handles that did not all lie in a single plane we also moved the brown 2-handle into the position shown above. As this brown 2-handle was intersecting the x-y plane, this intersection point must also move.

Finally, we note that the red 2-handle used to carry out the above cancellation intersected the y-z plane, hence we will get some new points of intersection in this plane. Furthermore, the moving of the brown 2-handle we did above will cause the two intersection points in the y-z plane labelled **DD'** to disappear.

The following picture shows the structure of the y-z plane after all the above has been carried out.

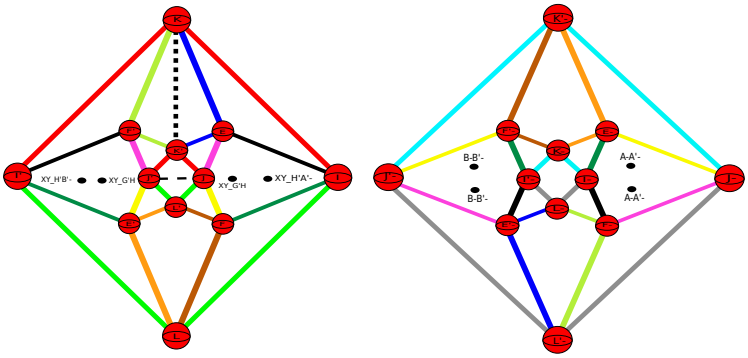

We can then cancel $B-, B'-$ with the blue 2-handle in the diagram corresponding to the twelve 2-handles that did not all lie in a single plane. The diagram changes as follows.

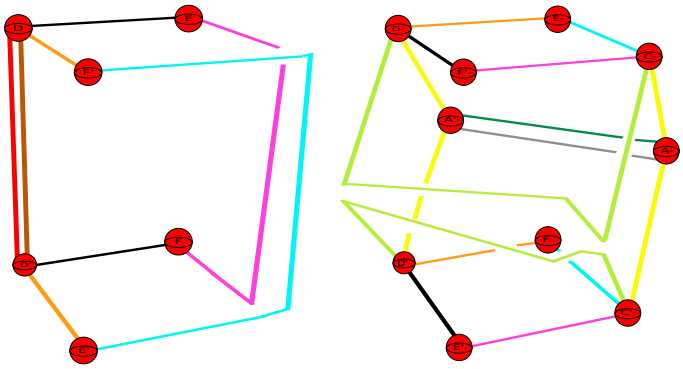

Note that the green 2-handle component that originally ran from $B-$ to $B'-$ slides to a zero framed unknot and can be immediately deleted from the diagram.

The cancellation also affects the x-y plane, which changes to the following.

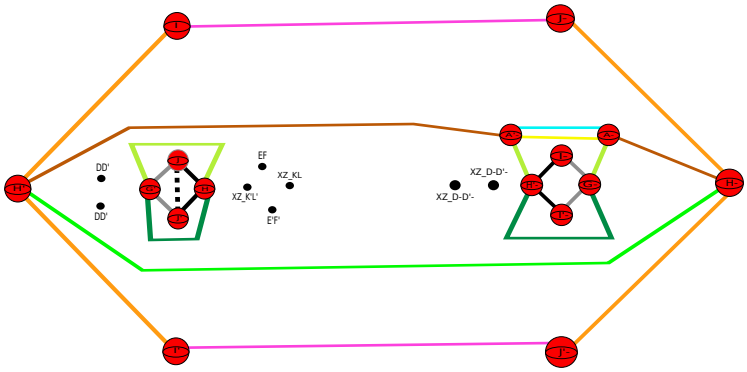

The blue 2-handle used to carry out the cancellation intersected the y-z plane, it is clear that the intersection points in the y-z plane change in the following way:

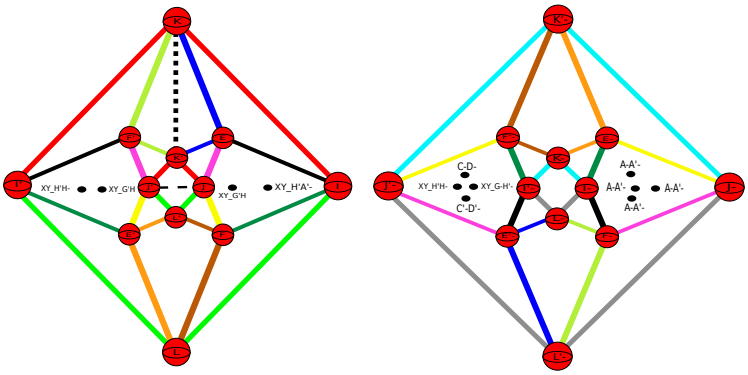

So far we have carried out five different handle cancellation moves. The following pictures collect together how the various diagrams have changed so far. The first picture shows the x-y and x-z planes respectively, and the second shows the y-z plane and the diagram corresponding to the twelve 2-handles that did not all lie in a single plane.

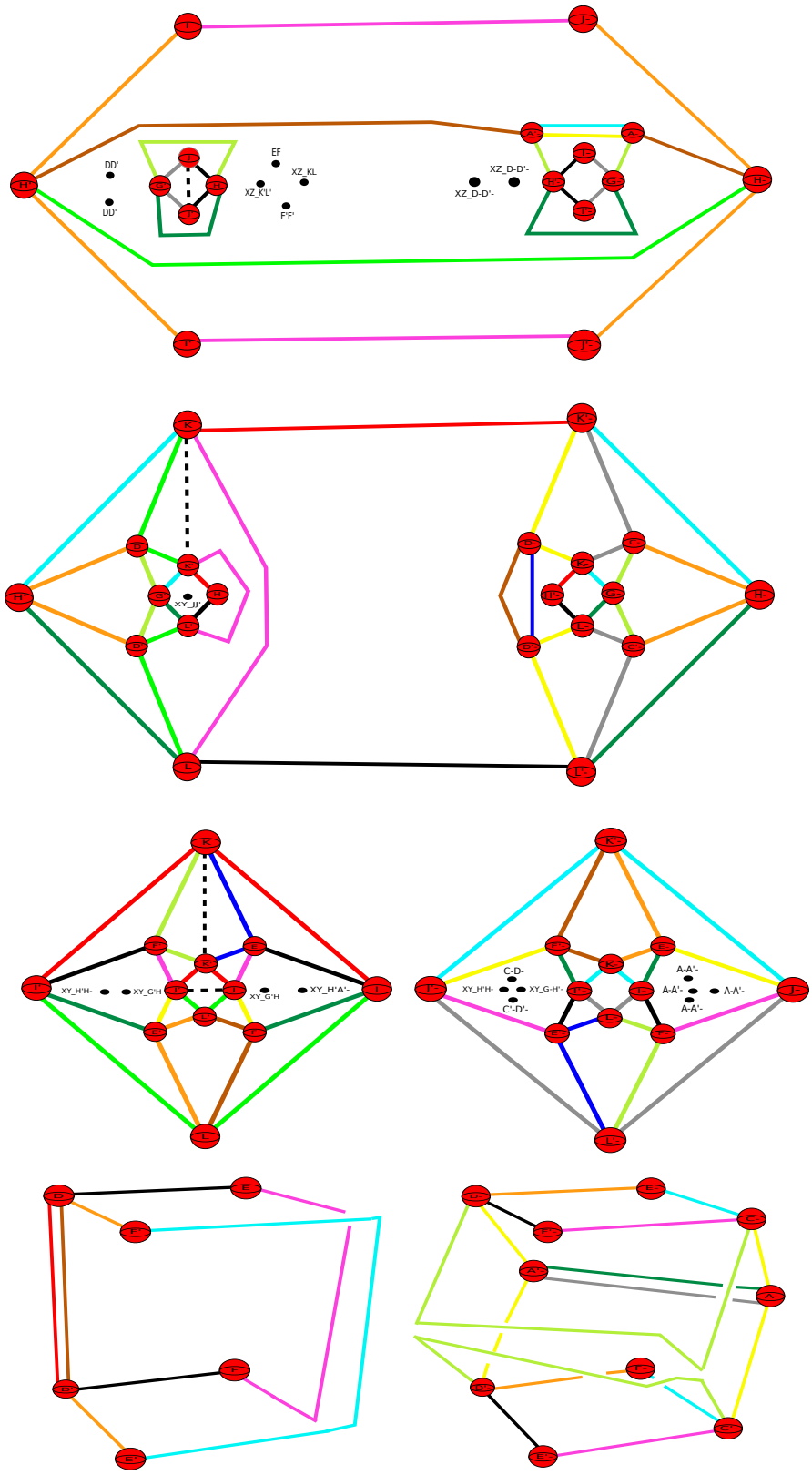

We move on to cancelling the 1-handle $A-, A'-$ using the yellow 2-handle in the x-y plane. This cancellation affects the x-y plane and the diagram corresponding to the twelve 2-handles

that did not all lie in a single plane.

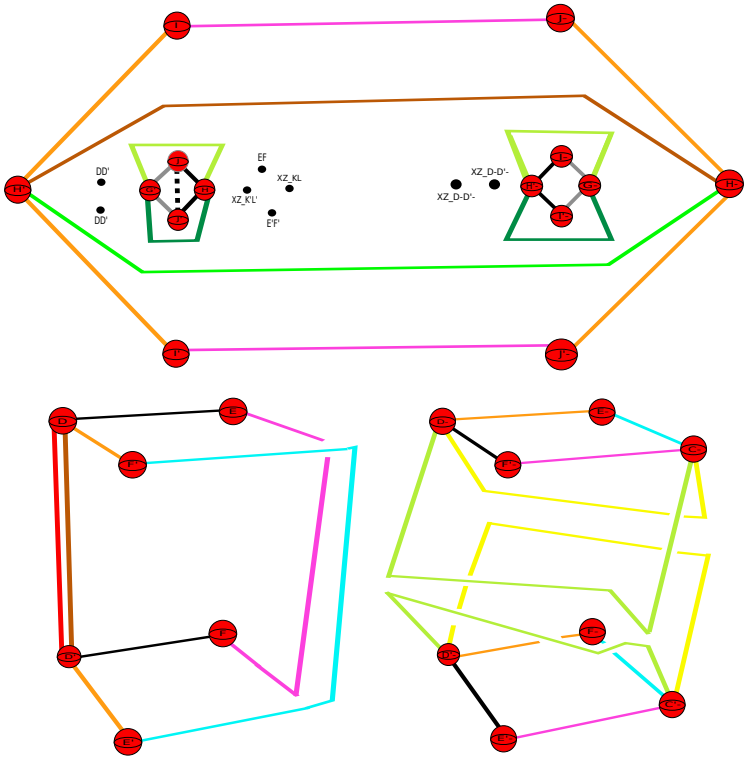

The intersection points in the y-z plane change as follows.

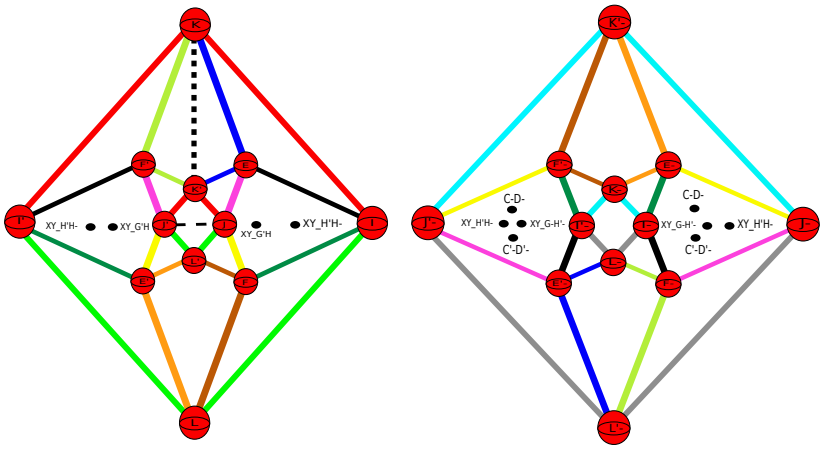

We can then cancel D, D' using the brown 2-handle in the diagram corresponding to the twelve 2-handles that did not all lie in a single plane. The result of this cancellation can be seen in the following picture.

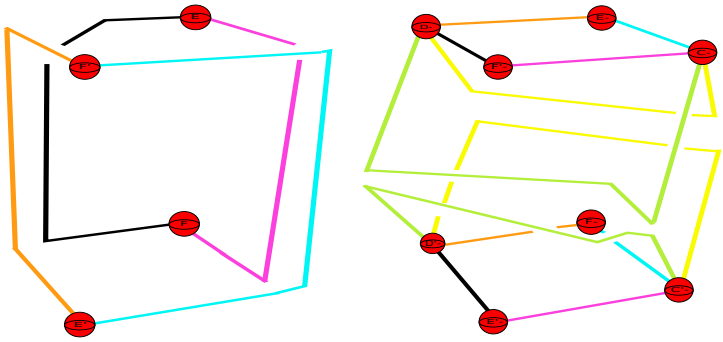

The cancellation also affects the x-z plane, which changes in the following way.

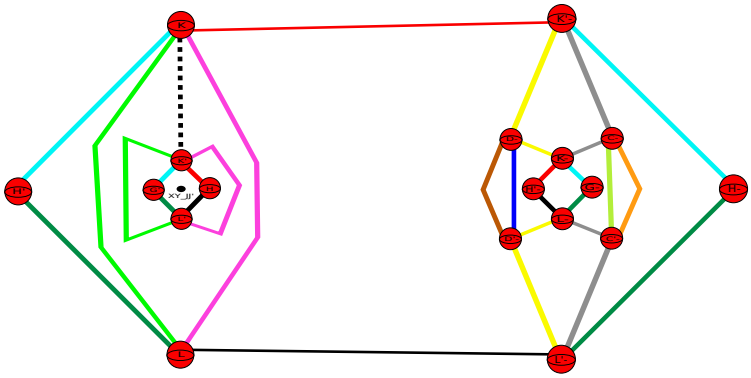

The intersection points in the x-y plane change in the following way.

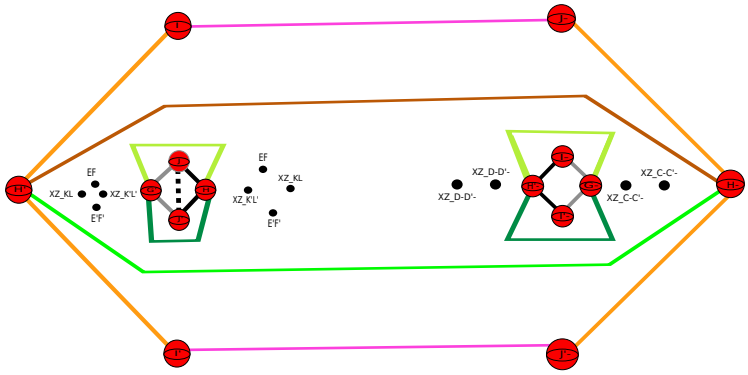

In the x-z plane we have the blue 2-handle that runs over $D-, D'-$ once, these then form a handle cancellation pair. Carrying out this cancellation, the x-z plane changes to:

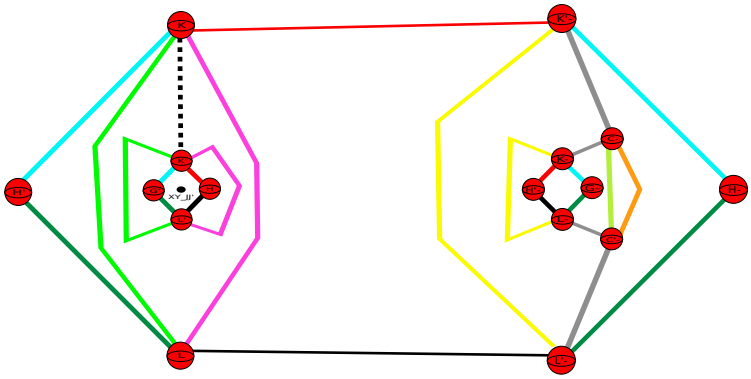

The diagram corresponding to the twelve 2-handles that did not all lie in a single plane will also be affected by this cancellation and change in the following way.

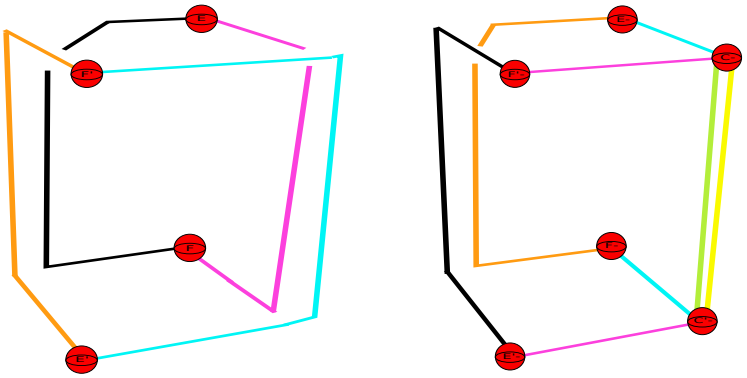

The intersection points labelled **C-D-** and **C'-D'-** will disappear from the y-z plane, no new intersection points will appear.

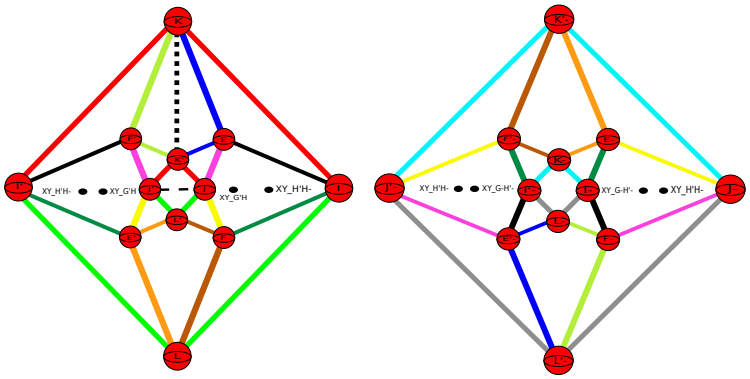

As for the x-y plane, we have that the intersection points labelled **XZ_D-D'-** will disappear but some new ones corresponding to the yellow 2-handles in the x-z plane, running from $K-$ to $L-$ and from $K'-$ to $L'-$, will appear. We will also see intersection points created by the two 2-handles running between $C-$ and $C'-$ in the diagram corresponding to the twelve 2-handles that did not all lie in a single plane.

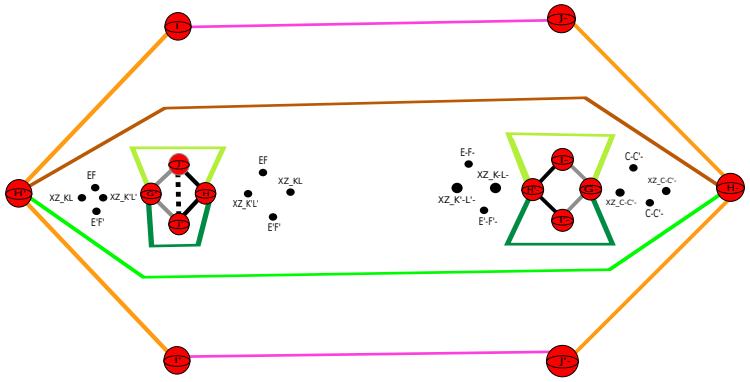

We can then cancel $C-, C'-$ with the light green 2-handle in the x-z plane that runs over it once. Note that when we carry out this cancellation a few 2-handles can be immediately deleted from our diagrams. Namely, the orange 2-handle in the x-z plane will slide to give a zero framed

unknot, and so will the light green and yellow 2-handles in the diagram corresponding to the twelve 2-handles that did not all lie in a single plane. These then each cancel a 3-handle and hence can be deleted from our diagrams.

The following picture shows how the x-z plane changes after this cancellation has been carried out.

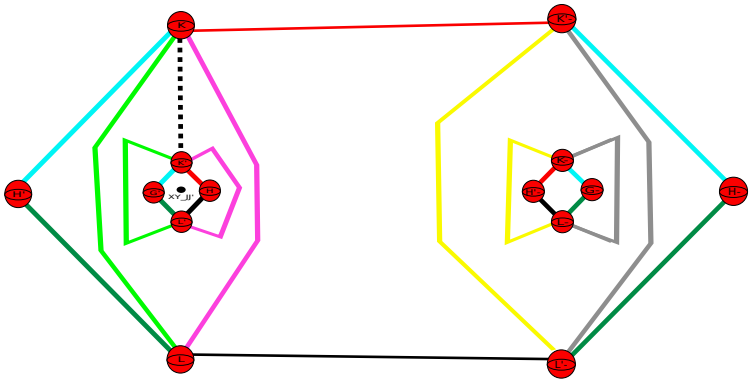

The diagram corresponding to the twelve 2-handles that did not all lie in a single plane changes in the following way.

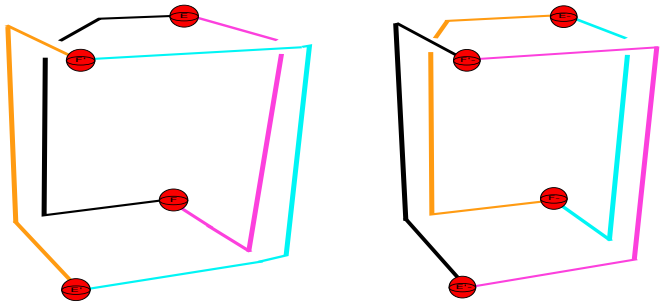

The intersection points labelled **XZ_C-C'-** and **C-C'-** in the x-y plane will disappear. The following picture shows the coding of the new ones that come into place.

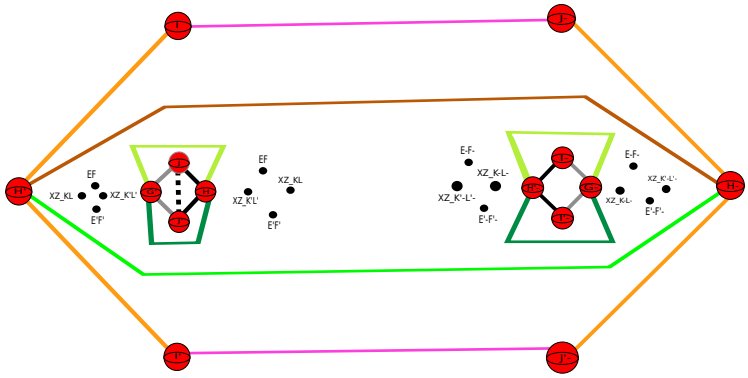

We move on to cancelling J, J' with the dashed black 2-handle that resides in the x-y and y-z planes. The x-y plane changes in the following way.

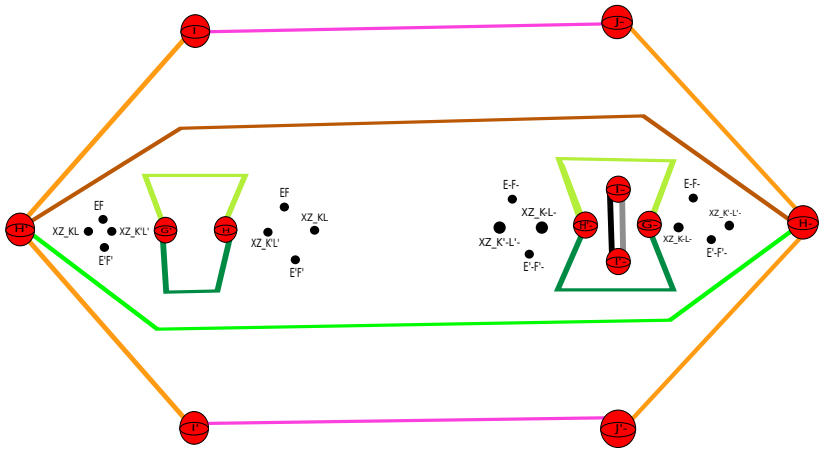

The reader should be aware that when we cancel J, J' with the dashed black 2-handle we obtain grey and black 2-handle components that loop back into G' and H. We can then push these through the pieces of 1-handles they loop back into and then do a handle slide to obtain grey and black 2-handles that run over $I-, I'-$ once, which can be seen in the above picture.

The y-z plane changes in the following way.

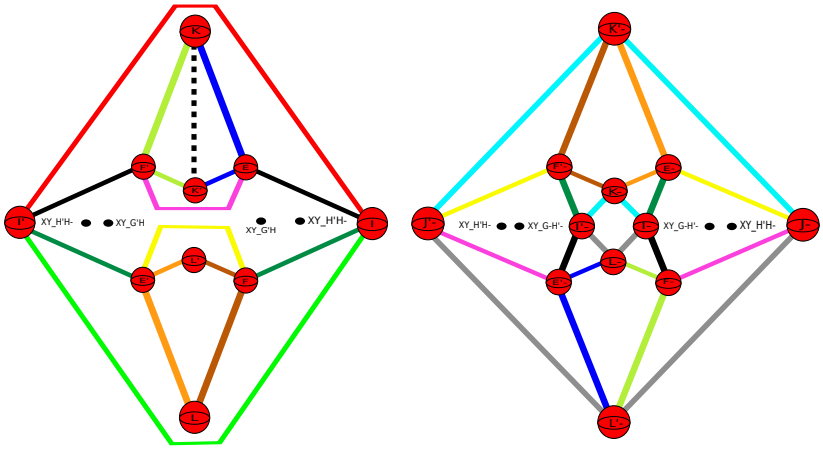

The reader should be aware that, as in the case of the x-y plane, we have carried out some handle slides as well. Namely, the cancellation creates a red 2-handle that loops back into K' and a green 2-handle that loops back into L', we can then slide these into the positions shown. The dashed black 2-handle that we used to cancel J, J' intersected the x-z plane, hence the cancellation will add some new points of intersection with the x-z plane. The following two diagrams show these new intersection points with the second one being a close up showing the coding of the intersection points in the middle of the diagram.

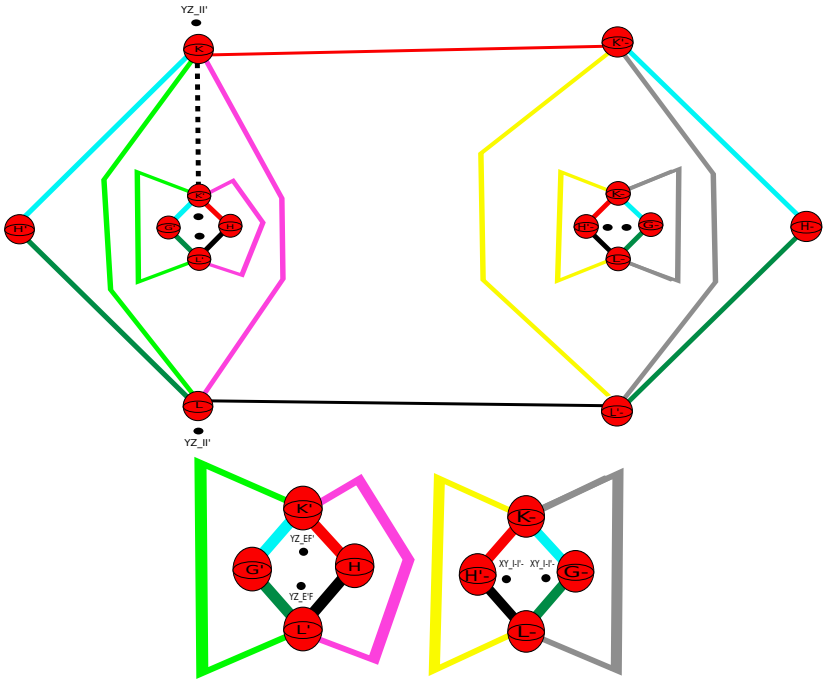

At this point we stop and collect together pictures of the four diagrams so far. This first picture shows the structure of the x-y and x-z planes, and the second picture shows the structure of the y-z plane and the 2-handles remaining in the diagram corresponding to the twelve 2-handles that did not all lie in a single plane.

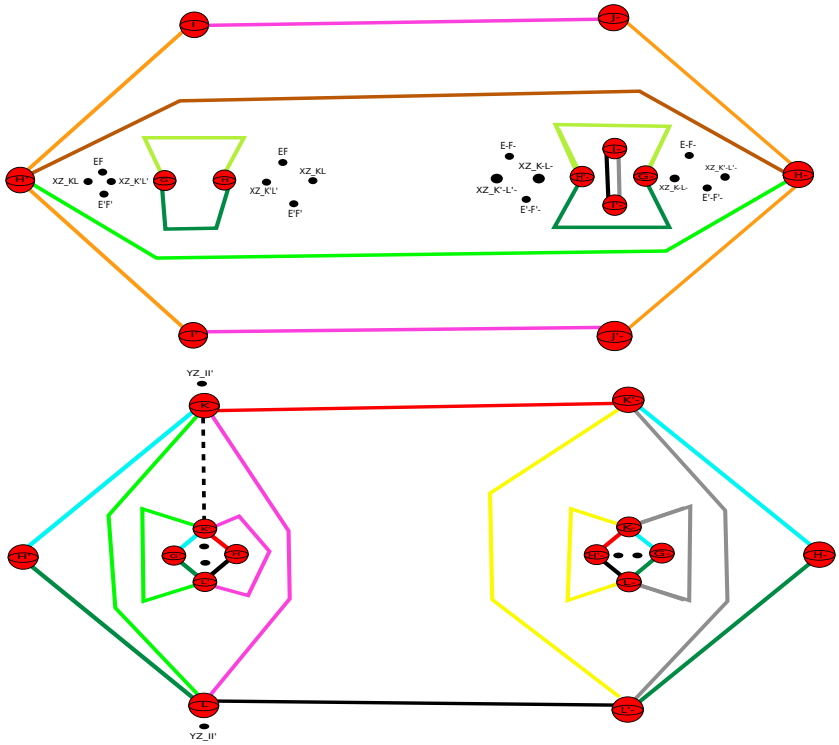

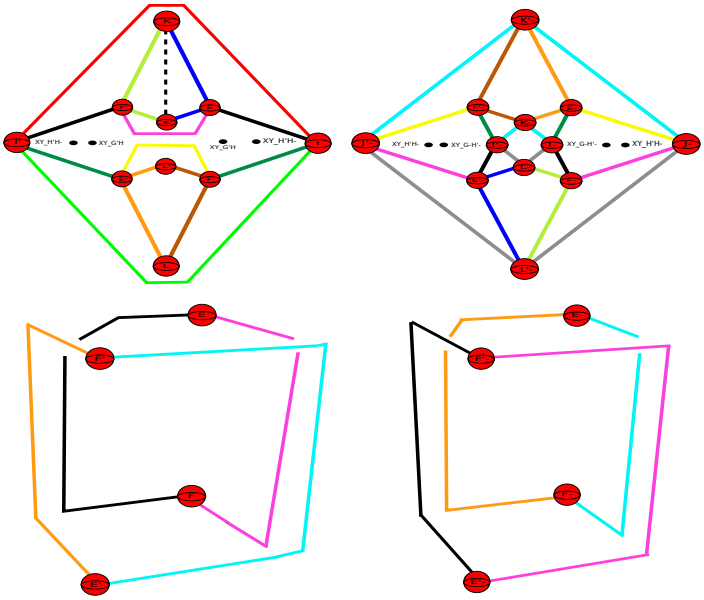

The next handle cancellation we carry out is to cancel K, K' with the black dashed 2-handle that sits in the x-z and y-z planes.

The following pictures shows how the x-z and y-z planes change respectively.

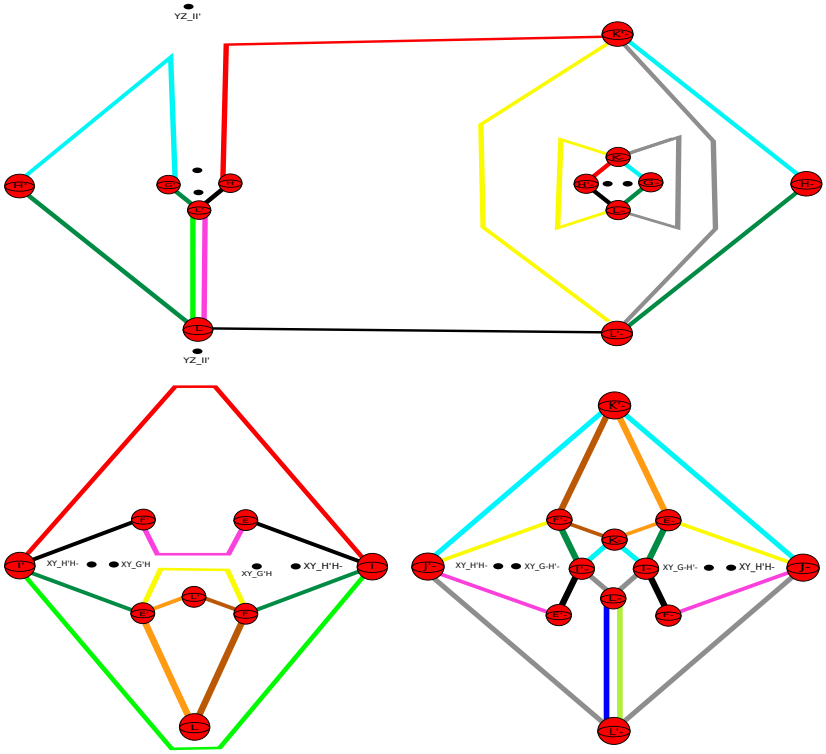

The dashed black 2-handle that was used to cancel K, K' did not intersect the x-y plane, hence on the level of intersection points the x-y plane does not change.

We can also cancel L, L' with the green 2-handle that runs over it once in the x-z plane. This cancellation will only affect the x-z and y-z planes. As the 2-handle we are using to perform

the cancellation does not intersect the x-y plane we find that the intersection points of the x-y plane remain the same.

The following pictures show how these diagrams look like after the cancellation has taken place.

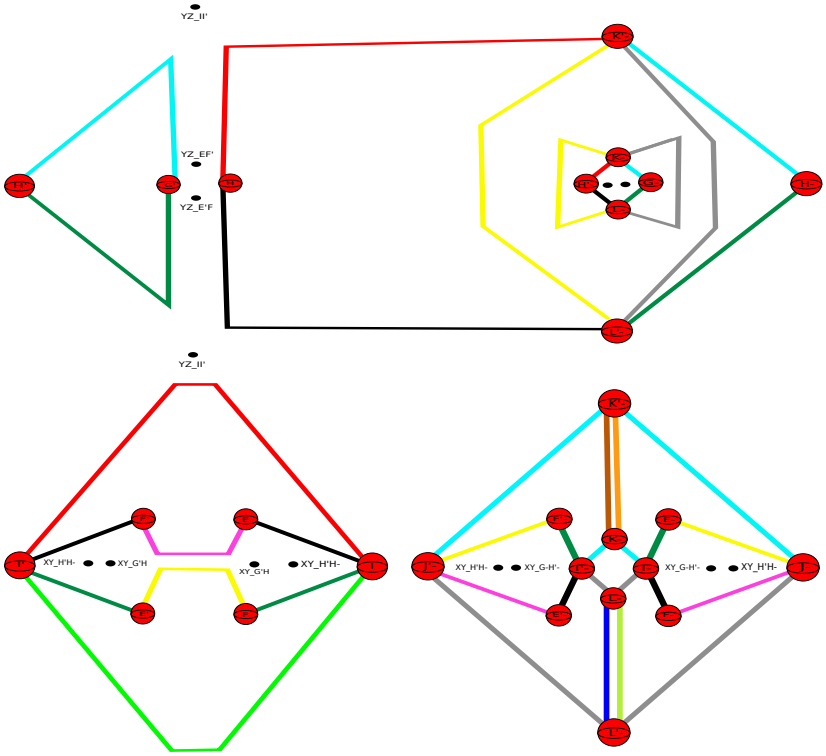

The reader should note that we have also carried out some handle slides. After performing the above cancellation we get an orange 2-handle component in the y-z plane that loops back into E', and a brown 2-handle component (in the y-z plane as well) that loops back into F. We can then perform a handle slide on both these components to obtain orange and brown 2-handles, in the y-z plane, that run over $K-, K'-$ once.

We can use either of these 2-handles to perform a cancellation with $K-, K'-$, again this will only affect the x-z and y-z planes. The following two pictures show how these planes change.

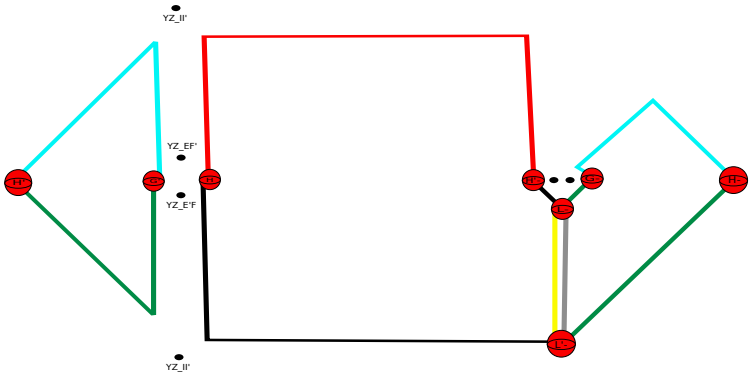

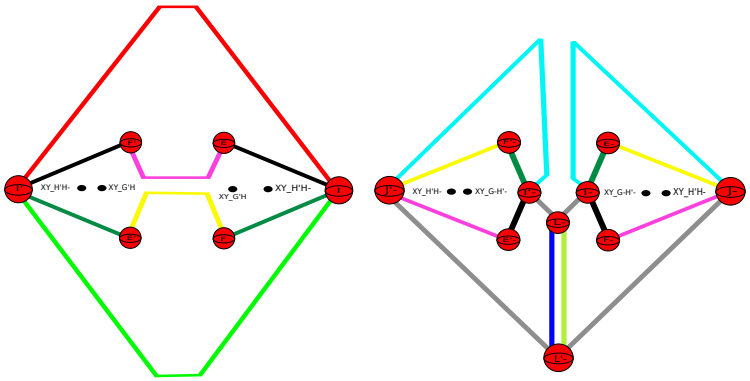

We can also cancel $L-, L'-$ with the blue 2-handle in the y-z plane, this cancellation only affects the x-z and y-z planes.

The x-z plane changes to the following diagram.

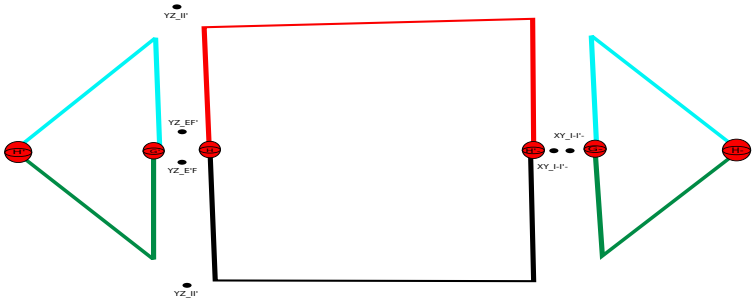

The y-z plane changes to the following diagram.

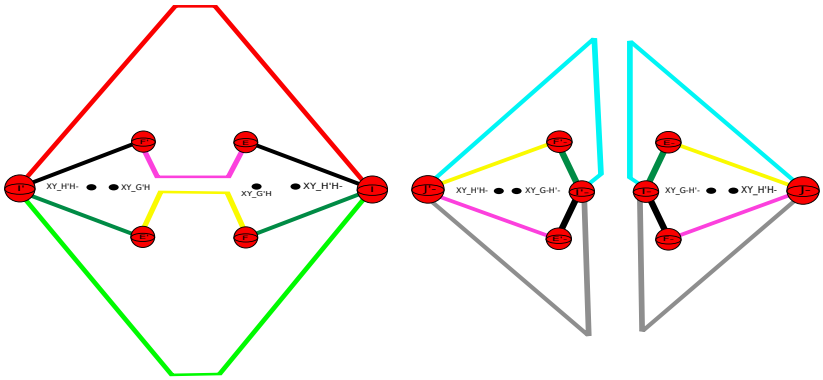

This cancellation does not affect the points of intersection in the x-y plane as the 2-handle we used in the cancellation did not intersect the x-y plane.

The next cancellation we undertake is to cancel $I-, I'-$ with the black 2-handle in the x-y plane. This cancellation only affects the 2-handles in the x-y and y-z plane.

The x-y plane changes to the following diagram:

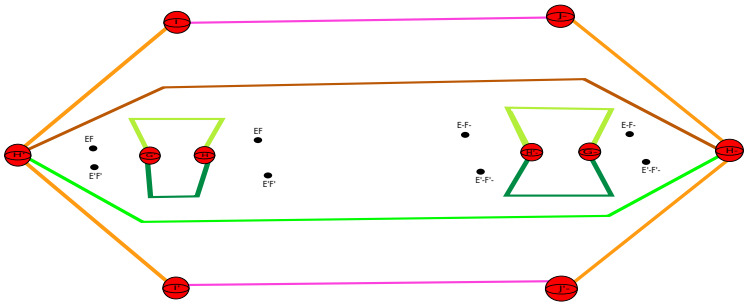

The y-z plane changes in the following way:

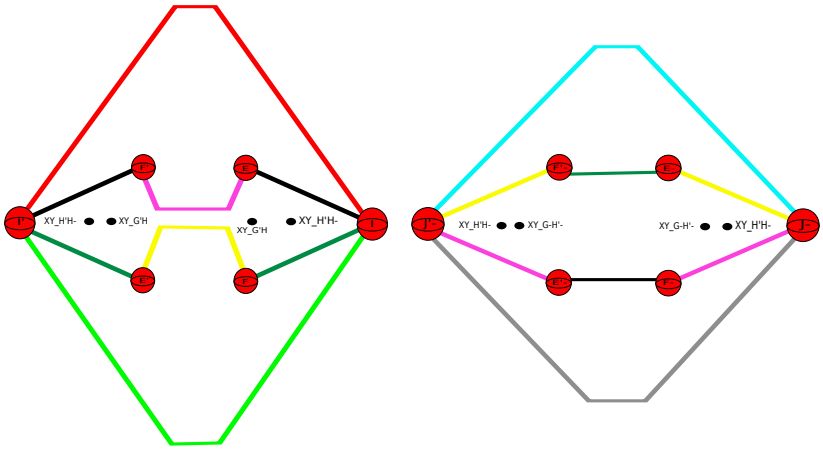

The black 2-handle used to carry out this cancellation intersected the x-z plane, the code was **XY_I-I'-**, therefore after the cancellation this intersection point disappears. However, many new intersection points arise from 2-handle components in the y-z plane. The following picture shows the coding of these new intersection points.

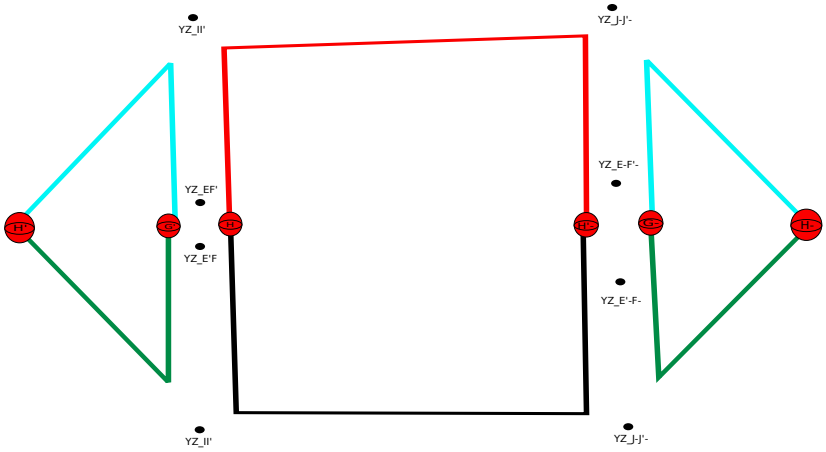

We have carried out a further five handle cancellations. This is a good point to stop and take stock of how our four different diagrams, showing the structure of all the 2-handles, look like.

The following picture shows the structure of the x-y and x-z planes respectively after all the above cancellations have been carried out.

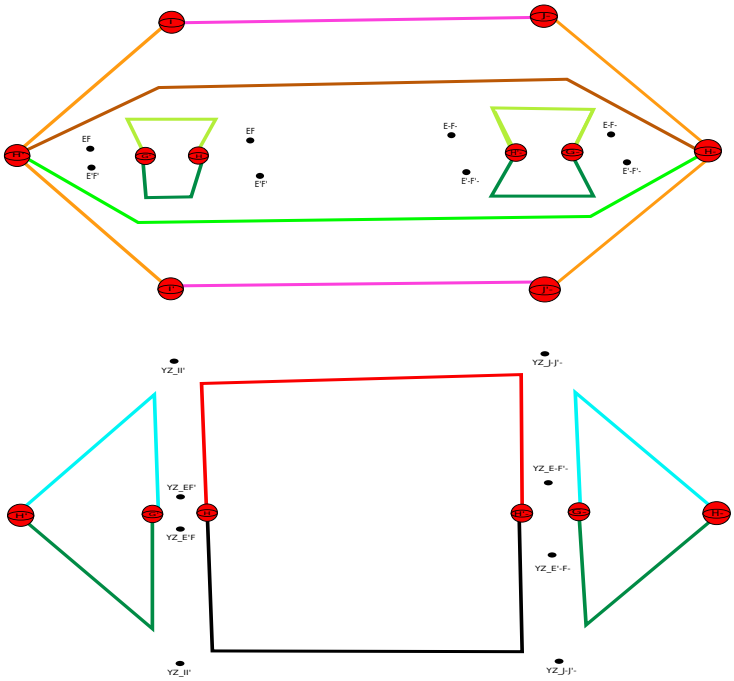

The following picture shows the structure of the y-z plane and the structure of the diagram corresponding to the twelve 2-handles that did not all lie in a single plane after all the above cancellations have been carried out.

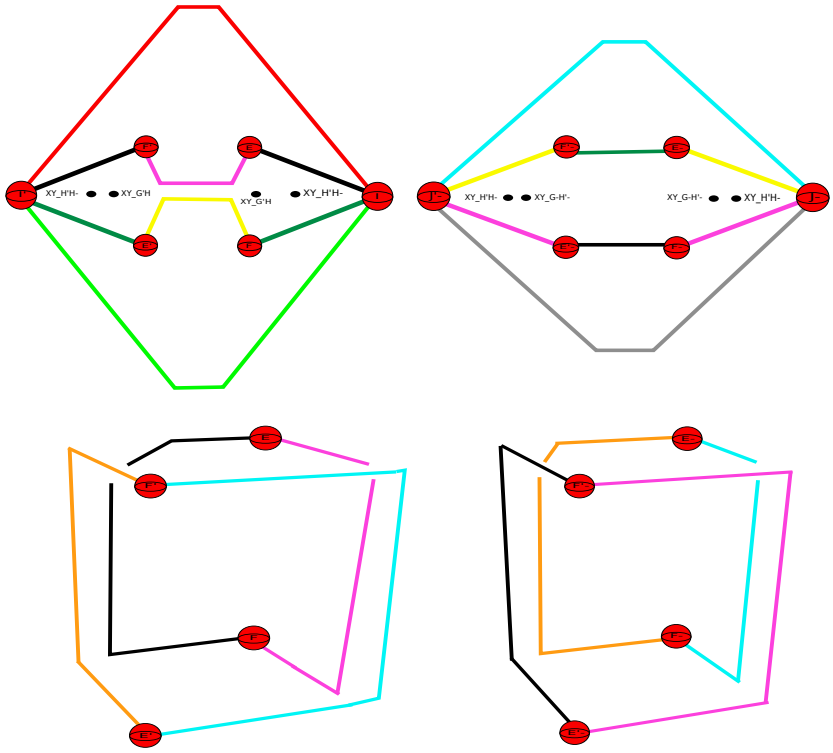

We remind the reader that all throughout the above cancellations there was a 2-handle that we were not showing in our diagrams. Namely, the 2-handle corresponding to the translation $e^{-1}heh^{-1}$. Recall that this 2-handle had four components running from E to H, $H'-$ to $E-$,

E' to H' and $H-$ to $E'-$. So far, the cancellations we have carried out have all been within the three planes, the x-y, x-z, y-z planes, or the diagram showing the twelve 2-handles not all lying in a single plane. The components of the 2-handle $e^{-1}heh^{-1}$ each pass between the y-z and x-y planes and so are not affected by any of the cancellations that are carried within the x-y, x-z or y-z planes. As for cancellations done within in the diagram corresponding to the twelve 2-handles that did not all lie in a single plane, two components, namely the ones running from E to H and $H'-$ to $E-$, are contained in the "inside" of the diagram, and it is easy to see that the cancellations we have carried out so far have not in any way interfered with these two components. As for the two components running from E' to H' and $H-$ to $E'-$, these run on the "outside" of the diagram, hence it is clear that the cancellations we have done so far have not interfered with these two components.

The next cancellation we are going to carry out is to cancel I, I' using the red 2-handle that resides in the y-z plane. This cancellation will affect the 2-handles in the y-z and x-y planes.

The y-z plane changes to the following diagram.

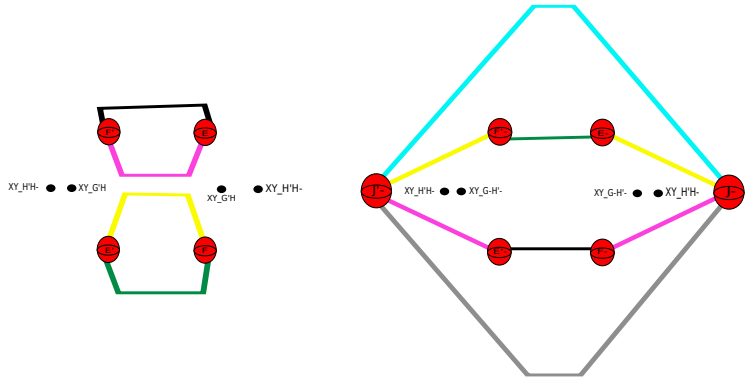

The x-y plane changes in the following way.

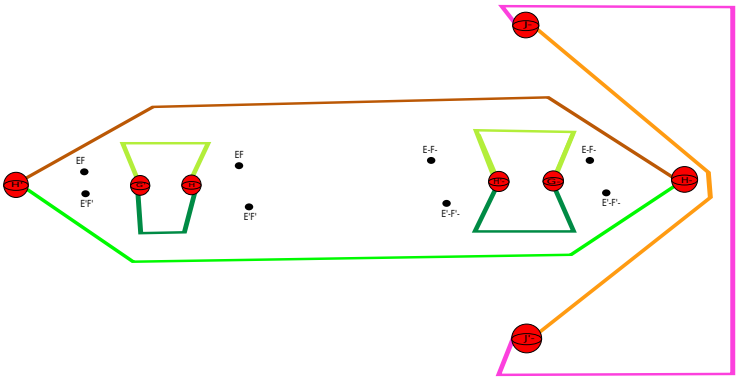

The 2-handle used to carry out the above cancellation intersected the x-z plane, the following diagram shows how the intersection points in the x-z plane change.

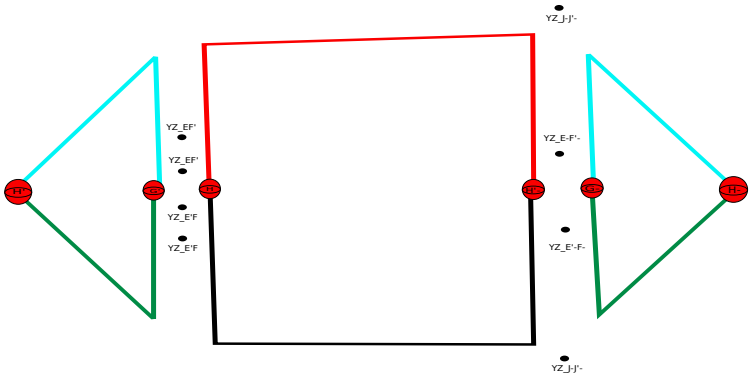

We move on to cancelling $J-, J'-$ with the orange 2-handle in the x-y plane, this cancellation only affects the 2-handles in the x-y and y-z planes.

The x-y plane changes in the following way

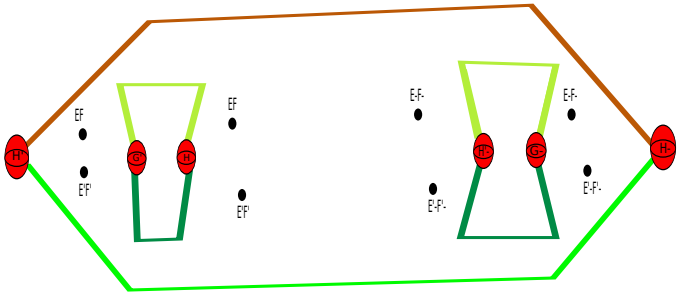

and the y-z plane changes to the following diagram.

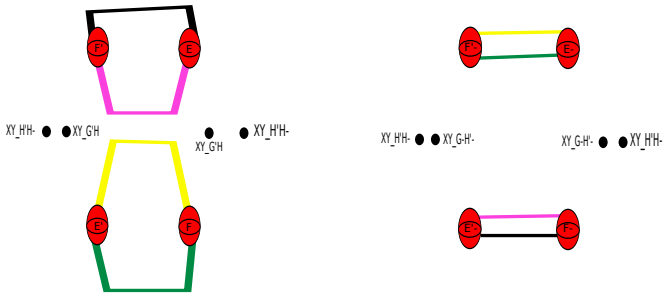

The orange 2-handle used in this cancellation intersected the x-z plane. The intersection points in the x-z plane changes to the following.

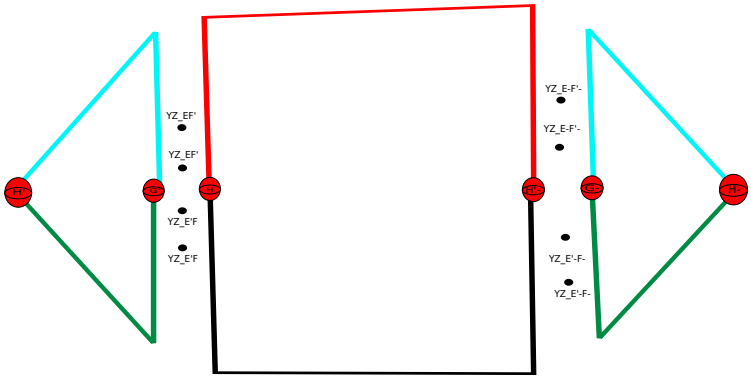

So far, the last few cancellations we have carried out have not interfered with the 2-handles that are left in the diagram corresponding to the twelve 2-handles that did not all lie in a single plane. We want to perform an isotopy of the 2-handles in this diagram.

The first picture shows the original position the 2-handles were in, and the picture following it shows the final position after we carry out the isotopy. It should be clear to the reader how the 2-handles move during this isotopy.

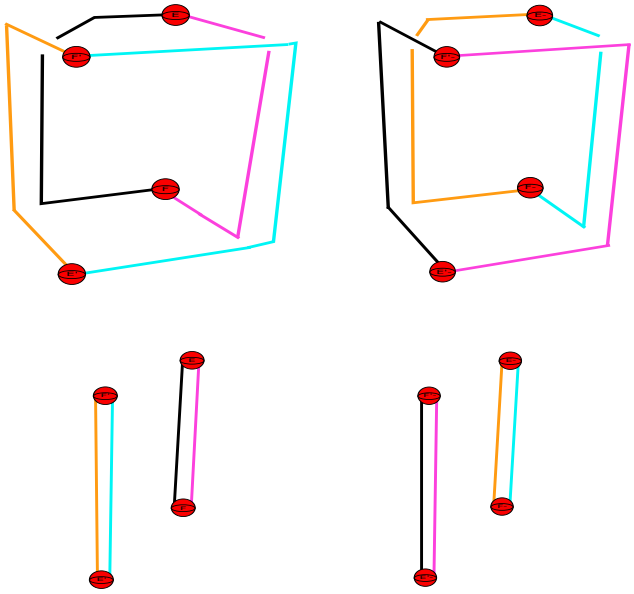

The next cancellation we are going to undertake is to cancel $H, H'-$ using the red 2-handle in the x-z plane. This cancellation affects the 2-handles in the x-z and x-y planes. It also affects the 2-handle corresponding to the translation $e^{-1}heh^{-1}$ that we have not been drawing so far.

We start with the x-z plane, the following picture shows how the x-z plane changes after we have carried out this cancellation.

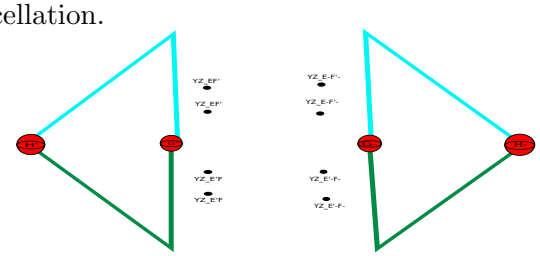

The x-y plane changes in the following way:

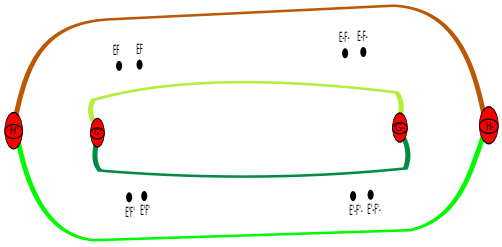

Recall that the 2-handle corresponding to the translation $e^{-1}heh^{-1}$ had in total four components, two of them in particular were such that one ran from E to H and another from $E-$ to $H'-$. When we perform the above cancellation these two components come together, giving one component running from E to $E-$.

The following picture shows how this new component runs between E and $E-$.

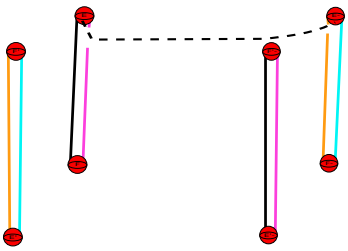

The cancellation carried out above causes the intersection points in the y-z plane to change. The following picture shows the y-z plane with these new intersection points.

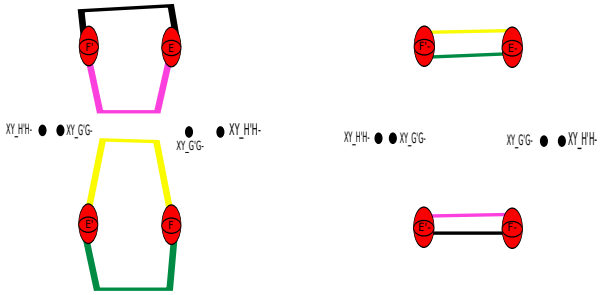

We can then cancel $H', H-$ with the green 2-handle in the x-y plane. This cancellation affects the 2-handles in the x-y plane and the x-z plane.

The x-y plane changes as follows.

The x-z plane changes to the following.

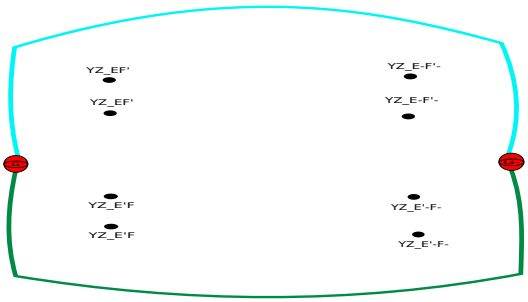

The translation $e^{-1}heh^{-1}$ that has been reduced to consisting of one component running from E to $E-$, another running from E' to H', and another running from $E'-$ to $H-$. When we cancel $H', H-$ with the green 2-handle in the x-y plane the components running from E' to H' and $E'-$ to $H-$ slide to form one component joining E' to $E'-$.

The following picture shows how this new component runs between E' and $E'-$.

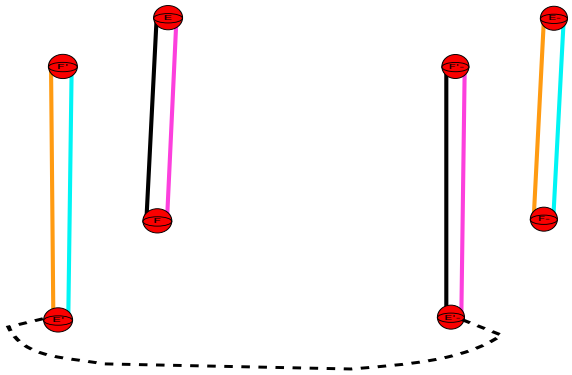

We now have two separate diagrams, the one coming from the x-y and x-z planes that involve 2-handles running over $G', G-$, and the 2-handles left in the diagram corresponding to the twelve 2-handles that did not all lie in a single plane, and the 2-handles in the y-z plane, which run over the 1-handles $E, E'-$, $E', E-$, $F, F'-$ and $F', F-$. It is easy to see that these two diagrams do not interact with each other in any way. Furthermore, the 2-handles that run over $G', G-$ (the ones coming from the x-y and x-z planes) do so once. Hence we can use any one of them to form a cancelling pair with $G', G-$. Carrying out this cancellation, all other 2-handles running over $G', G-$ slide to form zero framed unknot's, hence cancel with a 3-handle and can be deleted from the diagram. Thus we are left with the 2-handles running over the 1-handles $E, E'-$, $E', E-$, $F, F'-$ and $F', F-$.

We can then cancel $F', F-$ with the black 2-handle in the y-z plane. This will cause the pink 2-handle in the y-z plane to slide and have two components, one looping back into E and the other looping back into $E'-$. We can then slide one of these components through to obtain a zero framed unknot that cancels a 3-handle. Hence this 2-handle can be deleted from the diagram.

We can also cancel $F, F'-$ using the dark green 2-handle in the y-z plane. This cancellation causes the yellow 2-handle in the y-z plane to slide into a position where it has one component looping back into E' and another looping back into $E-$. We can then perform a handle slide to obtain a yellow coloured zero framed unknot. This then cancels with a 3-handle and can be deleted from the diagram.

The two cancellations we have just carried out also affect the other 2-handles, they reside in

the diagram corresponding to the twelve 2-handles that did not all lie in a single plane. It is straightforward to see how they change, the following diagram shows the position they slide into.

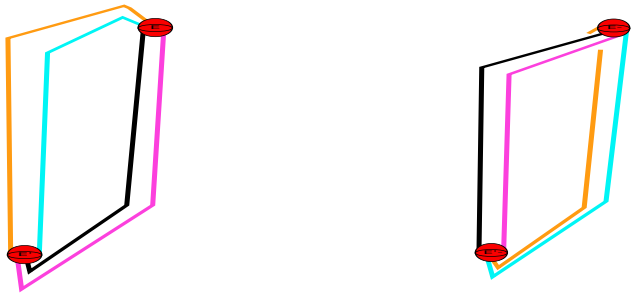

We also have an extra 2-handle that we have not shown in the above, it is the 2-handle that corresponded to the translation $e^{-1}heh^{-1}$. It has two components, one that runs from E to $E-$ and another that runs from E' to $E'-$. The following picture adds this 2-handle to the above diagram.

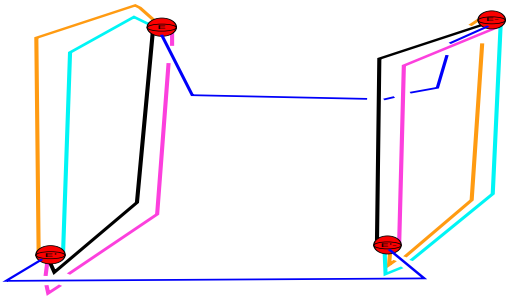

We can now carry out some handle slides. We can slide the orange 2-handle along the turquoise 2-handle to obtain the following diagram.

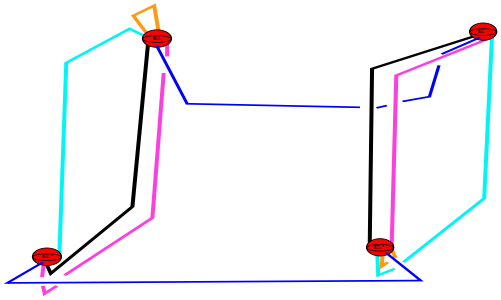

We then slide the pink 2-handle along the black 2-handle to obtain the following diagram.

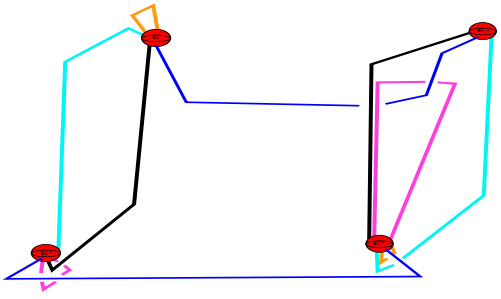

We can then slide the orange 2-handle to a zero framed unknot, which will then cancel a 3-handle. Therefore we can simply delete the orange 2-handle from our diagram. This gives us the following diagram.

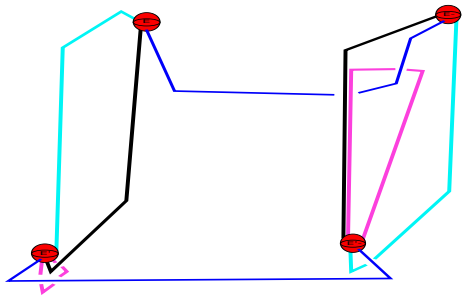

We can then slide the pink 2-handle into the following position.

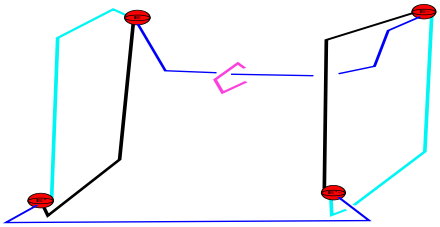

We can also slide the turquoise 2-handle along the black 2-handle to obtain the following diagram.

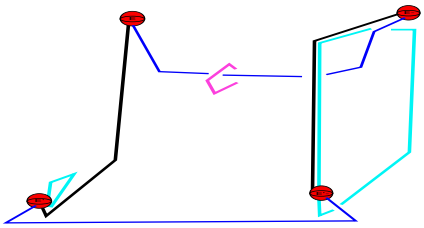

Then another handle slide produces:

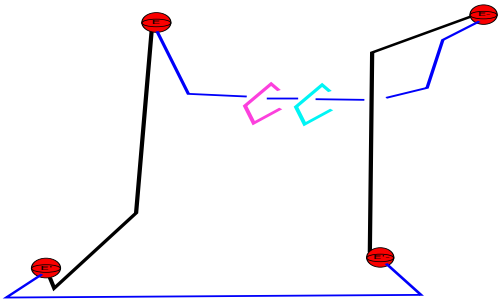

We can then cancel the 1-handle $E', E-$ with the black 2-handle producing the following diagram.

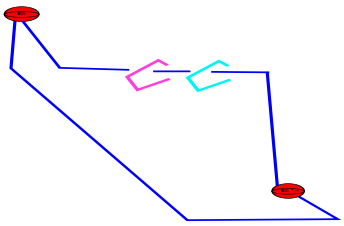

This is a Kirby diagram for the orientable manifold $\widetilde{M}$, which recall is the orientable double cover of M (manifold 35). Furthermore, it is clear that $\pi_1(\widetilde{M}) = \langle x \mid x^2 = 1 \rangle \cong \mathbb{Z}_2$. We want to take the double cover of this manifold, which we denoted by $\widetilde{M}_2$. Recall the procedure to do this, the one skeleton of $\widetilde{M}$ consists of $D^4 \cup (E, E'-)$ (the 0-handle union the 1-handle), which is a copy of $S^1 \times D^3$. The one skeleton of $\widetilde{M}_2$ will also consist of a copy of $S^1 \times D^3$ double covering the one skeleton of $\widetilde{M}$ in the usual way that $S^1 \times D^3$ double covers itself. Each of the remaining handles of $\widetilde{M}$ lift to two handles of $\widetilde{M}_2$. This means that the blue 2-handle in the above diagram, that passes over $E, E'-$ twice, will lift to two 2-handles each passing over the unique 1-handle in $\widetilde{M}_2$. The turquoise and pink 2-handles that loop around one component of the blue 2-handle in the above diagram, lift to two copies of each looping around one lift of the blue 2-handle. The following diagram shows how the Kirby diagram of the double cover, $\widetilde{M}_2$, looks like.

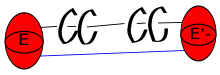

We can then cancel $E, E'-$ with the blue 2-handle, this will cause the diagram to change to.

We can then slide three of the linked circles over the fourth one so that each one gives a zero framed unknot. These each cancel with a 3-handle and we are left with the following diagram.

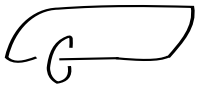

The diagram shows two zero framed linked 2-handles, which is precisely the Kirby diagram for $S^2 \times S^2$. Thus we can conclude that the simply connected closed 4-manifold $\widetilde{M}_2$, which is a four fold cover of M (manifold 35), is diffeomorphic to $S^2 \times S^2$. We have thus proved the following theorem:

Theorem 3.3.1. *There exists a collection L of ten linked tori embedded in a standard smooth $(S^2 \times S^2)$ such that the complement $(S^2 \times S^2) - L$ admits a finite volume hyperbolic geometry.*

Chapter 4

Topological link complements via spin structures

In this chapter we take up the problem of trying to identify the homeomorphism type of various fillings of the Ratcliffe-Tschantz manifolds. The problem is made drastically simpler through the use of a beautiful classification theorem of M. Freedman and S. Donaldson on the homeomorphism types of smooth, closed, simply connected 4-manifolds. Furthermore, another key ingredient is an understanding of which fillings admit a spin structure.

4.1 Spin structures

In this section we take up the problem of how trying to understand whether a Ratcliffe-Tschantz manifold and a filling of such a manifold can admit a spin structure. We explain how to understand such a structure through the use of a Kirby diagram and give explicit examples of manifolds that are spin. We then use these examples to construct topological hyperbolic link complements in $\#_3(S^2 \times S^2)$ and $S^2 \times S^2$.

Let E be a real vector bundle over a 4-manifold M, which we assume from here on in is orientable. We also assume that the fibres of E have dimension $m \geq 3$, this will always be the case of interest for us, in the general case one can sum with a trivial bundle to obtain this condition. To construct a *spin structure*, we begin with a trivialisation of $E|_{M_1}$, where M_1 denotes the 1-skeleton of M. We wish to extend this trivialisation τ over each 2-handle h of M. The 2-handle h is a copy of $D^2 \times D^2$, which being contractible implies $E|_h$ is trivial, so τ over the attaching circle determines an element of $\pi_1(SO(m)) \cong \mathbb{Z}_2$ (as we are assuming $m \geq 3$). It is then clear that τ extends over h if and only if this element in $\mathbb{Z}_2$ vanishes. Applying this to each 2-handle h of M, we obtain an element of $\mathbb{Z}_2$ assigned to each 2-handle. In other words, using the handle complex, we obtain a cochain $c(\tau) \in C^2(M; \mathbb{Z}_2)$. One can then prove that if we were to take another trivialisation τ_1 to start with, the cochains $c(\tau)$ and $c(\tau_1)$ will differ

by a coboundary, furthermore one can prove that for any trivialisation τ, $c(\tau)$ is closed. This implies we get a well-defined cohomology class denoted $w_2(E) = [c(\tau)] \in H^2(M; \mathbb{Z}_2)$. We can the conclude

Proposition 4.1.1. *An oriented vector bundle E over M admits a spin structure if and only if $w_2(E) = 0 \in H^2(M; \mathbb{Z}_2)$.*

The cohomology class $w_2(E)$ is known as the *second Stiefel-Whitney class* of E, the details of why $c(\tau)$ defines a cohomology class can be found in [8] p.180. Given an oriented 4-manifold M its tangent bundle is an oriented vector bundle over M of rank four. The second Stiefel-Whitney class of the tangent bundle associated to M will be denoted by $w_2(M)$.

Given a Kirby diagram of the oriented 4-manifold M the following proposition shows how we can compute the second Stiefel-Whitney class $w_2(M)$.

Proposition 4.1.2. *For an oriented manifold M given by a Kirby diagram, $w_2(M) \in H^2(M; \mathbb{Z}_2)$ is represented by the cocycle $c \in C^2(M; \mathbb{Z}_2)$ whose value on each 2-handle h is the framing coefficient of h modulo 2.*

The proof of this proposition can be found in [8] Proposition 5.7.1 and Corollary 5.7.3, p.185-186. There is a slight issue with the way we have stated this theorem. The problem is that a general Kirby diagram can have many 1-handles floating about (as is the case for us), and in these situations the concept of a framing as a unique integer is not a well-defined concept (we explained this at the end of chapter 1.). The theorem is normally stated with the idea that the Kirby diagram is given in *dotted circle notation*. The reader who is unfamiliar with the dotted circle notation can consult [8] chap.5.6, p.167. We will just mention that one way to think of how the dotted circle method comes in to play is to recall that we can cancel any 1-handle in a Kirby diagram by adding an appropriate 2-handle. Thus, adding a 1-handle to a Kirby diagram X is the same as removing the cancelling 2-handle. The point is that the cocore of the 2-handle corresponds to an unknotted 2-disk in X, obtained from a 2-disk in the boundary ∂X by pushing the interior of this 2-disk into the interior of X. In this way we can think of the addition of a 1-handle as being done by pushing the interior of a 2-disk, originally in ∂X, into the interior of X and then removing a tubular neighbourhood of the disk. This tubular neighbourhood is drawn as a circle decorated with a dot, hence the name the dotted circle notation. Using this viewpoint of a 1-handle one can transfer a usual Kirby diagram in to dotted circle notation. On the level of the actual diagram one can think of the passage to dotted circle notation as being carried out by choosing a collection of reference arcs, one for each pair of 1-handles running between the attaching spheres of the 1-handle, then taking a dotted meridian to each such reference arc and collapsing the associated 1-handle via the reference arc. This will cause the 2-handles running between the 1-handles to then run through the associated dotted

meridian parallel to the choice of reference arc (see [8] p.169). The problem here is that there is no canonical way to do this transformation, one has to make a choice of how the 1-handles are going to come together to form dotted circles i.e. one has to make a choice of reference arc. (see [8] p.169 for an example of this choice). Once one fixes a choice of such reference arcs, then in dotted circle notation all the 2-handles are knots in 3-space. They then have a notion of a framing integer (or as it is sometimes called framing coefficient). In general, the choices made in passing to dotted circle notation affect the framing of the associated 2-handles. In our case all the 2-handles have a planar framing, due to this it turns out that in many cases one can, in a straightforward manner, choose a system of reference arcs that will produce a Kirby diagram in dotted circle notation with every 2-handle knot having an even framing coefficient.

We will now go through an example of how one chooses a system of reference arcs and transforms a Kirby diagram associated to one of the Ratcliffe-Tschantz manifolds in to dotted circle notation. The example we are going to look at is the orientable double cover of manifold 1011. The construction of the Kirby diagram for the orientable double cover proceeds in exactly the same way as we did in chapter 3 when constructing the double cover of manifold 35, and the notation is exactly the same as used in that chapter. When we construct the orientable double cover we have to pick an orientation reversing element, the Kirby diagram then consists of reflecting everything through the 1-handle corresponding to this element. In this case we pick the side pairing g^{-1}, hence in our Kirby diagram everything needs to be reflected through the 1-handle component G. As G sits on the $x-y$ and $x-z$ plane we can think of this reflection as taking place in a plane parallel to the $y-z$ plane.

The following diagram shows that part of the Kirby diagram that lies in the $x-y$ plane.

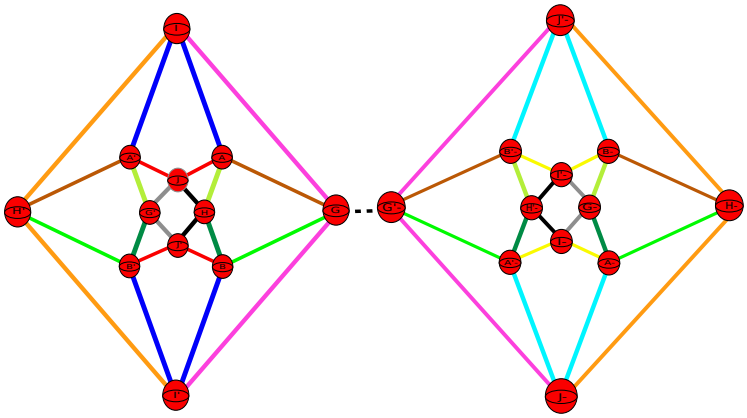

The following diagram shows that part of the Kirby diagram that lies in the $x-z$ plane.

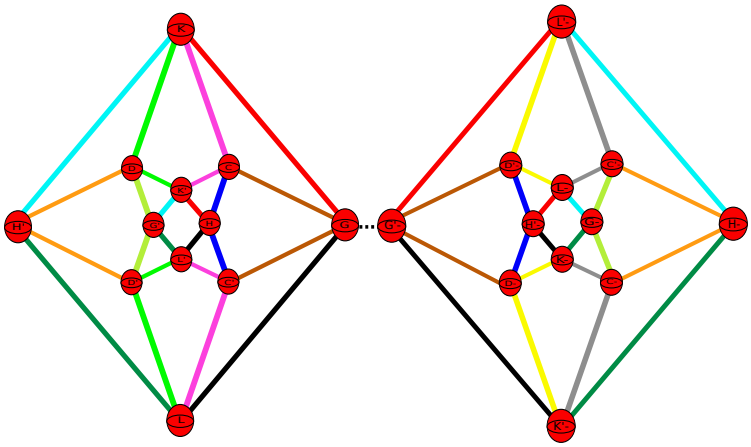

The following shows two diagrams, however in this case they both do not lie in the $y-z$ plane. The diagram on the left lies on the $y-z$ plane but the one on the right lies on a plane parallel to the $y-z$ plane (this is because we are reflecting across G).

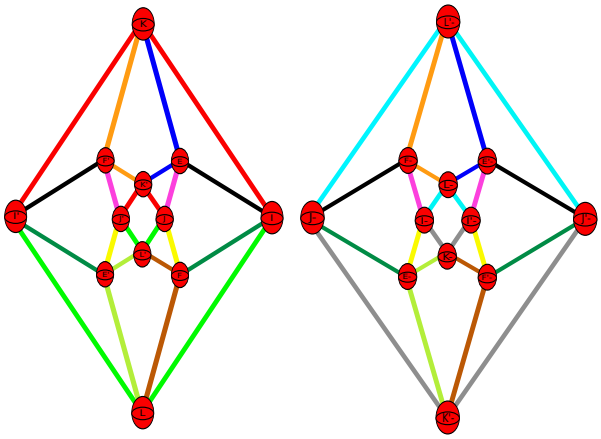

Finally, the following diagram shows those 2-handles that do not all lie in any one of the above planes, there are twelve such 2-handles in total.

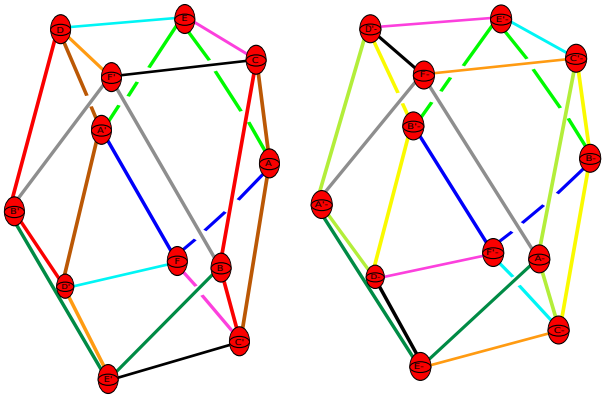

We want to show that we can pick a system of reference arcs for each 1-handle such that when we change to dotted circle notation the framing of each 2-handle will be congruent to zero

mod two. In order to do this we need a way to measure the framing from the diagram. A convenient choice to use is the **blackboard framing**, this involves projecting the knot onto a 2-plane giving a knot diagram. The framing coefficient is then computed as the signed number of self-crossings of the knot. Start with the $x-y$ plane, the following diagram shows a system of reference arcs for some of the 1-handles, they all lie in the x-y plane and have framing zero.

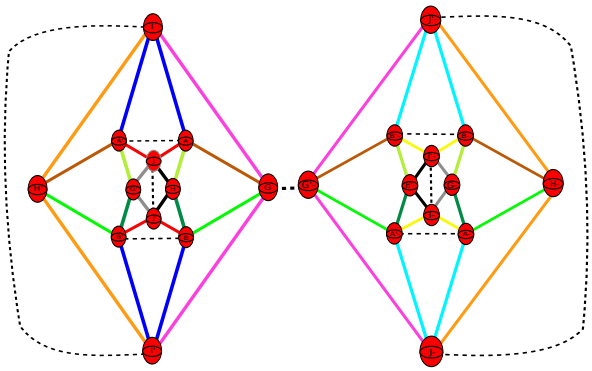

This leaves us with specifying reference arcs for the 1-handles $G, G'-$, $G', G-$, $H, H'-$ and $H', H-$. The reference arcs for some of these will have to leave the $x-y$ plane slightly as some other handles are in the way. The following diagram shows these reference arcs together with the ones shown above.

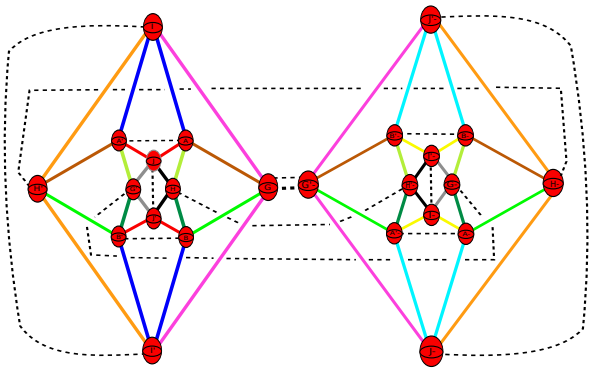

Once we have chosen a particular reference arc for a 1-handle in one diagram we have to use that same reference arc for any other diagram that the 1-handle resides in. For example since the 1-handles $G, G'-$, $G', G-$, $H, H'-$ and $H', H-$ also lie in the $x-z$ plane when we choose reference arcs for 1-handles in the $x-z$ plane we have to keep in mind that the reference arcs for $G, G'-$, $G', G-$, $H, H'-$ and $H', H-$ have already been chosen.

The following diagram shows the reference arcs for the 1-handles in the $x-z$ plane.

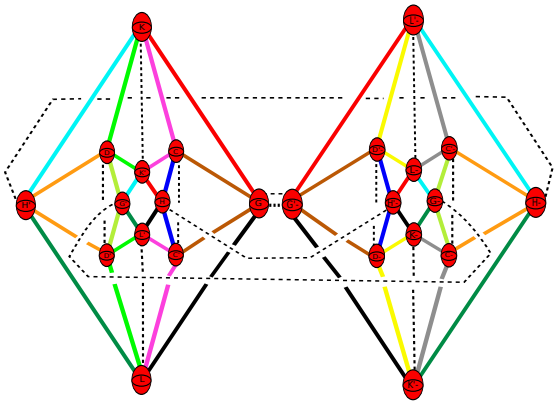

The arcs you see, in the above diagram, running between the 1-handles $G, G'-$, $G', G-$, $H, H'-$ and $H', H-$ represent projections, of the reference arcs chosen previously for these 1-handles, onto the $x - z$ plane. The next reference arcs we want to show are for those 1-handles in the diagram corresponding to the twelve 2-handles not all lying in a single 2-plane. To start with we show those reference arcs that have already been chosen when we considered the $x - y$ and $x - z$ planes.

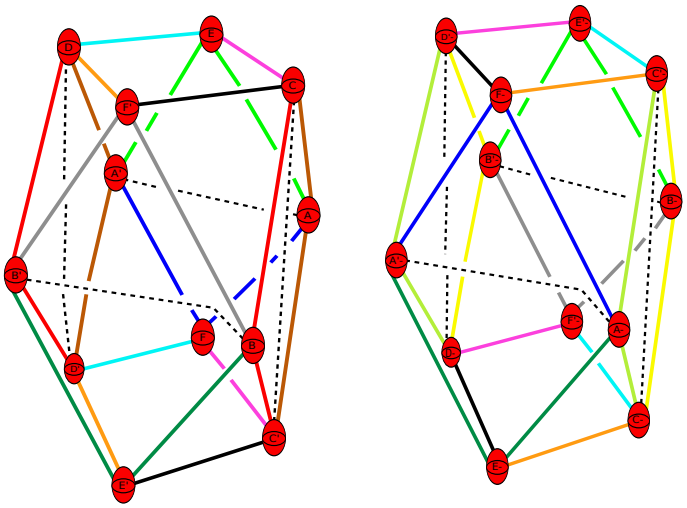

We are left with choosing arcs for $E, E'-$, $E', E-$, $F, F'-$ and $F', F-$. For the 1-handles $E, E'-$ and $F, F'-$ we choose horizontal arcs that run behind the diagram as the following shows.

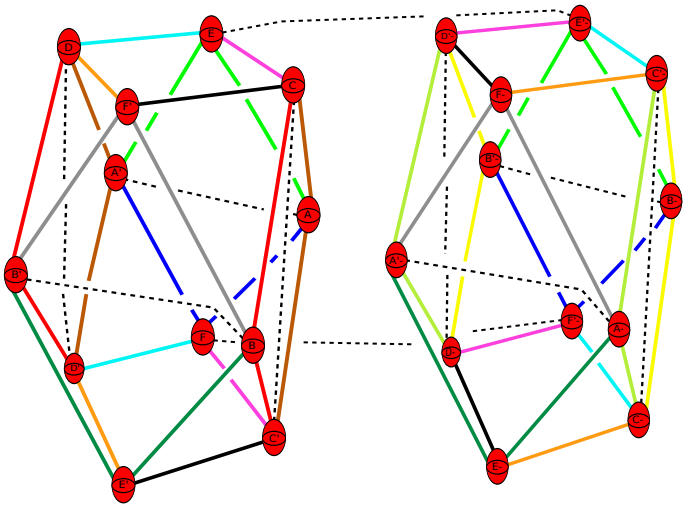

For the 1-handles $E', E-$ and $F', F-$ we choose horizontal arcs running in the front as the following shows.

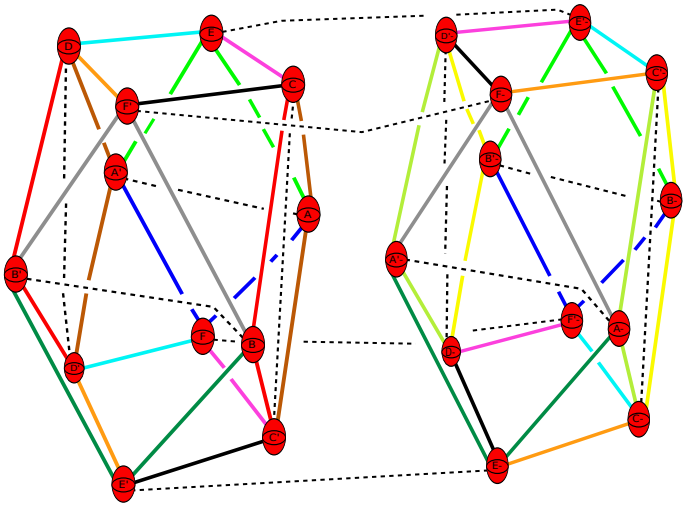

The final case to consider is the diagram that shows the $y-z$ plane and the plane parallel to the $y-z$ plane. For this diagram we choose the following arcs.

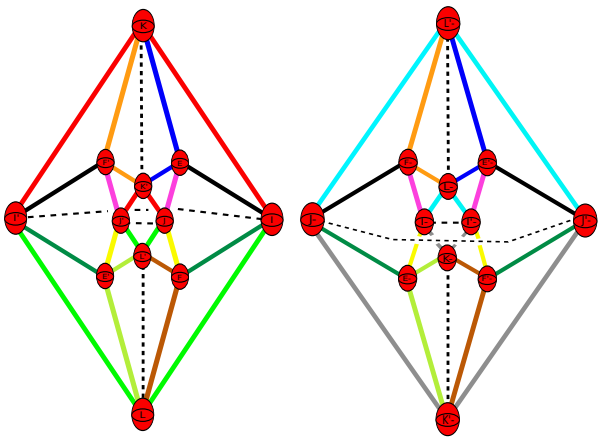

We have not shown how the arcs running between the 1-handles $E, E'-$, $E', E-$, $F, F'-$ and $F', F-$ look like from this plane. From our choice above it should be clear to the reader that they run horizontally outside the diagram.

We claim that with this system of zero framed reference arcs when we pass to dotted circle notation each 2-handle will have even framing. This is not too hard to see, one needs to take each 2-handle separately and then see what happens when we collapse a 1-handle it goes over using the reference arc for that 1-handle. Let us give a few examples.

Start with the 2-handles in the $x - y$ plane, look at the pink 2-handle in that plane. When we use our system of reference arcs to collapse the 1-handles it goes over we get that the pink 2-handle transforms to the following.

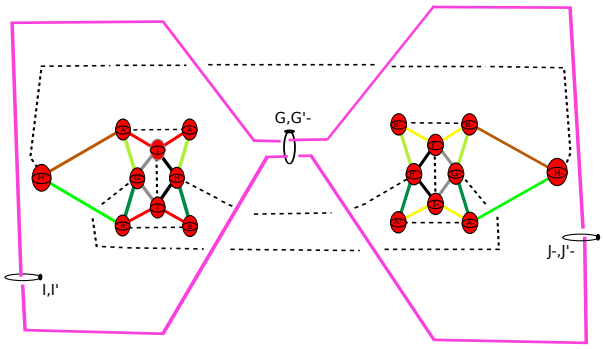

As we are only interested in framings of each 2-handle and not how they link with the other 2-handles we have thrown away some 2-handles so that the reader can easily see how the pink 2-handle will look like in dotted circle notation. It should be clear to the reader that the pink 2-handle transforms to a knot with zero framing (remember we are using the blackboard framing).

The green 2-handle also transforms in a similar way, the following diagram shows how it looks

like. The reader should notice that the framing is again zero.

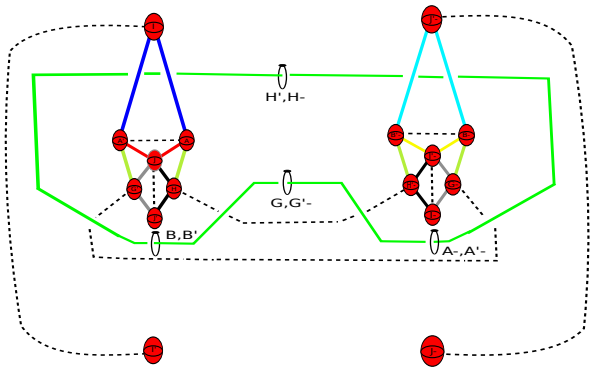

The following diagram shows how the red and blue 2-handles transform. It should be clear that the framing is zero for both of them.

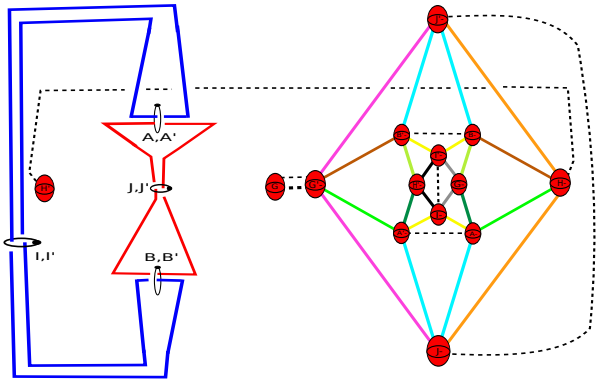

One can continue in this fashion checking each 2-handle, in this case one finds that all the 2-handles will have framing zero. The point is that since these 2-handles are all confined in a 2-plane one can easily find a system of reference arcs so that in dotted circle notation these 2-handles will have even framing. A computation similar to the above works for the $x-z$ plane as well, we leave the details to the reader. We want to move on to considering the diagram showing the twelve 2-handles that did not all lie in a single 2-plane.

The following diagram shows how the green 2-handle in that diagram transforms.

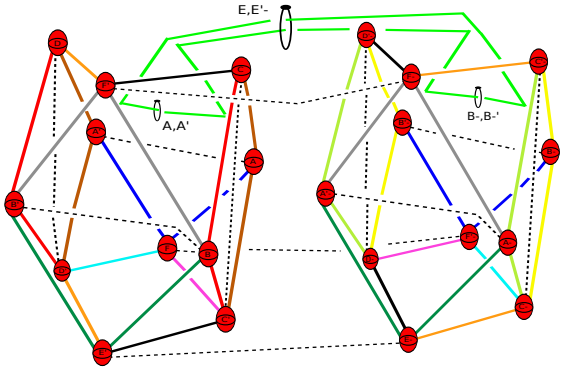

It is easy to see that the framing is again zero. So far all the 2-handles we have shown have had framing zero simply because when they transform they don't cross over themselves. It can happen that a 2-handle transforms to something that has self crossings. However, it is always the case that the number of self crossings is even, this means that the blackboard framing will always be congruent to zero mod two.

The following diagram shows how the black 2-handle transforms.

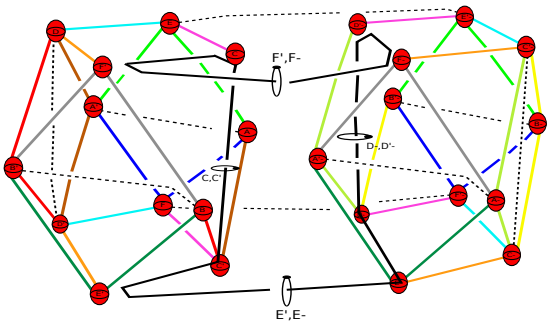

In this case you can see two self crossings, and if we were to project this to the plane then we would have framing zero (as we count the crossings with sign). Each of the other 2-handles in this diagram transform in a similar way. It is also the case that for the 2-handles in the diagram showing the $y-z$ plane and the plane parallel to the $y-z$ plane that when we transform to dotted circle notation, using the reference arcs we have chosen above, we always get 2-handles with an even number of self crossings, hence their framing must always be even. As the details are exactly analogous to what we have shown above we will not bother with the details.

In summary we have chosen a system of zero framed reference arcs that when used to transform the Kirby diagram in to dotted circle notation we obtain 2-handles all with an even framing. In particular, by proposition 4.1.2 we see that the double cover of manifold 1011 must be spin.

We would also like to mention that one can use the above system of reference arcs to show that a filling of a boundary component of manifold 1011 (which remember is a 3-torus) must also be spin. The way to do this is to first recall that we already identified translations corresponding to an S^1-fibre of each cusp of manifold 1011. They were given by the side pairing transformations c, a, j, k, $e^{-1}g$ (see chapter 2), a filling of anyone of these cusps corresponded to adding a 2-handle that ran between the 1-handles corresponding to the side pairing transformation. For example if we wanted to fill in the cusp who has an S^1-fibre corresponding to a on the level of our Kirby diagram we had to add a 2-handle running from A to A'. It is easy to check that, with respect to the system of reference arcs, such a 2-handle will have zero framing when we change to dotted circle notation. This same argument works for fillings of the other four cusps.

In general one finds that this procedure works for many of the Ratcliffe-Tschantz manifolds and can be used to show that many of them or their orientable double covers are spin. Also, by understanding the cusp structures one can show that many fillings of such manifolds are spin. The advantage of knowing that a particular manifold is spin is that it allows you to construct explicit hyperbolic complements up to homeomorphism as the next section shows.

4.2 Hyperbolic link complements with topological type $\#_{2k}(S^2 \times S^2)$

This section is devoted to constructing a hyperbolic link complement in a manifold that is homeomorphic to $(S^2 \times S^2)\#(S^2 \times S^2)$. The main idea is to construct a certain finite cover of manifold 1011 with the right Euler characteristic and then take a filling of this cover, using the fact that the double cover of manifold 1011 is spin we will be able to deduce that the filling must be homeomorphic to $(S^2 \times S^2)\#(S^2 \times S^2)$.

From here on in we will denote manifold 1011 by M, and its orientable double cover by N.

Recall that M had five cusps and the translations we chose to construct a filling of M were given by c, a, k, j, $e^{-1}g$. When we construct a filling on the level of the fundamental group what we were doing is adding the relations $c = a = k = j = e^{-1}g = 1$. If instead we add a power of one of the translations, then we can construct new fillings. For example instead of taking c we could take c^n for some $n > 1$. This is still a translation and so we can try and analyse what happens if we fill along this translation. On the level of the fundamental group what we are doing is adding the relations $c^n = a = k = j = e^{-1}g = 1$. Using some computer software, such as **Magma**, one can obtain that the presentation for the fundamental group with these added relations is $\langle c^n = e^2 = e^{-1}cec = 1 \rangle$. This is not quite a product as the e and c terms interact, however it is a semi direct product of $\mathbb{Z}_n$, generated by c, and $\mathbb{Z}_2$, generated by e, where e acts

on $\mathbb{Z}_n$ by $e^{-1}ce$. Therefore the filling will have fundamental group $\mathbb{Z}_n \rtimes \mathbb{Z}_2$, we can use this to construct more covers.

Let $\rho : \pi_1(M) \to \mathbb{Z}_n \rtimes \mathbb{Z}_2$ be the quotient homomorphism given by the above discussion. We know explicit generators of each parabolic subgroup associated to each cusp of M (see chapter 2 where this computation was done). Using these explicit generators one can show that the parabolic subgroups associated to the equivalence class of ideal vertices $(0, \pm 1, 0, 0)$, $(0, 0, \pm 1, 0)$, $(0, 0, 0, \pm 1)$, $(\pm 1/2, \pm 1/2, \pm 1/2, \pm 1/2)$ all map to the generator e under the above quotient homomorphism. Furthermore, the parabolic subgroup corresponding to the ideal vertex $(\pm 1, 0, 0, 0)$ has one generator (other than c) that maps to e, since c maps to c it follows that the image of the parabolic subgroup corresponding to $(\pm 1, 0, 0, 0)$ is the whole group $\mathbb{Z}_n \rtimes \mathbb{Z}_2$. This means that the image of the parabolic subgroup associated to $(\pm 1, 0, 0, 0)$ has index one, and the index of the image of all the other parabolic subgroups is n.

As the orientation reversing side pairing transformations of M are e and g, it follows that under the quotient map they map to $\mathbb{Z}_2$. This implies that the orientation preserving generators are sent to $\mathbb{Z}_n$, which in turn implies that that orientable double cover of M corresponds to the index two subgroup given by $\rho^{-1}(\mathbb{Z}_n)$. We also know that the kernel of this quotient homomorphism is contained in $\rho^{-1}(\mathbb{Z}_n)$ and has index $2n$. It follows that the cover corresponding to $ker(\rho)$ is also an n-fold cover of the orientable double cover of M. The associated deck transformation group to $ker(\rho)$ over the orientable double cover of M is $\mathbb{Z}_n$, which implies the $2n$ fold cover is a cyclic cover.

This discussion tells us that the orientable double cover N has an n sheeted cyclic cover for each n, or put another way M has a $2n$ sheeted cover for each n, where the case $n = 1$ corresponds to the orientable double cover N. The discussion before that tells us how each boundary torus corresponding to a parabolic subgroup lifts to each cover. The boundary component corresponding to the ideal vertex class $(\pm 1, 0, 0, 0)$ lifts to one torus. This means that the covering restricted to this boundary torus is the usual n fold covering of the 3-torus onto itself. All other boundary 3-tori each lift to n copies of itself. In other words, the orientable double cover N has an n sheeted cyclic cover which has $4n + 1$ cusps, each given by a 3-torus.

The question that arises at this point is can we identify the fillings of these cyclic covers? Observe that N has Euler characteristic 2 (as all the Ratcliffe-Tschantz manifolds have Euler characteristic 1). Therefore each such cyclic cover has Euler characteristic $2n$. In the case that n is odd we claim that we can identify the topological type of the associated filling.

The argument proceeds as follows, from the previous section we know that N is spin hence it induces a spin structure on each of its boundary 3-tori (there are five in total). The three torus has exactly eight spin structures, seven of them are given by having one S^1-factor taking the bounding spin structure induced from D^2, and each of these spin structures spin bounds a solid

3-torus. The eighth spin structure corresponds to taking the Lie group spin structure on each S^1 factor. This eighth spin structure does not spin bound a solid torus, rather it spins bounds the complement of a singular 2-torus fibre in $\mathbb{CP}^2\#_9\overline{\mathbb{CP}^2}$, viewed as an elliptic fibration over $\mathbb{CP}^1$. When we preform a filling on N we are gluing in a solid torus. When we do this the manifold we obtain is itself spin, meaning that the spin structure induced on each boundary torus must cross over the solid torus that we glued in. Hence the induced spin structure on each boundary component must be the one that spin bounds a solid torus, and in fact the fibre we are filling in must have the spin structure induced from D^2. As four of the boundary tori each lift to n disjoint tori in the cyclic cover it follows that the spin structure associated to these n boundary tori in the cyclic cover must have the same spin structure as their base. Thus we need only worry about the lift of the boundary 3-torus corresponding to the ideal vertex class $(\pm 1, 0, 0, 0)$. In this case the covering is given by the covering of $S^1 \times S^1 \times S^1$ onto itself induced by the n-fold cover of one S^1 factor onto itself. In the case that n is odd we have that the lifted spin structure on the associated boundary torus in the n sheeted cover must also be the one that spin bounds a solid torus. This implies that for n odd the associated filling of the n sheeted cover is a smooth closed simply connected spin 4-manifold. We can then make an appeal to the following classification theorem of S. Donaldson and M. Freedman (see [18] p.244, see also [6] and [5]).

Theorem 4.2.1. *Every smooth simply connected 4-manifold is homeomorphic to either* $\#_m\mathbb{CP}^2\#_n\overline{\mathbb{CP}^2}$ *or* $\#_m \pm \mathcal{M}E_8\#_n(S^2 \times S^2)$.

The manifold $\mathcal{M}E_8$ denotes the non-smoothable closed simply connected 4-manifold with intersection form the E_8 lattice. The reader can find a construction of this manifold and details about its intersection form in [18] p.86 and p.125. The manifold $-\mathcal{M}E_8$ denotes $\mathcal{M}E_8$ with opposite orientation.

When $n = 3$ the Euler characteristic of the 3 sheeted cover is six, using the classification theorem of S. Donaldson and M. Freedman (thm. 4.2.1) we can deduce that the filling of the associated 3 sheeted cover (remember a filling does not change the Euler characteristic) must be homeomorphic to one of $(S^2 \times S^2)\#(S^2 \times S^2)$, $\#_4\mathbb{CP}^2$, $\#_3\mathbb{CP}^2\#\overline{\mathbb{CP}^2}$, $\#_2\mathbb{CP}^2\#_2\overline{\mathbb{CP}^2}$, $\mathbb{CP}^2\#_3\overline{\mathbb{CP}^2}$ or $\#_4\overline{\mathbb{CP}^2}$. However only $(S^2\times S^2)\#(S^2\times S^2)$ is spin, we have thus proved the following theorem.

Theorem 4.2.2. *There exists a system L consisting of thirteen linked 2-tori embedded in a smooth closed 4-manifold X that is homeomorphic to $(S^2 \times S^2)\#(S^2 \times S^2)$, such that that the complement $X - L$ admits a finite volume hyperbolic geometry*

In the case that n is odd and greater than three we see from the above classification theorem that there could be components of $\pm\mathcal{M}E_8$ (the fact that $\pm\mathcal{M}E_8$ is spin follows from the converse to *Wu's theorem*, see [18] p.163). For example if we were to take $n = 5$, and consider the associated

5 sheeted cover, we would find that we have three options for the topological type of the filling. We could have $\pm\mathcal{M}E_8$ or $\#_4(S^2 \times S^2)$. We can rule out these extra manifolds by using the fact that their signatures will all be non-zero.

The following theorem of D. Long and A. Reid allows us to compute the signature of any non-compact finite volume hyperbolic 4-manifold.

Theorem 4.2.3. *Let M be a non-compact orientable finite volume hyperbolic 4-manifold. Then $\sigma(M) = \eta(\partial M)$, where σ denotes the signature and η is the eta invariant.*

The proof of this theorem can be found in [16] Theorem.2.1, p.173-174. We should mention that the above theorem is a special case of a more general theorem proved by M.F. Atiyah, V.K. Patodi and I.M. Singer. Namely, they prove a general signature formula for a $4k$-dimensional manifold with boundary see [2] Theorem.4.14, p.66. The proof of Long and Reid involves using the formula constructed by Atiyah, Patodi and Singer together with a theorem of Chern, which states that the Pontryagin classes of a hyperbolic manifold must vanish (see [4]), and some fine analysis to do with horoball neighbourhoods about each cusp cross section of the hyperbolic 4-manifold.

The eta invariant has also been computed for flat 3-manifolds and can be found in [19] Example 1, p.128. Recall, there are six distinct isometry classes of orientable closed flat 3-manifolds, which we have been denoting by **A**, **B**, **C**, **D**, **E**, **F** (or in Wolf's notation by $\mathcal{G}_1$, $\mathcal{G}_2$, $\mathcal{G}_3$, $\mathcal{G}_4$, $\mathcal{G}_5$, $\mathcal{G}_6$). From the classification theorem (see [22] Theorem.3.5.5, p.117) it is known that only **A** and **B** are S^1-fibre bundles over a compact surface, with **A** being a 3-torus fibering over a 2-torus and **B** fibering over a Klein bottle. As we are only interested in link complements we need only worry about the eta invariant of **A** and **B**. Using the computations carried out in [19] Example 1, p.128 we find that the eta invariant of both these 3-manifolds must vanish. One can then conclude that the signature of an orientable non-compact finite volume hyperbolic 4-manifold with cusp cross sections given by **A** or **B** must have vanishing signature.

Corollary 4.2.4. *Let M be an orientable non-compact finite volume hyperbolic 4-manifold with cusp cross sections of type **A** or **B**. Then $\sigma(M) = 0$.*

Appealing to the above corollary we can conclude $\sigma(N) = 0$, and that all of the n sheeted covers of N, constructed above, have vanishing signature. The cusps of each n sheeted cover of N is a 3-torus, and when we carry out a filling we are gluing in a solid 3-torus by filling in one of the S^1-fibres with a copy of D^2 (i.e. we are doing a filling with a fixed choice of meridian). A solid 3-torus also has vanishing signature, therefore when we perform a filling we are gluing two 4-manifolds with signature zero along their common boundary (via the identity map).

There is a beautiful theorem of S. Novikov that allows one to compute the signature of a gluing provided one knows the signature of the pieces that are being glued together (see [15] Thm.5.3, p.27).

Theorem 4.2.5. *Given two oriented $4n$-dimensional manifolds M and N such that $\partial M = \partial N$. Then $\sigma(M \cup_\partial N) = \sigma(M) + \sigma(N)$, where $M \cup_\partial N$ denotes M glued to N along the common boundary.*

This theorem implies that the filling of any of the n sheeted covers of N must have signature zero, furthermore for n odd we know that such a filling must be spin. This observation coupled with the classification theorem of S. Donaldson and M. Freedman allows us to establish the following theorem.

Theorem 4.2.6. *For $n > 1$ odd the n sheeted cover of N is a complement of $4n + 1$ 2-tori in a manifold X that is homeomorphic to $\#_{n-1}(S^2 \times S^2)$.*

We remark that in the case that n is even the bounding spin structure on the base S^1 can lift to the non-bounding (the Lie group spin structure) spin structure on the total space S^1, and it is this that obstructs us from being able to conclude that the n sheeted cover of N for n even is spin. When $n = 2$ one can construct the Kirby diagram of the 2 sheeted cover of N, similar to how we did in chapter 3. Using this Kirby diagram one can prove, again by taking a simple system of reference arcs, that the 2 sheeted cover must in fact be spin. This then allows one to construct a topological hyperbolic complement in $S^2 \times S^2$, we will not go in to the details.

We should also mention that the above finite covers of N were also constructed by D. Ivanšić in his paper [10], Thm.4.3, p.18. However he does not identify the homeomorphism types of any of the finite covers of N, but merely states that they exist.

4.3 A hyperbolic link complement with topological type $(S^1 \times S^3)\#(S^2 \times S^2)$

The purpose of this section is to show the reader that there are examples of Ratcliffe-Tschantz manifolds that have fundamental groups that are much more complicated than the ones we have been dealing with so far. Due to this, the Kirby diagrams of such manifolds turn out to be much more complicated, and in turn it becomes very difficult to try and identify the diffeomorphism type of a boundary filling of the orientable double cover of such a manifold. However, if we forgo the need to identify the diffeomorphism type of such boundary fillings and be content with trying to identify the homeomorphism type (as we have been so far in this chapter) then one can make some progress. The primary example we will be dealing with is the manifold numbered

40 in the census. We will show the Kirby diagram of a boundary filling of this manifold, we will then carry out a few handle cancellations and then show the reader the exact point where things start to get very complicated. Finally, we will show how using a very beautiful theorem of *Akio Kawauchi* and knowledge of spin structures we can identify the homeomorphism type of the orientable double cover of manifold 40.

The side pairing code for this manifold is **143CF9**. The explicit side pairings are given as:

$$S_{(+1,+1,0,0)} \xrightarrow[k_{(-1,+1,+1,+1)}]{a} S_{(-1,+1,0,0)} \qquad S_{(+1,-1,0,0)} \xrightarrow[k_{(-1,+1,+1,+1)}]{b} S_{(-1,-1,0,0)}$$

$$S_{(+1,0,+1,0)} \xrightarrow[k_{(+1,+1,-1,+1)}]{c} S_{(+1,0,-1,0)} \qquad S_{(-1,0,+1,0)} \xrightarrow[k_{(+1,+1,-1,+1)}]{d} S_{(-1,0,-1,0)}$$

$$S_{(0,+1,+1,0)} \xrightarrow[k_{(-1,-1,+1,+1)}]{e} S_{(0,-1,+1,0)} \qquad S_{(0,+1,-1,0)} \xrightarrow[k_{(-1,-1,+1,+1)}]{f} S_{(0,-1,-1,0)}$$

$$S_{(+1,0,0,+1)} \xrightarrow[k_{(+1,+1,-1,-1)}]{g} S_{(+1,0,0,-1)} \qquad S_{(-1,0,0,+1)} \xrightarrow[k_{(+1,+1,-1,-1)}]{h} S_{(-1,0,0,-1)}$$

$$S_{(0,+1,0,+1)} \xrightarrow[k_{(-1,-1,-1,-1)}]{i} S_{(0,-1,0,-1)} \qquad S_{(0,+1,0,-1)} \xrightarrow[k_{(-1,-1,-1,-1)}]{j} S_{(0,-1,0,+1)}$$

$$S_{(0,0,+1,+1)} \xrightarrow[k_{(-1,+1,+1,-1)}]{k} S_{(0,0,+,-)} \qquad S_{(0,0,-1,+1)} \xrightarrow[k_{(-1,+1,+1,+1)}]{l} S_{(0,0,-1,-1)} \ .$$

The coordinates of the sides are given in the following table:

A	$S_{(+1,+1,0,0)}$	$(\frac{1}{\sqrt{2}}, \frac{1}{\sqrt{2}}, 0)$	A'	$S_{(-1,+1,0,0)}$	$(\frac{-1}{\sqrt{2}}, \frac{1}{\sqrt{2}}, 0)$
B	$S_{(+1,-1,0,0)}$	$(\frac{1}{\sqrt{2}}, \frac{-1}{\sqrt{2}}, 0)$	B'	$S_{(-1,-1,0,0)}$	$(\frac{-1}{\sqrt{2}}, \frac{-1}{\sqrt{2}}, 0)$
C	$S_{(+1,0,+1,0)}$	$(\frac{1}{\sqrt{2}}, 0, \frac{1}{\sqrt{2}})$	C'	$S_{(+1,0,-1,0)}$	$(\frac{1}{\sqrt{2}}, 0, \frac{-1}{\sqrt{2}})$
D	$S_{(-1,0,+1,0)}$	$(\frac{-1}{\sqrt{2}}, 0, \frac{1}{\sqrt{2}})$	D'	$S_{(-1,0,-1,0)}$	$(\frac{-1}{\sqrt{2}}, 0, \frac{-1}{\sqrt{2}})$
E	$S_{(0,+1,+1,0)}$	$(0, \frac{1}{\sqrt{2}}, \frac{1}{\sqrt{2}})$	E'	$S_{(0,-1,+1,0)}$	$(0, \frac{-1}{\sqrt{2}}, \frac{1}{\sqrt{2}})$
F	$S_{(0,+1,-1,0)}$	$(0, \frac{1}{\sqrt{2}}, \frac{-1}{\sqrt{2}})$	F'	$S_{(0,-1,-1,0)}$	$(0, \frac{-1}{\sqrt{2}}, \frac{-1}{\sqrt{2}})$
G	$S_{(+1,0,0,+1)}$	$(1+\sqrt{2}, 0, 0)$	G'	$S_{(+1,0,0,-1)}$	$(-1+\sqrt{2}, 0, 0)$
H	$S_{(-1,0,0,+1)}$	$(-1-\sqrt{2}, 0, 0)$	H'	$S_{(-1,0,0,-1)}$	$(1-\sqrt{2}, 0, 0)$
I	$S_{(0,+1,0,+1)}$	$(0, 1+\sqrt{2}, 0)$	I'	$S_{(0,-1,0,-1)}$	$(0, 1-\sqrt{2}, 0)$
J	$S_{(0,+1,0,-1)}$	$(0, -1+\sqrt{2}, 0)$	J'	$S_{(0,-1,0,+1)}$	$(0, -1-\sqrt{2}, 0)$
K	$S_{(0,0,+1,+1)}$	$(0, 0, 1+\sqrt{2})$	K'	$S_{(0,0,+1,-1)}$	$(0, 0, -1+\sqrt{2})$
L	$S_{(0,0,-1,+1}$	$(0, 0, -1-\sqrt{2})$	L'	$S_{(0,0,-1,-1)}$	$(0, 0, 1-\sqrt{2})$

From here on in we will denote manifold 40 in the Ratcliffe-Tschantz census by M, we will not bother giving all the twenty four 2-handles in a separate table as we have been doing. Instead,

we will move on to showing which 2-handles lie in which plane, and those that do not lie in any single plane.

The 2-handles that lie in the x-y plane are shown in the following picture with the table following showing which colour corresponds to which 2-handle.

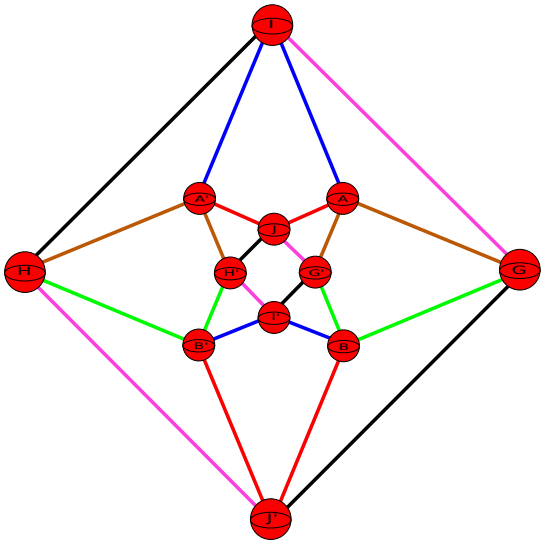

Colour	**Equivalence Class**
brown	$A \cap G \xrightarrow{a} A' \cap H \xrightarrow{h} A' \cap H' \xrightarrow{a^{-1}} A \cap G' \xrightarrow{g^{-1}} A \cap G$
red	$A \cap J \xrightarrow{a} A' \cap J \xrightarrow{j} B \cap J' \xrightarrow{b} B' \cap J' \xrightarrow{j^{-1}} A \cap J$
blue	$A \cap I \xrightarrow{a} A' \cap I \xrightarrow{i} B \cap I' \xrightarrow{b} B' \cap I' \xrightarrow{i^{-1}} A \cap I$
Green	$B \cap G \xrightarrow{b} B' \cap H \xrightarrow{h} B' \cap H' \xrightarrow{b} B \cap G' \xrightarrow{g^{-1}} B \cap G$
pink	$G \cap I \xrightarrow{g} G' \cap J \xrightarrow{j} H \cap J' \xrightarrow{h} H' \cap I' \xrightarrow{i^{-1}} G \cap I$
black	$G \cap J' \xrightarrow{g} G' \cap I' \xrightarrow{i^{-1}} H \cap I \xrightarrow{h} H' \cap J \xrightarrow{j} G \cap J'$

The 2-handles that lie in the x-z plane are shown in the following picture with the table following showing which colour corresponds to which 2-handle.

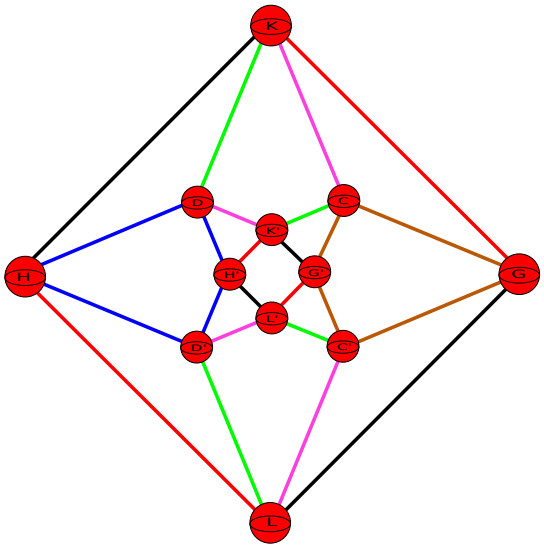

Colour	Equivalence Class
brown	$C \cap G \xrightarrow{c} C' \cap G \xrightarrow{g} C \cap G' \xrightarrow{c} C' \cap G' \xrightarrow{g^{-1}} C \cap G$
red	$G \cap K \xrightarrow{g} G' \cap L' \xrightarrow{l^{-1}} H \cap L \xrightarrow{h} H' \cap K' \xrightarrow{k^{-1}} G \cap K$
blue	$D \cap H \xrightarrow{d} D' \cap H \xrightarrow{h} D \cap H' \xrightarrow{d} D' \cap H' \xrightarrow{h^{-1}} D \cap H$
green	$C \cap K' \xrightarrow{c} C' \cap L' \xrightarrow{l^{-1}} D' \cap L \xrightarrow{d^{-1}} D \cap K \xrightarrow{k^{-1}} C \cap K'$
pink	$C \cap K \xrightarrow{c} C' \cap L \xrightarrow{l} D' \cap L' \xrightarrow{d^{-1}} D \cap K' \xrightarrow{k^{-1}} C \cap K$
black	$G \cap L \xrightarrow{g} G' \cap K' \xrightarrow{k^{-1}} H \cap K \xrightarrow{h} H' \cap L' \xrightarrow{l^{-1}} G \cap L$

The 2-handles that lie in the y-z plane are shown in the following picture.

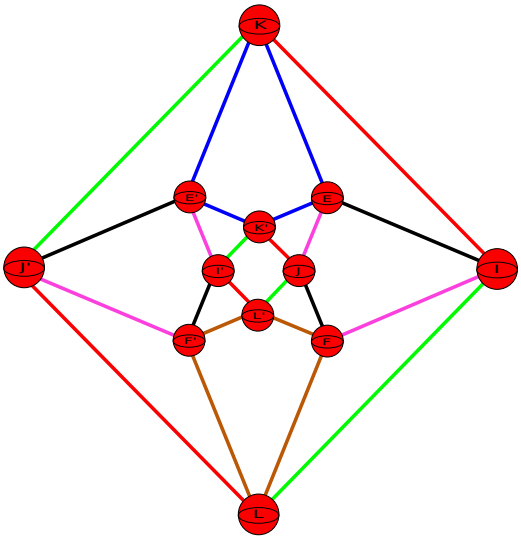

Colour	Equivalence Class
brown	$F \cap L \xrightarrow{f} F' \cap L \xrightarrow{l} F' \cap L' \xrightarrow{f^{-1}} F \cap L' \xrightarrow{l^{-1}} F \cap L$
red	$I \cap K \xrightarrow{i} I' \cap L' \xrightarrow{l^{-1}} J' \cap L \xrightarrow{j^{-1}} J \cap K' \xrightarrow{k^{-1}} I \cap K$
blue	$E \cap K \xrightarrow{e} E' \cap K \xrightarrow{k} E' \cap K' \xrightarrow{e^{-1}} E \cap K' \xrightarrow{k^{-1}} E \cap K$
green	$I \cap L \xrightarrow{i} I' \cap K' \xrightarrow{k^{-1}} J' \cap K \xrightarrow{j^{-1}} J \cap L' \xrightarrow{l^{-1}} I \cap L$
pink	$E \cap J \xrightarrow{e} E' \cap I' \xrightarrow{i^{-1}} F \cap I \xrightarrow{f} F' \cap J' \xrightarrow{j^{-1}} E \cap J$
black	$E \cap I \xrightarrow{e} E' \cap J' \xrightarrow{j^{-1}} F \cap J \xrightarrow{f} F' \cap I' \xrightarrow{i^{-1}} E \cap I$

Finally, the 2-handles that do not lie in any of the above three planes are shown in the following picture.

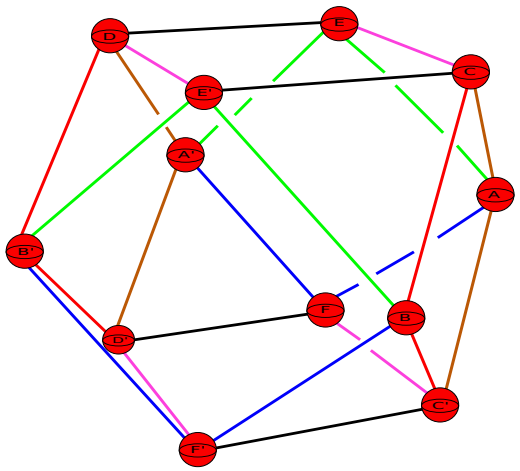

Colour	Equivalence Class
brown	$A \cap C \xrightarrow{a} A' \cap D \xrightarrow{d} A' \cap D' \xrightarrow{a^{-1}} A \cap C' \xrightarrow{c^{-1}} A \cap C$
red	$B \cap C \xrightarrow{b} B' \cap D \xrightarrow{d} B' \cap D' \xrightarrow{b^{-1}} B \cap C' \xrightarrow{c^{-1}} B \cap C$
blue	$A \cap F \xrightarrow{a} A' \cap F \xrightarrow{f} B \cap F' \xrightarrow{b} B' \cap F' \xrightarrow{f^{-1}} A \cap F$
green	$A \cap E \xrightarrow{a} A' \cap E \xrightarrow{e} B \cap E' \xrightarrow{b} B' \cap E' \xrightarrow{e^{-1}} A \cap E$
pink	$C \cap E \xrightarrow{c} C' \cap F \xrightarrow{f} D' \cap F' \xrightarrow{d^{-1}} D \cap E' \xrightarrow{e^{-1}} C \cap E$
black	$C \cap E' \xrightarrow{c} C' \cap F' \xrightarrow{f^{-1}} D' \cap F \xrightarrow{d^{-1}} D \cap E \xrightarrow{e} C \cap E'$

The manifold M has five boundary components each of which is a closed Euclidean 3-manifold that is an S^1-fibre bundle over some (possibly non-orientable) compact surface. We have already seen that in order to "fill in" each boundary component we need to choose translations in each parabolic subgroup, corresponding to each cusp, that represent the S^1-fibre. We have already explicitly shown how to compute the generators of each parabolic subgroup, and then how to identify which ones are translations. As the same technique works for any Ratcliffe-Tschantz manifold (and more generally any non-compact finite volume hyperbolic manifold) we will just

write down the translations we are going to use, leaving it to the interested reader to carry out the explicit computations if they so please.

The following table shows the translations and the ideal vertices they correspond to.

Ideal vertex	**Filling translation**
$\{(1,0,0,0),(-1,0,0,0)\}$	c
$\{(0,1,0,0),(0,-1,0,0)\}$	a
$\{(0,0,1,0),(0,0,-1,0)\}$	$e^{-1}k^{-1}$
$\{(0,0,0,1),(0,0,0,-1)\}$	$g^{-1}l$
$\{(\pm 1/2,\pm 1/2,\pm 1/2,\pm 1/2)\}$	$e^{-1}h^{-1}fg$

In the above Kirby diagram the attaching locus of the 2-handles, corresponding to a boundary filling with respect to the above translations, will consist of a line joining the 1-handles $C - C'$ and $A - A'$, corresponding to the translations c and a respectively, one line joining E to K' and another joining E' to K, corresponding to $e^{-1}k^{-1}$. A line joining G to L and another joining G' to L', corresponding to the translation $g^{-1}l$, and finally four more lines with one joining E to G, one joining E' to H, one joining F' to H' and one joining F to G', corresponding to the translation $e^{-1}h^{-1}fg$. We are going to show how these added 2-handles will look like in the above Kirby diagram, at the same time we will also show the intersection points they create with the other planes.

The following shows the x-y plane, you can see the added 2-handle corresponding to the translation a, it is the only one that lies in the x-y plane.

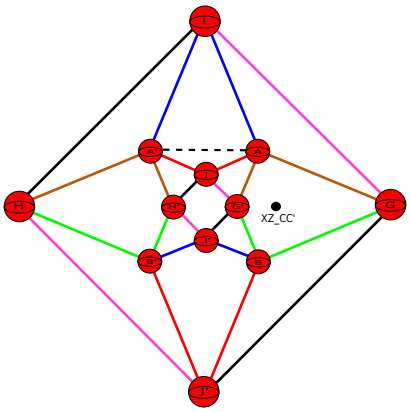

The added 2-handles corresponding to the translations c and $g^{-1}l$ lie in the x-z plane and can be seen in the following picture.

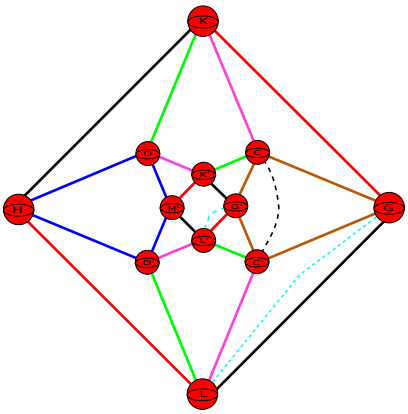

The added 2-handle corresponding to the translation $e^{-1}k^{-1}$ lies in the y-z plane and can be seen in the following picture.

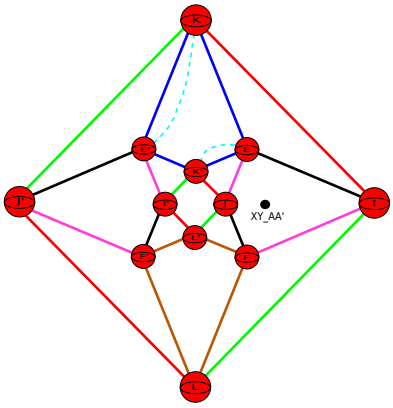

Finally, the added 2-handles corresponding to the translations a and c can also been seen in the diagram corresponding to the six 2-handles that do not all lie in a single plane.

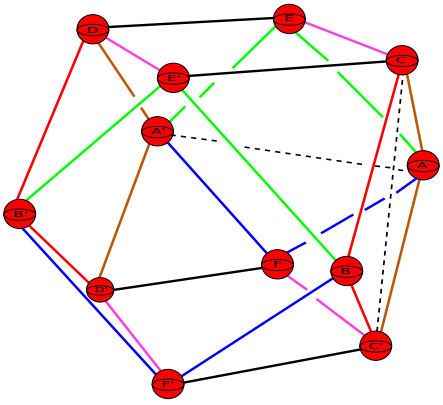

The attaching locus of the final 2-handle we are adding, which corresponds to the translation $e^{-1}h^{-1}fg$, lies outside the above four diagrams.

The following picture shows that part of the locus that runs between E and G

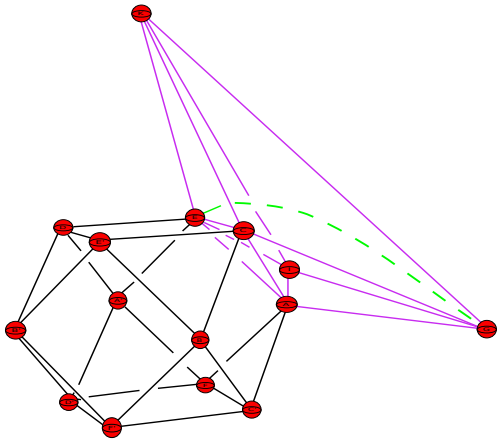

that part of the locus that runs between E' and H can be seen in the following picture

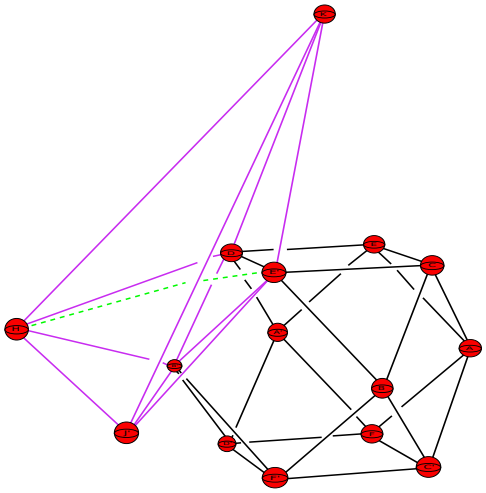

that part of the locus that runs between F' and H' can be seen in the following picture

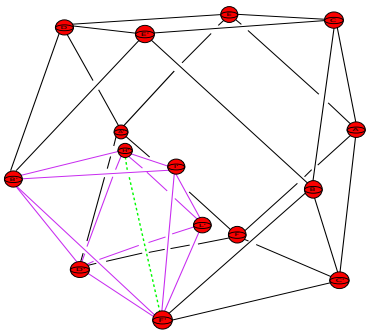

and finally the part that runs between F and G' can be seen in the following picture

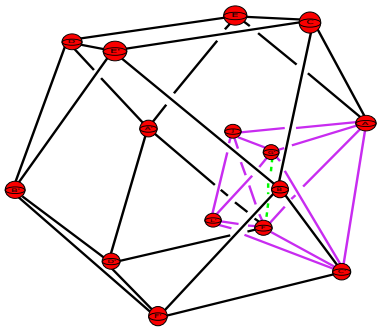

From these diagrams it is clear that there are a few cancellations that we can start carrying out in order to simplify the Kirby diagram. We are going to show the explicit details of these handle cancellations as we have been doing. Instead, let us just mention that to start with, one can carry out some easy cancellations. For example the added 2-handle corresponding to the translation a can be used to cancel A, A'. Similarly the added 2-handle corresponding to the translation c can be used to cancel C, C'. These two cancellations provide a 2-handle that runs over B, B' once, and one that runs over D, D' once. Hence we can use these 2-handles to cancel B, B' and D, D' respectively. It is at this point where the cancellations start to become much more tricky. The next step one can undertake is to cancel the 1-handle K, K' with the 2-handle in the y-z plane whose attaching locus runs from E to K' and E' to K, this is the added 2-handle that corresponded to the translation $e^{-1}k^{-1}$. The problem with carrying out this cancellation is that there are 2-handles in the x-z plane that run over $K - K'$ in the x-z plane. This means that when we cancel $K - K'$ using the 2-handle we just mentioned, we find that some 2-handles originally residing in x-z plane will have components that move into the y-z plane. It is these 2-handles that move from one plane into another that make the Kirby diagram much more complicated. Many more cancellations that one wants to proceed with also have similar problems, and in general getting passed these complications seems to be very difficult. We leave it to the reader to experiment for him/her-self as to how these Kirby diagrams start to look like when one carries out such cancellations.

Although we are in a position where using Kirby calculus to try and identify the diffeomorphism type of a boundary filling seems a daunting task, it is not so the case if instead we try and identify the homeomorphism type. The first step in carrying out such a program is to identify the fundamental group of the boundary filling of M (remember M denotes manifold 40). Let us denote the boundary filling of M by M_0. We already have a presentation for the fundamental group of M_0, its generators are the side pairing transformations making up M, and its relations are given by taking the twenty four 2-handle equivalence classes of M and adding the five relations c, a, $e^{-1}k^{-1}$, $g^{-1}l$ and $e^{-1}h^{-1}fg$. The addition of these five last relations allows the presentation to be simplified greatly. The easiest way to do this is to use a computer

program, for example one can input the presentation of M_0 into the software **Magma** and use the **ReduceGenerators** command to obtain $\pi_1(M_0) = \langle e, i \,|\, e^2 = i^2 \rangle$. Thus we see that the fundamental group of M_0 is isomorphic to the free product $\mathbb{Z}_2 * \mathbb{Z}_2$.

The orientable double cover is given by an index two subgroup, and any index two subgroup is determined by a homomorphism

$$\phi : \pi_1(M_0) \to \mathbb{Z}_2$$

however any such homomorphism is completely determined by where it sends the generators e and i. This leaves us with three choices:

- $\phi(e) = 1$ and $\phi(i) = 0$
- $\phi(e) = 0$ and $\phi(i) = 1$
- $\phi(e) = 1$ and $\phi(i) = 1$

In the case that the index two subgroup corresponds to an orientable double cover we know that the homomorphism ϕ maps all orientation preserving isometries to 0 and all orientation reversing ones to 1. In our case it is not hard to see that both e and i are orientation reversing, hence the homomorphism that corresponds to our case is number 3. It is clear that such a homomorphism has kernel generated by the product ei, hence is infinite cyclic. We are therefore able to conclude that M_0 has orientable double cover $\widetilde{M_0}$ with $\pi_1(\widetilde{M_0}) \cong \mathbb{Z}$. In order to identify the homeomorphism type of $\widetilde{M_0}$ we need a theorem of *A. Kawauchi*, see [13].

Theorem 4.3.1 (A. Kawauchi)**.** *A smooth closed 4-manifold M with infinite cyclic fundamental group is homeomorphic to $S^1 \times S^3 \# M'$, where M' is a closed simply connected 4-manifold.*

We would like to point out that the theorem is not true if the initial 4-manifold M is not assumed to admit a smooth structure. A very nice counter example to this case is in the paper [7]. In our case this is not a problem as it is clear from construction that both M_0 and hence $\widetilde{M_0}$ have smooth structures.

Appealing to the above theorem we can conclude that $\widetilde{M_0}$ is homeomorphic to the connected sum $S^1 \times S^3 \# M'$ for some closed simply connected manifold M'. What can M' be? Recall that filling in a manifold with boundary a compact Euclidean 3-manifold does not change the Euler characteristic. As all the Ratcliffe-Tschantz manifolds have Euler characteristic one, it follows that M_0 has Euler characteristic one and hence $\widetilde{M_0}$ has Euler characteristic two. The reader can check that $S^1 \times S^3$ has Euler characteristic zero, combining this with what we just said we obtain the following equation

$$2 = \chi(\widetilde{M_0}) = \chi(S^1 \times S^3) + \chi(M') - 2$$

from which we can conclude $\chi(M') = 4$. Applying the classification theorem on the homeomorphism type of a smooth simply connected 4-manifold by Freedman and Donaldson (see [18] p.244, see also [6] and [5]), we can conclude that M' is homeomorphic to $S^2 \times S^2$, $\mathbb{CP}^2\#\mathbb{CP}^2$, $\mathbb{CP}^2\#\overline{\mathbb{CP}^2}$ or $\overline{\mathbb{CP}^2}\#\overline{\mathbb{CP}^2}$ (in fact, using the signature theorem one can always rule out the possibility of $\mathbb{CP}^2\#\mathbb{CP}^2$ or $\overline{\mathbb{CP}^2}\#\overline{\mathbb{CP}^2}$, see next chapter). The key to deducing the homeomorphism type of M' rests on knowing that the orientable double cover $\widetilde{M_0}$ admits a spin structure. The way to see this is to proceed as in the case of the orientable double cover of manifold 1011. One constructs the Kirby diagram associated to the orientable double cover of M, then shows that there exists a system of reference arcs, which can be used to transform the Kirby diagram of the orientable double cover in to dotted circle notation such that each 2-handle transforms in to a knot with framing coefficient an even integer. One then shows the 2-handles that need to be added in order to carry out the filling process will also transform to knots with framing coefficient an even integer. We will not give the details of this process as it is exactly analogous to what we did for manifold 1011 (see section 4.1). This then allows us to conclude that the filling $\widetilde{M_0}$ must be spin, and hence that M' must be homeomorphic to $S^2 \times S^2$.

Theorem 4.3.2. *The manifold numbered 40 in the Ratcliffe-Tschantz census has orientable double cover a 7-cusped hyperbolic 4-manifold that is a complement in a 4-manifold that is homeomorphic to* $(S^1 \times S^3)\#(S^2 \times S^2)$.

Chapter 5

Hyperbolic link complements in $\#_r\mathbb{CP}^2\#_s\overline{\mathbb{CP}^2}$

In the previous chapter we witnessed the construction of hyperbolic link complements in closed 4-manifolds that were topologically given by $\#_{2k}(S^2 \times S^2)$, for $k > 0$. The identification proceeded via three steps, the first involved using the classification theorem of S. Donaldson and M. Freedman to give a finite list of manifolds, for each Euler characteristic, which we could choose from. The second step involved refining this list to have fewer possible choices by proving that the fillings we were dealing with had to admit a spin structure. The third and final step involved a further refinement by the understanding that the fillings also had to have vanishing signature. The need for the second step was primarily to do with the fact of understanding whether the manifolds we were dealing with could have the topological type of $\#_r\mathbb{CP}^2\#_s\overline{\mathbb{CP}^2}$. As the manifolds we were dealing with were all spin, and all the manifolds $\#_r\mathbb{CP}^2\#_s\overline{\mathbb{CP}^2}$ are not, we could cross these off our list. This brings forth the question of whether a manifold that is homeomorphic to $\#_r\mathbb{CP}^2\#_s\overline{\mathbb{CP}^2}$ could have a link complement that is hyperbolic? In this brief chapter we take up this question and show that a sufficient condition for such a link complement to exist is that $r = s$. The proof is not at all difficult and is based on the signature type argument we invoked in the previous chapter.

To make this chapter self-contained we will recall the theorems, used in the previous chapter, about the signature of a non-compact orientable finite volume hyperbolic 4-manifold.

The starting point was to use the following theorem of D. Long and A. Reid that involves a formula for computing the signature of a non-compact orientable finite volume hyperbolic 4-manifold in terms of the eta invariant.

Theorem 5.0.3. *Let M be a non-compact orientable finite volume hyperbolic 4-manifold. Then $\sigma(M) = \eta(\partial M)$, where σ denotes the signature and η is the eta invariant.*

The proof of this theorem can be found in [16] Theorem.2.1, p.173-174. As we did in the previous chapter, we mention that the above theorem is a special case of a more general theorem proved by M.F. Atiyah, V.K. Patodi and I.M. Singer. Namely, they prove a general signature formula for a $4k$-dimensional manifold with boundary see [2] Theorem.4.14, p.66. The proof of Long and Reid involves using the formula constructed by Atiyah, Patodi and Singer together with a theorem of Chern, which states that the Pontryagin classes of a hyperbolic manifold must vanish (see [4]), and some fine analysis to do with horoball neighbourhoods about each cusp cross-section of the hyperbolic 4-manifold.

The main importance of the above theorem is that it pushes the computation of the signature to the computation of the eta invariant of the cusp cross sections of the manifold. The cusp cross sections of a non-compact orientable finite volume hyperbolic 4-manifold fall into six classes, coming from the fact that there are six isometry classes of orientable closed flat 3-manifolds. We denoted these six classes by **A**, **B**, **C**, **D**, **E**, **F** (or in Wolf's notation by $\mathcal{G}_1$, $\mathcal{G}_2$, $\mathcal{G}_3$, $\mathcal{G}_4$, $\mathcal{G}_5$, $\mathcal{G}_6$). Therefore in order to understand the signature of a non-compact orientable finite volume hyperbolic 4-manifold one needs to understand what the eta invariant of the above six classes of flat 3-manifolds are.

The computation of the eta invariant for these six classes of flat 3-manifolds can be found in [19] Example 1, p.128. The following proposition gives the values of the eta invariant for these six classes.

Proposition 5.0.4.

$\eta(\boldsymbol{A}) = 0$

$\eta(\boldsymbol{B}) = 0$

$\eta(\boldsymbol{C}) = \frac{-2}{3}$

$\eta(\boldsymbol{D}) = -1$

$\eta(\boldsymbol{E}) = \frac{-4}{3}$

$\eta(\boldsymbol{F}) = 0$

From the classification theorem (see [22] Theorem.3.5.5, p.117) it is known that only **A** and **B** are S^1-fibre bundles over a compact surface, with **A** being a 3-torus fibering over a 2-torus and **B** fibering over a Klein bottle. As we are only interested in link complements we need only worry about the eta invariant of **A** and **B**. Using the above proposition we obtain the following corollary.

Corollary 5.0.5. *Let M be an orientable non-compact finite volume hyperbolic 4-manifold with cusp cross sections of type **A** or **B**. Then $\sigma(M) = 0$.*

From now on we assume M is a non-compact finite volume hyperbolic 4-manifold with cusp cross sections of type **A** or **B**. When we construct a filling of M we are gluing in disk bundles associated to the cusp-cross sections of type **A** or **B**. These disk bundles also have vanishing signature, hence the filling of M is made up from a collection of 4-manifolds each having vanishing signature.

Appealing to the following theorem of S. Novikov (see [15] Thm.5.3, p.27)

Theorem 5.0.6. *Let M and N be two oriented $4n$-dimensional manifolds such that $\partial M = \partial N$. Then $\sigma(M \cup_\partial N) = \sigma(M) + \sigma(N)$, where $M \cup_\partial N$ denotes M glued to N along the common boundary.*

We can conclude that the signature of such a filled in manifold must be zero. This allows one to deduce a simple restriction on such complements residing in a manifold that is homeomorphic to $\#_r\mathbb{CP}^2\#_s\overline{\mathbb{CP}^2}$.

Theorem 5.0.7. *Let M be a non-compact finite volume hyperbolic 4-manifold with cusps of type **A** or **B**. Suppose M is a complement in the connected sum $\#_r\mathbb{CP}^2\#_s\overline{\mathbb{CP}^2}$. Then we must have that $r = s$.*

Proof. If M is a complement in $\#_r\mathbb{CP}^2\#_s\overline{\mathbb{CP}^2}$, then the filling of M must be $\#_r\mathbb{CP}^2\#_s\overline{\mathbb{CP}^2}$. However, the filling of M must have signature zero. This can only happen if $r = s$. □

This theorem together with the work we did in the previous chapter (see 4.2) gives necessary conditions on those smooth simply connected closed 4-manifolds that admit a hyperbolic link complement.

Theorem 5.0.8. *Let M be a smooth closed simply connected 4-manifold that has a link complement that admits a finite volume hyperbolic geometry. Then the homeomorphism type of M falls into one of the following three categories:*

- S^4
- $\#_k(S^2 \times S^2)$, $k > 0$.
- $\#_k\mathbb{CP}^2\#_k\overline{\mathbb{CP}^2}$, $k > 0$.

Bibliography

[1] S. Akbulut. *4-manifolds.* available at http://www.math.msu.edu/ akbulut/, 2014.

[2] M.F. Atiyah, V.K. Patodi, and I.M. Singer. *Spectral asymmetry and Riemannian Geometry. I.* Math. Proc. Camb. Phil. Soc. (1975), 77, 43.

[3] R. Benedetti and C. Petronio. *Lectures on Hyperbolic Geometry.* Springer-Verlag, Berlin Heidelberg, 1992.

[4] S. Chern. *On curvature and characteristic classes of a Riemannian manifold.* Abhandlungen aus dem Mathematischen Seminar der Universitt Hamburg, 20, 1955.

[5] S.K. Donaldson. *An application of gauge theory to four-dimensional topology.* Journal of Differential Geometry, 18 (2): 279315, 1983.

[6] M.H. Freedman. *The topology of four-dimensional manifolds.* Journal of Differential Geometry, 17 (3): 357453, 1982.

[7] S. Friedl, I. Hambelton, P. Melvin, and P. Teichner. *Non-smoothable Four-manifolds with Infinite Cyclic Fundamental Group.* International Mathematics Research Notices, Vol. 22, No. 14.

[8] R.E Gompf and A.I Stipsicz. *4-manifolds and Kirby Calculus.* Graduate Studies in Mathematics, Providence, Rhode Island, 1999.

[9] W. Hantzsche and H. Wendt. *Dreidimensionale euklidische Raumformen.* Math. Ann. 110, 593-611, 1935.

[10] D. Ivanšić. *Hyperbolic structure on a complement of tori in the 4-sphere.* Adv. Geom. 4, no. 1, 119139, 2004.

[11] D. Ivanšić, J.G. Ratcliffe, and S.T. Tschantz. *Complements of tori and Klein bottles in the 4-sphere that have hyperbolic structure.* Algebr. Geom. Topol. 5, 9991026, 2005.

[12] D.L. Johnson. *Topics in the Theory of Group Presentations, London Mathematical Society Lecture Notes Series, 42.* Cambridge University Press, Cambridge, 1980.

[13] A. Kawauchi. *Splitting a 4-manifold with infinite cyclic fundamental group, revised.* Journal of Knot Theory and Its Ramifications, Vol. 22, No. 14.

[14] R. Kirby. *A Calculus for Framed Links in S^3.* Inventiones math., 45, 35-56, 1978.

[15] R. Kirby. *Topology of 4-manifolds.* Springer-Verlag Berlin Heidelberg, 1989.

[16] D. Long and A. Reid. *On the geometric boundaries of hyperbolic 4-manifolds.* Geometry & Topology, Vol. 4 (2000) no. 5, p.171-178.

[17] J.G Ratcliffe and S.T Tschantz. *The Volume Spectrum of Hyperbolic 4-manifolds.* Experimental Mathematics, Vol. 9, No.1, 2000.

[18] A. Scorpan. *The Wild World of 4-Manifolds.* American Mathemtical Society, Providence, Rhode island, 2005.

[19] A. Szczepański. *Eta invariants for flat manifolds.* Annals of Global Analysis and Geometry, February 2012, Volume 41, Issue 2, pp 125-138.

[20] W. Thurston. *The geometry and topology of three-manifolds.* Princeton Univ. Math. Dept. Notes, Available at http://www.msri.org/communications/books/gt3m, 1979.

[21] W. Thurston. *Three-dimensional manifolds, Kleinian groups and hyperbolic geometry.* Bull.Amer. Math. Soc. (N.S.)6, no. 3, 357381, 1982.

[22] J.A Wolf. *Spaces of constant curvature.* McGraw-Hill, Inc., United States of America, 1967.